

Doctoral Dissertation

**Fundamental Study on Indoor Thermal Environments in High-Rise
Apartments in Hot-Humid Climates of Indonesia**

MUHAMMAD NUR FAJRI ALFATA

Graduate School for International Development and Cooperation
Hiroshima University

March 2018

**Fundamental Study on Indoor Thermal Environments in High-Rise
Apartments in Hot-Humid Climates of Indonesia**

D140332

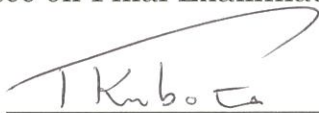
MUHAMMAD NUR FAJRI ALFATA

A Dissertation Submitted to
the Graduate School for International Development and Cooperation
of Hiroshima University in Partial Fulfillment
of the Requirement for the Degree of
Doctor of Engineering

March 2018

We hereby recommend that the dissertation by Mr. MUHAMMAD NUR FAJRI ALFATA entitled "Fundamental Study on Indoor Thermal Environments in High-Rise Apartments in Hot-Humid Climates of Indonesia" be accepted in partial fulfillment of the requirements for the degree of Doctor of Engineering.

Committee on Final Examination:



KUBOTA Tetsu, Associate Professor

Chairperson



ZHANG Junyi, Professor



YAMAMOTO Haruyuki, Professor



NISHINA Daisaku, Professor



LEE Hansoo, Associate Professor

Date: 13 Feb. 2018

Approved:



BABA Takuya, Professor

Dean

Date: February 23, 2018

Graduate School for International Development and Cooperation
Hiroshima University

*For:
Allah SWT,
Muhammad SAW,
Indonesia,
Puskim,
My Wife, and
My Family*

Contents

Abstract	v
Acknowledgement	ix
List of Figures	xi
List of Tables	xxiii
List of Acronyms	xxv
Nomenclature	xxvii
List of Publications	xxix
1 Introduction	1
1.1 Backgrounds	1
1.1.1 Development of middle class and apartments in Indonesia	2
1.1.2 Energy consumption and CO ₂ emissions in Indonesia	4
1.2 Problem statement and research scope	5
1.3 Research objectives	7
1.4 Contribution of the research	7
2 Literature Review: Passive Cooling of Apartment Buildings	9
2.1 Passive cooling techniques of buildings in the tropics	9
2.2 Thermal comfort in the tropics	13
2.3 Studies on vernacular passive techniques in hot-humid climates	16
2.4 Recent developments of passive cooling techniques in apartments in hot-humid climate	18
3 Thermal Comfort in Existing Apartments of Indonesia	21
3.1 Apartments in Indonesia	21
3.2 Case study apartments	25
3.3 Methods	27
3.3.1 Field measurements	27
3.3.2 Questionnaires and face to face interview	30
3.3.3 Computer simulation	31
3.3.3.1 The simulation program used and simulation conditions	31

3.3.3.2.	Base model apartments and simulation cases	34
3.4	Thermal comfort in unoccupied units	39
3.4.1	Field investigation of indoor thermal environments	40
3.4.1.1	Indoor thermal environments in different natural ventilation conditions	40
3.4.1.2	Vertical distribution of air temperature in master bedroom	49
3.4.1.3	Surface temperatures in the master bedroom	51
3.4.1.4	Air tightness of master bedroom	57
3.4.1.5	Thermal comfort evaluation	60
3.4.2	Numerical simulation of indoor thermal environments	63
3.4.2.1	Validation of the base model	63
3.4.2.2	Indoor thermal environments in different natural ventilation conditions	66
3.4.2.3	Indoor thermal comfort	69
3.5	Thermal comfort in occupied units	72
3.5.1	Field investigation of indoor thermal environments	72
3.5.2	Thermal comfort evaluation	73
3.5.3	Factors influencing thermal conditions	74
3.6	Discussion	78
3.6.1	Current problems of design of apartments in Indonesia	78
3.6.2	Potential passive cooling techniques	82
3.7	Summary	82
4	Field Investigation of Indoor Thermal Environments in Dutch Colonial Buildings	85
4.1	Introduction	85
4.2	Case study buildings in Bandung	88
4.3	Methods	91
4.3.1	Field measurement	91
4.3.2	Questionnaires	93
4.4	Case study 1	93
4.4.1	Indoor thermal environments in different natural ventilation conditions	93
4.4.2	Vertical distribution of air temperatures	97
4.4.3	Thermal comfort evaluation	98
4.5	Case study 2	103
4.5.1	Indoor thermal environments in different natural ventilation conditions	103
4.5.2	Vertical distribution of air temperatures	106
4.5.3	Thermal comfort evaluation	107
4.6	Case study 3	108
4.6.1	Indoor thermal environments in different natural ventilation conditions	108
4.6.2	Vertical distribution of air temperatures	112

4.6.3	Thermal comfort evaluation	113
4.7	Discussion	114
4.7.1	The effects of corridor spaces on indoor thermal environments	114
4.7.2	The effects of ceiling height	115
4.7.3	Comfort ventilation in Dutch colonial buildings	116
4.7.4	Cooling strategies employed in the Dutch colonial buildings: Recommendation for modern houses	117
4.8	Summary	118
5	Parametric Study of Cooling Strategies for High-Rise Apartments	119
5.1	Introduction	119
5.2	Methods	119
5.2.1	TRNSYS and COMIS	120
5.2.2	Computational Fluid Dynamics (CFD): STREAM	120
5.2.3	Validation: Model specifications and simulation conditions	125
5.3	Base model and simulation test cases	136
5.3.1	Base model and simulation test cases for CFD STREAM	136
5.3.2	Base model and simulation test cases for TRNSYS-COMIS	138
5.4	Results: Naturally ventilated conditions	139
5.4.1	Structural cooling in the living room	140
5.4.1.1	The effects of thermal mass	141
5.4.1.2	The effects of ratio of opening area to floor area	147
5.4.1.3	The effects of ceiling height	153
5.4.1.4	The effects of window position	157
5.4.1.5	Optimum combination	167
5.4.2	Comfort ventilation in the living room	169
5.4.2.1	The effects of ratio of opening area to floor area	170
5.4.2.2	The effects of ceiling height	175
5.4.2.3	The effects of window position	179
5.4.2.4	Optimum combination	183
5.5	Results: Air-conditioned conditions	185
5.5.1	Effects of structural cooling	185
5.5.1.1	Insulation	187
5.5.1.2	Ceiling height	188
5.5.1.3	Optimum combination	188
5.7	Summary	189
6	Recommendations	193
6.1	Introduction	193
6.2	Proposal of design guidelines for high-rise apartments	193
7	Conclusions	197
6.1	Key findings	197
6.2	Study limitations and further studies	203

Contents

References	205
Appendix A	219
Appendix B	229
Appendix C	237
Appendix D	247
Appendix E	261
Appendix F	273
Appendix G	283

Abstract

Currently, the number of high-rise apartments in Indonesia is increasing and it is projected to be further increasing in the future. As the increasing of high-rise apartments, the energy consumption particularly electricity consumption will be further increasing. The aims of this doctoral thesis are to gather all the fundamental data and information regarding current conditions of existing apartments in Indonesia particularly in the middle-class high-rise apartment and to propose the comprehensive cooling techniques for middle-class high-rise apartments in Indonesia towards energy-saving guidelines. The significance of this research also presented in this chapter.

The review in Chapter 2 particularly focused on the development of passive cooling techniques for the high-rise apartments building in hot-humid climatic regions. As reviewed, there are few studies of passive cooling strategies in apartments in the tropics except for Singapore. Moreover, proper guidelines or regulations and practices of energy-saving apartments particularly through passive cooling strategies are still lack. The existing standards for energy-saving on buildings that rely on the single value of OTTV (for building envelope) alone are not enough in the case of hot-humid climatic regions since ventilation requirements are crucial and important aspect in determining thermal comfort.

Chapter 3 explained the current condition of existing apartments in Indonesia, particularly in the middle-class high-rise apartment. Three types of apartments were selected for in depth field experiments, they are: old public apartment, new public apartment and private apartment. Results of field measurements revealed that under unoccupied condition, old public apartment had better indoor thermal environment compared to two other apartment types. Newly constructed middle-class high-rise apartment are designed on the premise of using air-conditioning. Based on the generalization through computer simulation, it is concluded that it is difficult to achieve thermal comfort without relying on air-conditioning particularly in the middle-class high-rise apartment. Under occupied condition, nocturnal indoor air temperature in the public apartments were higher than that of under unoccupied condition, and even higher than the daytime indoor air temperature under same condition (i.e. unoccupied condition). By using multiple regression analysis, it is found that factors influencing indoor air temperature

in occupied units were physical variables (such as orientation, floor level and window to wall ratio) at the daytime and windows/doors opening behavior at the night-time. Current problems particularly in the middle-class high-rise apartments are the absence of shading devices, lower ventilation rate due to single-side ventilation and uninsulated external wall. Furthermore, potential passive cooling techniques for the middle-class high-rise apartments are proper building orientation, proper shading devices and proper design of thermal buffer zones (such as balcony and corridor spaces).

Chapter 4 explained the some key findings extracted from the field investigation on the one of the vernacular buildings in Indonesia, Dutch colonial buildings. Three Dutch colonial buildings were selected in this study after carefully selecting from hundreds lists of Dutch colonial buildings in Bandung. It is found that daytime indoor air temperatures in Dutch colonial buildings maintained lower than the corresponding outdoors. Indoor thermal comfort evaluation showed that operative temperature exceeded the 80% upper comfortable limit during the daytime. However, thermal comfort in those rooms was improved by increased wind speeds. Thermal comfort survey revealed that as the wind sensation increases due to stronger winds, occupants tend to feel cooler. Passive cooling strategies found in the Dutch colonial buildings are thermal mass, natural ventilation, corridor spaces, high ceiling and permanent openings above windows/doors. Corridor spaces played important roles as thermal buffer zone and shading device as well as encourage cross ventilation for improving wind speed. Meanwhile, high ceiling (5.3-5.7m) contributed in maintaining indoor air temperatures at occupied level (1.1m) at lower values even when windows/doors were open during the daytime.

Chapter 5 discussed the results of a numerical simulation study and proposal of passive cooling attempted guidelines for high-rise apartments. One of the field experiment apartment buildings, i.e. middle-class high-rise apartments, was modelled using the TRNSYS-COMIS and Computational Fluid Dynamics (CFD) STREAM programs. The main objectives of these simulations are to obtain the combination of some parameters including ventilation strategies in structural cooling (i.e. night ventilation) and comfort ventilation (i.e. full-day ventilation). Parametric study under night ventilation and full-day conditions were carried out by varying thermal mass, ceiling height, window positions and ratio of openings area to the total floor area. The results showed that that daytime indoor air temperature would be reduced if thermal mass increased (i.e. 2,000 kg/m²). However, increasing thermal mass caused nocturnal indoor air temperature increasing as well. This increasing could be overcome by increasing ratio of opening area to floor area, in order to allow cool air enter the indoor space from the outdoor. Nevertheless, the window position should be further considered to reduce more indoor air temperature. Upper and lower window position significantly cooled the building structures (i.e. walls, floor and ceiling) and effectively reduced indoor air temperature even during the daytime. Although changing window position would not significantly affect the indoor air temperature, but it reduce indoor wind speed by more than half compared to the previous cases. This is important since some standards such as ASHRAE-55 allowed maximum indoor air velocity not exceeded to 1.2 m/s. Furthermore, ceiling height should be considered to optimize

the indoor air temperature. From the simulation results, the optimum result was obtained when the applying thermal mass of 2,000 kg/m², ratio of opening area to floor area of 0.15, ceiling height of 5.0m, and upper/lower windows at back-side while maintaining central window at windward side (front-side).

Under full-day ventilation condition, simulation results showed that indoor air temperature at daytime are not significantly different amongst all cases. Instead, applying all parameters affected the nocturnal indoor air temperature. However, these effects were diminished due to the air infiltration during the daytime. Meanwhile, the significant results was found in wind speed profiles particularly when upper and lower windows are applied. It reduced more than half of wind speed compared to that when central windows are applied. It is obtained that the unit employing central windows and increasing window opening ratio to floor area significantly increased wind speed, and therefore lowered the SET* values. Hence, it is found that the unit with ratio of opening area to floor area of 0.10 and employing central windows at the both sides enjoyed lower SET* values and larger distribution area of these values during the peak hours regardless ceiling height. Furthermore, the cooling load in air-conditioned room (master bedroom) reduced almost half from the base model (around 43.9%) by applying the combined techniques, i.e. internal insulation and ceiling height of 2.2m. It should be noticed that the unit is facing North/South and the master bedroom applied daytime ventilation while living room applied night ventilation. Moreover, air-conditioning unit is turned on in the night-time only

Chapter 6 discussed recommendation of proposal for design guidelines of energy saving in the middle-class high-rise apartment. For final conclusions, Chapter 7 summarized the main findings of this study and recommended key areas for further studies based on the limitations of this thesis.

Acknowledgements

This thesis was made possible with the greatest continuous support from many people and organizations. First, I sincerely thank my academic advisor, Associate Prof. Tetsu Kubota, for giving me this fine opportunity to complete the thesis at the BUESA laboratory in the Graduate School for International Development and Cooperation of Hiroshima University. Throughout the development of the thesis, Associate Prof. Tetsu Kubota has provided invaluable advice, knowledge, meaningful discussion and exemplary effort not only in the laboratory but also in field work. I wish to thank also my academic co-advisors, Prof. Zhang Junyi and Prof. Haruyuki Yamamoto, together Prof. Daisaku Nishina and Prof. Hansoo Lee for examining my thesis and giving useful comments.

I extend my sincerest gratitude to Indonesia Endowment Fund for Education (LPDP) of the Republic of Indonesia for providing the scholarship, study opportunity and various kinds of support that enabled me to pursue this doctoral degree in Japan. In particular, I would like to thank all of the staff at the institution and university for kindly supporting and granting my application. The work in this thesis would not have been possible without the financial support for the related projects. Research grants by the Nichias Corporation, is gratefully acknowledged. During the course of this study, I am grateful for opportunities that were given through this program to support my field work in Surabaya, Indonesia which is the g-echo Internship Program in summer 2014. I thank the staff of the program and my graduate school for their kind support and assistance.

I wish to thank Dr. Agung Murti Nugroho of University of Brawijaya (UB) Malang and Dr. IGN Antaryama and Dr. Nastiti Ekasiwi of Sepuluh November Institute of Technology (ITS) Surabaya, Dr. Tomoko Uno of Mukogawa Women's University, Hyogo and Dr. Arif Sarwo Wibowo of Bandung Institute of Technology (ITB) Bandung for supporting the research projects. My thanks are extended to the Building Science Laboratory of the Research Institute for Human Settlements (Puskim), Ministry of Public Works of Indonesia, for measuring instruments and field equipment as well as kindly support. Special thanks are due to members of Puskim who have helped in the research work, including Prof. Anita Firmanti, Prof. Arif Sabarudin, Arvi Argyantoro, MA, and Dr. Maryoko Hadi. Special thanks are also due to Dr. Wahyu Sujatmiko, Nugraha Budi Rahardja, MSc and Fefen Suhedi for their valuable advice particularly for measurement methods.

Acknowledgements

Data for the research were invaluable. Our sincerest gratitude is given to municipal governments of Surabaya, East Java, and Bandung, West Java, and the management of PT. PGN (Persero) for giving permission to do field measurements in the existing apartments in Surabaya and Dutch colonial buildings in Bandung. Special thanks are due to Meita Tristida Arethusia, Naoto Hirata, Prima Adi Yudha, Ariono Taftazani, Kanoasa Akbar, Bonita Ratih Permatasari, Takashi Hirose, and Shoi Nozoe for the overwhelmingly support in collecting data through field measurements and field surveys in both Surabaya and Bandung, and analyzing them. I also wish to thanks to the principal and teachers of SMA Negeri 3 Bandung and SMPN 5 Bandung, and also to students of both schools for their participation in the field survey. The list of Dutch colonial buildings in Bandung provided by the Bandung Heritage is invaluable and therefore is greatly appreciated. I am also very grateful for the useful comments given by reviewers of our papers that helped to improve this work. Several professors whom I had the great opportunity to meet during the course of this study are a source of inspiration.

I had the opportunity to work with many fellow students of Hiroshima University in the research projects, including Mohd. Azuan bin Zakaria, Andhang Rakhmat Trihamdhani, Susumu Sugiyama, Toshichika Kusunoki, Masato Morishita, Seiji Abe, Makoto Ohashi, Daiki Kanao, Kento Sumida, and many others who assisted in the field measurement and questionnaire surveys. It was a pleasure to learn together and I thank all of their effort.

I am most indebted to my beloved wife, Puji Rahmawati Nurchayani, for her continuously support, my parents, my siblings and closest family members for their love, encouragement, prayers and support. Above all, I greatly thanks to the Merciful God, Allah SWT, for this blessed life.

List of Figures

Figure 1.1	Global energy consumption in building sectors, including residential and commercial buildings (EIA, 2016)	2
Figure 1.2	Development of middle class in Indonesia from 1999 to 2010 (the World Bank, 2010; ADB, 2011)	3
Figure 1.3	Development of private apartment in Surabaya (Arethusa, 2014)	3
Figure 1.4	Final energy consumption by sector In Indonesia from 1990 to 2009 (Ministry of Energy and Mineral Resources, 2010)	4
Figure 2.1	Framework of passive cooling strategies in energy-efficient buildings (Geetha and Velraj, 2012)	11
Figure 3.1	Views of old public apartments	22
Figure 3.2	Views of new public apartments	22
Figure 3.3	Typical floor plan of unit in (a) old public apartment and (b) new public apartment (Arethusa, 2014)	22
Figure 3.4	(a) Views of private apartments and (b) typical floor plan of unit of private apartment	23
Figure 3.5	(a) Example of layout of <i>Rusunami</i> tower and (b) Example of floor plan of unit in <i>Rusunami</i> (Ministry of Public Works, 2007)	24
Figure 3.6	(a) View of selected old public apartment and (b) floor plan of selected unit	26
Figure 3.7	(a) View of selected new public apartment and (b) floor plan of selected unit	26
Figure 3.8	(a) View of selected middle-class private apartment and (b) floor plan of selected unit	27
Figure 3.9	Instruments for (a) indoor measurement and (b) outdoor measurement	28
Figure 3.10	Components and data transfer in the TRNSYS-COMIS simulation	35
Figure 3.11	(a) Location of the selected unit in the model and (b) front view of the old public apartment. Surfaces in purple are shading objects and their heat transfers are not simulated	35
Figure 3.12	(a) Location of the selected unit in the model and (b) front view of the new public apartment. Surfaces in purple are shading objects and their heat transfers are not simulated	35

Figure 3.13	(a) Location of the selected unit in the model and (b) front view of the middle-class high-rise apartment. Surfaces in purple are shading objects and their heat transfers are not simulated	36
Figure 3.14	Temporal variations of indoor thermal environments in the old public apartment under (a) daytime ventilation and (b) night ventilation conditions	41
Figure 3.15	Temporal variations of indoor thermal environments in the new public apartment under (a) daytime ventilation and (b) night ventilation conditions	42
Figure 3.16	Temporal variations of indoor thermal environments in the middle-class private apartment under (a) daytime ventilation and (b) night ventilation conditions	43
Figure 3.17	Temporal variations of indoor thermal environments in the old public apartment under (a) full-day ventilation) and (b) no ventilation condition	44
Figure 3.18	Temporal variations of indoor thermal environments in the new public apartment under (a) full-day ventilation) and (b) no ventilation condition	45
Figure 3.19	Temporal variations of indoor thermal environments in the middle-class private apartment under (a) full-day ventilation) and (b) no ventilation condition	46
Figure 3.20	Illustration of solar radiation through windows in (a) old public apartment and (b) new public apartment	47
Figure 3.21	Illustration of solar radiation through windows in the middle-class private apartment in (a) master bedroom and (b) living room	47
Figure 3.22	Statistical summary (5 th and 95 th percentile, mean and \pm one standard deviation) of indoor and outdoor air temperatures and relative humidity in old public apartment	48
Figure 3.23	Statistical summary (5 th and 95 th percentile, mean and \pm one standard deviation) of indoor and outdoor air temperatures and relative humidity in the new public apartment	48
Figure 3.24	Statistical summary (5 th and 95 th percentile, mean and \pm one standard deviation) of indoor and outdoor air temperatures and relative humidity in the middle-class private apartment	49
Figure 3.25	Comparison of the statistical summary of indoor and outdoor air temperatures and relative humidity in in the three apartments under (a) daytime ventilation, (b) night ventilation, (c) full-day ventilation and (d) no ventilation conditions	49
Figure 3.26	Vertical distribution if indoor air temperatures in the master bedroom of old public apartment under (a) daytime ventilation, (b) night ventilation, (c) full-day ventilation and (d) no ventilation	50
Figure 3.27	Vertical distribution if indoor air temperatures in the master bedroom of the new public apartment under (a) daytime ventilation, (b) night ventilation, (c) full-day ventilation and (d) no ventilation	51

Figure 3.28	Vertical distribution of indoor air temperatures in the master bedroom of the middle-class high-rise apartment under (a) daytime ventilation, (b) night ventilation, (c) full-day ventilation and (d) no ventilation	52
Figure 3.29	Comparison of the measured and calculated heat flux at the external wall of the master bedroom in (a) new public apartment and (b) middle-class high-rise apartment	53
Figure 3.30	Surface temperature of inside wall in the old public apartment under (a) daytime, (b) night, (c) full-day and (d) no ventilation conditions	53
Figure 3.31	Heat flux of the wall surface in the old public apartment under (a) daytime, (b) night, (c) full-day and (d) no ventilation conditions	53
Figure 3.32	Surface temperature of wall in the new public apartment under (a) daytime, (b) night, (c) full-day and (d) no ventilation conditions	54
Figure 3.33	Heat flux of the wall surface in the new public apartment under (a) daytime, (b) night, (c) full-day and (d) no ventilation conditions	54
Figure 3.34	Surface temperature of wall in the middle-class high-rise apartment under (a) daytime, (b) night, (c) full-day and (d) no ventilation conditions	55
Figure 3.35	Heat flux of the wall surface in the middle-class high-rise apartment under (a) daytime, (b) night, (c) full-day and (d) no ventilation conditions	55
Figure 3.36	Profile of wall surface temperatures using thermal viewer in the old public apartment at (a) daytime and (b) night-time	56
Figure 3.37	Profile of wall surface temperatures using thermal viewer in the new public apartment at (a) daytime and (b) night-time	56
Figure 3.38	Profile of wall surface temperatures using thermal viewer in the middle-class high-rise apartment at (a) daytime and (b) night-time	56
Figure 3.39	Results of air change rate (ACH) calculation using CO ₂ concentration decay method	58
Figure 3.40	Thermal comfort evaluation using adaptive comfort equation in the old public apartment, under (a) daytime ventilation, (b) night ventilation, (c) full-day ventilation and (d) no ventilation	60
Figure 3.41	Thermal comfort evaluation using adaptive comfort equation in the new public apartment, under (a) daytime ventilation, (b) night ventilation, (c) full-day ventilation and (d) no ventilation	61
Figure 3.42	Thermal comfort evaluation using adaptive comfort equation in the middle-class private apartment, under (a) daytime ventilation, (b) night ventilation, (c) full-day ventilation and (d) no ventilation	61
Figure 3.43	Comparison of simulation results and the field experiment results in the old public apartment in (a) master bedroom and (b) corridor space	64
Figure 3.44	Comparison of simulation results and the field experiment results in the new public apartment in (a) master bedroom and (b) living room and (c) corridor space	64
Figure 3.45	Comparison of simulation results and the field experiment results in the middle-class high-rise apartment in (a) master bedroom and (b) living room and (c) corridor space	65

Figure 3.46	Simulation results for indoor thermal environments in (a) old public apartment and (b) new public apartment and (c) middle-class private apartment, under different orientations	66
Figure 3.47	Statistical summary (5 th and 95 th percentile, mean and \pm one standard deviation) of indoor and outdoor air temperatures of master bedrooms in (a) old public apartment, (b) new public apartment and (c) middle-class private apartment, under different orientations	66
Figure 3.48	Simulation results of indoor thermal environments of master bedroom in the old public apartment under different ventilation conditions for (a) east-facing and (b) north-facing orientations	67
Figure 3.49	Simulation results of indoor thermal environments of master bedroom in the new public apartment under different ventilation conditions for (a) east-facing and (b) north-facing orientations	67
Figure 3.50	Simulation results of indoor thermal environments of master bedroom in the middle-class private apartment under different ventilation conditions for (a) east-facing and (b) north-facing orientations	68
Figure 3.51	Statistical summary (5 th and 95 th percentile, mean and \pm one standard deviation) of indoor and outdoor air temperatures of master bedrooms in in the three apartments under (a) daytime ventilation, (b) night ventilation, (c) full-day ventilation and (c) no ventilation	68
Figure 3.52	Thermal comfort evaluation in the three apartments in east-facing unit under (a) daytime ventilation and (b) night ventilation conditions based on computer simulation	69
Figure 3.53	Thermal comfort evaluation in the three apartments in north-facing unit under (a) daytime ventilation and (b) night ventilation conditions based on computer simulation	69
Figure 3.54	Mean temporal variation of air temperature in the old public apartment in (a) daytime ventilated units and (b) night-ventilated and full-day ventilated units	72
Figure 3.55	Mean temporal variation of air temperature in the new public apartment in (a) daytime ventilated units and (b) night-ventilated and full-day ventilated units	72
Figure 3.56	Thermal comfort evaluation using adaptive comfort equation in (a) old public apartment and (b) new public apartment under occupied condition	74
Figure 3.57	Results of multiple regression analysis for indoor air temperature using enter method	77
Figure 3.58	Problem of single-sided ventilation in the middle-class private apartment	79
Figure 3.59	Problem of uninsulated external wall for the middle-class private apartment	79
Figure 3.60	Heat flow in the three apartments based on the simulation results under daytime ventilation condition at east-facing unit in (a) old public apartment, (b) new public apartment and (c) middle-class private apartment	81

Figure 4.1	Timeline of colonial architecture in Indonesia	87
Figure 4.2	Case study buildings: (a) Views of Case study 1, (b) Floor plan of Case study 1 and (c) Floor plan and section of selected rooms (Room 1-1 and Room 1-2)	89
Figure 4.3	Louver windows and ventilation openings above windows/door	89
Figure 4.4	Case study buildings: (a) Views of Case study 2, (b) Floor plan of Case study 2 and (c) Floor plan and section of selected room (Room 2-1)	90
Figure 4.5	Case study buildings: (a) Views of Case study 3, (b) Floor plan of Case study 3 and (c) Floor plan and section of selected rooms (Room 3-1 and 3-2)	91
Figure 4.6	Measurement setting in (a) class room, (b) corridor space and (c) outdoor	92
Figure 4.7	Temporal variations of thermal parameters in Case study 1 (a) Room 1-1 (ground floor) and (b) Room 1-2 (first floor)	94
Figure 4.8	Statistical summary (5% percentile, average, 95 percentile and average \pm standard deviation) of air temperatures in (a) Room 1-1 and (b) Room 1-2 under different ventilation conditions	94
Figure 4.9	Surface temperature of walls, floor and ceiling in the Case study 1	95
Figure 4.10	Correlation of indoor, corridor space and outdoor air temperature in Case study 1 for (a) ground floor (Room 1-1) and (b) first floor (Room 1-2)	96
Figure 4.11	Solar radiation of the ground floor and the first floor in the Case study 1, (a) including outdoor solar radiation and (b) excluding outdoor solar radiation	96
Figure 4.12	Vertical distribution of indoor air temperature in Case study 1 under (a) daytime ventilation and (b) night ventilation conditions	97
Figure 4.13	Thermal comfort evaluation using adaptive comfort evaluation and SET* in (a) Room 1-1 (ground floor) and (b) Room 1-2 (first floor) ...	99
Figure 4.14	Results of thermal comfort survey in Case study 1, (a) Thermal perception, (b) Humidity perception and (c) Wind speed perception ...	100
Figure 4.15	Mann-Whitney U test results for comparing the significant difference between (a) GF and 1F, (b) GF-Morning and 1F-Morning, (c) GF-Afternoon and 1F-Afternoon, (d) GF-Morning and GF-Afternoon and (e) GF-Afternoon and 1F-Afternoon	101
Figure 4.16	Relationship between thermal sensation and wind sensation in Rooms 1-1 and 1-2	102
Figure 4.17	Temporal variations of thermal parameters in Case study 2 (Room 2-1)	103
Figure 4.18	Statistical summary (5% percentile, average, 95 percentile and average \pm standard deviation) of air temperatures in Case study 2 (Room 2-1) under different ventilation conditions	104
Figure 4.19	Illustration of solar radiation through the window in Case study 2 (Room 2-1)	104

Figure 4.20	Solar radiation of the ground floor and the first floor in the Case study 2, (a) including outdoor solar radiation and (b) excluding outdoor solar radiation	105
Figure 4.21	Surface temperature of walls, floor and ceiling in the Case study 2 (Room 2-1)	105
Figure 4.22	Solar radiation of the ground floor and the first floor in the Case study 2, (a) including outdoor solar radiation and (b) excluding outdoor solar radiation	106
Figure 4.23	Vertical distribution of indoor air temperatures in Case study 2 for (a) daytime ventilation and (b) night ventilation conditions	107
Figure 4.24	Thermal comfort evaluation using adaptive comfort evaluation and SET* in the Case study 2 (Room 2-1)	108
Figure 4.25	Temporal variations of thermal parameters in Case study 3 under (a) daytime ventilation, (b) night ventilation, (c) full-day ventilation and (d) no ventilation	109
Figure 4.26	Statistical summary (5% percentile, average, 95 percentile and average \pm standard deviation) of air temperatures in Case study 3, (a) Room 3-1 and (b) Room 3-2, under different ventilation conditions	110
Figure 4.27	Surface temperatures of walls, floor and ceiling in the Room 3-2 under (a) night ventilation, (b) daytime ventilation, (c) full-day ventilation and (d) no ventilation conditions	110
Figure 4.28	Correlation between corridor space, indoor and outdoor air temperatures in (a) Case 1 and (b) Case 2 under different ventilation conditions	111
Figure 4.29	Vertical distribution of indoor air temperatures in Case study 3 building under (a) daytime ventilation and (b) night ventilation conditions	112
Figure 4.30	Thermal comfort evaluation using adaptive comfort evaluation and SET* in Case study 3 building under (a) daytime ventilation, (b) night ventilation, (c) full-day ventilation and (d) no ventilation conditions ...	113
Figure 4.31	Average wind speeds of indoor, corridor and outdoor spaces at daytime and night-time in Case study 1	115
Figure 5.1	Main components and structures of the CFD STREAM (Cradle, 2015)	121
Figure 5.2	Flowchart of simulation in the CFD STREAM (Cradle, 2015)	123
Figure 5.3	Computational domain for CFD simulation	123
Figure 5.4	Flowchart of STsolver in STREAM	125
Figure 5.5	Model of middle-class apartment for CFD simulation in (a) Google SketchUp and (b) Preprocessor (STpre)	126
Figure 5.6	Comparison between the measured and calculated global horizontal solar radiation under (a) no ventilation, (b) full-day ventilation and (c) night ventilation conditions	129
Figure 5.7	View of meshing division in (a) object and computational domain, (b) middle-class private apartment model and (c) connected regions in model	131

Figure 5.8	Validation results of indoor air temperature and relative humidity in (a) master bedroom, (b) living room and (c) corridor space under no ventilation condition	132
Figure 5.9	Validation results of indoor wind speed including and excluding outdoor wind speed in (a) master bedroom, (b) living room and (c) corridor space under no ventilation condition	132
Figure 5.10	Validation results of indoor air temperature and relative humidity in (a) master bedroom, (b) living room and (c) corridor space under full-day ventilation condition	133
Figure 5.11	Validation results of indoor wind speed including and excluding outdoor wind speed in (a) master bedroom, (b) living room and (c) corridor space under full-day ventilation condition	133
Figure 5.12	Validation results of indoor air temperature and relative humidity in (a) master bedroom, (b) living room and (c) corridor space under night ventilation condition	134
Figure 5.13	Validation results of indoor wind speed including and excluding outdoor wind speed in (a) master bedroom, (b) living room and (c) corridor space under night ventilation condition	135
Figure 5.14	3D model for simulation, (a) front view, (b) front view with the surrounding, (c) back view and (d) back view with the surrounding	137
Figure 5.15	(a) 3D view of base model in Preprocessor, and view of meshing division in (a) object and computational domain, (b) middle-class private apartment model and (c) connected regions in model	137
Figure 5.16	Comparison of simulation results of indoor air temperature at 1.1m above floor under different thermal masses	141
Figure 5.17	View of distribution of indoor air temperature (left: y-axis at 1.4m, right: z-axis at 1.1m) at thermal mass of (a) 1,000 kg/m ² and (b) 2,000 kg/m ² during daytime (14:00)	142
Figure 5.18	View of distribution of indoor air temperature (left: y-axis at 1.4m, right: z-axis at 1.1m) at thermal mass of (a) 1,000 kg/m ² and (b) 2,000 kg/m ² during night-time (02:00)	142
Figure 5.19	Comparison of simulation results of indoor wind speed at 1.1m above floor under different thermal mass	143
Figure 5.20	View of distribution of indoor wind speed (left: y-axis, right: z-axis) at thermal mass of (a) 1,000 kg/m ² and (b) 2,000 kg/m ² during daytime (14:00)	144
Figure 5.21	View of distribution of indoor wind speed (left: y-axis, right: z-axis) at thermal mass of (a) 1,000 kg/m ² and (b) 2,000 kg/m ² during night-time (21:00)	144
Figure 5.22	Comparison of surface temperature of walls, floor and ceiling under different thermal masses at ceiling height of 3.0m	145
Figure 5.23	Comparison of surface temperature of walls, floor and ceiling under different thermal masses at ceiling height of 5.0m	146
Figure 5.24	View of surface temperature of walls, floor and ceiling at the peak hour (14:00) at thermal mass of (a) 1,000 kg/m ² and (b) 2,000 kg/m ² ...	147

Figure 5.25	View of surface temperature of walls, floor and ceiling at the night-time (02:00) at thermal mass of (a) 1,000 kg/m ² and (b) 2,000 kg/m ² ...	147
Figure 5.26	Comparison of simulation results of indoor air temperature at 1.1m above floor under different ratio of opening area to floor area	148
Figure 5.27	View of distribution of indoor air temperature (left: y-axis at 1.4m, right: z-axis at 1.1m above floor) at opening ratio of (a) 0.05 and (b) 0.15 during daytime (14:00)	149
Figure 5.28	View of distribution of indoor air temperature (left: y-axis at 1.4m, right: z-axis at 1.1m above floor) at opening ratio of (a) 0.05 and (b) 0.15 during night-time (02:00)	149
Figure 5.29	Comparison of simulation results of indoor wind speed at 1.1m above floor under different ratio of opening area to floor area	150
Figure 5.30	View of distribution of indoor wind speed (left: y-axis, right: z-axis) at opening ratio of (a) 0.05 and (b) 0.15 during night-time (21:00)	150
Figure 5.31	Comparison of surface temperature of walls, floor and ceiling under different ratios of opening area to floor area at ceiling height of 3.0m ..	151
Figure 5.32	View of surface temperature of walls, floor and ceiling during the daytime (14:00) at opening ratios of (a) 0.05 and (b) 0.15	152
Figure 5.33	View of surface temperature of walls, floor and ceiling during the night-time (02:00) at opening ratios of (a) 0.05 and (b) 0.15	152
Figure 5.34	Comparison of simulation results of indoor air temperature at 1.1m above floor under different ceiling heights	153
Figure 5.35	View of distribution of indoor air temperature (left: y-axis at 1.4m, right: z-axis at 1.1m above floor) at the ceiling heights of (a) 3.0m and (b) 5.0m at the peak hour (14:00)	154
Figure 5.36	View of distribution of indoor air temperature (left: y-axis at 1.4m, right: z-axis at 1.1m above floor) at the ceiling heights of (a) 3.0m and (b) 5.0m at the peak hour (14:00)	154
Figure 5.37	Comparison of simulation results of indoor wind speed at 1.1m above floor under different ceiling heights	155
Figure 5.38	View of indoor wind flow (y-axis) at ceiling height of (a) 0.05 and (b) 0.15 at the night-time (21:00)	155
Figure 5.39	Comparison of surface temperature of walls, floor and ceiling under different ceiling height at ratio of opening area to floor area of 0.05 ...	156
Figure 5.40	Comparison of surface temperature of walls, floor and ceiling under different ceiling heights at ratio of opening area to floor area of 0.15 ...	157
Figure 5.41	View of surface temperature of walls, floor and ceiling at the ceiling heights of (a) 3.0m and (b) 5.0m during daytime (14:00)	157
Figure 5.42	View of surface temperature of walls, floor and ceiling at the ceiling heights of (a) 3.0m and (b) 5.0m during night-time (02:00)	158
Figure 5.43	Comparison of simulation results of indoor air temperature at 1.1m above floor under different window positions	159
Figure 5.44	View of indoor air temperature (y-axis) at the peak hour (14:00) in the unit applying (a) central window and (b) upper and lower window at back-side	159

Figure 5.45	View of indoor air temperature (y-axis) at the night-time (02:00) in the unit applying (a) central window and (b) upper and lower window at back-side	160
Figure 5.46	Comparison of simulation results of indoor wind speed at 1.1m above floor under different window positions	160
Figure 5.47	View of indoor wind speed pattern (y-axis) at the unit with (a) central windows and (b) upper/lower windows at the night-time (21:00)	161
Figure 5.48	Comparison of surface temperature of walls, floor and ceiling under different window positions at ceiling height of 3.0m	161
Figure 5.49	Comparison of surface temperature of walls, floor and ceiling under different window positions at ceiling height of 5.0m	162
Figure 5.50	View of surface temperature of walls, floor and ceiling in the unit with (a) central window (b) upper and lower window at the peak hour (14:00)	163
Figure 5.51	View of surface temperature of walls, floor and ceiling in the unit with (a) central window (b) upper and lower window at the night-time (02:00)	163
Figure 5.52	Comparison of indoor air temperature in the unit with (a) central windows at both sides, (b) upper/lower windows at back-side, (c) upper/lower windows at front side and (d) upper/lower at both sides ...	164
Figure 5.53	View of indoor air temperature profiles (y-axis) during the daytime (14:00) in unit employs (a) central windows at both sides, (b) upper/lower windows at back-side, (c) upper/lower windows at front side and (d) upper/lower at both sides	164
Figure 5.54	View of indoor air temperature profiles (y-axis) at the night-time (02:00) in the unit with (a) central windows at both sides, (b) upper/lower windows at back-side, (c) upper/lower windows at front side and (d) upper/lower at both sides	165
Figure 5.55	Comparison of indoor wind speed in the unit with (a) central windows at both sides, (b) upper/lower windows at back-side, (c) upper/lower windows at front side and (d) upper/lower at both sides	165
Figure 5.56	View of indoor wind flow pattern at the night-time (21:00) in the unit with (a) central windows at both sides, (b) upper/lower windows at back-side, (c) upper/lower windows at front side and (d) upper/lower at both sides	166
Figure 5.57	View of surface temperatures of walls, floor and ceiling at the peak hour (14:00) in the unit with (a) central windows at both sides, (b) upper/lower windows at back-side, (c) upper/lower windows at front side and (d) upper/lower at both sides	167
Figure 5.58	View of surface temperatures of walls, floor and ceiling at the night-time (21:00) in the unit with (a) central windows at both sides, (b) upper/lower windows at back-side, (c) upper/lower windows at front side and (d) upper/lower at both sides	167
Figure 5.59	Profiles of (a) air temperature and (b) wind speed in indoor space and balcony in Case 16	169

List of Figures

Figure 5.60	Profiles of surface temperatures of (a) south- and north-wall (b) west- and east-wall and (c) floor and ceiling in Case 16	169
Figure 5.61	Comparison of indoor air temperature under different ratios of opening area to floor area for full-day ventilation condition	171
Figure 5.62	Comparison of indoor relative humidity under different ratios of opening area to floor area for full-day ventilation condition	171
Figure 5.63	View of distribution of indoor air temperature (left: y-axis, right: z-axis at 1.1m) at opening ratios of (a) 0.05 and (b) 0.10 at the peak hour (14:00)	172
Figure 5.64	View of distribution of indoor air temperature (left: y-axis, right: z-axis at 1.1m) at opening ratios of (a) 0.05 and (b) 0.10 at the night-time (21:00)	172
Figure 5.65	Comparison of indoor air temperature under different ratios of opening area to floor area for full-day ventilation condition	173
Figure 5.66	View of wind flow pattern (left: y-axis, right: z-axis at 1.1m) at opening ratios of (a) 0.05 and (b) 0.10 at the peak hour (14:00)	173
Figure 5.67	View of wind flow pattern (left: y-axis, right: z-axis at 1.1m) at opening ratios of (a) 0.05 and (b) 0.10 at the night-time (21:00)	174
Figure 5.68	View of MRT values (left: y-axis, right: z-axis at 1.1m above floor) at opening ratios of (a) 0.05 and (b) 0.10 at the peak hour (14:00)	174
Figure 5.69	View of SET* patterns (left: y-axis, right: z-axis at 1.1m above floor) at opening ratios of (a) 0.05 and (b) 0.10 at the peak hour (14:00)	175
Figure 5.70	View of SET* patterns (left: y-axis, right: z-axis at 1.1m above floor) at opening ratios of (a) 0.05 and (b) 0.10 at the night-time (21:00)	175
Figure 5.71	Comparison of indoor air temperature under different ceiling heights for full-day ventilation condition	177
Figure 5.72	Comparison of indoor relative humidity under different ceiling heights for full-day ventilation condition	177
Figure 5.73	View of distribution of indoor air temperature (left: y-axis, right: z-axis at 1.1m) at ceiling heights of (a) 3.0m and (b) 5.0m at the peak hour (14:00)	178
Figure 5.74	Comparison of indoor wind speed under different ceiling heights for full-day ventilation condition	178
Figure 5.75	View of wind flow pattern (left: y-axis, right: z-axis at 1.1m) at ceiling heights of (a) 3.0m and (b) 5.0m at the peak hour (14:00)	179
Figure 5.76	View of MRT values (left: y-axis, right: z-axis at 1.1m above floor) at ceiling heights of (a) 3.0m and (b) 5.0m at the peak hour (14:00)	179
Figure 5.77	View of SET* values (left: y-axis, right: z-axis at 1.1m above floor) at ceiling heights of (a) 3.0m and (b) 5.0m at the peak hour (14:00)	180
Figure 5.78	Comparison of indoor air temperature under different window positions for full-day ventilation condition	181
Figure 5.79	Comparison of indoor relative humidity under different window positions for full-day ventilation condition	181

Figure 5.80	View of distribution of indoor air temperature (left: y-axis, right: z-axis at 1.1m) in the unit with (a) central windows and (b) upper/lower windows at the peak hour (14:00)	182
Figure 5.81	Comparison of indoor wind speed under different window positions for full-day ventilation condition	182
Figure 5.82	View of wind flow pattern (left: y-axis, right: z-axis at 1.1m) in the unit with (a) central windows and (b) upper/lower windows at the peak hour (14:00)	183
Figure 5.83	View of MRT values (left: y-axis, right: z-axis at 1.1m) in the unit with (a) central windows and (b) upper/lower windows at the peak hour (14:00)	183
Figure 5.84	View of wind flow pattern (left: y-axis, right: z-axis at 1.1m) in the unit with (a) central windows and (b) upper/lower windows at the peak hour (14:00)	184
Figure 5.85	Views of (a) MRT and (b) SET* values (left: y-axis, right: z-axis at 1.1m) in the unit with central windows at both sides, opening ratio of 0.10 and ceiling height of 5.0m	186
Figure 5.86	Cooling load in master bedroom under different combination of ventilation conditions of master bedroom and living room	187
Figure 5.87	Cooling load in master bedroom under different orientations	187
Figure 5.88	Installation of (a) internal insulation and (b) external insulation	188
Figure 5.89	Simulation results of cooling load for insulation applications in master bedroom	189
Figure 5.90	Simulation results of cooling load for different ceiling heights in master bedroom	190
Figure 5.91	Simulation results of cooling load for combined techniques in master bedroom	190
Figure 6.1	Comfort requirements and proposed design guidelines for (a) living room and (b) master bedroom during the night-time	194
Figure 6.2	Comfort requirements and proposed design guidelines for (a) living room and (b) master bedroom during the daytime	195

List of Tables

Table 2.1	Proposed adaptive thermal comfort equation and related criteria for naturally ventilated buildings in hot-humid climate	15
Table 2.2	Vernacular passive cooling techniques in hot-humid climatic regions from previous studies	17
Table 2.3	Passive cooling techniques of the high-rise apartments in hot-humid climatic regions from previous studies	20
Table 3.1	Description of measurement instruments used in the selected apartments	29
Table 3.2	Thermal properties of the building materials in the base models	37
Table 3.3	Constructional layers and reference U-values of the base models	38
Table 3.4	Flow coefficients and flow exponents of the base model. Note: Selected data from Orme and Leksmono, 2002	39
Table 3.5	The simulation test cases and their test conditions	39
Table 3.6	Windows/doors opening conditions for the adjacent rooms of master bedroom for the CO ₂ measurement	59
Table 3.7	Measured air change rates in master bedrooms	59
Table 3.8	Results of thermal comfort evaluation using adaptive comfort equation under different ventilation conditions	62
Table 3.9	Summary of statistical error tests of the base model under no ventilation condition	65
Table 3.10	Results of adaptive thermal comfort evaluation in the master bedroom under different ventilation conditions based on the simulation results	70
Table 3.11	Profile of measured units	71
Table 3.12	Summary of household size and indoor air temperatures (descending order of mean indoor air temperature)	73
Table 3.13	Variables used in Multiple Regression Analysis (MRA)	75
Table 3.14	Results of multiple regression analysis for indoor air temperature using step-wise method (n=32)	76
Table 4.1	Description of measurement instruments used in the selected rooms ..	92
Table 4.2	Summary of indoor thermal environments in Case study 1 during thermal comfort survey	98

List of Tables

Table 4.3	Results of adaptive comfort evaluation in Case study 1 building under different ventilation conditions	99
Table 4.4	Results of adaptive comfort evaluation in Case study 2 building under different ventilation conditions	108
Table 4.5	Results of adaptive comfort evaluation in Case study 3 building under different ventilation conditions	114
Table 5.1	Thermal properties of the building materials in the base models	126
Table 5.2	Surface film coefficient (ASHRAE, 2013)	128
Table 5.3	Typical values of ground reflectance of foreground surfaces (ASHRAE, 2013)	128
Table 5.4	Summary of statistical error tests of the validation results	135
Table 5.5	Case designs for CFD simulation for naturally ventilated living room	138
Table 5.6	Case designs for ventilation conditions in the master bedroom	139
Table 5.7	Case designs for simulation of the air-conditioned master bedroom ...	139
Table 5.8	Simulation cases for structural cooling in the living room	138
Table 5.9	Additional simulation test cases based on the different window positions	163
Table 5.10	Summary of the simulation results of indoor air temperatures and wind speeds for structural cooling (night ventilation) in the living room	168
Table 5.11	Simulation cases for comfort ventilation in the living room	170
Table 5.12	Summary of the simulation results of indoor air temperatures, relative humidity and wind speeds for comfort ventilation (full-day ventilation) in the living room	185
Table 5.13	Summary of the simulation results of indoor MRT, PMV and SET* for comfort ventilation (full-day ventilation) in the living room	185
Table 6.1	Proposal of design guidelines for high-rise apartment buildings in hot-humid climate of Indonesia	196

List of Acronyms

ACH	Air changes per hour
ACS	Adaptive Comfort Standard
ADB	Asian Development Bank
ASHRAE	American Society of Heating, Refrigerating and Air-Conditioning Engineers
BAPPENAS	<i>Badan Perencanaan Pembangunan Nasional</i> (Agency for National Development Planning)
BP	British Petroleum
BPS	<i>Badan Pusat Statistik</i> (Center for Statistic Agency)
BSI	British Standards Institute
BUESA	Building and Urban Environmental Science in Asia
CFD	Computational Fluid Dynamics
CO₂	Carbon dioxide
COMIS	Conjunction of Multi-zone Infiltration Specialists
EIA	US Energy Information Administration
EN	European Norms
ET	Effective Temperature
ET*	New Effective Temperature
GHG	Greenhouse Gas
Gt	Giga Ton
HVAC	Heating, ventilating and air-conditioning
IEA	International Energy Agency
IMF	International Monetary Fund
IPCC	Intergovernmental Panel on Climate Change
ISO	International Organization for Standardization
LBL	Lawrence Berkeley National Laboratory
LR	Living Room
MB	Master Bedroom
MBE	Mean Bias Error
MRT	Mean Radiant Temperature
OT	Operative Temperature

List of Acronyms

OTTV	Overall Thermal Transfer Value
PCM	Phase Change Material
PMV	Predicted Mean Vote
RH	Relative humidity
RMSE	Root Mean Square Error
<i>Rusunami</i>	<i>Rumah Susun Sederhana Milik</i> (Owned Simple Subsidized High-rise Apartment)
<i>Rusunawa</i>	<i>Rumah Susun Sederhana Sewa</i> (Rented Simple Subsidized Low-rise Apartment)
SET*	Standard Effective Temperature
SF	Shading Factor
SMAN	<i>Sekolah Menengah Atas Negeri</i> (National Senior High School)
SMPN	<i>Sekolah Menengah Pertama Negeri</i> (National Junior High School)
SNI	<i>Standar Nasional Indonesia</i> (Indonesia National Standard)
TMY	Typical meteorological year
TRNSYS	Transient Systems Simulation Program
UNEP	United Nations Environment Program
UNFCCC	United Nations Framework Convention on Climate Change
US	United States of America
USD	US Dollar
VF	View Factor

Nomenclature

A	Area (m^2)
a	Y-intercept in regression model (-)
b	Slope in regression model (-)
C	Courant number
C_0	Concentration of gas at initial condition (ppm)
C_a	Concentration of gas at the outdoor (ppm)
C_p	Specific heat at constant pressure (J/kg.K)
C_Q	Volume flow coefficient (m^3/sPa^n)
$C(t)$	Concentration of gas at final condition (ppm)
g_i	Gravity (m/s^2)
h	Sun altitude (rad)
h_t	Heat transfer coefficient ($\text{W/m}^2\text{K}$)
J_c	Solar radiation from cloud ($\text{W/m}^2\text{K}$)
J_d	Direct solar radiation ($\text{W/m}^2\text{K}$)
J_r	Reflected solar radiation ($\text{W/m}^2\text{K}$)
J_s	Sky solar radiation ($\text{W/m}^2\text{K}$)
J_t	Global solar radiation on horizontal face (W/m^2)
J_0	Solar constant ($1,330 \text{ W/m}^2$)
K	Thermal conductivity ($\text{W/m}^2\text{K}$)
k	Turbulent kinetic energy (m^2/s^3)
L_{im}	i th measured value (unit of the variable)
L_{is}	i th simulated value (unit of the variable)
LR	Ratio of convective and evaporative heat transfer coefficient (dimensionless)
n	Flow exponent (-)
N	Total number of observations or data pairs (-)
P	Atmospheric transmissivity (dimensionless)
p	Pressure of fluid (N/m^2)
p_a	Barometric pressure (kPa)

Nomenclature

p_{ET^*}	Saturated vapor pressure at new effective temperature (kPa)
Q	Volume flow (m ³ /s)
\dot{Q}	Energy or heat flow (W)
R^2	Coefficient of determination (-)
RH	Relative humidity (%)
T_a	Air temperature (°C)
T_g	Globe temperature (°C)
T_{op}	Operative temperature (°C)
T_{out}	Outdoor temperature (°C)
\bar{T}_r	Mean radiant temperature (°C)
T_{comf}	Indoor comfort temperature (°C)
T_{lower}	Lower comfort operative temperature limit (°C)
T_{neutop}	Indoor neutral operative temperature (°C)
T_{outdm}	Daily mean outdoor air temperature (°C)
T_{outmm}	Monthly mean outdoor air temperature (°C)
T_w	Wall surface temperature (°C)
t	Time (second)
T_{upper}	Upper comfort operative temperature limit (°C)
v	Indoor air speed (m/s)
w_{im}	Skin wittedness (dimensionless)
x	Independent variable in regression model (unit of the variable)
x_i	X-axis coordinate in the object coordinate system (-)
y	Dependent variable in regression model (unit of the variable)
ΔL	Element size (m)
ΔP	Pressure difference (Pa)
Δt	Time step (s)

Greek letter

λ	Air change rate (times/hour)
μ	Viscosity of fluid (kg/ms)
ρ	Density of fluid (kg/m ³)
β	Thermal expansion coefficient (1/K)
ε	Dissipation rate (m ² /s ³)
σ	Stress tensor (dimensionless)
σ_r	Reflectance of ground or foreground surface (dimensionless)

List of Publications

Referred Journal and Book Chapter

Alfata, MNF, N. Hirata, T. Kubota, AM. Nugroho, T. Uno, IGN. Antaryama, and SNN. Ekasiwi, 2015: Thermal Comfort in Naturally Ventilated Apartments in Surabaya, Indonesia. *Procedia Engineering*, 121, 459-467.

Alfata, MNF, N. Hirata, T. Kubota, AM. Nugroho, T. Uno, SNN. Ekasiwi and IGN Antaryama, 2015: Field investigation of Indoor Thermal Environments in Apartments of Surabaya, Indonesia: Potential Passive Cooling Strategies for Middle-class Apartments. *Energy Procedia*, 78, 2947-2952.

Wibowo, AS., MNF **Alfata** and T. Kubota, 2018 (*in press*): Indonesia: Dutch Colonial Buildings. *Sustainable Houses and Living in the Hot-Humid Climates of Asia*. Springer.

Kubota, T., MNF. **Alfata**, MT. Arethusa, T. Uno, IGN. Antaryama, SNN. Ekasiwi and AM. Nugroho, 2018 (*in press*): Indoor Thermal Environments in Apartments of Surabaya, Indonesia. *Sustainable Houses and Living in the Hot-Humid Climates of Asia*. Springer.

Referred Conference Papers

Alfata, MNF, T. Hirose and T. Kubota. Field Investigation of Indoor Thermal Environments of Dutch Colonial Buildings in Bandung, Indonesia: Potential of Passive Cooling Strategies. *ISAIA 2016*, Japan.

Alfata, MNF, T. Kubota and AS. Wibowo, 2017: The effects of veranda space on indoor thermal environments in Dutch colonial buildings in Bandung, Indonesia. *PLEA 2017 Conference*, Volume III, 3858-3865.

Non-Referred Conference Papers

Hirata, N., MNF **Alfata**, T. Kubota. and Uno, T. (2015). Thermal Environment of Apartments for Middle Class in Surabaya. Summary of Technical Papers of Annual Meeting, AIJ, September 4-6, Tokai, Japan.

Alfata, MNF, N. Hirata, T. Hirose, and T. Kubota. Analysis of Passive Cooling Strategies Employed in Dutch Colonial Buildings in Indonesia. *AIJ 2016, Japan*.

1

Introduction

Currently, there is little need to justify the drive to minimize the use of energy in our daily life. Global warming and climate change have become main issues in our society, in addition to the scarcity of energy resources due to the increase in energy consumption and the depletion of energy production. In face of the above issues, the excessive use of energy from fossil fuels becomes a main concern. Motivation may now have moved from reducing costs and saving scarce resources towards minimizing carbon dioxide emissions. There are at least three pathways to reduce energy consumption: lower the demand and use less energy, more efficient use of energy and substitute fossil fuels with renewable energy sources. This thesis takes the first pathway as a fundamental approach towards energy-saving in buildings, focusing on cooling strategies to achieve indoor comfort needs.

1.1 Backgrounds

Nowadays, worldwide energy consumption increased rapidly as reported by BP (2017), and it is projected that world energy consumption would rise by 28% between 2015 and 2040 (EIA, 2016). Today, buildings are responsible for more than 40% of global energy consumption, and as much as one third of global greenhouse gas emissions, both in developed and developing countries (UNEP, 2009). Energy use in buildings is projected to increase by 32% between 2015 and 2040 while electricity use grows 2% annually by 2040 as shown in Figure 1.1 (EIA, 2016).

Buildings are known as major energy consumers. Their operational energy is commonly supplied in the form of electricity which is generated from fossil fuels. IPCC (2014) reported that greenhouse gas (GHG) emissions from the building sector have more than doubled since 1970 to reach 9.18 GtCO₂-eq in 2010, representing 19% of all global 2010 GHG emissions. Most of GHG emissions (6.02 Gt) are indirect CO₂ emissions from electricity use in buildings, and these emissions have shown dynamic growth in contrast to direct emissions, which have roughly stagnated over the last four decades. Furthermore, around 32-34% of the global final

energy consumption in both residential and commercial buildings were used for room air-conditioning (i.e. space heating and cooling). IPCC (2014) also estimated that heating and cooling energy use in residential and commercial buildings will grow by 79% and 83%, respectively, over the period 2010-2050. In residential buildings, both the growing number of households and the floor area per household tend to increase energy consumption. However, the building sector has the largest potential in reducing greenhouse gas emissions compared to the other major emitting sectors (UNEP, 2009).

Due to the vulnerability of land and living to the impacts of climate change, the Paris Agreement proposed to keep the increase in global average temperature below 2°C above pre-industrial levels and to pursue efforts to limit the temperature increase by 1.5°C above pre-industrial levels after 2020. This agreement implies that reduction of CO₂ emissions is necessary to achieve the above targets. Therefore, some mitigation strategies across sectors, particularly in the sectors that heavily depend on fossil fuel are necessary.

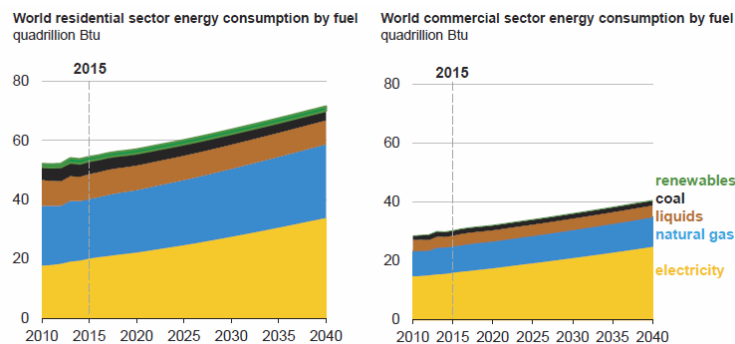


Figure 1.1. Global energy consumption in building sectors, including residential and commercial buildings (EIA, 2016)

1.1.1 Development of middle class and apartments in Indonesia

Indonesia is the fourth most populous nation with more than 250 million people in 2014. It is projected that Indonesian population will reach more than 305 million people in 2035, with around 78% of them will concentrate in the Java island. The percentage of people living in urban areas is predicted to increase from about 49.8% in 2010 to 66.6% in 2035 (McDonald, 2014; Bappenas *et al.*, 2014). In addition, Indonesia has been experiencing high economic growth in recent years with the relatively stable growth rates of around 6.1-6.5% (The World Bank, 2012). The nationwide per capita income increased more than five times from around USD 600 in 2000 to around USD 3,500 in 2013, and it is projected to see higher economic growth in the future (IMF, 2014). Indonesia also aims to earn its place as one of the world’s developed countries by 2025 with expected per capita income of USD 14,250-15,500, and will further increase to USD 44,500-49,000 by 2045 (Coordinating Ministry for Economic Affairs, 2011). The increase in both population and economic growth in Indonesia bring the consequences to the rise of middle-class in Indonesia. As the World Bank defines, the

Government of Indonesia also defines the middle-class people as those who have daily expenditures between US\$ 2 and US\$ 20. In particular, for the ownership of subsidized middle-class high-rise apartments, a monthly income-based definition is used by the government. In this case, middle-class people is defined as those who earn monthly income from IDR 4,500,000 to 7,000,000 (or around USD 350-540) (Ministry of Finance, 2015). Meanwhile, lower class and lower middle class are defined as those who have monthly income of up to IDR 2,500,000 (or USD 190) and from IDR 2,500,000 to 4,500,000 (or USD 190-350), respectively (Ministry of Public Works, 2007). Figure 1.2 shows that Indonesian middle-class population (defined by daily expenditure) increased more than doubled over the ten years from 1999 to 2010 (ADB, 2010; The World Bank, 2011), and it is predicted that the emerging middle class will reach up to 141 million people and 16.5 million people will be affluent by 2020 (Rostogi *et al.*, 2013). Based on the continued strong growth and current distribution patterns, more people will enter the upper segments of the middle income over the next few decades (The World Bank, 2011).

The rise of middle class is likely to make significant impacts on the structure of the economy, particularly in terms of demands of consumers towards durable and luxurious items such as houses. Due to the rise of middle-class in Indonesia, it is expected that the housing

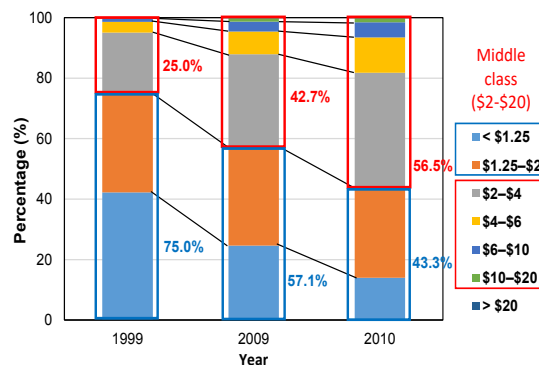


Figure 1.2. Development of middle class in Indonesia from 1999 to 2010 (the World Bank, 2010; ADB, 2011)

(a) Private apartments

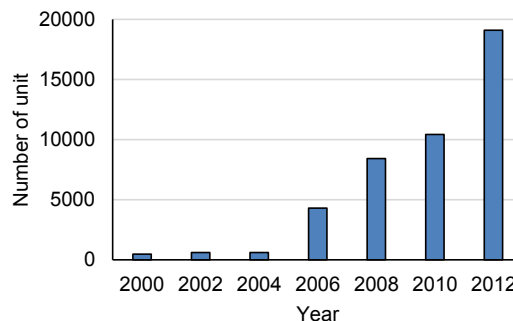


Figure 1.3. Development of private apartment in Surabaya (Arethusa, 2014)

demand including those for apartments will continuously increase. Since 2003, the central government of Indonesia initiated urban redevelopment program and provided rented apartments for low-middle and middle-middle income people. This type of apartments gradually increased since the central government allocate budget to develop this kinds of apartments by around 250 towers (with 94-108 units/tower) annually (Ministry of Public Works, 2012). In 2007, the national government of Indonesia launched the so-called “1,000 towers program” to stimulate and accelerate the development of apartments for the middle-class. Since that, the number of newly emerging middle-class apartments particularly so-called *Rusunami* dramatically increased (Figure 1.3). Since most of the major cities in Indonesia are already densely populated, the demand for apartments is expected to increase in the future.

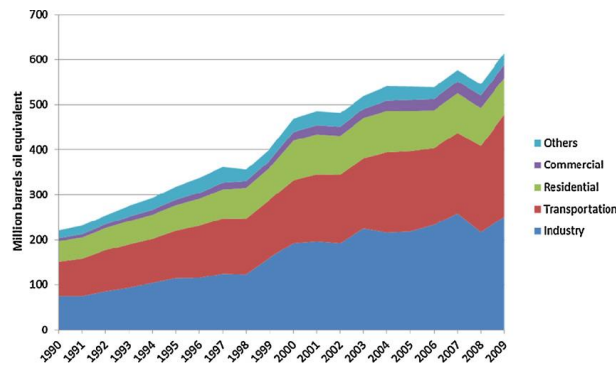


Figure 1.4. Final energy consumption by sector In Indonesia from 1990 to 2009 (Ministry of Energy and Mineral Resources, 2010)

1.1.2 Energy consumption and CO₂ emissions in Indonesia

Indonesia currently is facing problem of rapid depletion in energy resources particularly oil and gas, while at the same time, energy consumption rapidly increased. Final energy consumption has been drastically increasing due to the rapid industrialization and urbanization. As shown in Figure 1.4, the industrial sector dominated final energy consumption in Indonesia in 2009, followed by transportation and residential sectors. In particular, the residential sector shows steady increase. In a depth review on the situation of energy in Indonesia has been discussed by Hasan *et al.* (2012a), Gunningham (2013) and Mujiyanto and Tiess (2013). While energy consumption increased, CO₂ and other greenhouse gas emissions showed similar patterns in Indonesia. Hasan *et al.* (2012b) calculated total emissions from power plants in Indonesia, and the results implied a rapid increase. Over the past 23 years, the average annual growth rate of emissions from power plants was 7.6% for CO₂, 10.1% for NO_x, 4.4% for SO₂ and 6.4% for CO. Meanwhile, in other report, residential sector shared 2.2% of total emissions from fuel combustion, or equal to 16.73 MtCO₂ (IEA, 2012).

As the number of middle class increases, the electricity consumption in Indonesia is predicted to increase further. By 2012, the households sector consumed electricity by around 41% of total nationwide consumption and it has been increasing with time (Ministry of Energy,

2014). In the tropical regions such as Indonesia, the cooling demand was found to have a significant contribution to the household energy consumption especially when air-conditioning is used (Surahman and Kubota, 2012). The energy consumption for cooling in households is reported relatively larger compared to those for other needs (Wijaya and Tezuka, 2013). However, the studies of electricity consumption for cooling in apartments in Indonesia are still rarely found. As a comparison, it is reported that the electricity consumption in apartments in subtropical Hong Kong during the hot summer months was about twice as much as during other seasons, mainly due to the demand for cooling (Lam, 2000), and it is said to be almost three times larger than those in other study (Yao, 2012). Indoor thermal environment significantly affects the energy consumption for thermal comfort and HVAC systems.

1.2 Problem statement and research scope

As previously discussed, one of the pathways in reducing energy consumption without sacrificing thermal comfort need is applying some cooling strategies to the buildings. Based on the review, it has been reported that the thermal comfort range in the tropics can be altered particularly under the naturally ventilated conditions. Recent studies showed that through thermal adaptations, comfort temperature can vary with changing outdoor conditions, thus reducing indoor-outdoor temperature differences and required cooling loads of buildings (de Dear and Brager, 2002; Nicol *et al.*, 2012). Nonetheless, studies that attempt to improve thermal performance of apartments particularly in hot and humid climates remain few and fragmented. Some researches on cooling strategies mainly focused on the design of building envelope alone such as U-values, orientation, WWR, insulation, etc. (see Liping *et al.*, 2007, Mirrahimi *et al.*, 2016, Yildiz and Arsan, 2011, Wong and Li, 2007 and Liping and Wong, 2007) while other studies focused on the ventilation strategies only (see Liping and Wong, 2007; Nguyen and Reiter, 2012 and Prajongsan and Sharples, 2012). The former was mostly conducted in the air-conditioned buildings where the air change rates were controlled as minimum as possible to reduce the cooling load while the latter was undertaken in the naturally ventilated apartments where wind speed and air change rate were essential for the design (see Table 2.2). Yet, the studies combining the above two aspects can still be hardly found.

Meanwhile, the existing energy-saving standards for buildings mainly focus on the reduction of heat entering the indoor spaces through the building envelopes. In European countries as well as North American countries, energy-saving performance is evaluated using U-value for each part or whole of building envelopes. Meanwhile, heat transfer coefficient values for each part of building envelope are used as the energy efficiency requirements for residential buildings in Japan (IEA, 2008). As such, energy saving requirements for the building in the tropics to date solely depend on the single parameter such as OTTV (Overall Thermal Transfer Values), as can be found in Singapore and Indonesia (BCA, 2004; BSN, 2011). This requirement is highly associated with the insulation performance whereas the ventilation strategies are rather difficult to be included in the standards.

Indonesia is currently the Southeast Asia's largest economy and ranks among the most advanced of the developing countries. As previously described, more than half of the population will live in the urban areas in the future. As reported by Ministry of Public Works (2012), housing backlog is now becoming a main problem in addition to providing good living

space for the population. Housing programs initiated by the government including 1,000 tower program are expected to fill out this gap. Hence, the increase in greenhouse gasses needs to be addressed as a consequence of the increase in housing.

Indonesia has ratified Paris Agreement in October 2016. By ratifying this agreement, Indonesia has committed to reduce the emissions by 29% under the business as usual scenario by 2030 and up to 41% with the international supports. Indonesia targets to reduce greenhouse gas emissions from energy sector by around 11%-14% from the baseline scenario by 2030. As one of the biggest energy consumers as well as the highest contributors in greenhouse gas emissions, the building sector has the largest potential in reducing emissions in Indonesia. Nevertheless, although the Indonesian government particularly increases the provision of high-rise apartments to accommodate the growing number of middle class, the current design guidelines for apartments in Indonesia don't include the aspects of energy-saving. The building regulations for apartments to date still don't specify any requirements for achieving indoor thermal comfort, except for requiring natural ventilation openings to be at least 5% of the net floor area in each room (Ministry of Public Works, 2012; BSN, 2001). In addition, some standards regarding energy conservation in Indonesia were adopted from the European or Western standards which are designed for subtropical or temperate regions without considering the local hot and humid conditions. These standards rely fully on the requirements of the building envelope performance represented by a single value such as OTTV (Overall Thermal Transfer Value).

In response to the above research gap, this study attempts to propose cooling strategies for high-rise apartments in the hot-humid climate of Indonesia by combining envelope strategies and ventilation strategies. As such, this study examines cooling strategies comprehensively in three-dimensional perspective. Furthermore, the cooling strategies target not only naturally ventilated rooms but also air-conditioned rooms in high-rise apartments.

This work is a fundamental study to accumulate the basic information and data that can be useful in developing the above-mentioned cooling strategies for the high-rise apartments in Indonesia. First, this study aims to understand indoor thermal environments and thermal comfort of the existing apartments in major cities of Indonesia, focusing especially on the middle-class high-rise apartments, the so-called *Rusunami*. Second, this study investigates the passive cooling techniques embedded in the Dutch colonial buildings located in the city of Bandung with the aim of applying these traditional techniques to the modern houses. Third, the effects of cooling techniques on indoor thermal comfort as well as cooling load reduction in high-rise apartments are analyzed comprehensively through a series of parametric studies using numerical simulations. Fourth, the design guidelines for high-rise apartments towards energy-saving are proposed based on the results of the field measurements and simulations. This research was conducted as part of the joint research project between the research group for Building and Urban Environmental Science in Asia (BUESA) at Hiroshima University and Research Institute for Human Settlements/*Pusat Penelitian dan Pengembangan Permukiman* (Puskim), Ministry of Public Works and Housing of Indonesia. The ultimate goal of this project is to construct an experimental house, i.e. apartments, for full-scale experiments, and to propose new energy-saving guidelines for the high-rise apartments, i.e. *Rusunami*, as a national standard of Indonesia.

1.3 Research objectives

The main objective of this thesis is to provide fundamental and comprehensive data and information on newly constructed high-rise apartments, *Rusunami*, in Indonesia, which are useful in developing new energy-saving guidelines and standards for these apartments. As described before, these subsidized high-rise apartments have constructed especially from 2007 in order to accommodate the growing number of middle class in Indonesia. Because these apartments are still new in Indonesia, their indoor thermal conditions as well as thermal comfort are not yet studied in detail. The specific objectives are as follows:

1. To understand the existing situation and current problems of the existing apartments through investigation of detailed indoor thermal environments in the three types of apartments in Surabaya, Indonesia; to investigate the effects of ventilative cooling on indoor thermal environments of apartment units under unoccupied condition; and to investigate factors influencing indoor thermal environments under occupied condition. Primary data are collected through field experiments and questionnaire surveys while computer simulation is used to further investigate the effects of several cooling techniques.
2. To evaluate indoor thermal environments of vernacular houses, i.e. Dutch colonial buildings, and to find out their cooling techniques that are worthwhile of applying to the modern high-rise apartments. Vernacular houses adapted to the hot and humid local climates for a long time without relying on mechanical cooling techniques. It is, therefore, logical to make scientific references to past local vernacular buildings for designing energy-saving techniques for modern houses. Several field measurements were conducted in Dutch colonial buildings located in the city of Bandung.
3. To examine the effects of the selected cooling techniques on indoor thermal environments of the high-rise apartments through parametric studies using numerical simulations. The three-dimensional perspective of cooling techniques, comprising natural ventilation, envelope techniques and building volume, is considered in this simulation. Both multi-zone thermal simulation (TRNSYS-COMIS) and Computational Fluid Dynamic (CFD) STREAM are used to assess the cooling load and indoor thermal conditions, respectively.
4. To evaluate the cooling potential of the different combinations of cooling techniques and to propose cooling strategies for the high-rise apartments of Indonesia.

1.4 Significance of the research

1. As previously described, the number of newly emerging high-rise apartments, *Rusunami*, has been rapidly increasing in Indonesia over the last several years (since 2007). To date, the current conditions of indoor thermal environment in these apartments have not yet been revealed: this study is probably the first attempt. The comprehensive data on these apartments that will be provided by this study would be a fundamental and useful information in developing design guidelines towards energy-saving and low-carbon societies in Indonesia.

2. Indonesia is a quite diverse country in terms of social and cultural aspects, and therefore there are very rich variations in vernacular architecture as well, ranging from well-ventilated wooden traditional houses with raised floor to brick colonial architecture. This study focuses especially on the Dutch colonial buildings because of similarities of building materials and building size with those of the modern high-rise apartments. Although numerous studies were conducted to investigate the thermal environments of vernacular buildings, most of the studies deal with the traditional wooden houses and there are few studies that analyze the Dutch colonial buildings in Indonesia.
3. High-rise apartments are still rare in the developing countries such as those located in Southeast Asia, although they are rapidly increasing as can be seen in Indonesia. Therefore, extensive and comprehensive studies in apartments in the tropics are still limited in the field of building science. An exception is Singapore, where the apartments account for about 94.2% of the total housing stocks (ADB, 2016). However, most of the apartments in Singapore are no longer low-to-medium-cost apartments and therefore their building design and attributes are different from those located in developing countries such as Indonesia.
4. Furthermore, the existing studies on high-rise apartments are still limited within one or two dimensional perspective(s) of cooling strategies: either envelope technique or ventilation technique, or combining both techniques. Accordingly, most of the building regulations/guidelines on cooling/heating strategies for apartments often focus on the building envelope alone such as by U-value and OTTV (Overall Thermal Transfer Values). This study employs three-dimensional perspective of cooling strategies and attempts to provide completely new insights in developing energy-saving standards for high-rise apartments in the hot-humid climates.
5. In the hot-humid climatic regions such as Indonesia, diurnal temperature variation is larger than the seasonal variation. Thus, the cooling techniques may have to distinguish for daytime and night-time conditions respectively, rather than to respond to the seasonal changes. This study employs different comfort requirements for daytime and night-time respectively and determines the different cooling strategies.

2

Literature Review: Passive Cooling of Apartment Buildings

This chapter presents a literature review of relevant studies of passive cooling in buildings, particularly in the apartment buildings. First of all, some fundamental principles and development of passive cooling and thermal comfort particularly in the tropics are explained (Sections 2.1 and 2.2). Vernacular passive techniques not only in colonial buildings but also other vernacular buildings are considered in Section 2.3. From these sections, the information of passive cooling techniques and their thermal performances as well as the method how to develop the techniques are extracted. Eventually, the recent developments of passive cooling techniques for the high-rise buildings in the hot-humid climatic regions are considered from the review in Section 2.5

2.1 Passive cooling techniques of buildings in the tropics

Historically, the term passive in relation to the integral heating and cooling of buildings was firstly used in the United States in the early 1970s to describe the space conditioning systems that are primarily driven by natural resources, as the counterpart of passive heating (Cook, 1989). Meanwhile, cooling is defined as the transfer of energy from the space or the air supplied to the space, to achieve a lower temperature and/or humidity level than those of the natural surroundings (Balaras, 1996). Furthermore, Givoni (1994) defined passive cooling techniques as various simple cooling techniques that enable the indoor air temperatures of building to be lowered through the use of natural energy resources. In this term, the use of a fan or a pump to enhance the indoor performance is included. Even though, the similar term had been already used to describe the same phenomena such as bioclimatic design (Olgay, 1963), tropical architecture (Koenigsberger *et al.*, 1974) in the context of tropical regions, and later in this early century, as green buildings (Bauer *et al.*, 2010; Bonta and Snyder, 2008) and eco-house (Roaf, 2013).

Comprehensive references on passive cooling can be found in Cook (1989), Givoni (1994), and Santamouris (2007). Basically, passive cooling strategies for buildings should be designed

at three levels: (1) prevention of the heat gain; (2) modulation of the heat gains by effective solar control; and (3) rejection of heat from building to the heat sinks through ventilation or air infiltration, evaporative cooling, radiative cooling and earth cooling (Dimoudi, 1996, Geetha and Velraj, 2012; Al-Obaidi *et al.*, 2014). Natural heat sinks as the passive cooling resources are the sky, the atmosphere, the earth (Cook, 1989), and water (Givoni, 1994). Preventing the heat gain or minimizing cooling needs, can be achieved by appropriate architectural design such as building layout and form, orientation of building, shading devices, window size, color of building envelopes, insulation, etc. (Givoni, 1994). Meanwhile, heat modulation related to the thermal mass of materials such as brick and concrete, and thermal properties of material (i.e. heat storage capacity). Phase Change Material (PCM) is a new type of material that currently growing as one of the passive cooling techniques, in terms of heat modulation (Akeiber *et al.*, 2016; Kenisarin and Mahkamov, 2016). Passive cooling systems are thus classified into several systems, they are comfort ventilation, nocturnal ventilative cooling, radiant cooling, evaporative cooling (both direct and indirect evaporative cooling), soil (earth) cooling and cooling of outdoor spaces (Givoni, 1994; 2011). Geetha and Velraj (2012) developed a comprehensive framework of passive cooling strategies including the new techniques such as PCM, direct hybrid air, etc., as indicated in Figure 2.1.

Since firstly introduced in the 1970s, the researches and practices of passive cooling (or in other terms, bioclimatic design, etc.) for energy-efficient buildings have increased cover various climatic conditions. Givoni (2011), Santamoris *et al.* (2007) and Santamouris and Kolokotsa (2013) for instance, presented the research results of various passive cooling strategies in naturally ventilated buildings under different climatic conditions, including in the hot-humid regions. Their review included the utilization of new passive techniques, such as smart ventilation and smart shading, *Skytherm* system, *NightSky* cooling system, earth to air heat exchanger and so on. Sabzi *et al.* (2015) evaluated three types of passive cooling strategies applied on the roof, namely: water jacket, water pond and radiation shield on roof, in the moderate tropics of Iran. Those above evaluation strategies implied that passive cooling strategies can lowering the indoor air temperatures and provide comfort in naturally ventilated buildings and decrease the cooling load in air-conditioned buildings. Innovation and new techniques were developed and broadly used in building recent days. Pires *et al.* (2013) developed a prototype of innovative element for passive cooling techniques and investigated its performance in Portugal. On the other hand, PCM recently obtains growing attentions due to its ability of storing thermal energy within a small volume (Al-Saadi and Zhai, 2013), and broadly used as heat storage system to improve the building thermal environments in many different fields including buildings and industries (Zhou *et al.*, 2012; Al-Saadi and Zhai, 2013; Akeiber *et al.*, 2016) through several different ways: passive, active and free cooling (de Gracia and Cabeza, 2015; Alam *et al.*, 2017). Passive cooling would be more important in the future mainly related to the growth and development of the air-conditioning, primarily affected by local climatic conditions, global warming, increase of the earth's population, growth of local income and gross domestic product (GDP), electricity and equipment prices and technological aspect of the equipment (efficiency and energy performance) (Santamouris, 2016).

A tropical zone (or hot-humid climatic region) is the part of the earth that lies between the Tropic of Cancer (23°27'N) and the Tropic of Capricorn (23°27'S) (Ayoade in Al-Obaidi *et al.*, 2014). The tropical region is an uncomfortable climate zone that receives a large amount of

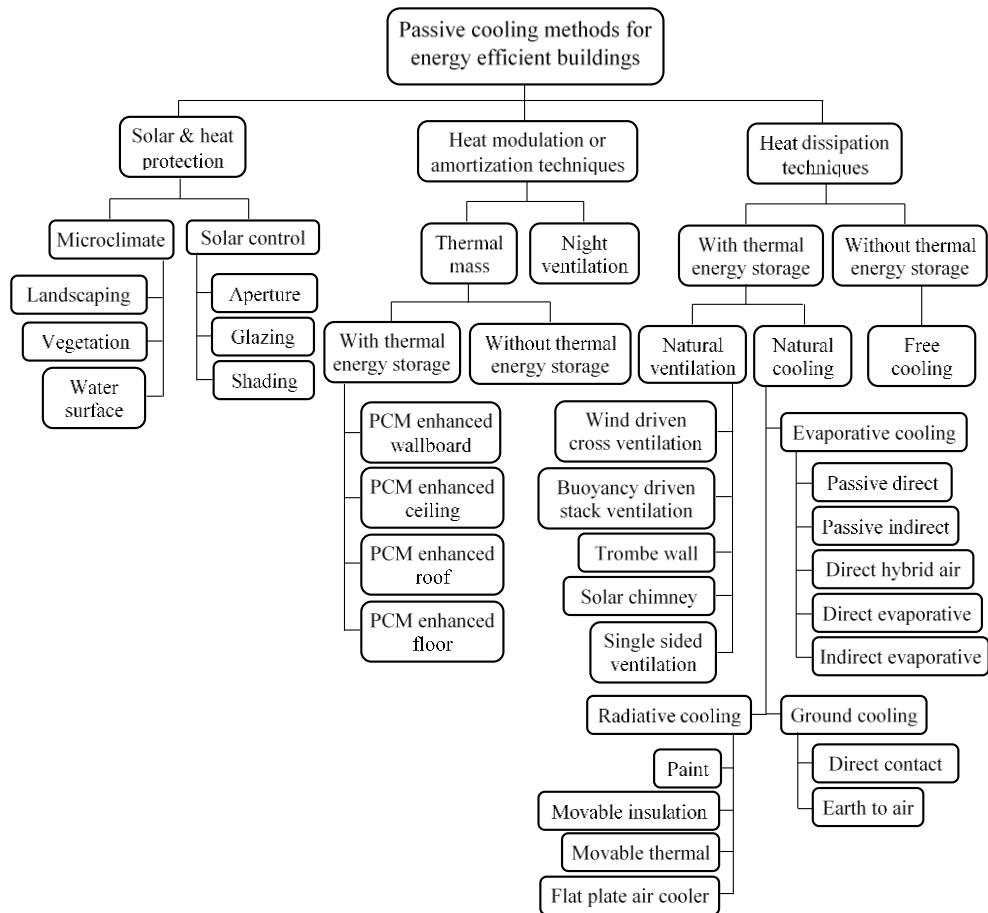


Figure 2.1. Framework of passive cooling strategies in energy-efficient buildings (Geetha and Velraj, 2012)

solar radiation, high temperature (annual mean temperature of 27°C) and follow a very constant diurnal pattern throughout the year, high level of relative humidity and long periods of sunny days throughout the year (Al-Obaidi *et al.*, 2014; Givoni, 1976), and small diurnal temperature variation (Szokolay, 2004). Although the overheating is not as great as in hot-dry regions, but tropical area is aggravated by high humidity so that restricting the evaporation potential (Szokolay, 2004). Above conditions make the tropical is a difficult climatic regions to be dealt with in terms of passive cooling design. In order to fulfill the physiological thermal requirements in tropical regions, Givoni (1976, 1994) suggested some building design principles by emphasizing on provision of continuous and efficient ventilation; protection from the sun, rain and insects; prevention of internal temperature elevation during the day and minimizing during the night and evening. Since the humidity in the tropical regions is very high, then the continuous ventilation is the most important comfort requirements by increasing

the efficiency of sweat evaporation and avoid the discomfort due to moisture on skin and clothes. Therefore, it affects all aspects of building design such as orientation, the size and location of windows (openings), layout of the surroundings, etc.

Numerous studies on the passive cooling strategies for hot-humid climatic regions have been carried out this recent years. De Waal (1993) proposed recommendation for building design in the tropics based on his long research, in order to achieve thermally comfortable building. Some of the recommendations for naturally ventilated buildings are ventilation strategies, building materials and thickness of the envelope (thermal mass), insulation, and many other strategies. Ventilation is considered to be one of the effective means to achieve thermal comfort in naturally ventilated buildings. Ventilation strategies, including night ventilation still became main strategies for cooling of building in hot-humid climate regions, in addition insulated roof and shading devices (Borda-Diaz *et al.*, 1989). The effect of ventilation strategies further studied by Liping and Wong (2007) and Kubota *et al.* (2009). Both studies concluded different results in terms of ventilation strategies. By using computer simulation, Liping and Wong (2007) demonstrated that full-day ventilation was effective to provide better thermal comfort for hot-humid climate in Singapore. Meanwhile, from field investigation, Kubota *et al.* (2009) found that night ventilation had larger cooling effect than other ventilation strategies. Liping and Wong (2007) also suggested to increase the window to wall ratio to 0.24 so that indoor thermal comfort improve largely by increasing wind speeds. In another study, Liping *et al.* (2007) suggested U-values for different façade orientations for naturally ventilated residential buildings in hot-humid Singapore. Shading devices, window to wall ratio (WWR) and orientation were also considered as effective passive cooling strategies in residential buildings of Singapore (Liping *et al.*, 2007; Wong and Li, 2007). However, the performance of ventilation strategies partly depend on the orientation of building units and its elevation (its height above ground) of unit, in case of high-rise residential buildings (Aflaki *et al.*, 2016). Hirunlabh *et al.* (1999; 2001) claimed that modification of wall and roof through utilization of metallic solar wall (MSW) and roof solar collector (RSF) significantly improved ventilation and air flow rate in the tropical buildings. Khedari *et al.* (2004) proposed an innovation building materials (for wall) to enhance natural ventilation in the tropical houses of Thailand.

Building envelopes also play important roles in reducing solar heat gain and maintaining a good indoor thermal environment. Mirrahimi *et al.* (2016) summarized some possible passive facades and discussed its effects to thermal comfort and energy saving in hot-humid buildings. Some of them are orientation, insulated external wall, design of external roof, glazing material and external shading devices. By simulation, Liping *et al.* (2007) recommended U-values for design guideline for naturally ventilated buildings in Singapore; 2 W/m²K for west- and east-facing orientation and 2.5W/m²K for south- and north-facing orientation. Wong and Li (2007) suggested to use thicker external wall facing east or west than that facing south or north to reduce heat gain from east- and west-side and increase time lag. In lightweight buildings, color of envelope surface has significant effect on indoor temperature; the darker, the higher maximum temperature and thus, the larger the diurnal swings, while this effect could not be seen clearly when thermal mass is applied. However, thermal mass should be carefully applied in the tropics, since it is sometimes benefit and sometimes not (Cheng *et al.*, 2005). Lei *et al.* (2017) found that cool colored coating integrated to (PCM) further reduced the surface and air temperatures and saving energy annually by 8.5%,

as compared to when those techniques (i.e. PCM, cool paint) applied alone. Cool paint is a type of cool material used on surfaces, characterized by high solar radiation reflectance and high infrared emittance.

Roof is one of the most important building envelope in the tropics since it received strong direct solar radiation throughout the day, and receive about 70% of the total heat gain (Al-Obaidi *et al.*, 2014). Therefore, reducing heat gain through the roof is essential for the tropical buildings. Solar and heat protection can be achieved by using reflective coatings on the roof of buildings. The application of reflective and radiative roofs, as well as ventilated roof in the hot-humid climatic regions of Southeast Asia has been reviewed by Al-Obaidi *et al.* (2014a, 2014b, 2014c), and Roslan *et al.* (2016). It is found that reflective and radiative roofs enhanced environmental sinks for heat dissipation and thus reduced internal heat gain although their efficiency depends on the building type, occupancy pattern and climatic boundaries. It is also found that Malaysia environment, and hot-humid environmental condition in general, cannot rely only on the natural climate to extract heat from the attic, and using ventilator provides a better solution. The effectiveness of night radiant cooling on the roof in the tropics were also investigated by Khedari *et al.* (2000) and Vangtook and Chirattananon (2007). Both studies showed that night radiant cooling with different configuration can be used in the context of hot-humid regions, although its performance depend on the weather condition at night-time (cloudiness, for instance). Moreover, cooling tower also could be employed to provide cooling water for radiant cooling and for pre-cooling of ventilation air to achieve thermal comfort.

Other than above passive techniques, courtyard can be considered as passive cooling strategies in hot-humid climatic regions (Rajapakhsa *et al.*, 2003; Kubota *et al.*, 2017). Courtyard functioned as cooling source to the surrounding spaces and as an air funnel discharging indoor air into the sky, rather than as suction zone inducing air from its sky opening. It is recommended to apply closed and cross-ventilated courtyards with a low sky view factor in the hot-humid climates.

2.2 Thermal comfort in the tropics

The main function of passive cooling is to cool a building's structure and its indoor space so that enable to provide thermal comfort for the occupants. Therefore, conditions for thermal comfort would be the main assessment criteria of the performance of the passive cooling techniques. Thermal comfort is one of the most important aspects of user satisfaction and energy consumption in buildings (Nicol *et al.*, 2012). ASHRAE defined thermal comfort as '*the condition of mind that expresses satisfaction with the thermal environment*' and therefore it is contextually dynamic (ASHRAE, 2013). This definition implied that thermal comfort has subjective definition, and therefore it is related to the principles of adaptation of people to respond their discomfort environments by seeking appropriate methods to restore their comfort levels through physiological, psychological and behavioral adjustments (Humphreys and Nicol, 1998; Brager and de Dear, 1998; Humphreys *et al.*, 2007). Since this thesis deals with naturally ventilated buildings, adaptive comfort standards and field studies of thermal comfort are of main interest. The adaptive model provides flexibility in matching optimal indoor temperatures with outdoor climate, particularly in naturally ventilated buildings (de Dear and Brager, 2002; Nicol and Humphreys, 2010).

Adaptive model investigates the dynamic relationship between occupants and their thermal conditions based on the principle that people tend to react to changes that produce discomfort by seeking methods of restoring their comfort levels (Humphreys and Nicol, 1998). Some studies in the tropics regions, for instance, indicated that people of those regions showed higher thermal comfort level as compared to what PMV model has predicted, and how the ability of people in modifying and adjusting the environment as well as particular behaviors to enable themselves to compensate for the less comfortable thermal conditions (Karyono, 2000; Givoni, 2004; Feriadi and Wong, 2004; Nguyen *et al.*, 2012). Orosa and Oliveira (2011) noted that climatic differences affect comfort perception and thus achieving a good level of agreement between the thermal sensation and adaptive models. Mishra and Ramgopal (2013) in their review concluded that people vote closer to comfort if they are given more adaptive opportunities, including adaptive opportunities in the building structure (i.e. passive cooling techniques).

Over the past decades there has been increase in the number of thermal comfort field studies in the tropics. The first attempt to investigate thermal comfort in the tropics was carried out by Webb more than half century ago (1949-1950) and followed by Ellis in 1953 (Feriadi and Wong, 2004). Some of the studies attempted to find out the range of comfort zone in the hot-humid climatic regions and compare them with the available standards. In his study in Indonesia, Karyono (2000) reported that neutral temperature in both naturally ventilated and air-conditioned buildings of Jakarta was found at operative temperature of 26.7°C with the comfort range at 23.5°C ≤ OT ≤ 29.9°C. In another study, neutral temperature in the naturally ventilated building of Yogyakarta, Indonesia, was found at operative temperature of 29.7°C (Feriadi and Wong, 2004). Damiati *et al.* (2016) reported that the highest comfort temperature in the mixed mode ventilation building of Indonesia is around of 27.5°C operative temperature. Meanwhile, Djamila *et al.* (2015) found that optimum neutral temperature in Malaysia was about 30.0°C, providing 95% fiducial limits of about -0.3°C and +0.6°C. Similar studies also carried out in different climatic zones of India, including hot-humid climatic area, by Indraganti (2010), Indraganti *et al.* (2014), Mishra and Ramgopal (2015) and Manu *et al.* (2016), while field study in Vietnam was reported by Nguyen *et al.* (2012). Above studies demonstrated that Fanger's static PMV model consistently overestimates the actual sensation and therefore under-predict the comfort temperature values in the tropics regions. In addition, above studies emphasize on the importance of control to the environment in order to adjust the thermal conditions in accordance to their preference (such as windows opening).

Further, studies which encountered higher air speeds reported that comfort temperatures voted by respondents also increased accordingly (Cândido *et al.*, 2010a; Khedari *et al.*, 2000). Cândido *et al.* (2010) suggested that subject's acceptance of higher air velocities increase to compensate for elevated temperature and humidity. The minimal air velocities were at least 0.4 m/s for an operative temperature of 26.0°C and rising to 0.9 m/s for that of 30.0°C. Khedari *et al.* (2000) recommended air speed above 3.0m/s for air temperature above 34.0°C. ASHRAE (2013) permit to use the increasing of air velocities up to 1.2m/s for increasing of operative temperature to 2.2°C. Although values of the wind speeds and the corresponding comfort temperatures are different among the studies, however, it is agreeable that poor ventilation is probably the most important reason for the discomfort of occupants in naturally ventilated buildings in the humid tropics (Yang and Zhang, 2008). Above studies also strongly

Table 2.1. Proposed adaptive thermal comfort equation and related criteria for naturally ventilated buildings in hot-humid climate.

No.	Aspect	Criterion	Note
(i)	Climate type	All A climate types; and Summer season of Cfa climate type.	Climate type refers to the Köppen-Geiger climate classification system.
(ii)	Neutral operative temperature, T_{neutop} (°C)	$T_{neutop} = 0.57T_{outdm} + 13.8$	T_{outdm} is daily mean outdoor air temperature (°C), i.e. the 24-hour arithmetic mean for the day in question.
(iii)	Daily mean outdoor air temperature, T_{outdm} (°C)	Range from 19.4 to 30.5.	Recommended applicable range for criterion no. (ii).
(iv)	Lower comfort operative temperature limit, T_{lower} (°C)	No required limit.	-
(v)	Upper comfort operative temperature limit, T_{upper} (°C)	$T_{upper} = T_{neutop} - 0.7$ for 80% comfortable thermal sensation votes.	Graphical representation can be referred in Figure 3.7a (continuous line in the right figure) for a different percentage of comfortable thermal sensation votes.
(vi)	Indoor air speed, v (m/s)	<0.65 at and below neutral operative temperature; ≥0.65 above neutral operative temperature.	Recommended to provide non-still air and occupants' control to adjust the indoor air speeds according to their preferences.
(vii)	Indoor humidity, RH (%)	No required limit.	-

imply that the adaptive comfort model provide appropriate approach in evaluating thermal comfort, particularly in naturally ventilated buildings.

Standards on indoor thermal environment are important factors considered in building designs, in terms of balancing reductions in cooling/heating energy requirements and improving thermal comfort in the same time. Basically, there are two types of thermal comfort assessments: prescriptive method based on the heat balance model (PMV) and adaptive comfort methods. Current standards are essentially based on both models. The most notable example of the former is the predicted mean vote (PMV) model developed by Fanger (1972), which is applied in ISO 7730 (BSI, 2006) and ASHRAE Standard 55-2013. The latter model is also used in ASHRAE Standard 55-2013 as the code for naturally conditioned spaces for buildings without mechanical cooling systems during cooling season. Naturally conditioned spaces are defined as those spaces where the occupants have control of operable windows to regulate the indoor thermal conditions (ASHRAE, 2017). Thus, adaptive standards are thus considered more appropriate for supporting comfort in low-energy buildings (de Dear and Brager, 2002; Humphreys *et al.*, 2007; Nicol and Humphreys, 2002; Nicol *et al.*, 2012).

The adaptive comfort standard in ASHRAE (2013) applied a simple thermal index to

characterize the indoor comfort temperature, i.e. operative temperature. The simpler temperature index is sufficient and very useful when indoor thermal environment is close to the standard environment, which is at low air speed and 50% RH (Humphreys *et al.*, 2007). However, the conditions might not be so in hot-humid climate, especially when high air speed is essential and promoted by the adaptive model to aid evaporative heat loss by sweat. To be used as a standard particularly for hot-humid climate, this may bring two implications – under provision of the required air speed to building occupant and underestimation of the potential for higher comfort temperature under increased air speed (Toe, 2014). Some studies reviewed that comfort temperatures in tropical regions overestimate than those in ASHRAE’s adaptive comfort standard (Mishra and Ramgopal, 2015; Manu *et al.*, 2016; Nguyen *et al.*, 2012).

Besides ASHRAE (2013), some researchers developed adaptive comfort equation for hot-humid climatic regions based on the field survey in the specific locations, such as Karyono (2000), Nguyen *et al.* (2012), Indraganti (2010), Indraganti *et al.* (2014), and Manu *et al.* (2016). Toe and Kubota (2013) developed adaptive comfort standard based on the statistical meta-analysis of the ASHRAE RP-884 database. The proposed adaptive thermal comfort criteria for naturally ventilated buildings in hot-humid climate based on the present study findings are summarized in Table 2.1. This proposed criteria are used throughout this thesis to evaluate thermal performance of passive cooling techniques.

2.3 Studies on vernacular passive techniques in hot-humid climates

Vernacular architecture comprises the dwellings and other buildings of the people. Related to their environmental contexts and available resources, they are customarily owner- or community-built, utilizing traditional technologies. All forms of vernacular architecture are built to meet specific needs, accommodating the values, economies and ways of living of the cultures that produce them (Oliver in Bronner, 2006). It is believed that vernacular buildings have already withstood time and are subtly crafted over generations in response to experience of conditions and use including the local climate and human comfort needs (Oliver, 2006). Zhai and Previtali (2010) and Previtali and Zhai (2016) classified ancient vernacular buildings around the world and categorizing them based on the climatic zones and cultural heritage particularly language families used. Tropical vernacular buildings were characterized by the lightweight construction, thatched roof, vaulted ceilings, elevated floor, and other characters involving room arrangement, building shape, building story, window and infiltration, and shading devices. Large openings protected from the sun are common features of vernacular buildings in the tropics since ventilation is very important but in the same time, the radiation is also very intense (Coch, 1998). This indicates that vernacular buildings have evolved with the need to create thermal comfort conditions, and it is found that thermal performance of vernacular buildings is better than that of modern houses thanks to passive strategies (Chandel *et al.*, 2016).

In-depth both qualitative and quantitative studies with regard to passive environment control techniques of vernacular buildings in the tropics are remain few including in Indonesia. Some of them were conducted by Labaki and Kowaltowski (1998), Hassan and Ramli, (2010), Dili *et al.* (2010), Shanthi Priya *et al.* (2012), Nugroho (2012), Nguyen *et al.* (2011) and Hoseini *et al.* (2014). A detailed study that examined a specific traditional passive cooling

Table 2.2 Vernacular passive cooling techniques in hot-humid climatic regions from previous studies.

Reference	Country	Type of vernacular buildings	Passive cooling techniques
Toe and Kubota, 2015	Malaysia	Malay traditional house and Chinese shop-house	Microclimate modification (to reduce outdoor air temperature) and courtyard
Kubota et al., 2017	Malaysia	Chinese shop-house	Courtyard
Hoseini et al., 2014	Malaysia	Malay traditional house	Large openings area, open plan layout
Nugroho, 2012	Indonesia	Flores traditional house	Room arrangement, shading devices and roof insulation (thick roof)
Shanti Priya, et al., 2012	India	Nagapattinam traditional house	Courtyard with wind catchers, thick external wall, verandas, and sloping roof
Dili, Naseer and Varghese, 2010	India	Kerala traditional house	Building orientation, room arrangement, internal courtyard, large openings
Nguyen et al., 2011	Vietnam	Vietnamese traditional house and Colonial buildings	Corridor spaces, shading devices, large openings, high ceiling height.

techniques in the tropics was conducted by Toe and Kubota (2015). The passive cooling techniques such as night ventilation, roof insulation, window and wall shading devices, presence of courtyards were found to be effective strategies to maintain indoor comfort temperature and humidity levels. Table 2.2 summarized the environmental techniques employed in the vernacular buildings from the previous studies.

Using above definitions of vernacular buildings, in the context of Indonesia, Dutch colonial buildings is considered to be vernacular buildings, since these buildings have developed for generations even by local people and transformed with the local context (i.e. cultures and environment) (Hartono and Handinoto, 2006; Ardiyanto *et al.*, 2015). In addition, these buildings were intentionally broadened to include large-scale city development and country planning and left a very strong imprint on the built environment of the Indonesian archipelago. Nevertheless, during this long process, Dutch colonial buildings unequivocally showed the influence of cultural exchange with the various traditions that already existed in Indonesian archipelago (Wuisman, 2007). Further, Nguyen *et al.* (2011) considered French colonial buildings as one of vernacular buildings in Vietnam.

Dutch colonial building is one of the vernacular architectures that had adopted to the local climatic conditions and providing thermal comfort (Widodo, 2007; Passchier, 2007). The Dutch adopted specific elements and architectural features of autochthonous traditions of Indonesian architecture into their own building tradition (Wuisman, 2007). However, most of the studies on colonial buildings particularly in Indonesia were focus on the others than thermal performance such as design, cultural heritage, architectural history, urban planning and so on (Handinoto and Hartono, 2006; van Dulleman, 2012; Adiyanto *et al.*, 2015; Wibowo, 2015; and Wan Ismail and Nadarajah, 2016). In the other hand, studies on the thermal performance of colonial buildings, both qualitatively and quantitatively, in the hot-humid climatic regions including Indonesia are hardly found. Kowaltowski *et al.* (2007) and Nguyen *et al.* (2011) qualitatively studied thermal performance of Portuguese colonial buildings and French colonial building in their respective home-country, Brazil and Vietnam. Through field

measurement and computer simulation, Santoso (2001) compared the thermal performance of three different houses in Indonesia, i.e. traditional building, colonial building and modern house. It is found that Dutch colonial building has the best thermal performance compare two other types of buildings. Its advantages mostly due to the high thermal mass so that has low U-value and longer time lag for heat modulation.

2.4 Recent developments of passive cooling techniques in apartments in hot-humid climate.

As previously discussed, a proper passive cooling strategies can achieve indoor thermal comfort as well as saving energy for cooling in residential buildings including apartments. A number of passive cooling strategies for high-rise residential buildings in hot-humid climatic regions had been studied although still limited. Aflaki *et al.* (2015) reviewed the natural ventilation as one of passive cooling strategies through building facade and ventilation openings in hot-humid climatic regions. They found that the stack effect and wind force would be the main and basic principles to produce air movement (and produce thermal comfort as well) although its efficiency depends on certain factors; difference in temperature as well as vertical distance between inlet and outlet. They also found that building layout, size and form of balcony on the external surface of building facade were the most relevant architectural variables. In another field study, Aflaki *et al.* (2016) compared four different scenarios of apartment units and investigated indoor thermal environment under single-sided ventilation conditions. The study revealed that unit facing prevailing wind received maximum amount of heat radiation but in the same time, the sufficient wind velocity removed the heat effectively through single-sided ventilation. Nevertheless, unit elevation influenced the performance of this ventilation. Meanwhile, it is reported that full-day ventilation is the most effective strategy for thermal comfort in apartment in Singapore (Liping and Wong, 2007) and in Danang City of Vietnam (Nguyen and Reiter, 2012). Nonetheless, both studies agreed that structural cooling through nocturnal ventilative cooling (i.e. night ventilation and full-day ventilation) are more effective in cooling the building than other ventilation strategies. Thermal mass did not have any positive contributions on the thermal environment in low rise apartment building (Nguyen and Reiter, 2012) while in the high-rise apartment buildings, thermal mass inertia is ideal option for naturally ventilated apartment buildings (Liping and Wong, 2007).

To enhance natural ventilation in the apartment buildings, Liping *et al.* (2007) recommended combination of window to wall ratio (WWR) and U-values for different orientation. This study suggested to use optimum WWR at 0.24 with U-value of 2.0 W/m²K for east-/west-facing unit and 2.5 W/m²K for north-/south-facing unit. However, for west and east orientation, large WWR should be avoided when the wind direction is parallel with the facade. Other studies to improve natural ventilation in the apartments were carried out by Prajongsan and Sharples (2012) and Priyadarsini *et al.* (2014). Prajongsan and Sharples (2012) showed that natural ventilation can be achieved by using ventilation shafts in each unit. The ventilation shaft is an effective wind-induced ventilation system for creating cross ventilation and relatively high indoor air velocities that can enhance thermal comfort in a single-sided residential unit during summer, depend on the external environment. Meanwhile, Priyadarsini *et al.* (2004) demonstrated that stack effect applied in the apartment unit effectively provide

Table 2.3 Passive cooling techniques of the high-rise apartments in hot-humid climatic regions from previous studies.

Reference	Country	Apartment type	Method	Passive cooling techniques
Yildiz and Arsan, 2011	Turkey	Air-conditioned	Sensitivity analysis	Window area, U-values and SHGC depending orientation (specific values are not given)
Bojic et al., 2002	Hong Kong	Air-conditioned	Computer Simulation (HTB2)	Thermal insulation of the external wall and partition wall.
Bojic, Yik and Sat, 2001	Hong Kong	Air conditioned	Computer Simulation (HTB2)	Thermal insulation of the external wall
Cheung, Fuller and Luther, 2005	Hong Kong	Air conditioned	Computer simulation (TRNSYS)	Internal insulation for external wall, light color of external wall, Low-E glazing and shading devices (saving 31.4% of cooling load)
Wong and Li, 2007	Singapore	Naturally ventilated	Field measurement and computer simulation (TAS)	Orientation (South/North), roof thermal buffer, thicker wall in east- and west-external wall, and window shading devices
Liping and Wong, 2007	Singapore	Naturally ventilated	Computer Simulation (TAS) and CFD	Full-day ventilation, high thermal mass, north- or south-facing orientation and window to wall ratio
Priyadarsini, Cheong and Wong 2004	Singapore	Naturally ventilated	Lab experiment (wind tunnel) and Computer Simulation (CFD)	Active stack system.
Prajongsan and Sharples, 2012	Thailand	Naturally ventilated	Computer Simulation (CFD)	Ventilation shaft
Nguyen and Rieter, 2012	Vietnam	Naturally ventilated	Field measurement and computer simulation (COMFIE)	Night-ventilation, reflectance building envelope, shading devices, low U-value openings.

thermal comfort for the occupants with the 85-95% of satisfaction. The design of stack ventilation also given in their study.

In addition to natural ventilation strategies, some proper parameters of building envelope to the high-rise residential buildings were investigated by Mirrahimi *et al.* (2016). They summarized particular techniques of building envelope for both achieving thermal comfort and saving energy, respectively. These parameters orientation, building form, width, length and height; external wall, external roof, glazing and external shading devices. However, no study has been reported on application of such elements in a specific study investigating as a complementary concept. The importance of building form in cooling load reduction was highlighted by Yildiz and Arsan (2011) and Choi *et al.* (2012). Furthermore, Wong and Li (2007) studied effectiveness of orientation, roof thermal buffer, thermal mass and window

shading devices in reducing cooling load of high-rise apartment building. They pointed out that around 2.6-11.6% of energy were saving when above passive cooling strategies are applied in the apartments of Singapore. In the other studies, combination of several passive strategies (i.e. thermal mass, shading devices, glazing type and reflectance coating) reduced annual sensible cooling energy in apartments of Hongkong up to 31.4% (Cheung *et al.*, 2005). However, potential of cooling load reduction only given for particular strategies in this study. Meanwhile, the use of shading devices (i.e. overhang and blind system) generally reduced yearly cooling load in apartments in Hong Kong during summer time, depend on the slat angle (Kim *et al.*, 2012). Slat angle of 0° to be has the highest cooling load reduction and became the lowest when slat angel is 60°. The similar findings were reported by Bojic and Yik (2005) and Bojic *et al.* (2001, 2002). Further, Bojic *et al.* (2001) investigated the thermal performance of insulation positions in building envelopes. Six configuration of insulation in the building envelopes were examined. It is found that the highest decreasing in the yearly cooling load of 7.3% is obtained when a 5cm thermal insulation layer faces either the inside and outside of the flat. Air tightness of buildings, thermal properties of glazing and window were found to be important factors in high-rise apartment buildings to reduce cooling energy consumption (Yildiz and Arsan, 2011). Other studies also showed that thermal comfort as well as energy saving also can be achieved by occupant's behavior related to the openings usage as a response to the indoor thermal environment (Arethusa *et al.*, 2014; Indraganti, 2010; Kang *et al.*, 2012).

As reviewed above, there are few studies of passive cooling strategies in apartments in the tropics except for Singapore. Studies on the thermal performance and passive cooling strategies for energy saving in apartments in Indonesia were hardly to find. Table 2.3 presents the review of previous studies for the passive techniques in the high-rise apartments in hot-humid climate regions.

3

Thermal Comfort in Existing Apartments of Indonesia

As previously discussed, there are two types of thermal comfort standards: prescriptive method based on the Fanger's heat balance model (PMV) and adaptive comfort methods. Those two models are currently used as thermal comfort standards, such as ISO 7730 and ASHRAE 55. Since thermal comfort has subjective definition, then adaptive comfort model provide appropriate approach in evaluating thermal comfort particularly in naturally ventilated buildings. This chapter begins with the description of condition of apartments in Indonesia, including their types and the developments (Section 3.1) and then selection of case study apartments is discussed in the Section 3.2. Section 3.3 explains the methods of field experiments as well as numerical computer simulation conducted to investigate the indoor thermal environments of the existing apartments. The current situations and problems of the existing apartments are discussed in Section 3.4 for unoccupied condition and Section 3.5 for the occupied condition.

3.1 Apartments in Indonesia

Act No. 20/2011 regarding Apartments distinguished apartments in Indonesia into four categories, they are public apartments, special apartments, state apartments and private apartments. The main difference amongst above apartment types is the target people (or occupants) of each category: low-income people, special groups or communities, civil servants, and general market to obtain benefit, respectively. In this study, only the private and public apartments were considered since the special and state apartments categories are built for special purposes, the number and development of those apartments are limited. In recent years, these two categories (i.e. private and public apartments) are highly demanded by emerging low-to-middle class market in major cities of Indonesia due to the previously mentioned reasons: population growth and land availability issues (Arethusa, 2014).

The public apartments are broadly divided into two types, they are old public apartment and new public apartment. In local term, public apartments are usually known as *Rusunawa*, abbreviation for *Rumah Susun Sederhana Sewa* (Rented Simple Apartments). The public apartments, which is targeted low- and middle-low income people, are built and managed by both the central and local government. Initially, the old public apartments were built as a part of urban redevelopment program undertaken by the government to relocate the slum squatters to such apartment for providing better living environments (Darmawan, 2011). Since 2003, the new public apartment was built by the government to extend the target to wider social classes, especially for low to middle classes due to the increasing of housing demand (Arethusa, 2014) although this is still part of urban redevelopment program (Ministry of Public Works, 2012). By the time, old public apartments have been replaced by the new public apartments



Figure 3.1. Views of old public apartments.



Figure 3.2. Views of new public apartment

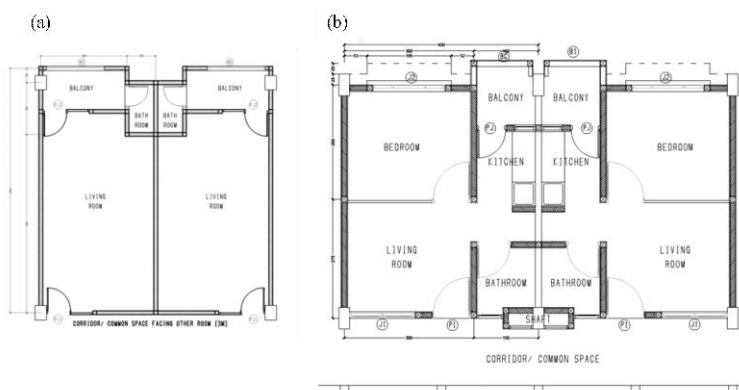


Figure 3.3. Typical floor plan of unit in (a) old public apartment and (b) new public apartment.

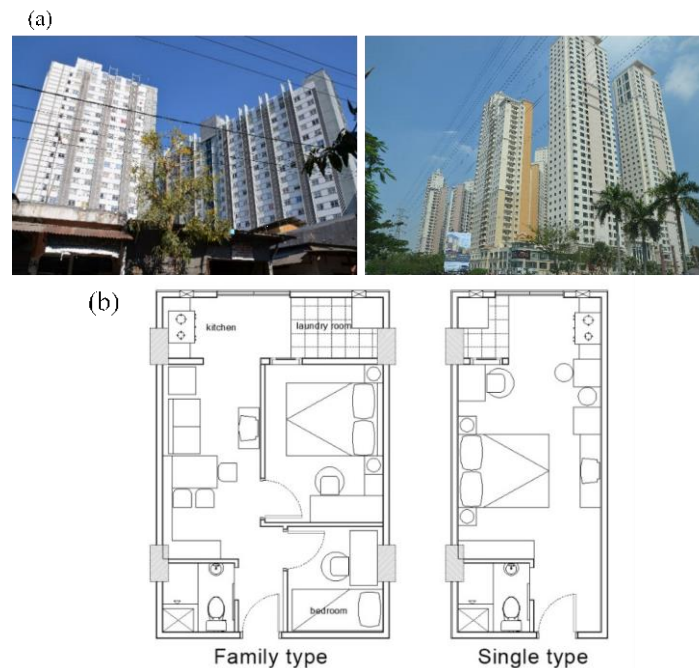


Figure 3.4. (a) Views of private apartments and (b) typical floor plan of unit of private apartment.

and since that time, more than 46,000 units of this apartment were built by 2015 and will be increase in the future (Ministry of Public Works, 2012).

In addition the establishment year, the differences between old and new public apartments can be recognized from the design between them. Since the public apartments are built by the government, thus both old and new public apartments have typical construction and design forms. Figures 3.1 and 3.2 are view of old public and new public apartments, respectively. Old public apartments generally are four storeys building while new public apartments consist of five floor level, with the ground floor functioned as common spaces. Both types of apartment are normally double loaded apartment type whereas each units are connected by corridor spaces. Both old public and new public apartments are naturally ventilated.

Figure 3.3 illustrated the typical floor plan of old public and new public apartments, respectively. In the old public apartments, typical unit is one room with floor areas of 18-21m². More than 70% of the units in those apartments have private bathroom, whereas the rest of units uses shared bathroom. Meanwhile, the new public apartment typically has different room arrangements. The room is slightly larger (24-32m²) and divided by functions: a bathroom, a bedroom, a living room, and a kitchen. All of the units in both types of public apartments have one small veranda which connects the indoor unit with outdoor environment (Arethusa, 2014). However, corridor space in the new public apartments is different than that in the old public apartments. Corridor space in the old public apartments is typically semi-open corridor space

while that in the new public apartment is open corridor space facing void space. The corridor in these apartments may also be functioned as a social gathering area.

The private apartment is constructed and owned by private companies for profit oriented. It normally high-rise buildings which consist of 14-33 floor heights and almost all of the units are equipped with air-conditionings. The private apartments have floor areas of 18-38 m² and consist of two typical types: single (or studio type) and family type unit. The single type contains only one room, functioning bedroom and kitchen, and one private bathroom. The family room has one living room which is connected directly with kitchen and dining room, two bedrooms, and one private bathroom (Arethusa, 2014). As the public apartments, this apartment type is double loaded apartment type and the units are connected by the corridor space. But unlike the public apartments, the corridor spaces are enclosed and relatively narrower. Figures 3.4 showed the views of sample of private apartments and typical floor plan of units of private apartment, respectively.

In further development, there is another type of private apartment so called *Rusunami*, abbreviated for *Rumah Susun Sederhana Milik* (Owned Simple Apartment), as a consequence

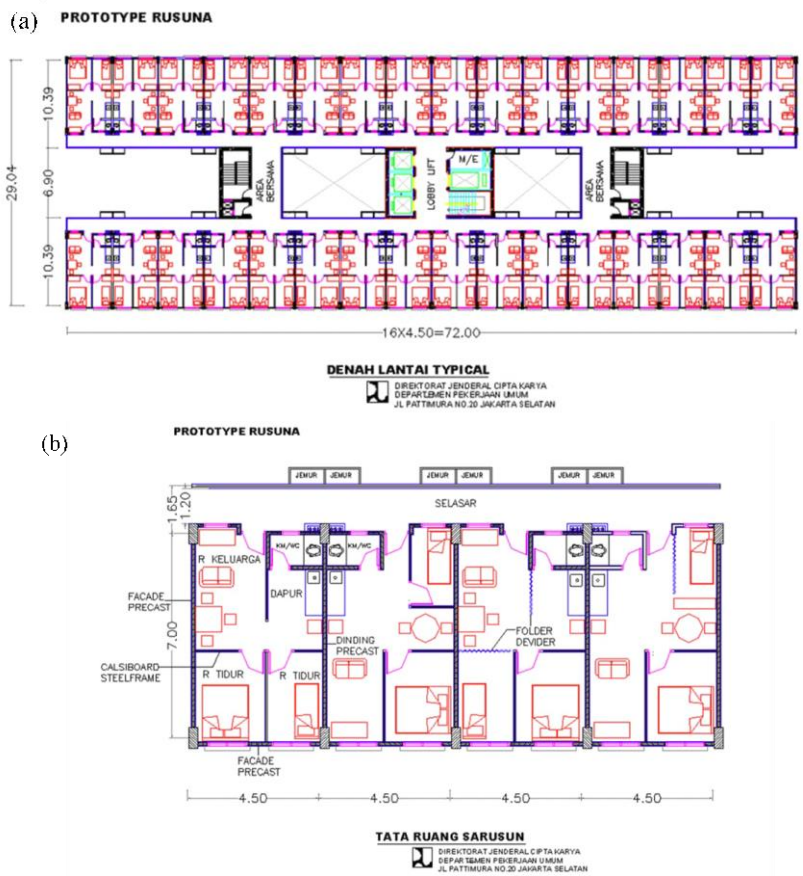


Figure 3.5. (a) Example of layout of *Rusunami* tower and (b) Example of floor plan of unit in *Rusunami* (Ministry of Public Works, 2007).

of a 1000 tower program launched by the central government in 2007 that specifically targeted middle-class population in urban area (Darmawan, 2011). Hereafter, this type of apartment named by middle-class high-rise apartment. This apartment is an official category of apartment that developed by individual or company that fulfil specifications and requirements as stipulated by Regulation of Ministry of Public Works Number 7 year 2007. The government interfered the development of this kind of apartment through subsidies and incentives such as free of value added tax, fixed lower interest rate with longer duration for mortgage, and subsidy for down payment and other costs free such as permit costs, land providing, public facilities and mechanical electrical facilities (Ministry of Public Works, 2007; 2015; 2016; Ministry of Finance, 2014).

As subsidized middle-class high-rise apartment, the development must comply with the requirements of government. As regulated by the Regulation of Ministry of Public Works Number 7 year 2007, the floor level of this apartment is determined more than 8 floor levels but not exceeded to 20 floors. Ground floor should be used for public spaces while first floor above used for the residential purpose. The unit has maximum total floor area of 30m² (some regulations such as Decree of Ministry of Finance say around of 36m²) consists of two bedrooms, one living room, one bathroom and one service space (for washing and kitchen). The regulation also determined the construction types, material used, architectural designs and so on in detail. Figures 3.5 illustrated the typical of this subsidized high-rise apartment type as regulated by the government. In this thesis, middle-class high-rise apartment as officially defined by Indonesian government is used.

3.2 Case study apartments

To understand the current conditions of the existing apartments of Indonesia, field experiments had been carried out in the city of Surabaya, Indonesia. As mentioned in the Section 1.3, the aims of this chapter are to investigate the detailed thermal environments and to evaluate thermal comfort in the three types of apartments in Indonesia.

Surabaya is the capital of East Java Province and the second biggest city in Indonesia with a total area of 326.4 km² and population of about 3.2 million by 2014. Located in 07°09'-07°21'S and 112°36'-112°54'E and situated in the coastal area. Surabaya has hot-humid climatic conditions, with the monthly average air temperature of 27.9-30.2°C and relative humidity of 64-92%. The maximum air temperature could reach up to 35.8°C while the maximum relative humidity could reach up to 99%. The city receives monthly average wind speeds of 3.1-4.1 m/s with major direction to East and West (BPS, 2014). Surabaya is one of the pilot project cities for development of public apartments so that it has larger proportion of public apartments compared to other cities in Indonesia (Darmawan, 2011). Meanwhile, the number of private apartments including middle-class high-rise apartments are also increasing in Surabaya (Arethusa, 2014).

One of the typical apartments from these three types (i.e., old public apartment, new public apartment and middle-class high-rise apartment) was selected for the field measurements, respectively. All the selected apartment buildings were located in the urban area. The selected old public and new public apartments were located about 10 km and 3.5 km from the downtown while the middle-class apartment was located about 6 km from the city center.

The selected old public apartment is a four storey building with 48 units (Figure 3.6a). The measurement was conducted in the south-facing unit located on the second floor. The unit has a standard size of 21m² with a semi-open corridor space. This corridor space is relatively wide (3.1m width) and well-ventilated. A multi-functional balcony is placed in between the indoor unit and outdoors (Figure 3.6b). Meanwhile, the new public apartment is a five storey building with 96 units (Figure 3.7a). The measurement was carried out in the west-facing unit located on the top floor. The unit size is slightly larger (24m²) but the corridor space is narrower (1.9m width) than that of the old public apartment. The corridor space is opened and adjacent to the void space (Figure 3.7b). Both of the public apartments are naturally ventilated. The main structure of both apartments are reinforced concrete and concrete block for walls with relatively high thermal capacities. The per-unit thermal mass of these apartments was calculated at 2,031 kg/m² for the old public apartment and 1,873 kg/m² for the new public apartment.

Meanwhile, the middle-class high-rise apartment is a 19 storey high-rise building comprising 762 units (Figure 3.8a). Almost all the units are equipped with one or two air-conditioner(s). The measurement was conducted in the west-facing unit located on the eighth floor, with a total floor area of 31m². The small balcony is only used for placing the outdoor units of air-conditioners (Figure 3.8b). Unlike the above public apartments, the long corridor



Figure 3.6. (a) View of selected old public apartment and (b) floor plan of selected unit.



Figure 3.7. (a) View of selected new public apartment and (b) floor plan of selected unit.

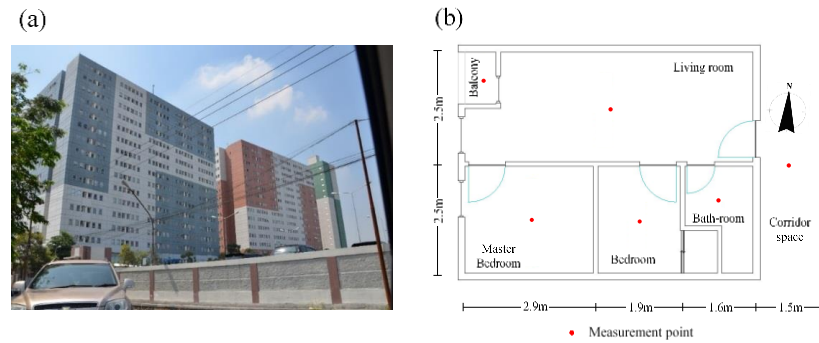


Figure 3.8. (a) View of selected middle-class private apartment and (b) floor plan of selected unit.

space is not well-ventilated. Reinforced concrete construction was used for the main structure while pre-cast concrete and aerated lightweight concrete were used for external wall and partition walls respectively. The per-unit thermal mass was calculated at $1,100 \text{ kg/m}^2$ which is 41-46% smaller than those for public apartments. Thermal insulation was not applied to ceiling/roof and walls in all the three apartments. This study focuses especially on the private apartments subsidized by the government for middle-class groups (Figure 3.8). Appendix A presents the floor plan and detail façade of respective case study apartments.

3.3 Methods

To investigate the current conditions of the existing apartments, first, field measurements were carried out in the unoccupied units of the above mentioned three types of apartments. At the same time, thermal responses of the occupants were collected through questionnaires and face to face interview whilst indoor thermal environments in the occupied units were measured. Finally, computer simulation was carried out to generalize the results of field measurements.

3.3.1 Field measurements

Field measurements were carried out during the hottest period in dry season of Surabaya, from August to October 2014. Detailed measurements of physical thermal comfort variables including air temperature, relative humidity, air velocity and globe temperature were measured at the center of one or two main rooms at 1.1m above floor in the selected units from the three apartments, respectively. Air temperatures in the other spaces including corridor spaces, balcony, kitchen and bathroom were also measured at 1.1m above floor level (see Figures 3.6b, 3.7b and 3.8c). These indoor measurements were carried out in unoccupied units under different natural ventilation conditions, they are: daytime ventilation, night ventilation, full-day ventilation and no ventilation. For the daytime ventilation, windows and all other openings were opened from 6:00 to 18:00. In contrast, all of them were opened from 18:00 to 6:00 during the night ventilation condition.

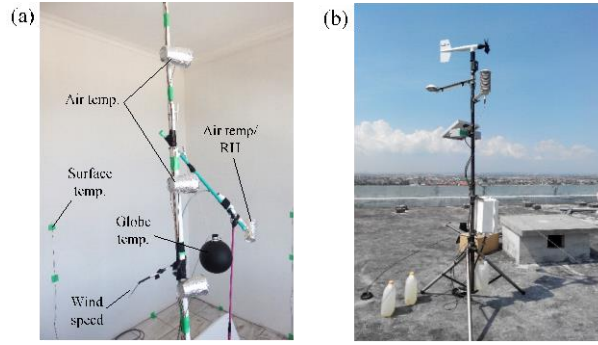


Figure 3.9. Instruments for (a) indoor measurement and (b) outdoor measurement.

Furthermore, vertical distribution of air temperature was measured at 0.1m, 0.6m, 1.1m, 1.5m, 2.0 m and 2.6m (and 2.4m in the case of the new public apartment) above floor level. Surface temperature was measured at the centers of each part of building fabric including floor, ceiling and walls (Figure 3.9a). The measurement for each ventilation condition was conducted for 7-8 days. During the measurements, the outdoor thermal conditions were recorded by weather stations placed on unobstructed and unshaded spaces (i.e., on the top of roof) in the measurement site (Figure 3.9b). All measurements were logged automatically at 10-minute intervals. Table 3.1 presents the measurement instruments used during the field measurements.

Before analyzing indoor thermal environment as well as thermal comfort in the existing apartments, some variables such as mean radiant temperature and operative temperature are calculated using equations in order to make the data processing consistent throughout this thesis. Mean radiant temperature is defined as the uniform temperature of an imaginary enclosure in which radiant heat transfer from the human body equals the radiant heat transfer in the actual non-uniform enclosure (ASHRAE, 2017). Meanwhile, mean radiant temperature is calculated based on the globe temperature, which is in case of natural convection is expressed by following equation (BSI, 2002):

$$\bar{T}_r = \left[(T_g + 273)^4 + \frac{1.1 \times 10^8 \times v^{0.6}}{\epsilon_g \times D^{0.4}} (T_g - T_a) \right]^{1/4} - 273 \quad (3.1)$$

where \bar{T}_r is mean radiant temperature (°C), T_g is globe temperature (°C), v is air speed (measured at the level of the globe) (m/s), ϵ_g is emissivity of the black globe (-) and D is diameter of the globe (m). The emissivity of the black globe is taken as 0.98 in all the calculations in this thesis.

Meanwhile, operative temperature is calculated from the same standard as follow:

$$T_{op} = \frac{T_a \sqrt{10v} + \bar{T}_r}{1 + \sqrt{10v}} \quad (3.2)$$

where T_{op} is the operative temperature (°C), v is wind speed (m/s), and \bar{T}_r is mean radiant temperature (°C). This operative temperature expresses the uniform temperature of an imaginary black enclosure in which an occupant would exchange the same amount of heat by radiation plus convection as in the actual non-uniform environment (ASHRAE, 2017).

Table 3.1. Description of measurement instruments used in the selected apartments.

Measured variable	Instrument model	Accuracy
<i>Master Bedroom (old public apartment)</i>		
Air temperature and RH	T&D TR-72U	±0.3°C; ±5% RH
Globe temperature	Thermocouple type T inside 150mm black globe	±0.1%+0.5°C plus ±0.5°C for cold junction compensation
Wind speed	Kanomax probe 0965-03	±0.15 m/s at 0.1 – 4.99 m/s
<i>Master Bedrooms (new public and private apartments)</i>		
Air temperature and RH	Vaisala HMP155	±0.10°C; ±1.0% RH at 0-75% RH
Globe temperature	Thermocouple type T inside 150mm black globe	±0.1%+0.5°C plus ±0.5°C for cold junction compensation
Wind speed	Kanomax probe 0965-03	±0.15 m/s at 0.1 – 4.99 m/s
<i>Living rooms (new public and private apartments)</i>		
Air temperature and RH	T&D TR-72U	±0.3°C; ±5% RH
Globe temperature	Thermocouple type T inside 75mm black globe	±0.1%+0.5°C plus ±0.5°C for cold junction compensation
Wind speed	Kanomax probe 0965-03	±0.15 m/s at 0.1 – 4.99 m/s
<i>Corridor space</i>		
Air temperature and RH	T&D TR-72U	±0.3°C; ±5% RH
Globe temperature	T&D TR-52i inside black ping-pong ball	±0.3°C
Wind speed	Kanomax probe 0965-03	±0.15 m/s at 0.1 – 4.99 m/s
<i>Other rooms</i>		
Air temperature	Thermocouple type T	±0.1%+0.5°C plus ±0.5°C for cold junction compensation
<i>Weather Station (old public apartments)</i>		
Air temperature and RH	HOBO Pro v2 U23-001	±0.2°C; ±2.5% RH at 10-90% RH
Wind speed and direction	Onset S-WCA-M003	±0.5m/s; ±5°
Global horizontal solar radiation	Onset S-LIB-M003	±10 W/m ² or ±5% plus ±0.38 W/m ² K for additional temp.
Rainfall	Onset S-RGB-M002	±1.0% at up to 20 mm/hr
<i>Weather Station (new public and private apartments)</i>		
Air temperature and RH	Vaisala HMP155A	±0.3°C; ±5% RH
Wind speed and wind direction	Young 05103	±0.3 m/s or 1% of reading; ±3° for wind direction
Global horizontal solar radiation	Hukseflux SR20	±2 W/m ²

Finally, adaptive comfort standards are used as instruments to evaluate thermal comfort (ACE) in the existing apartments of Indonesia. In particular, adaptive thermal comfort equations for naturally ventilated in the hot-humid climatic conditions developed by Toe and Kubota (2013) are employed. Equation 3.3 calculates the neutral temperature in terms of operative temperature (OT) while the 80% of upper comfortable limit is calculated using Equation 3.4.

$$T_{neutop} = 0.57T_{outdm} + 13.8 \quad (3.3)$$

$$T_{upper} = T_{neutop} - 0.7 \quad (3.4)$$

where T_{neutop} is neutral operative temperature (°C), T_{outdm} is daily mean outdoor air temperature (°C), i.e., the 24-hour arithmetic mean for the day in question, and T_{upper} is upper comfort operative temperature limit (°C).

In addition, Standard Effective Temperature (SET*) is used to evaluate thermal comfort particularly the cooling effect of wind speed. SET* is defined as the equivalent air temperature of an isothermal environment at 50% of relative humidity in which a subject, wearing clothing standardized for the activity concerned, has the same heat stress and thermoregulatory strain as in the actual environment (ASHRAE, 2017). As defined, the SET is calculated by a thermophysiological simulation of human body by reducing any combination of real environmental and personal variables into the temperature of imaginary standard environment, which is at 0.57 clo and 1.25 met (Szokolay, 2004). Thus, this model enables air speed effects on thermal comfort to be related across a wide range of air temperatures, radiant temperatures and humidities. The SET* is calculated using following equation (ASHRAE, 2017):

$$SET^* = T_{op} + w_{i_m} LR(p_a - 0.5p_{ET^*,s}) \quad (3.5)$$

where SET^* is standard effective temperature (°C), T_{op} is operative temperature (°C), w_{i_m} is skin wittedness (dimensionless), LR is ratio of convective and evaporative heat transfer coefficients (dimensionless), p_a is barometric pressure (kPA) and $p_{ET^*,s}$ is saturated vapor pressure at effective temperature (kPA).

3.3.2 Questionnaires and face to face interview

The field survey was conducted at the same time as the field measurements conducted. The survey is composed of face-to-face interview and one-week thermal measurements. Face-to-face interviews were conducted using a questionnaire form list covered socio-demographic profile of respondents, average daily occupancy in both weekdays and weekends; ownership and the usage of cooling appliances; thermal sensations and preferences during the daytime and night-time; indoor air quality and windows/doors opening behavior. A 7-scale of thermal sensation was used to evaluate thermal sensation (from -3 for cold to 3 for hot). The same scale also used to assess wind sensation (from -3 for too still to 3 for too breezy) and humidity sensation (from -3 for too dry to 3 for too humid). Meanwhile, thermal preferences and humidity preference of the occupants were assessed by a 5-scale of thermal preference and humidity preference was used (from -2 for much cooler/much more humid to 2 for much warmer/much drier) whilst a-7 scale of wind preferences was used (from -3 for much more still to 3 for much more breezy). Moreover, during field survey, room arrangement and window devices were sketched. Appendix B presents the detailed drawing of respective occupied units while the detailed questionnaires used during field survey in the occupied units of public apartments, while are presented in Appendix C.

Thermal measurements were conducted in total 42 apartment units for one week period: 15 units for old public apartment, 17 units for new public apartment, and 10 houses for middle-high-rise apartments. Two data-loggers were attached in a stand pole at 1.1 m above floor level to measure indoor air temperature, indoor relative humidity and globe temperature. Indoor air

temperature and relative humidity were measured using TR-72ui (accuracy of $\pm 0.3^{\circ}\text{C}$ for air temperature and $\pm 5\%$ for relative humidity), while globe temperature was measured using T&D TR-52i (accuracy of $\pm 0.3^{\circ}\text{C}$) by inserting the sensor into a black-painted ping-pong ball. The equipment was installed in the living room and set to avoid direct solar radiation. In addition to weather station, outdoor air temperature and relative humidity were measured using TR-73Ui (accuracy of $\pm 0.3^{\circ}\text{C}$ for air temperature and $\pm 5\%$ for relative humidity). The outdoor data logger was installed in a large open space at a certain height under the shade to prevent the effect of solar radiation.

3.3.3 Computer simulation

As described in the Section 3.2, conditions of selected apartments for field measurements were different. To generalize the indoor thermal environment of current existing apartments under the same conditions, computer simulation was carried out to investigate its response to changing conditions inside and outside the building. Simulation test cases and weather conditions are considered in this section after base models are developed. The models represent the actual building forms with some simplifications and material properties of the buildings.

3.3.3.1 The simulation program used and simulation conditions

Over the past 50 years, hundreds of building energy programs have been developed, enhanced and are in use, and some of them were reviewed (Crawley *et al.*, 2008). Since naturally ventilated apartments were going to be simulated, TRNSYS and COMIS were used in this simulation. TRNSYS and COMIS are a multi-zone airflow network program, in coupled simulations; indoor temperatures and air flow rates are interdependent in naturally ventilated buildings.

TRNSYS 3.3 is the transient systems simulation program that has been available since 1975 and remains as one of the most flexible energy simulation software packages by facilitating the addition of mathematical models, available add-on components, the capabilities of the multi-zone building model, and the ability to interface with other programs. It has a module structure, where some components (called Type) are connected graphically in the Simulation Studio and compiled internally as a TRNSYS input file (known as the deck file) for the simulation engine. The Simulation Studio is a complete simulation package that integrates the simulation engine, components, components' connections of components, and output in the form of user interface tools. During the simulation, the components were called by the TRNSYS engine and their mathematical models iterated until convergence was reached within the specified tolerances. Output files were generated and post-processed in Excel spreadsheets after the simulation (Toe, 2013). Meanwhile, COMIS is known as a multi-zone airflow network model that can simulate infiltration and ventilation through crack flow and flow through large openings in multi-zone buildings (Dorer *et al.*, 2005; Feustel, 1999). In this simulation, COMIS version 4.2.0.28 was used. It works in a modular structure that is similar to TRNSYS in the Simulation Studio.

TRNSYS Type56 'Multi-zone Building' was used to model the thermal zones of the

apartment buildings, and then coupled with COMIS via Type 157 in TRNSYS. The building model in Type56 is an energy balance model describing the thermal behavior of the building, which is divided into different thermal zones and air nodes through TRNBUILD user interface. This component requires the number of building information, e.g. building material data, wall construction data, windows opening schedule, etc. The heat balance model of the whole building basically considers (1) convective heat fluxes to the air node; (2) coupling with other zones; and (3) radiative heat flows to the wall and windows. Mathematical equation for convective heat flux to the air node is showed in the Equation 3.6 while radiative heat flows to the wall and windows is indicated in Equation 3.7 (Klein *et al.*, 2012).

$$\dot{Q}_i = \dot{Q}_{surf,i} + \dot{Q}_{inf,i} + \dot{Q}_{vent,i} + \dot{Q}_{g,c,i} + \dot{Q}_{cplg,i} + \dot{Q}_{solair,i} + \dot{Q}_{ISHCCI,i} \quad (3.6)$$

where \dot{Q}_i is convective heat flux to the air node (W), $\dot{Q}_{surf,i}$ is the convective gain from surfaces (W), $\dot{Q}_{inf,i}$ is the infiltration gains (air from outside only) (W), $\dot{Q}_{vent,i}$ is the ventilation gains (W), $\dot{Q}_{g,c,i}$ is the internal convective gains (by people, equipment, etc.) (W), $\dot{Q}_{cplg,i}$ is the gain due to air from other zones (W), $\dot{Q}_{solair,i}$ is the fraction of solar radiation entering an air node through external windows which is immediately transferred as a convective gain to the internal air (W), and $\dot{Q}_{ISHCCI,i}$ is the absorbed solar radiation on all internal shading devices of zone and directly transferred as a convective gain to the internal air (W).

$$\dot{Q}_{r,w_i} = \dot{Q}_{g,r,w_i} + \dot{Q}_{sol,w_i} + \dot{Q}_{long,w_i} + \dot{Q}_{wall-gain} \quad (3.7)$$

where \dot{Q}_{r,w_i} is the radiative gains for the wall surface (W), \dot{Q}_{g,r,i,w_i} is the radiative air node internal gain received by wall (W), \dot{Q}_{sol,w_i} is the solar gains through windows received by wall (W), \dot{Q}_{long,w_i} is the long-wave radiation exchange between this wall and all other wall and windows (W), and $\dot{Q}_{wall-gain}$ is the specified heat flow to the wall or window surface (W).

The development of simulation model was refer to the previous works of Toe (2013), as shown in the Figure 3.10. Figure 3.10 describes the coupling relationship between the two programs in the whole simulation model. In this coupling method, Type 157 was treated like any other TRNSYS components and COMIS was thus called together in each iteration step until the mass and energy balance per zone reached convergence (Toe, 2013). As shown, data of the air flow rates per zone were transferred from Type 157 to Type 56 and in exchange, the zone air temperatures data were transferred from Type 56 to Type 157. The air flow included flow from outside and flow between zones. The Modified-Euler method was selected, and the successive solution method that should be used for buildings and systems with a thermal capacity was applied. All of the simulations attained convergence within a tolerance of 0.01.

The building in COMIS was modelled as a network of pressure nodes linked by air-mass flow paths including flow resistances caused by open or closed doors and windows as well as air leakage through walls and other building surfaces. The air volume (i.e. the room or zone) represented by each internal pressure node is assumed to be well mixed and has a fixed uniform pressure and temperature at each time step. Meanwhile, the wind pressure field around the building is attributed to external pressure nodes. Air leakage characteristics of the building constructional joints and surfaces for the whole building envelope as well as internal surface

were represented by crack flow, which is calculated by the power law equation as follow (Feustel and Raynor-Hoosen, 1990; Orme *et al.*, 1998):

$$\dot{Q} = C_{\dot{Q}}(\Delta P)^n \tag{3.8}$$

where \dot{Q} is volume flow (m^3/s), $C_{\dot{Q}}$ is volume flow coefficient (m^3/sPa^n), ΔP is pressure difference across the link (Pa) and n is flow exponent (-).

Temperature correction in the crack was not applied in this study due to the unavailability of the measurement data to determine the actual air leakage temperature. Instead, the standard reference data were used for the flow coefficients. Nevertheless, it is assumed that the air and the wall would have the same temperatures since apartment buildings have the tiny crack form in the wall constructions. It is also assumed that no thermal gradient over the height of the air flow component.

Since natural ventilation through open windows is a main interest of this simulation, windows and doors were modelled as large vertical openings. In COMIS, large opening is divided into several vertical layers at equal distance, and the mass flow is then solved for each layers. When they closed, pressure difference calculations are applied to the entire window frame including bottom crack, top crack and vertical side cracks. Furthermore, bi-directional flow is calculated when they are open by incorporating a discharge coefficient that represents a contraction effect on the flow due to the opening and effective opening area. The air flow for the vertical cracks is calculated by the summation of the flows over the vertical height (Feustel, 1999).

In this simulation, each thermal zones contained one air-node. Basically, the heat balance model of the whole building considers: (1) convective heat fluxes to the air-nodes; (2) short-wave and long-wave radiation, conduction and convection heat fluxes to the walls and

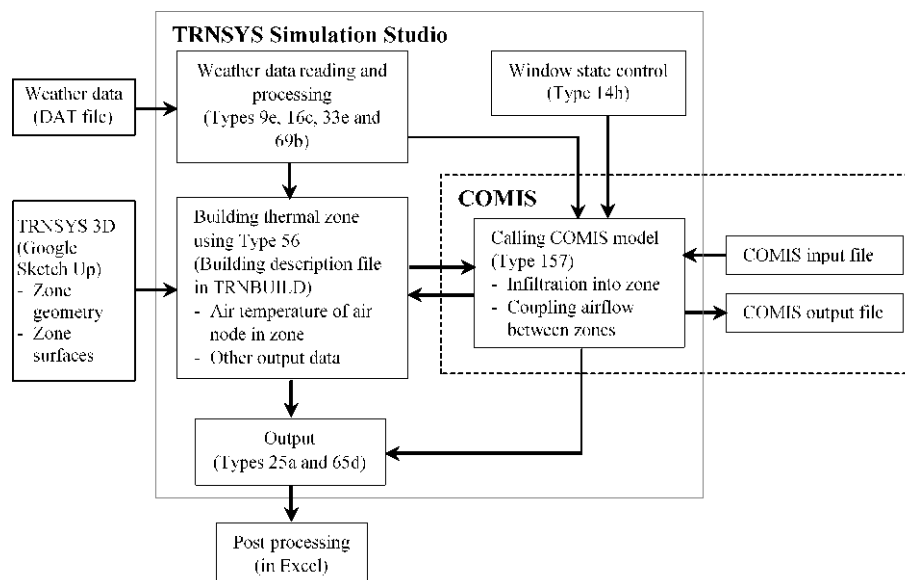


Figure 3.10. Components and data transfer in the TRNSYS-COMIS simulation.

windows; and (3) the thermal history of high thermal mass walls (Klein *et al.*, 2012). Standard models for beam and diffuse radiation distributions to inside surfaces and long-wave radiation exchange within each zone were used since the apartments had ordinary constructions comprising opaque facades and windows. Moreover, moisture balance was calculated in the Type 56 by considering the free floating humidity ratios in the naturally ventilated zones.

The weather data, simulation time and schedules were defined in TRNSYS and used simultaneously by both TRNSYS and COMIS models. The weather data that were measured on site directly during the field measurements from the weather stations were employed in the simulation. The raw weather data covered dry bulb temperature, relative humidity, wind speed, wind direction, barometric pressure and global horizontal solar radiation. In TRNSYS, these weather data were first read by Type 9e as average values over the data time interval without interpolation. Several other weather variables were derived to provide the necessary input for the simulation. The total horizontal radiation was divided into its beam and sky diffuse components on the horizontal surface by Type 16c. The incident radiation components received on respective building surfaces including vertical and tilted surfaces were then estimated internally as defined in Type 56. The long-wave radiation exchange from external surfaces of the building to the atmosphere; effective sky temperature was estimated by Type 69b as a function of the dry bulb temperature, dew point temperature, atmospheric pressure and cloudiness factor of the sky. Furthermore, moist air properties were estimated from the known dry bulb temperature and relative humidity using a psychrometric processor, i.e. Type 33e. The derived variables were humidity ratio, dew point temperature, densities of air with and without water vapor, and enthalpy.

3.3.3.2 Base model apartments and simulation cases

Each of apartment buildings that used to be performed in the field measurements, i.e. old public apartment, new public apartment and middle-class high-rise apartment were modelled for the purpose of this simulation study in order to validate the base model. Since the selected apartments represent the typical apartments in Indonesia, in terms of spatial design and building structures (see Sections 3.1 and 3.2), and thus they matched with the objectives of this study. The base model followed the data as well as the experimental setup outlined in the previous section.

The geographical location of the base model followed that of the actual apartments, i.e. 7°15'00"S and 112°45'00"E at an elevation of 6m above sea level. Weather data that was measured on site throughout the field experiment period, i.e. 01-30 October 2014, was used. The simulation time step was set to coincide with the weather data at 10-minute intervals. The building orientations were different, and represented the actual situation of the measured apartments. External façade of the master bedroom in old public apartment faces toward south while that of in new public and middle-class high-rise apartments face west respectively.

The apartment models for this simulation were modelled in three dimensions using the TRNSYS 3D plug-in in Google SketchUp interface so that the three dimensional data were read in TRNBUILD. The apartment models were developed based on the actual conditions with some modifications in order to simplify the models. It is impossible to build a complete model as the real conditions due to the limited capacity of this software in modelling the air-

nodes, which is up to 200 air-nodes only. The heat in the selected unit are assumed to be transferred through not only between the indoor and outdoor through thermal boundary, but also through surrounding spaces (i.e. other units and corridor space).

Figure 3.11 illustrates exterior views of the old public apartment model. In the old public apartment model, the number of simulated units was reduced from 48 units to 12 units. Meanwhile, the length of corridor space was shortened with maintaining the ratio of openings to total floor area which is around of 0.178. Thus, this model comprises 17 thermal zones, which was consist of three thermal zones in the selected unit and 13 thermal zones in neighboring rooms (e.g. left- and right-side of the selected unit and upper- and lower-side of the selected unit) and corridor space. The above three thermal zones represent each partitioned rooms as follows: main room, balcony, and restroom. The ground floor was considered as single thermal zone while the top floor was considered as the shading objects and their heat transfers were not simulated (see Figure 3.11b).

Figure 3.12 shows exterior views of the new public apartment model. In this model, the selected unit which is located on the top floor comprised five thermal zones represent

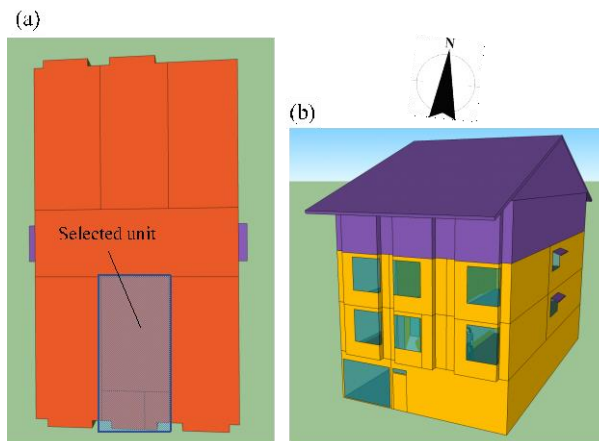


Figure 3.11. (a) Location of the selected unit in the model and (b) front view of the old public apartment. Surfaces in purple are shading objects and their heat transfers are not simulated.

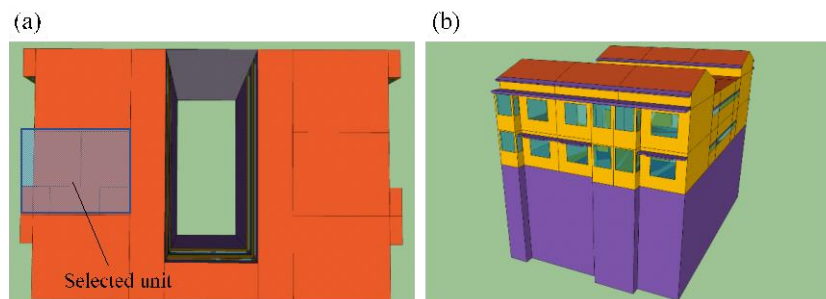


Figure 3.12. (a) Location of the selected unit in the model and (b) front view of the new public apartment. Surfaces in purple are shading objects and their heat transfers are not simulated.

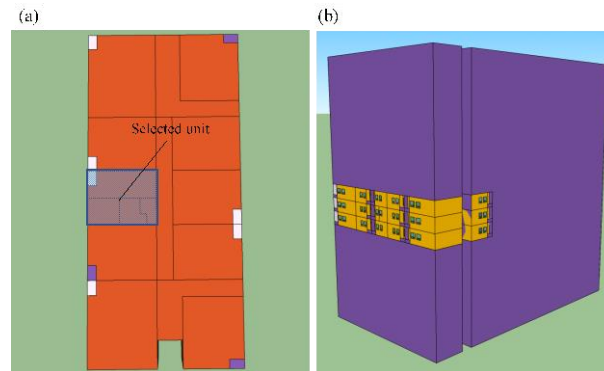


Figure 3.13. (a) Location of the selected unit in the model and (b) front view of the middle-class high-rise apartment. Surfaces in purple are shading objects and their heat transfers are not simulated.

following spaces: living room, master bedroom, bathroom, kitchen and balcony (see Figure 3.7b). Meanwhile, neighboring units and corridor spaces were considered as a single thermal zone and connected to main thermal zones. In this model, the total of 28 thermal zones were developed and connected each other after the number of units simulated was reduced from 96 units to 12 units. In spite of the selected unit, these thermal zones represent neighboring units and corridor spaces. Unlike old public apartment model, this model considered the roof as single thermal zone for each units. Meanwhile, the length of corridor space was shortened without maintaining the ratio of openings to total floor since it is open corridor spaces. From the ground floor to the third floor were considered as the shading objects and therefore their heat transfers were not considered (see Figure 3.12b).

Figure 3.13 illustrates the simplified model of the middle-class high-rise apartment model. In this model, simulated model was located on the eighth floor consist of four thermal zones represent living room, master bedroom, bedroom and bathroom (see Figure 3.8b). Like public apartments models (i.e. old public and new public apartments), each of neighboring units and corridor spaces were considered as single thermal zones. The spaces above 9th floor level and below 7th floor level were considered as shaded objects and thus no heat transfers occurred in those spaces (Figure 3.13b). After simplified from the total of 762 units to 30 units, this model comprised of 42 thermal zones. As old public apartment model, this model shortened the length of the corridor spaces whilst maintaining the ratio of openings to total floor since it is enclosed corridor spaces.

Table 3.2 shows the thermal properties of the building materials that were assigned to the each base models (i.e. old public apartment, new public apartment and middle-class apartment). Since the thermal property of material data of Indonesia are not available, then some properties such as density, specific heat capacity and thermal conductivity of each material were refer to the reference books (such as Szokolay, 2004), manufacturer's datasheet (Hebel, 2018; Boral, 2018) and related national standard of Indonesia (see BSN, 2002, 2013). The thermal properties of the windows (glazing and frame) were standard data in the WINDOW (Mitchell *et al.*, 2011). The constructional layers and reference U-values of respective building elements

Table 3.2. Thermal properties of the building materials in the base models.

Material	Density (kg/m ³)	Specific heat capacity (kJ/kgK)	Thermal conductivity (kJ/hmK)	Thermal resistance (hm ² K/kJ)
<i>Old public apartment</i>				
Cement plaster	1250	0.840	2.595	n/a
Concrete hollow block	2300	1.000	5.868	n/a
Concrete slab	2400	0.880	6.264	n/a
Ceramic tile	2022	1.250	3.987	n/a
Plywood (door)	480	1.680	0.468	n/a
PVC door pane	1200	1.000	0.540	n/a
<i>New public apartment</i>				
Cement board	550	0.960	1.843	n/a
Cement plaster	1250	0.840	2.595	n/a
Concrete block	2100	1.000	1.630	n/a
Concrete slab	2400	0.880	6.264	n/a
Ceramic tile	2022	1.250	3.987	n/a
Plywood (door)	620	1.300	0.497	n/a
PVC door pane	1200	1.000	0.540	n/a
Roof tile	1700	1.000	1.800	n/a
<i>Middle-class private apartment</i>				
Aerated light concrete	780	0.920	0.536	n/a
Cement board	550	0.960	1.843	n/a
Cement plaster	1250	0.840	2.595	n/a
Concrete slab	2400	0.880	6.264	n/a
Ceramic tile	2022	1.250	3.987	n/a
Precast concrete	2100	0.840	5.040	n/a
PVC door pane	1200	1.000	0.540	n/a
Timber (door)	620	1.300	0.497	n/a

are listed in Table 3.3. A time base of 1h was set for the transfer function to represent the thermal mass behavior of the walls. Initial zone air temperatures and relative humidity for the simulation were based on the field experiment data.

Wind pressure coefficients in this simulation were estimated using a parametrical model developed by Grosso (1992, 1995) known as CPCALC⁺. The tool applies to rectangular block buildings without overhangs (Grosso, 1992). The calculation considers terrain roughness (wind velocity profile exponent), surrounding buildings (building height and density), aspect ratios and wind direction. Considering that, a wind velocity profile exponent of 0.28 was used to represent the urban area. Discharge coefficients were calculated internally in COMIS while flow coefficients and flow exponents of cracks and openings were selected from references given by Orme and Leksmono (2002), as summarized in Table 3.4.

The simulation test cases mainly focus on parameters for generalization of indoor thermal environments in the existing apartments due to the limitation of field measurements. As previously described, the field measurements were conducted in different conditions (i.e. orientation, floor levels) and thus the simulation cases varying the ventilation conditions on

the orientations and unit positions. The test cases related to natural ventilation condition replicated the window opening patterns of the field experiment to represent night ventilation, daytime ventilation, no ventilation and full-day ventilation conditions while those related to the orientation evaluate the external wall's orientation of the units (i.e. North-facing, South-facing, East-facing and West-facing). The simulation was conducted under the same position, which is in the intermediate floors with the assumption that the number of units located on the top floor and the ground floor is smaller than that in the intermediate floors (between the ground level and top floor). Finally, all the simulation cases evaluate and compare the selected units under the same conditions (i.e. ventilation condition, orientation and position of unit). Table 3.5 summarizes the simulation test cases and their test conditions.

Table 3.3. Constructional layers and reference U-values of the base models.

Building element	Constructional layers	Reference U-value ^a (W/m ² K)
<i>Old public apartment</i>		
Ceiling	Cement plaster (2mm thick)+ concrete slab (200mm) + cement plaster (20mm) + ceramic tile (5mm)	3.194
External and party walls	Cement plaster (2mm)+ concrete hollow block (110mm) + cement plaster (2mm)	4.115
Floor	Ceramic tile (5mm) + cement plaster (20mm) + concrete slab (200mm) + cement plaster (2mm)	3.194
Window	Single layer float glass (6mm)	5.610
<i>New public apartment</i>		
Ceiling	Cement board (12mm)	3.482
Floor	Ceramic tile (5mm) + cement plaster (20mm) + concrete slab (150mm) + cement plaster (2mm)	3.768
External and party wall	Cement plaster (2mm)+ concrete block (140mm) + cement plaster (2mm)	2.087
Internal wall (living room)	Cement board (6 mm) + air gap (80 mm) + cement board (6 mm)	1.743
Pitched roof	20mm thick clay roof tile + 25mm thick timber batten	4.762
Window	Single layer float glass (6mm)	5.610
<i>Private apartment</i>		
Ceiling	Cement board (6mm)+ concrete slab (150mm) + cement plaster (20mm) + ceramic tile (5mm)	3.193
Floor	Ceramic tile (10mm) + cement plaster (20mm) + concrete slab (150mm) + cement plaster (2mm)	3.090
External wall	Cement plaster (2mm)+ precast concrete (80mm) + cement plaster (2mm)	4.546
Internal wall (bedrooms)	Cement board (12 mm) + air gap (80 mm) + cement board (12 mm)	0.244
Internal wall (bathroom)	Ceramic tile (5mm) + cement plaster (10mm) + lightweight concrete (120 mm) + cement plaster (2mm)	1.978
Party wall	Cement plaster (2mm)+ lightweight concrete (120mm) + cement plaster (2mm)	2.035
Window	Single layer float glass (6mm)	5.610

Table 3.4. Flow coefficients and flow exponents of the base model. Note: Selected data from Orme and Leksmono, 2002.

Building element	Flow coefficient	Flow exponent (-)
<i>Crack component^a</i>		
	Unit: kg/sm ² Pa ⁿ	
Plastered brick wall	2.18 x 10 ⁻⁵	0.85
Concrete slab	2.54 x 10 ⁻⁵	0.84
Tiled roofing ^b	9.68 x 10 ⁻³	0.55
Fibre ceiling board	1.14 x 10 ⁻⁴	0.76
<i>Large opening component^c</i>		
	Unit: kg/smPa ⁿ	
Window (hinged, with rubber seal)	1.57 x 10 ⁻⁴	0.60
Window (hinged, without rubber seal)	8.95 x 10 ⁻⁴	0.60
Window (sliding)	2.78 x 10 ⁻⁴	0.60
Window (louvred) ^d	2.88 x 10 ⁻³	0.60
External door (hinged)	1.45 x 10 ⁻³	0.60
Internal door	1.57 x 10 ⁻³	0.60

^a The flow coefficient is given per surface area.

^b Less airtight construction was assumed by applying a multiplication factor of 2 to the original value.

^c The flow coefficient is given per length of joint.

^d The given flow coefficient per louvre is 4.114 x 10⁻⁴ kg/smPaⁿ.

Table 3.5. The simulation test cases and their test conditions.

Parameters	Test conditions			
	1	2	3	4
Natural ventilation conditions	<i>Night ventilation</i> • Closed 6 a.m.-6 p.m. Open 6 p.m.-6 a.m.	<i>Daytime ventilation</i> • Open 6 a.m.-6 p.m. Closed 6 p.m.-6 a.m.	<i>No ventilation</i> • Closed 24h	<i>Full-day ventilation</i> • Open 24h
Orientation (external-wall)	North-facing	South-facing	East-facing	West-facing

3.4 Thermal comfort in unoccupied units

As previously described, this section addresses the current problems of the existing apartments under unoccupied condition by investigating the indoor thermal environments and evaluating thermal comfort inside mainly focus on the master bedrooms of respective apartment types. The results of field measurements are presented in sub-section 3.4.1, which is divided into four main sub-sections, i.e. daytime ventilation, night ventilation, full-day ventilation and no ventilation. Sub-section 3.4.2 presents the results of computer simulation on the respective existing apartment types under same parameters, to compare the indoor thermal environment as well as to evaluate indoor thermal comfort.

3.4.1 Field investigation of indoor thermal environments

3.4.1.1 Indoor thermal environments in different natural ventilation conditions

The outdoor air temperature during the field measurements ranged from 22.2-34.6°C with the average of 28.3°C, while the outdoor relative humidity ranged from 22-86%. Daily global horizontal solar radiation recorded at 21.1-27.3 MJ/m² on these days. There were no rainy days during the field measurements. The average outdoor wind speeds at the same height of the measured units were 0.7 m/s (old public), 1.4 m/s (new public) and 2.1 m/s (middle-class high-rise apartment), respectively. Figures 3.14-3.16 show the temporal variations of the thermal variables measured in the master bedrooms, living rooms and corridor space in the respective apartment types at 1.1m height above floor with the corresponding outdoor conditions for daytime and night ventilation condition, respectively. Based on the previous study (Arethusa, 2014), open the windows during the daytime and close them during night-time, i.e. daytime ventilation, is common practice of occupants of apartments in Indonesia.

When daytime ventilation was applied, the indoor air temperatures of the master bedroom of the old public apartment are relatively stable at 28.0-30.9°C. The maximum indoor air temperatures are around of 30.6-30.9°C, which is 3.1-3.8°C lower than the corresponding outdoors. In the other hand, during the night-time, indoor air temperatures are 4.8-5.2°C higher than the outdoors (Figure 3.14a). Indoor air temperature is well stabilized due to the relatively high thermal mass, which is around of 2,031 kg/m². The other reason for relatively lower indoor air temperature is the building orientation (south-facing) so that does not receive direct solar radiation (see Figure 3.20a). Although windows were open during the daytime, the indoor air temperatures in old public apartments are not closer to the outdoors mainly due to the existence of large balcony as shading devices and the semi-open corridor space as thermal buffer zone. As shown in Figures 3.14a, although the large corridor space was well ventilated during the daytime as shown in the wind speed measurements, the corresponding air temperature maintained lower values than the outdoors. Since it is semi-open space, the corridor space reduces internal heat gain particularly during the peak hours although its air temperature during the night-time still higher than the outdoors due to the high thermal mass effect.

When the night ventilation is applied, the maximum indoor air temperatures in the master bedroom of the old public apartment are 4.0-4.6°C lower than the outdoors (Figure 3.14b); these differences are about 0.9°C lower than those of when daytime ventilation is applied. In contrary, nocturnal indoor air temperatures shows the opposite pattern; about 3.3-4.1°C higher than the outdoors. These values are 1.1-1.5°C lower than those of when daytime ventilation is applied. This is due to the nocturnal ventilative cooling through open windows and thermal mass effect of the cooled building structures from the respective previous nights.

In contrast, during the peak hours, daytime indoor air temperatures in master bedrooms as well as in the living rooms in both new public and middle-class high-rise apartment are higher than the outdoors, around of 2.2-3.3°C and 3.0-3.6°C higher, respectively. As shown, the nocturnal indoor air temperatures in both rooms also much higher than the outdoors, which are around 3.1-6.0°C and 4.1-6.6°C higher, respectively (Figures 3.15-3.16). In the case of new public apartment, the average air temperature in the master bedroom was approximately

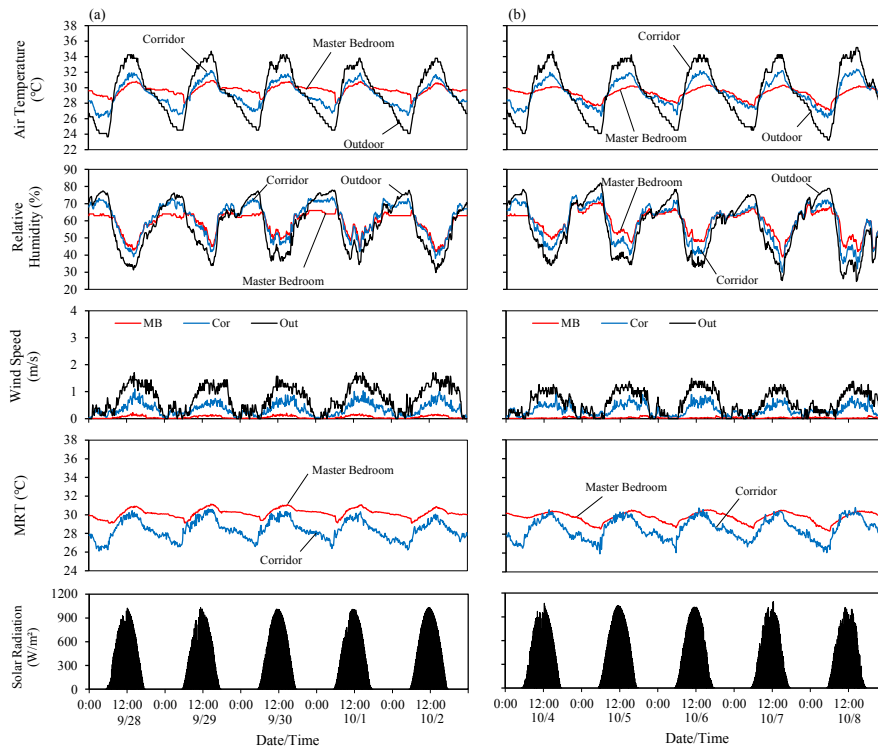


Figure 3.14. Temporal variations of indoor thermal environments in the old public apartment under (a) daytime ventilation and (b) night ventilation conditions.

1.8-3.5°C higher than the outdoors and 1.0-2.7°C higher than those in the corridor space. Meanwhile, the average air temperature in the master bedroom in the middle-class h apartment was approximately 1.6-2.9°C higher than the outdoors and 1.1-2.5°C higher than those in the corridor space (Figure 3.15a). The heat from the outdoor air is stored in the building structures and radiates to the indoor spaces at night. Since windows are closed during night-time, heat is confined inside the house and nocturnal indoor air temperature in the daytime ventilated room maintains higher than the night ventilated room on average. Since both apartments, i.e. new public and middle-class high-rise apartments are west-facing oriented, the effects of solar radiation must be taken into account into the higher indoor air temperatures. Meanwhile, the relatively higher nocturnal indoor air temperatures were caused by the thermal mass effects in the above three apartments. Further, wind speeds of new public apartment are relatively higher than those of other apartments mainly because of the cross ventilation due to the existence of open corridor space. Although the outdoor wind speeds in the middle-class high-rise apartment are much higher (up to 6.1 m/s) due to the altitude of the unit, but cross ventilation is not occurred and therefore it has low ventilation rate, which is averagely of 0.1-0.2 m/s (see Figure 3.16a).

During the peak hours, indoor air temperatures in the living room were slightly lower than those in the master bedroom, most probably due to the room-adjacent corridor spaces. As shown in Figure 3.15a, the profile of corridor space's air temperatures tends to follow the outdoors, since the corridor space in the new public apartment is open space. As the old public apartment, nocturnal air temperatures of corridor space are higher than the outdoors for the same reason, thermal mass effect. Meanwhile, corridor spaces in the middle-class high-rise apartment are enclosed space and therefore the profile of its air temperatures completely different than previous public apartments. The profile of corridor space's air temperature is relatively stable (Figure 3.16a).

The same phenomena do not occurred in both new public and middle-class high-rise apartments when the night cooling is applied. During the peak hours, the indoor air temperatures are almost the same as, and even higher than those in the old public apartment, which is around of 3.3-4.1°C and 2.5-4.2°C higher than the outdoors, respectively (Figures 3.15b-16b) . The effects of nocturnal ventilative cooling are cut off by the direct solar radiation entering the rooms, since both units are facing west and are not equipped with proper shading devices (see Figures 3.20b). As shown, the units of the new public apartment received direct solar radiation in both living room and master bedroom. The living room received the solar radiation through the window for about 50 minutes, from 6:30 to 7:20, while the master bedroom received it for more than four hours, from 12:50 to 17:00. The external shading of

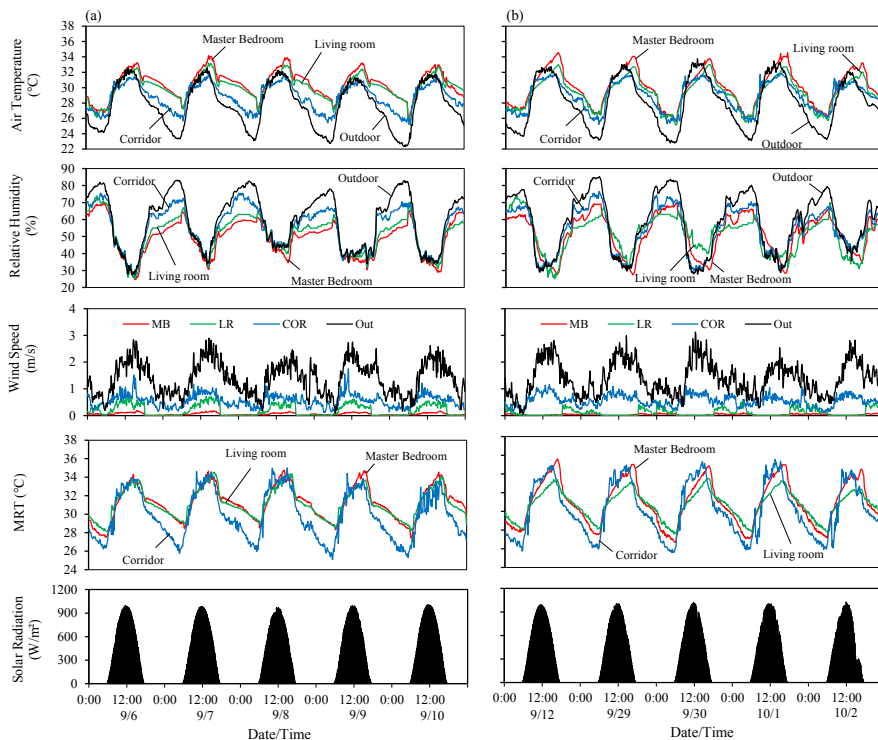


Figure 3.15. Temporal variations of indoor thermal environments in the new public apartment under (a) daytime ventilation and (b) night ventilation conditions.

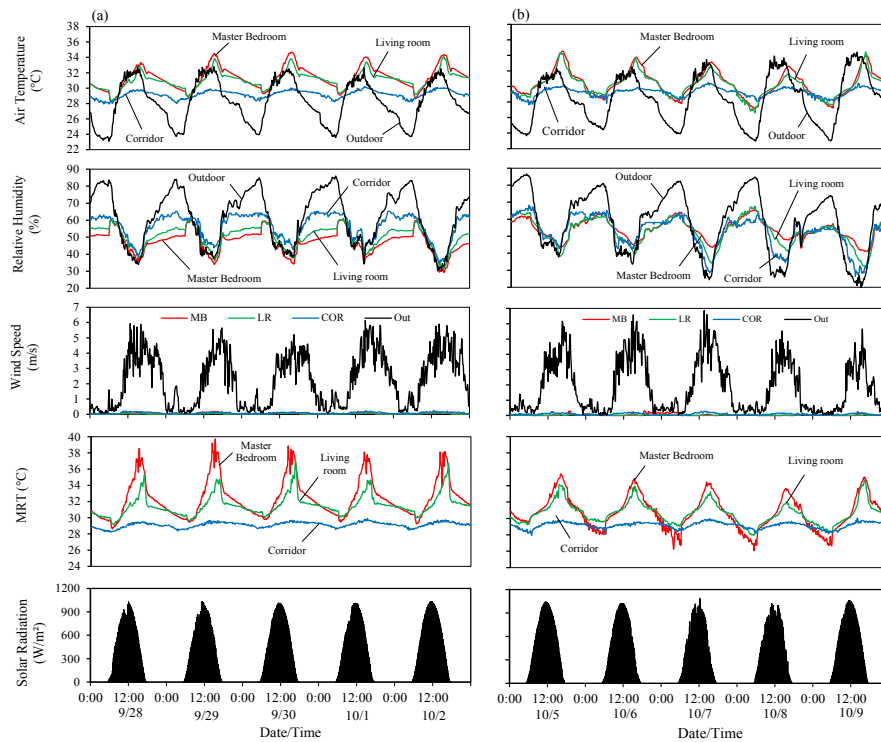


Figure 3.16. Temporal variations of indoor thermal environments in the middle-class private apartment under (a) daytime ventilation and (b) night ventilation conditions.

overhang was not sufficient in shading the master bedroom after 12:50. In the case of middle-class high-rise apartment, the direct solar radiation penetrated into the master bedroom and living room for more than five hours, from 11:50 to 17:10. As shown, the middle-class high-rise apartment was not equipped with external shading device (Figure 3.21). Although the windows were open during the night-time, the nocturnal indoor air temperatures of living room cannot lower to the same level as the outdoors because of the higher air temperature in the corridor space. As shown, the indoor wind speeds are almost not exist in both new public and middle-class high-rise apartment (around of 0.04 m/s, in average). As the daytime ventilation, thermal mass effects can be seen by the occurrence of the peak indoor air temperatures by 1-2 hours compared to the outdoors. Furthermore, nocturnal indoor air temperatures dropped up to 24.9°C in the new public apartment when the windows were opened, showing relatively large decrease compared with the old public apartment. This is probably because the ventilation rates in the new public apartment was larger than that in the old public apartment.

Profiles of indoor thermal environments in the each rooms of respective apartment types for full-day and no ventilation conditions are shown in Figures 3.17-19. In the master bedroom of old public apartment, the temperature differences between indoor and outdoor during the peak hours when the windows are open whole the day (i.e. full-day ventilation), are similar to those of when daytime ventilation is applied, which is around of 2.9-3.8°C lower than the

outdoors. Meanwhile, the nocturnal indoor air temperatures are around 3.5-4.4°C higher than the outdoors (Figure 3.17a). These values are slightly higher than those of night ventilation, because the building structures are heated more when windows are open during daytime. As the mean outdoor wind speeds drop from about 0.9-1.8 m/s during the day to about 0.1-1.0 m/s at night, the night-time ventilation rate might be insufficient to cool the heated structure of the full-day ventilated house properly at night due to its high thermal capacity.

When full-day ventilation is employed, the profile of indoor air temperatures of rooms in both new public and middle-class high-rise apartments are almost the same as the previous ventilation conditions (i.e. daytime and night ventilations); almost the whole day, indoor air temperatures are relatively higher than the outdoors. During the peak hours, indoor air temperatures of master bedroom in new public apartment are around of 33.5-34.5°C or about 2.9-3.9°C higher than the outdoors, while those of living room are around 32.0-33.0°C or about 1.9-2.8°C higher than the outdoors (Figure 3.18a). In the middle-class high-rise apartment, daytime indoor air temperatures of master bedroom and living room are 3.2-4.6°C and 2.8-4.4°C higher than the outdoors, respectively (Figure 3.19a). As the night ventilation condition, the nocturnal ventilative cooling effects are cut off by the strong direct solar radiation since these units facing west, in addition to the heated building structured during the daytime. As indicated, the nocturnal indoor air temperatures of the respective master bedroom and living room of new public apartment are 24.9-27.1°C and 24.2-26.1°C, while those of middle-class

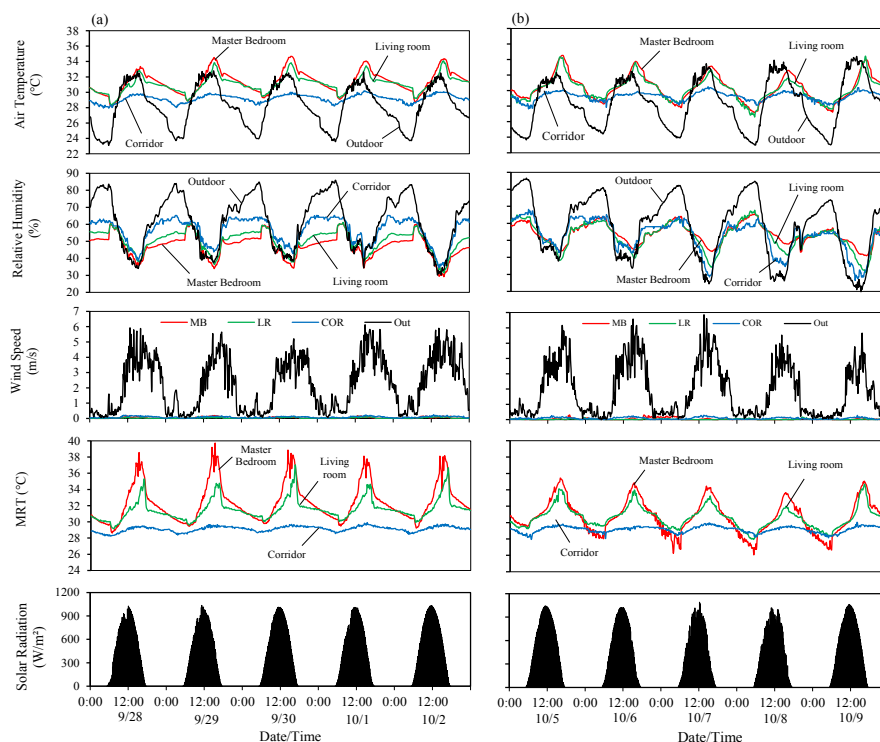


Figure 3.17. Temporal variations of indoor thermal environments in the old public apartment under (a) full-day ventilation) and (b) no ventilation condition.

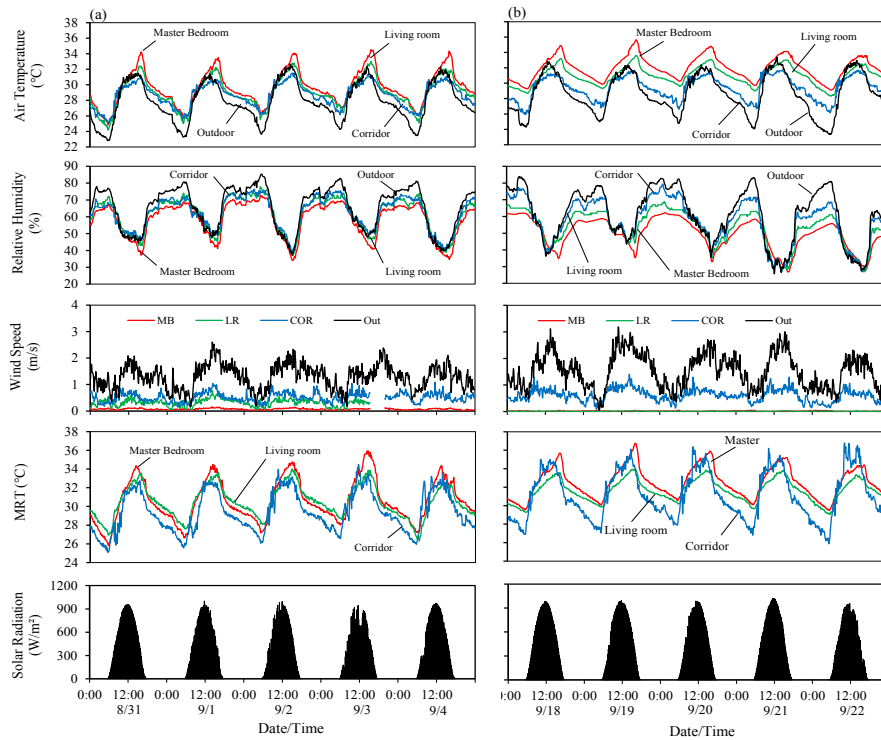


Figure 3.18. Temporal variations of indoor thermal environments in the new public apartment under (a) full-day ventilation) and (b) no ventilation condition.

high-rise apartment are 27.8-29.2°C, respectively. Furthermore, cross ventilation occurred in the living room of new public apartments while in the middle-class high-rise apartment, cross ventilation did not occur although windows are open throughout the day.

During no ventilation condition, indoor air temperatures in old public apartments showed stable values at 29.7-31.2°C with average of 30.5°C (Figure 3.17b). In case of new public apartment, the indoor air temperatures of master bedroom are much higher than those when other ventilation conditions are applied, which is around of 3.3-5.2°C higher than the corresponding outdoors (Figure 3.18b). It is found that without night cooling, maximum indoor air temperatures in the unventilated room are 1.1°C higher than the night ventilated ones, although windows were closed during daytime. Meanwhile, the profile of indoor air temperatures in the middle-class high-rise apartment almost the same as compare to other ventilation conditions, with the maximum indoor air temperatures are 2.7-4.0°C higher than the outdoors (Figure 3.19b).

Figures 3.22-24 further presents a statistical summary of the measured air temperature and humidity in the master bedrooms on fair weather days for respective apartment types under different ventilation conditions. As indicated, the average indoor air temperatures in the master bedroom and the corridor space in the old public apartment were nearly the same as the outdoors with the difference of only 0.1-0.2°C, regardless of the ventilation conditions. In

terms of air temperature, Figure 3.22 confirmed that night ventilation together with the full-day ventilation in case of old public apartment shows lower statistical values than the other ventilation conditions. The mean indoor air temperatures in the night ventilated room are almost similar to or lower than the mean outdoor air temperatures. It is found that indoor air temperatures will be lower when night ventilative cooling is applied. In terms of relative humidity, both night ventilation and full-day ventilation show higher statistical values.

In case of new public apartment and middle-class public apartment, no ventilation condition shows the highest statistical values of indoor air temperatures compared to other ventilation conditions. The average air temperatures in the rooms and the corridors in both new public and middle-class high-rise apartments were generally higher than the outdoors (Figures 3.23-24). In the case of new public apartment, the average air temperatures in the master bedroom were approximately 1.8-3.3°C higher than the outdoors and 0.7-1.0°C higher than those in the corridor space (Figure 3.23). Meanwhile, the average air temperatures in the master bedroom in the middle-class high-rise apartment was approximately 2.0-3.2°C higher than the outdoors and 0.7-1.0°C higher than those in the corridor space (Figure 3.24). As previously described, applying night ventilative cooling will not significantly affecting the indoor air temperatures during the peak hours due to the direct solar radiation. In the new public apartment, these difference cannot be seen clearly even if compared to the daytime

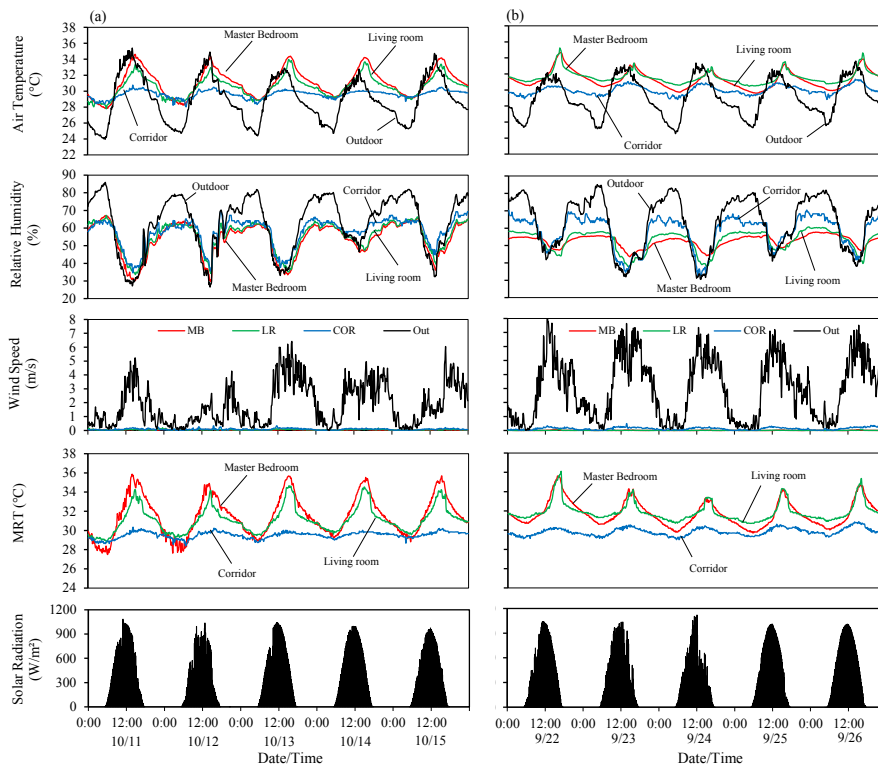


Figure 3.19. Temporal variations of indoor thermal environments in the middle-class private apartment under (a) full-day ventilation) and (b) no ventilation condition.

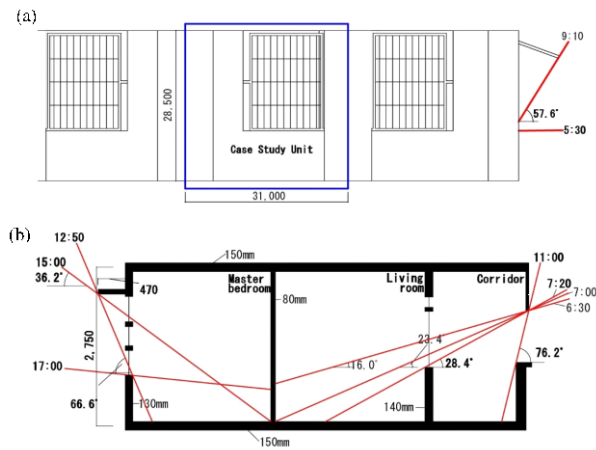


Figure 3.20. Illustration of solar radiation through windows in (a) old public apartment and (b) new public apartment.

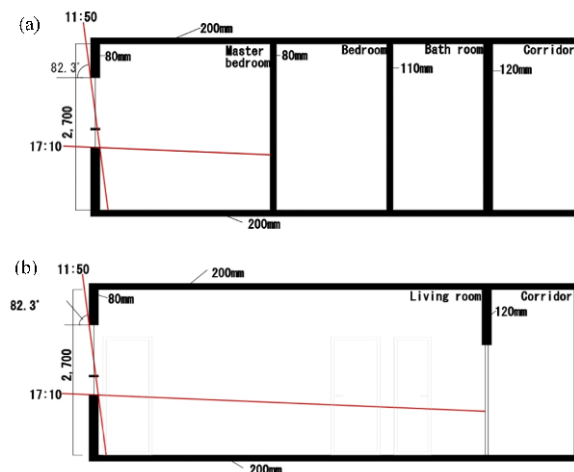


Figure 3.21. Illustration of solar radiation through windows in the middle-class private apartment in (a) master bedroom and (b) living room.

ventilation condition. Moreover, night ventilation lowers the average indoor air temperatures in the middle-class high-rise apartment by 0.6-1.3°C lower than those of when the windows open at daytime (i.e. full-day ventilation and daytime ventilation).

Figure 3.25 shows the comparison of the statistical summary of the three apartments under different ventilation conditions. As shown, old public apartment has the lowest statistical values of indoor air temperatures compared to other apartment types, regardless ventilation conditions. Meanwhile, middle-class high-rise apartment has the highest statistical values amongst other apartment types, for almost all ventilation conditions except for no ventilation

condition. If compared to the corresponding outdoors, the highest indoor air temperature can be found in the new public apartment under no ventilation condition and in the middle-class high-rise apartment under daytime ventilation condition, with averagely 3.3°C and 3.2°C higher than the outdoors respectively. In case of new public apartment, this is simply because the unit of the new public apartment is located on the top floor and thus received heat more than the middle-class apartment. Moreover, this heat then accumulated and could not be released to the outdoors due to no ventilation condition. During the daytime condition, the indoor air temperature is averagely 2.8°C higher than the corresponding outdoors. Furthermore, the corridor space in the new public apartment was semi-opened and therefore the air temperature in the space followed the outdoor temperature particularly during the daytime. On the other hand, the corridor space in the middle-class high-rise apartment was enclosed and therefore the air temperature in the space was quite stable and averagely higher than the outdoors. In this circumstance, even if the living rooms in the two apartments do not receive any direct solar radiation, the daytime indoor air temperature would not become the same level as the outdoors because of the higher air temperature in the corridor space.

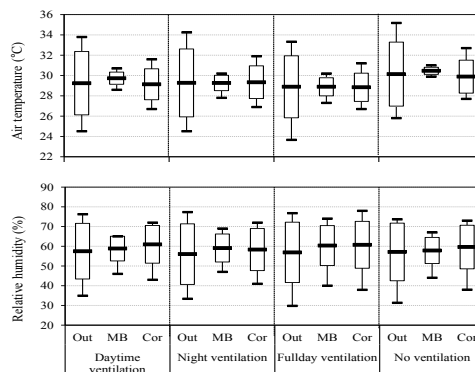


Figure 3.22. Statistical summary (5th and 95th percentile, mean and \pm one standard deviation) of indoor and outdoor air temperatures and relative humidity in old public apartment.

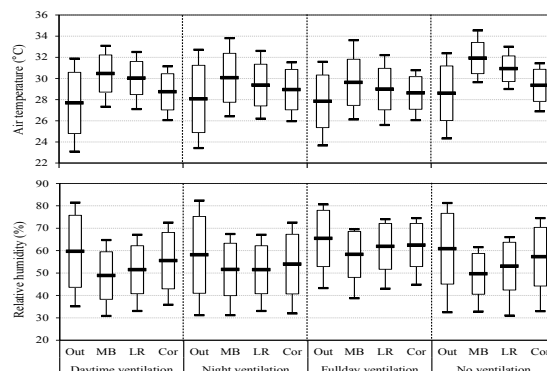


Figure 3.23. Statistical summary (5th and 95th percentile, mean and \pm one standard deviation) of indoor and outdoor air temperatures and relative humidity in the new public apartment.

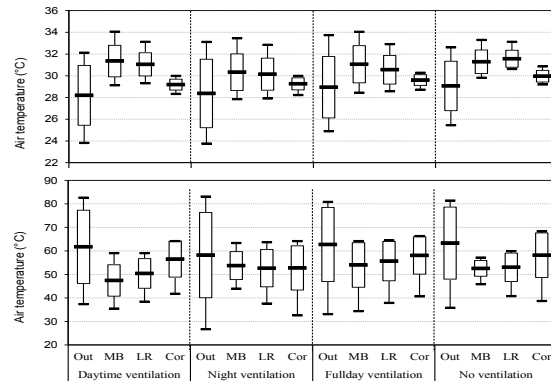


Figure 3.24. Statistical summary (5th and 95th percentile, mean and \pm one standard deviation) of indoor and outdoor air temperatures and relative humidity in the middle-class private apartment.

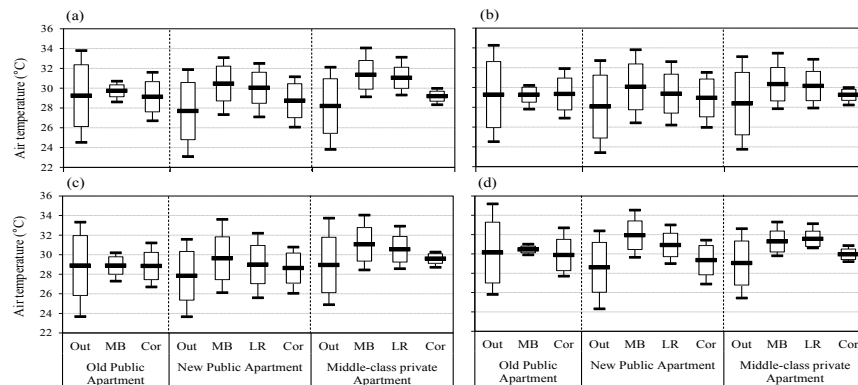


Figure 3.25. Comparison of the statistical summary of indoor and outdoor air temperatures and relative humidity in the three apartments under (a) daytime ventilation, (b) night ventilation, (c) full-day ventilation and (d) no ventilation conditions.

3.4.1.2. Vertical distribution of air temperature in master bedroom

Figures 3.26-28 show the vertical distributions of air temperatures in the three apartment types under different ventilation conditions. The profiles of vertical distribution of indoor air temperatures are represented the highest and the lowest outdoor air temperatures, at 14:00 pm and 05:00 am, respectively. As shown in Figure 3.26, the surface temperatures of the floor and ceiling in the old public apartment were almost constant throughout the day, ranging from 28.1 to 31.0°C regardless of the ventilation conditions. When the windows were open during the night-time (i.e. night ventilation and full-day ventilation), the steep temperature gradient can be seen at the morning time indicating that the building structure cooled by the nocturnal ventilative cooling. As indicated, the surface temperatures of floor and ceiling are lower than those of the other ventilation conditions. At the daytime, the temperature gradient can be seen

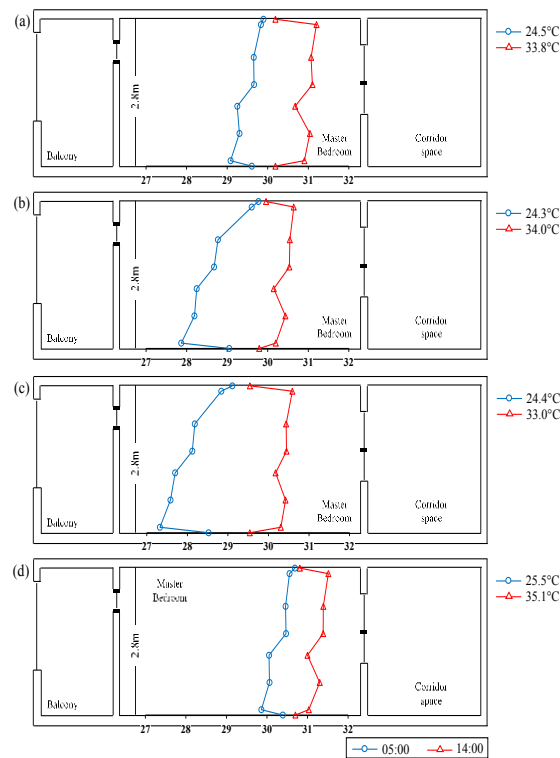


Figure 3.26. Vertical distribution of indoor air temperatures in the master bedroom of old public apartment under (a) daytime ventilation, (b) night ventilation, (c) full-day ventilation and (d) no ventilation.

clearly. The temperature differences between indoor and the surface increases when the windows open during the daytime.

In contrast, the surface temperature of ceiling varied largely (24.5-40.8°C) in the new public apartment because the unit was located on the top floor (Figure 3.27). Thermal insulation was not applied to the roof and ceiling. The surface temperature of the floor was also increased during the late afternoon due to the direct solar radiation (see Figure 3.20b). The steep temperature gradient can be seen during the peak hours when the windows were closed (i.e. night ventilation) due to the nocturnal cooling effect. Nocturnal indoor air temperatures dropped up to 26.4°C in the new public apartment when the windows were opened, showing relatively large decrease compared with the old public apartment. This is probably because the ventilation rates in the new public apartment was larger than that in the old public apartment partly because the unit was located on the higher floor level. In the case of middle-class high-rise apartment, the temperature gradient is seen during night-time even when the windows were open (Figure 3.28). This is probably because the ventilation rates were not sufficient mainly due to the single-sized small opening as well as single-sided ventilation. As previously described, middle-class high-rise apartment received direct solar

radiation during the peak hours and therefore the gradient could not be seen at that time regardless of ventilation conditions.

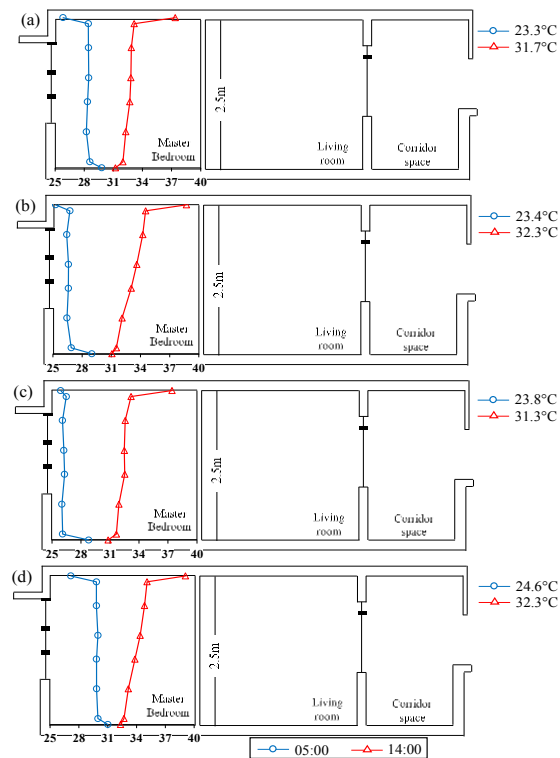


Figure 3.27. Vertical distribution of indoor air temperatures in the master bedroom of the new public apartment under (a) daytime ventilation, (b) night ventilation, (c) full-day ventilation and (d) no ventilation.

3.4.1.3. Surface temperatures and the heat flux in the master bedroom

Surface temperatures were measured using thermocouple type T (the detail information of thermocouple used can be seen in Table 3.1) in the center of respective inside wall surfaces (i.e. north-, south-, east- and west- wall, and floor and ceiling) in the master bedrooms. Meanwhile, heat fluxes were measured using heat flux sensor Hukseflux HFP01. This sensor measures the heat flux ranged from -2000 to 2000 W/m^2 with sensitivity of 60×10^{-6} $V/(W/m^2)$. With thermal resistance of 71×10^{-4} $K/(W/m^2)$, it can measure heat flux under operating temperature range of -30 to $70^\circ C$. Due to the limitation of sensor (and the data acquisition system as well), then the measurement of heat flux were carried out at the external wall alone in the new public apartment and middle-class high-rise apartment. Heat flux of other surfaces was calculated based on the Equations 3.6 and 3.7, with considering the convective heat transfer and radiative heat transfer. Those values, i.e. convective and radiative heat transfers, were calculated using following equations:

$$Q_c = h_c A(T_s - T_a) \tag{3.9}$$

$$Q_r = \varepsilon \sigma A(T_s^4 - T_a^4) \tag{3.10}$$

where Q_c is convective heat transfer (W/m^2), h_c is convective heat transfer coefficient ($\text{W/m}^2\text{K}$), A is surface area (m^2), ε is emissivity of the surface ($0 \leq \varepsilon \leq 1$), σ is Stefan-Boltzmann constant ($5.67 \times 10^{-8} \text{ W/m}^2\text{K}^4$), T_s is wall surface temperature ($^\circ\text{C}$) and T_a is indoor air temperature ($^\circ\text{C}$).

The convective heat transfer coefficient vary depend on the position of the surfaces. For horizontal heat flow (vertical surface), the h_c is $3 \text{ W/m}^2\text{K}$, while those for vertical heat flow (horizontal surface) are around of $1.5 \text{ W/m}^2\text{K}$ and $4.3 \text{ W/m}^2\text{K}$ for downward heat flow and for upward heat flow respectively (Szokolay, 2004). In addition, the emissivity of wall surface is typically 0.9. Using Equations 3.9 and 3.10, the results of calculated heat flux in the external wall of the master bedroom were closely correlated to the measured heat flux ($R^2=0.96$) while that in the middle-class high-rise apartments was around of 0.89. Figure 3.29 showed the comparison of measured and calculated heat flux.

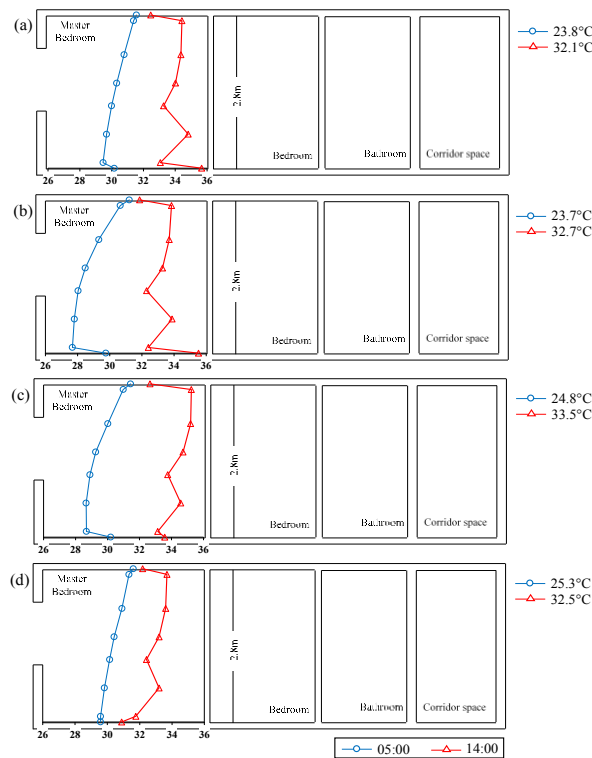


Figure 3.28. Vertical distribution of indoor air temperatures in the master bedroom of the middle-class high-rise apartment under (a) daytime ventilation, (b) night ventilation, (c) full-day ventilation and (d) no ventilation.

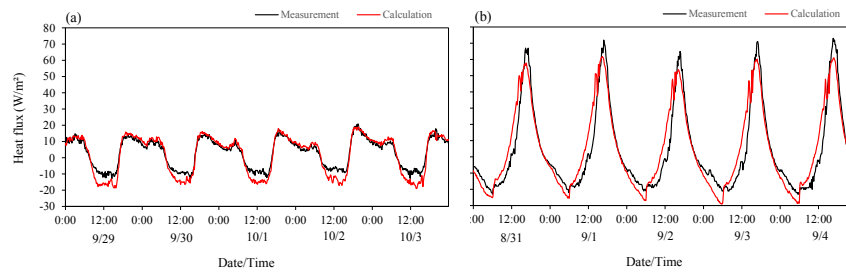


Figure 3.29. Comparison of the measured and calculated heat flux at the external wall of the master bedroom in (a) new public apartment and (b) middle-class high-rise apartment.

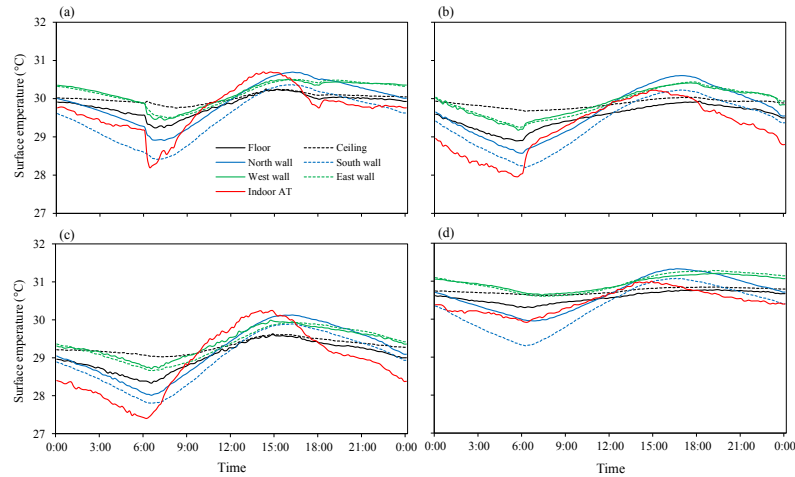


Figure 3.30. Surface temperature of inside wall in the old public apartment under (a) daytime, (b) night, (c) full-day and (d) no ventilation conditions.

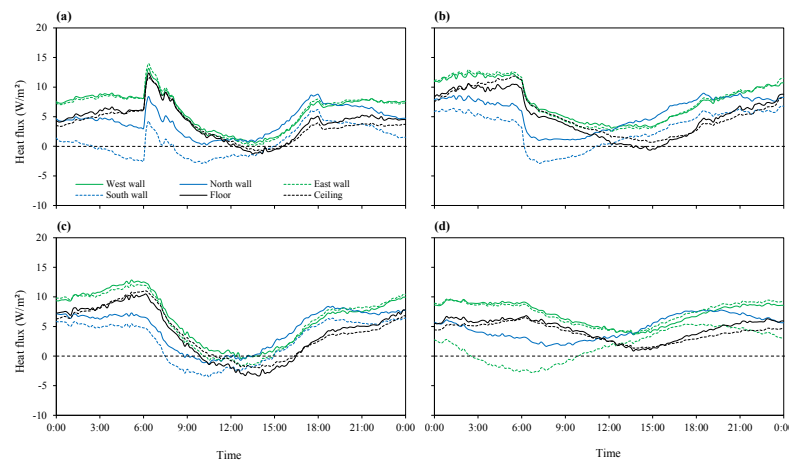


Figure 3.31. Heat flux of the wall surface in the old public apartment under (a) daytime, (b) night, (c) full-day and (d) no ventilation conditions.

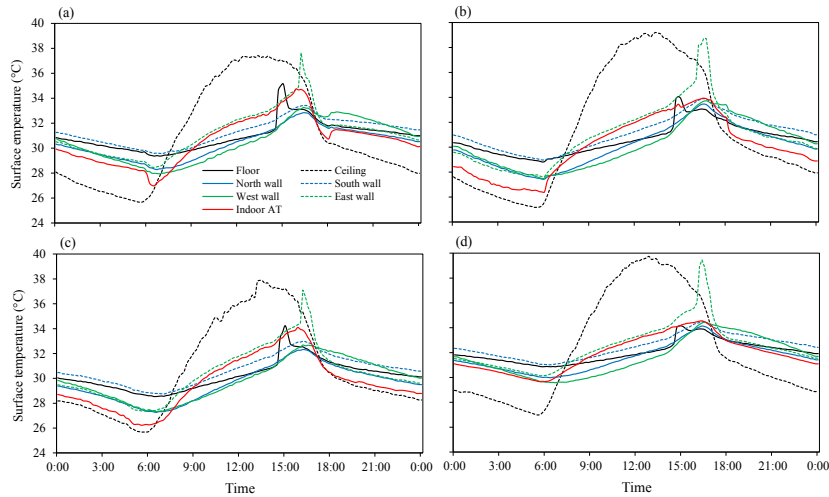


Figure 3.32. Surface temperature of wall in the new public apartment under (a) daytime, (b) night, (c) full-day and (d) no ventilation conditions.

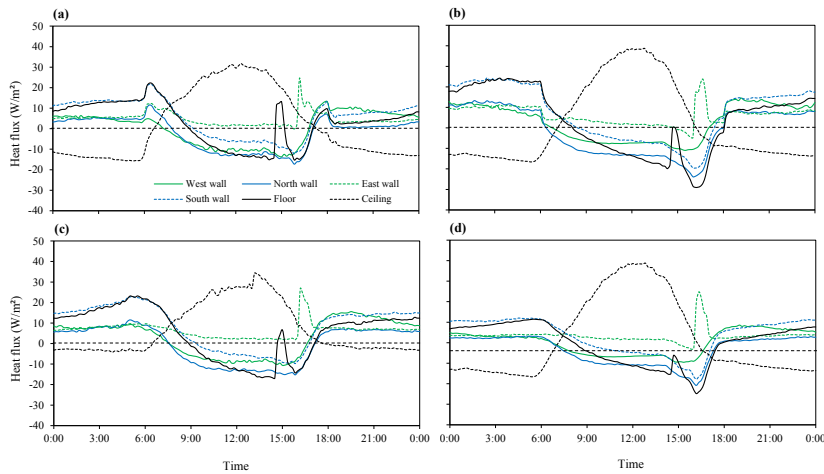


Figure 3.33. Heat flux of the wall surface in the new public apartment under (a) daytime, (b) night, (c) full-day and (d) no ventilation conditions.

As the indoor air temperatures, surface temperatures in the old public apartment were relatively stable at 27.6-30.7°C, except for no ventilation condition, which is slightly higher at around of 29.4-31.4°C. The surface temperatures were generally higher than the corresponding indoor air temperature except at the daytime when the windows were open (i.e. daytime ventilation and full-day ventilation) (Figure 3.30). It is found that the nocturnal cooling lowers the surface temperatures. The external wall (south-facing) recorded the lowest values particularly during night-time mainly due to low outdoor air temperature and unexposed directly to the outdoors, regardless ventilation conditions. When no ventilation condition is

applied, the surface temperatures averagely the highest throughout the day compared to the other ventilation conditions. This is mainly because there is no heat transfer between the walls and the outdoors as the heat sinks. Analysis of heat flow shows that the heat fluxes of respective wall surfaces were mostly had positive values (above 0 W/m^2) throughout the day regardless ventilation condition (Figure 3.31). It means that the heat flows from the wall surfaces to the indoor space. It is calculated that the maximum heat fluxes from the wall were around of $11.4\text{-}20.9 \text{ W/m}^2$. It explains why the measured globe temperatures in the master bedroom were higher than the indoor air temperature throughout the day (see Figure 3.14).

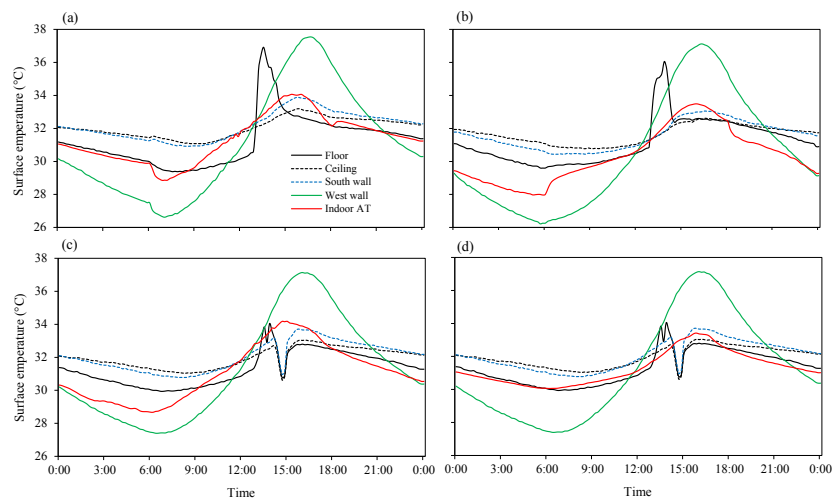


Figure 3.34. Surface temperature of wall in the middle-class high-rise apartment under (a) daytime, (b) night, (c) full-day and (d) no ventilation conditions.

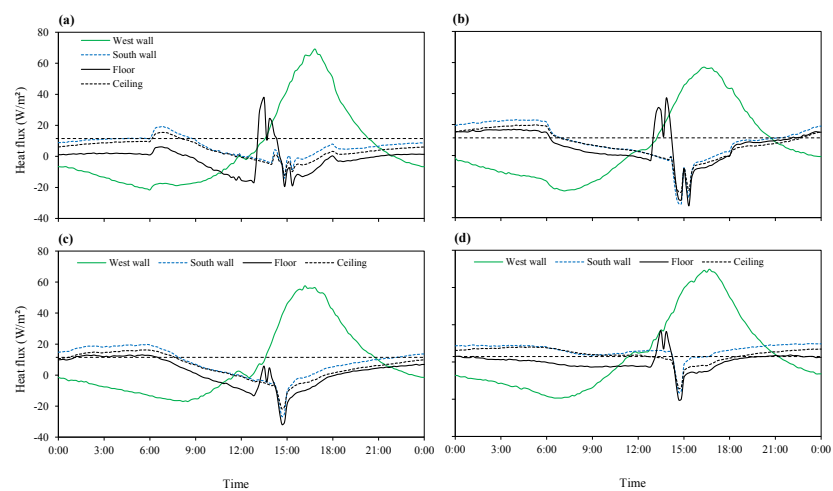


Figure 3.35. Heat flux of the wall surface in the middle-class high-rise apartment under (a) daytime, (b) night, (c) full-day and (d) no ventilation conditions.

As shown in Figure 3.32, ceiling in the case of new public apartment received the heat from the roof after transmitting through the attic space and therefore it has the highest surface temperature amongst other surfaces during the peak hours. As previously described, the roof and ceiling in the new public apartment are not insulated. It is calculated that the maximum heat fluxes from the ceiling ranged from 31.7 W/m² to 41.7 W/m² (Figure 3.33). The east wall received the direct solar radiation through the windows, thus increased the surface temperatures particularly during peak hours (15:00-17:00). As the old public apartment, the surfaces temperatures of walls under no ventilation conditions were averagely higher than those under other ventilation conditions, mainly for the same reason. Except for the ceiling, analysis of heat flux indicated that heat flow from the wall surface into the indoor space during the night-time (18:00-06:00). It should be noted that heat fluxes in the west wall (i.e. external wall) was obtained positive values throughout the day regardless ventilation condition (see Figure 3.33). It indicates that the external wall constantly transmitted the heat to the indoor space. It is important to provide proper shading devices in order to avoid direct solar radiation, and also insulate the external wall to reduce the amount of heat transferred to the indoor space.

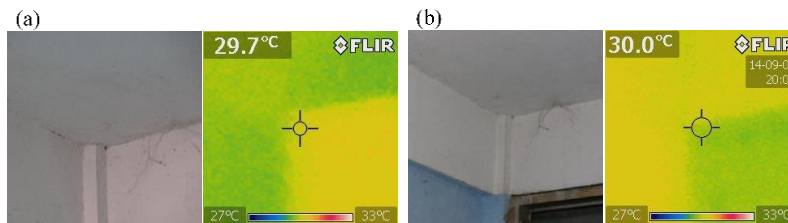


Figure 3.36. Profile of wall surface temperatures using thermal viewer in the old public apartment at (a) daytime and (b) night-time.

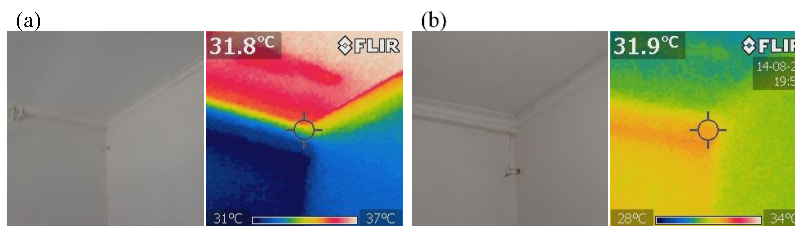


Figure 3.37. Profile of wall surface temperatures using thermal viewer in the new public apartment at (a) daytime and (b) night-time.

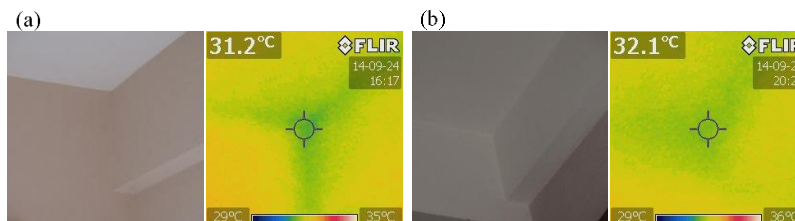


Figure 3.38. Profile of wall surface temperatures using thermal viewer in the middle-class high-rise apartment at (a) daytime and (b) night-time.

In the case of middle-class high-rise apartment, the surface temperatures of the external wall (west wall) varied largely from 25.3 to 38.6°C and recorded the highest value during the peak hours (Figure 3.34). Unlike new public apartment, the heat flux in the external wall showed different pattern. It had positive values during the daytime and negative during the night-time. Most of the heat from building envelopes came from this external wall, with the maximum heat flux reached to 49.6-69.2 W/m² (Figure 3.35). This is mainly because of thin wall structure (80mm) with relatively low thermal capacity used in the middle-class high-rise apartment. During the daytime, it easily transmitted the heat from the outdoor to the indoor space while in the night-time, the heat stored in the external wall released to the lower outdoor air temperature. Surface temperatures of floors in both new public and middle-class high-rise apartments increased in response to receiving the direct solar radiation during the afternoon hours. It should be noted that east- and north-wall of master bedroom in the middle-class high-rise apartment were not measured. As the new public apartment, it is important to provide proper shading devices and insulate the external wall in order to avoid direct solar radiation and to reduce the amount of heat transferred to the indoor space.

Profiles of surface temperatures of walls in the three types of apartments using FLIR thermal camera are shown in Figures 3.36-38, while completed distribution profiles of surface temperature are presented in the Appendix D. It should be noticed that FLIR thermal camera could capture the surface temperature ranged from -20 to 250°C with the sensitivity of 0.045°C.

3.4.1.4. Air tightness of master bedrooms

Air tightness of the rooms was investigated to examine the efficiency of air-conditioning in the master bedrooms using a CO₂ concentration decay method. The CO₂ concentration was measured in the closed master bedrooms under different open-window/door conditions for the adjacent space, as summarized in the Table 3.6. Since the unit of old public apartment has only single room without adjacent room, two phases of measurements were conducted. The first phase was carried out by normally closed the doors and windows without any treatments while the second phase was conducted by covering the gap between the windows/doors panes and windows/doors frames including the permanent ventilation holes. Both new public apartment and middle-class high-rise apartments employed four phases of measurement.

Firstly, CO₂ gas was injected into the closed room until reached a certain concentration level. After reached 2,500-3,000 ppm with a steady level, then the CO₂ concentration decay was measured at regular time intervals, i.e. 15 second. Indoor CO₂ concentration was measured using TESTO Serie 435-4 with CO₂ probe Part No. 0632 1535 (accuracy ±50ppm, ±2% reading). Other than the master bedroom, outdoor CO₂ concentration was also measured using T&D TR-76Ui (accuracy ±50ppm, ±5% reading).

The air change rate was calculated using the equation from Lausmann and Helm (2011) as follows:

$$C(t) = (C_0 - C_a)e^{-\lambda t} + C_a \quad (3.11)$$

where $C(t)$ is the final CO₂ gas concentration (ppm); C_0 is the initial concentration of CO₂ gas (ppm); C_a is the outdoor CO₂ gas concentration (ppm); λ is air change rate (times/hour) and t is time (second).

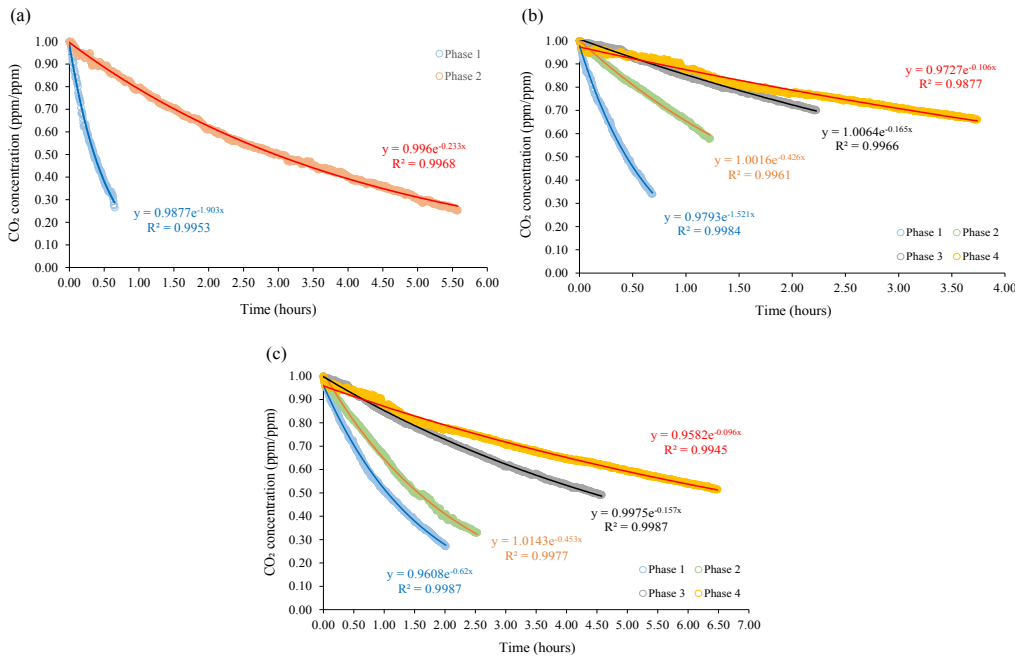


Figure 3.39. Results of air change rate (ACH) calculation using CO₂ concentration decay method.

By using the Equation 3.11, the results of calculation are presented in Figures 3.39 while the air change rates of the master bedrooms in the three apartments units were summarized in Table 3.7. As shown, under normal condition (open/closed adjacent rooms without any treatments), the air change rates were 1.9 ACH in the old public apartment, 1.0-1.5 ACH in the new public apartment and 0.4-0.7 ACH in the middle-class high-rise apartment respectively. The unit of middle-class high-rise apartment showed better air tightness compared to the other two types of apartments. The air change rates of the master bedrooms were slightly higher when the windows/doors of the adjacent rooms were opened. For instance, in the case of new public apartment, the air change rate was measured at 1.5 ACH under the opened windows/doors conditions while that in the closed conditions was 1.0 ACH. As stated by Sfakianaki (2008), the results from the tracer gas method particularly in naturally ventilated condition, are affected largely by the average wind speed and the indoor/outdoor temperature difference.

One of the factors influencing the air leakage rate is the size and distribution of leakage paths (Awbi, 2003). As indicated in Table 3.7, aluminum sash was used for the windows in all the apartments, but the old public apartment unit had relatively larger opening areas (3.4 m² in total). The old public apartment unit was equipped with the permanent ventilation holes (with opening area of about 0.02-0.05 m²) above windows and doors. Furthermore, there were relatively large cracks at joints in doors, windows and ceiling in the case of old public apartment. By filling all the cracks and gaps of joints with a special tape in the old public apartment, the air change rate was reduced to 0.2 ACH. This indicates that in the current

conditions of old public apartment, air-conditioning cannot be used efficiently unless air tightness is improved.

Table 3.6 Windows/doors opening conditions for the adjacent rooms of master bedroom for the CO₂ measurement.

Type of apartment	Adjacent room	Measurement phases	Windows/doors opening of adjacent rooms
Old public apartment	n/a	Phase 1	Closed
		Phase 2	Closed and cover the gap between doors/windows panes and doors/windows frames, including permanently ventilation holes, with the tape.
New public apartment	Living room and kitchen	Phase 1	Open
		Phase 2	Closed
		Phase 3	Open, and cover the gap between doors/windows panes and doors/windows frames of master bedroom, with the tape
		Phase 4	Closed, and cover the gap between doors/windows panes and door/windows frames of master bedroom, with the tape
Middle-class private apartment	Living room	Phase 1	Open
		Phase 2	Closed
		Phase 3	Open, and cover the gap between doors/windows panes and doors/windows frames of master bedroom, with the tape
		Phase 4	Closed, and cover the gap between doors/windows panes and doors/windows frames of master bedroom, with the tape

Table 3.7. Measured air change rates in master bedrooms.

Type of apartment	Opening area (m ²)	Floor area (m ²)	Air change rate (1/h)	Material
Old public apartment	Windows: 1.3 Door: 2.8 Vents: 0.6	16.6	Phase 1: 1.9 Phase 2: 0.2	Front window: Two single pane, aluminium window sash; Rear window: single pane, aluminium window sash; Door pane: plywood; Door frame: aluminium
New public apartment	Window: 0.5 Door: 1.3	7.3	Phase 1: 1.5 Phase 2: 1.0 Phase 3: 0.5 Phase 4: 0.3	Window: Two single pane, aluminium window sash, aluminium frame; Door pane: plywood; Door frame: aluminium
Middle-class private apartment	Window: 0.6 Door: 1.5	7.1	Phase 1: 0.7 Phase 2: 0.4 Phase 3: 0.2 Phase 4: 0.1	Window: single pane, aluminium window sash. Door pane: wood; door frame: wood

3.4.1.5 Thermal comfort evaluation

Evaluation of thermal comfort in the master bedrooms was carried out by using the adaptive comfort equations (Equations 3.3-4), which was developed for the use in hot-humid climatic regions (Toe and Kubota, 2013). In these equations, the 80% acceptability upper limit of indoor operative temperature is a function of the daily mean outdoor air temperature. The indoor operative temperature was calculated based on the Equations 3.1-2, while SET* calculated based on Equation 3.5. Temporal variations of the indoor operative temperatures in the three apartments under different ventilation conditions are plotted in Figures 3.40-42. The 80% comfortable upper limits range between 28.4-30.3°C, 27.3-28.9°C and 28.0-29.4°C for respective old public apartment, new public apartment and middle-class high-rise apartment regardless ventilation conditions. The evaluation is also summarized in terms of indoor operative temperature deviations from the 80% comfortable upper limits and the exceeding periods in Table 3.8.

As shown, the indoor operative temperatures in all the three apartments exceeded the 80% upper limits for the whole day-time period, regardless ventilation conditions. When the windows were closed throughout the day (i.e. no ventilation), almost all the day exceeded the 80% upper comfortable limits in all three apartments. As indicated, the peak operative temperatures between daytime ventilation and no ventilation conditions are almost the same, which is about of 30.7-31.0°C and 31.0-31.3°C, respectively (Figure 3.40). The deviation of operative temperature from the upper limit under these conditions are 0.8-1.2°C and 1.0-1.2°C, respectively. This is mainly because the night-time indoor operative temperature is remain high without ventilation. In the other hand, when nocturnal ventilative cooling was applied, the operative temperatures at the peak hours decreased 0.4-0.5°C compared to those when daytime ventilation. As shown, full-day ventilation received the shortest exceeding periods amongst other ventilation conditions, which is around of 33.8%, 5.1% lower than that when night ventilation is applied (Table 3.8).

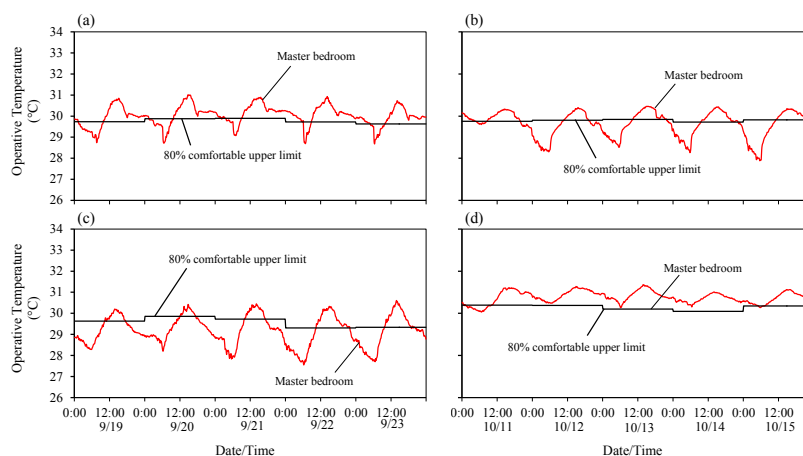


Figure 3.40. Thermal comfort evaluation using adaptive comfort equation in the old public apartment under (a) daytime ventilation, (b) night ventilation, (c) full-day ventilation and (d) no ventilation.

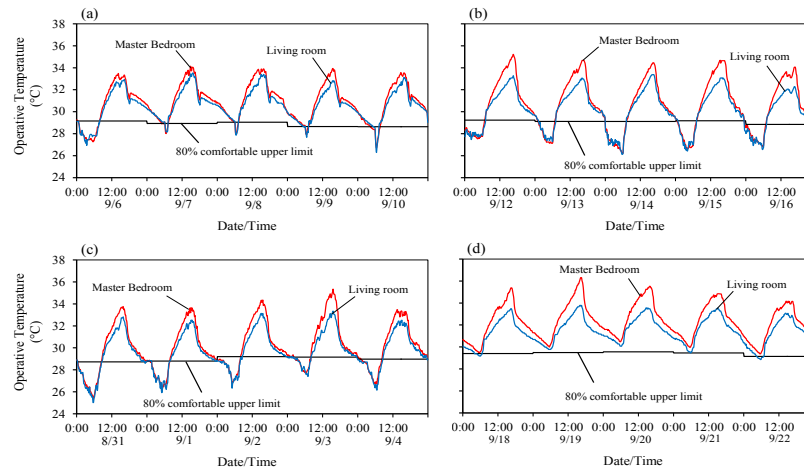


Figure 3.41. Thermal comfort evaluation using adaptive comfort equation in the new public apartment, under (a) daytime ventilation, (b) night ventilation, (c) full-day ventilation and (d) no ventilation.

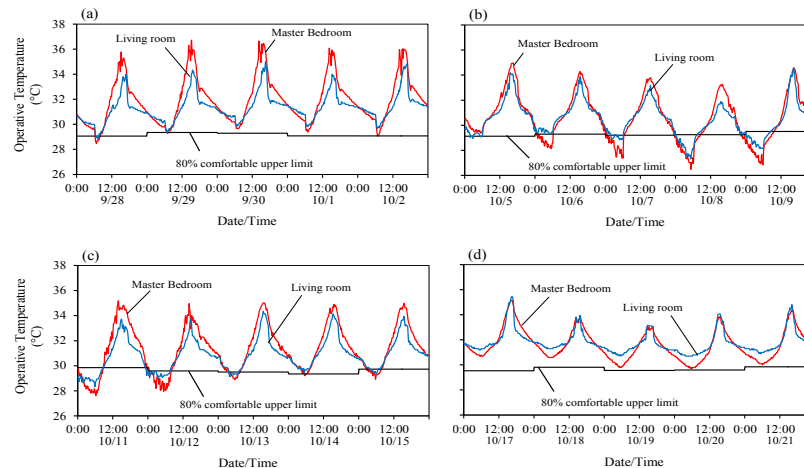


Figure 3.42. Thermal comfort evaluation using adaptive comfort equation in the middle-class private apartment, under (a) daytime ventilation, (b) night ventilation, (c) full-day ventilation and (d) no ventilation.

In the case of new public apartment, the operative temperatures of the living room generally were lower than those of the master bedroom throughout the days, regardless of ventilation conditions. As previously discussed, the operative temperatures in the master bedroom during the peak hours were relatively higher than those in the living room simply due to the direct solar radiation. When the windows opened during the night-time, i.e. night ventilation and full-day ventilation, the operative temperatures drop by 26.0°C due to high the ventilation rates during the night-time (see Figures 3.41). As shown in Table 3.8, daily maximum indoor operative temperatures in the night ventilated rooms are higher than the 80% comfortable

upper limits by 5.2-6.0°C (in case of the living room, 3.4-4.3°C) and 4.5-6.2°C (in case of the living room, 3.6-4.2°C) on the afternoons of fair weather days in above two cases. This is likely caused by the incoming solar radiation through the windows during the daytime as well as heat through the ceiling. Although full-day ventilation received the shortest exceeding periods, nevertheless it is only 2.1% shorter than that of the night ventilation.

Meanwhile, the operative temperatures of both master bedroom and living room during daytime ventilation and no ventilation conditions were exceeded the 80% upper comfortable limits throughout the day (Figure 3.42). During the night-time, the operative temperatures of the living room were higher than those of the master bedroom regardless ventilation conditions, because the heat emitted by the wall in the living room much higher due to the higher thermal mass. It is noted that night ventilation obtained the shortest exceeding period. Nevertheless, the exceeding periods in the case of middle-class high-rise apartment generally were higher than 70% even under night ventilation condition (Table 3.8). The radiant and convective heat through daytime ventilation further increases the maximum indoor operative temperatures in the daytime ventilated rooms. Their maximum operative temperatures exceeded the 80% comfortable upper limits by 6.7-7.4°C (in case of the living room, 4.9-5.8°C) on the afternoons of fair weather days. These results clearly indicate that it is very difficult to achieve thermal comfort in the middle-class high-rise apartment only by means of natural ventilation.

Table 3.8. Results of thermal comfort evaluation using adaptive comfort equation under different ventilation conditions.

Type of apartments	Ventilation conditions	Room	Deviation of OT and 80% upper comfortable limit		Exceeding period (%)
			Daily min. (°C)	Daily max. (°C)	
Old public apartment	Daytime	Master Bedroom	-0.5 to 0.3	1.0 to 1.2	74.4
	Night	Master Bedroom	-1.9 to -0.1	0.5 to 0.7	48.9
	Full-day	Master Bedroom	-1.9 to -0.6	0.6 to 1.3	33.8
	No	Master Bedroom	-0.3 to 0.5	0.8 to 1.2	90.8
New public apartment	Daytime	Master Bedroom	-1.9 to 1.9	4.3 to 5.3	87.8
		Living room	-2.2 to 1.7	3.8 to 4.6	89.3
	Night	Master Bedroom	-2.9 to 0.4	5.2 to 6.0	71.5
		Living room	-3.0 to 0.5	3.4 to 4.3	71.5
	Full-day	Master Bedroom	-3.4 to 0.2	4.5 to 6.2	69.4
		Living room	-3.7 to 0.0	3.6 to 4.2	66.0
	No	Master Bedroom	0.1 to 2.2	5.0 to 6.8	100.0
		Living room	-0.3 to 1.6	3.9 to 4.3	96.0
Middle-class private apartment	Daytime	Master Bedroom	0.4 to 2.3	6.7 to 7.4	98.2
		Living room	0.7 to 2.3	4.9 to 5.8	99.2
	Night	Master Bedroom	-2.8 to 0.6	4.0 to 5.8	72.4
		Living room	-1.9 to 0.6	2.6 to 5.1	81.7
	Full-day	Master Bedroom	-2.1 to 1.3	5.3 to 4.6	78.8
		Living room	-1.5 to 1.2	3.9 to 4.9	80.4
	No	Master Bedroom	0.1 to 2.3	3.5 to 5.6	100.0
		Living room	1.1 to 2.3	3.6 to 5.9	100.0

3.4.2 Numerical simulation of indoor thermal environments

3.4.2.1 Validation of the base model

Validation of the base model was carried out by comparing the simulation results with the field experiment data. This validation was conducted in the master bedroom, living room and corridor space. The validation period spans about three weeks in total. It begins at least a week after the simulation start time for all conditions, thus allowing the model to acquire sufficient thermal history. Two statistical error tests, the mean bias error (MBE) and the root mean square error (RMSE), are used to validate this model through checking the deviations of simulation results from actual measurement data. These two error test are calculated as follows:

$$\text{MBE} = \frac{\sum_{i=1}^N (L_{is} - L_{im})}{N} \quad (3.12)$$

$$\text{RMSE} = \sqrt{\frac{\sum_{i=1}^N (L_{is} - L_{im})^2}{N}} \quad (3.13)$$

where L_{im} is the i th simulated value, L_{is} is the i th measured value and N is the total number of data pairs (Jiang, 2009). A smaller error generally means better predictions by the evaluated model.

Figures 3.43-45 show the temporal variations of the simulation results of the base model compared to the measurement data in the three types of apartment under no ventilation condition, while Table 3.9 shows that the MBE and RMSE of respective rooms of the respective apartments. In case of old public apartment, the simulated results for air temperatures in both master bedroom and corridor space are consistently higher than the measured data by around of 1.0°C. Following the air temperature, the simulation results of both the relative humidity and absolute humidity showed the contrast results but constantly lower than those of the measurement data. This is most probably because air infiltration modelling in the old public apartment is too difficult to match the actual condition since there are many ventilation holes, constructional joints, and structural cracks. As shown in Table 3.9, the MBEs of air temperature of master bedroom and corridor space are 0.56 and 0.84 respectively while the RMSEs are 0.68 and 0.91 respectively. Coefficients of determination (R^2) then further test the linear relationships between the simulated and measured values. The R^2 values for air temperature in the master bedroom is slightly low ($R^2=0.63$) while that at the corridor space is quite high ($R^2=0.95$).

In the cases of new public and middle-class high-rise apartments, the results mostly demonstrate good agreement between the simulation and measurement data in terms of air temperature, relative humidity and absolute humidity in all the rooms of respective apartments, except for the absolute humidity of master bedroom of middle-class high-rise apartment ($R^2=0.36$). The MBEs of respective rooms (i.e. master bedroom, living room and corridor space) in the new public apartment are obtained at -0.51, 0.02 and 0.09 respectively while the RMSEs are obtained at 0.84, 0.36 and 0.9 respectively. Meanwhile, in the middle-class high-rise apartment, the MBEs of the same rooms are -0.30, -0.56 and 0.67 respectively while the RMSEs are 0.51, 0.62 and 0.72 respectively. In the new public apartment, master bedroom has the coefficients of determination (R^2) for air temperature above 0.80 while in the other rooms have R^2 values of 0.94 respectively. Meanwhile, the R^2 values for air temperature at the rooms

in the middle-class high-rise apartment are above 0.80 (see Table 3.9). Nevertheless, their daily patterns approximate those of the field measurement.

The temperature errors and corresponding R^2 values of this model are slightly higher to or smaller than errors reported in other validation works that simulated ventilative cooling techniques. In their study, Finn *et al.* (2007) reported MBE and RMSE of 0.46°C and 0.88°C for air temperature in a night ventilated building model. In another work, Shadafi *et al.* (2011)

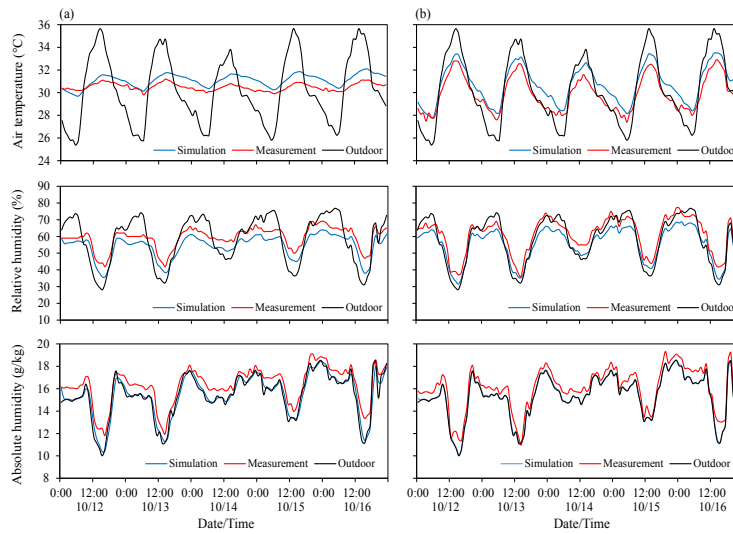


Figure 3.43. Comparison of simulation results and the field experiment results in the old public apartment in (a) master bedroom and (b) corridor space.

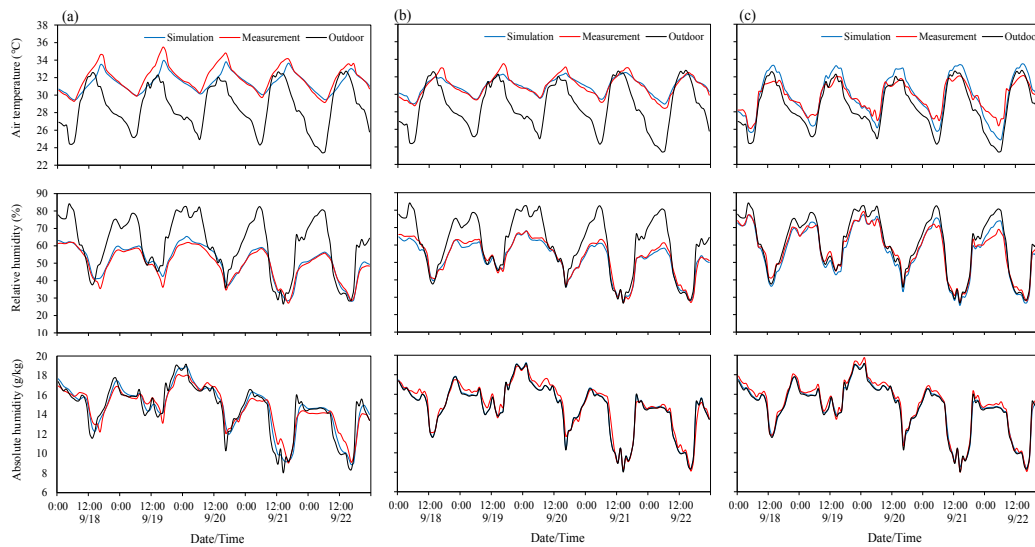


Figure 3.44. Comparison of simulation results and the field experiment results in the new public apartment in (a) master bedroom and (b) living room and (c) corridor space.

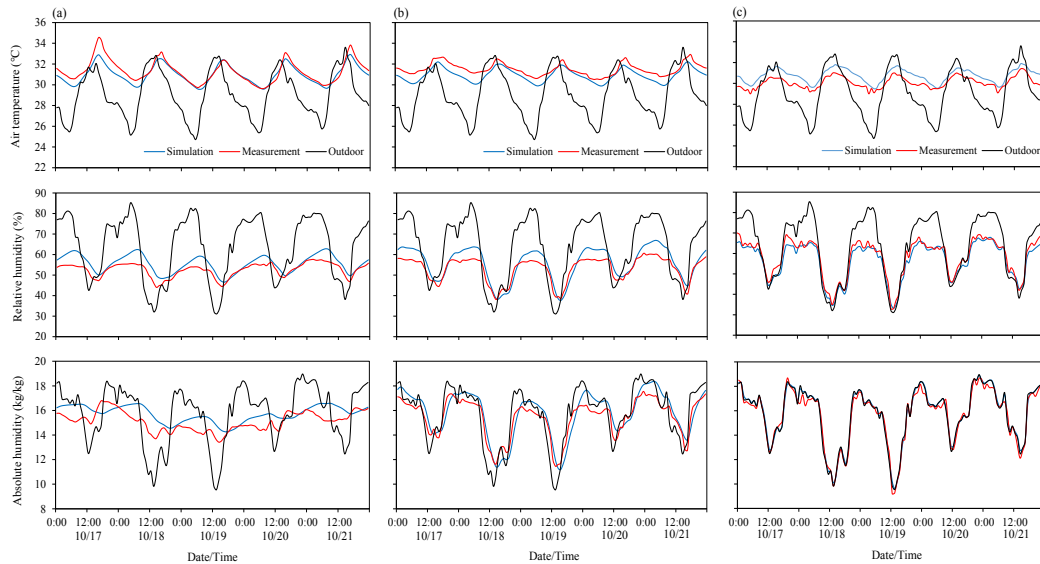


Figure 3.45. Comparison of simulation results and the field experiment results in the middle-class high-rise apartment in (a) master bedroom and (b) living room and (c) corridor space.

Table 3.9. Summary of statistical error tests of the base model under no ventilation condition.

Room	Air temperature			Relative humidity			Absolute humidity		
	MBE (°C)	RMSE (°C)	R ²	MBE (°C)	RMSE (°C)	R ²	MBE (g/kg ³)	RMSE (g/kg ³)	R ²
<i>Old public apartment</i>									
MB	0.56	0.68	0.63	-5.02	5.23	0.96	-0.87	0.95	0.97
Corridor	0.84	0.91	0.95	-5.42	5.68	0.98	-0.69	0.78	0.97
<i>New public apartment</i>									
MB	-0.51	0.84	0.83	1.13	1.99	0.97	3.08	6.16	0.95
LR	0.02	0.36	0.94	-0.98	1.81	0.98	2.94	6.24	0.96
Corridor	0.09	0.95	0.94	-0.95	2.89	0.97	-0.25	0.39	0.99
<i>Middle-class private apartment</i>									
MB	-0.30	0.51	0.86	2.95	3.65	0.75	0.60	0.88	0.36
LR	-0.56	0.62	0.83	2.76	3.92	0.92	0.31	0.75	0.87
Corridor	0.67	0.72	0.84	-1.77	2.33	0.97	0.15	0.35	0.98

Note:

MB : Master Bedroom
LR : Living Room

found that the average air temperature difference between simulation and field measurement was 0.4°C while Geros *et al.* (1999) employed a building model which had a mean difference between measured and simulated temperatures of about 0.3°C with R² value of about 0.90 when they performed simulation using TRNSYS. It is concluded that the base models of this study are generally satisfactorily describing the thermal behavior of the apartment buildings.

3.4.2.2 Indoor thermal environments in different natural ventilation conditions

Figure 3.46 shows the simulation results of indoor air temperatures and relative humidity of master bedroom in the three apartments under different orientations while Figure 3.47 presents the statistical summary of those indoor air temperatures of master bedrooms under different orientations. It should be noticed that the simulations were conducted under no ventilation conditions. As shown, building orientations do not significantly affect the indoor air temperatures of master bedroom in the old public apartment. The indoor air temperatures stabilized at around 27.3-30°C (Figure 3.46a). Nonetheless, east- and west-facing unit received slightly higher daytime indoor air temperatures, around 0.1-0.4°C higher than north- and south-facing unit (Figure 3.47a) simply due to the solar radiation effects. This effects are not as high as in the new public apartment and middle-class high-rise apartment due to the existence of balcony. As previously described, unit of old public apartment is equipped by the large balcony played role as a shading devices as well as thermal buffer zone so that the indoor air temperatures maintain low.

In the case of new public and middle-class high-rise apartments, east- and west-facing units show relatively higher indoor air temperatures compared to north- and south-facing units (Figure 3.46bc) due to the solar radiation entering the building during the morning time and afternoon. Maximum indoor air temperatures in both apartments at east- and west-facing are

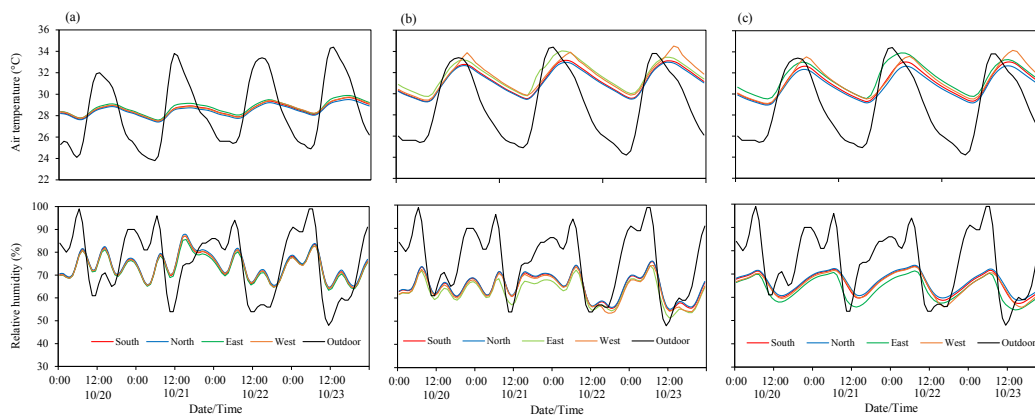


Figure 3.46. Simulation results for indoor thermal environments in (a) old public apartment and (b) new public apartment and (c) middle-class private apartment, under different orientations.

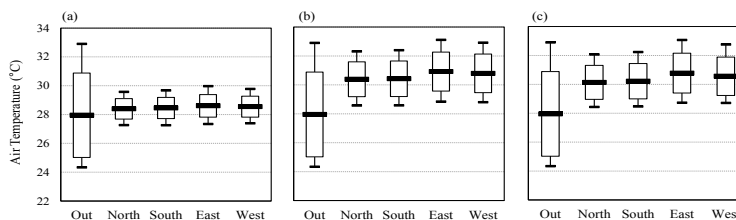


Figure 3.47. Statistical summary (5th and 95th percentile, mean and \pm one standard deviation) of indoor and outdoor air temperatures of master bedrooms in (a) old public apartment, (b) new public apartment and (c) middle-class private apartment, under different orientations.

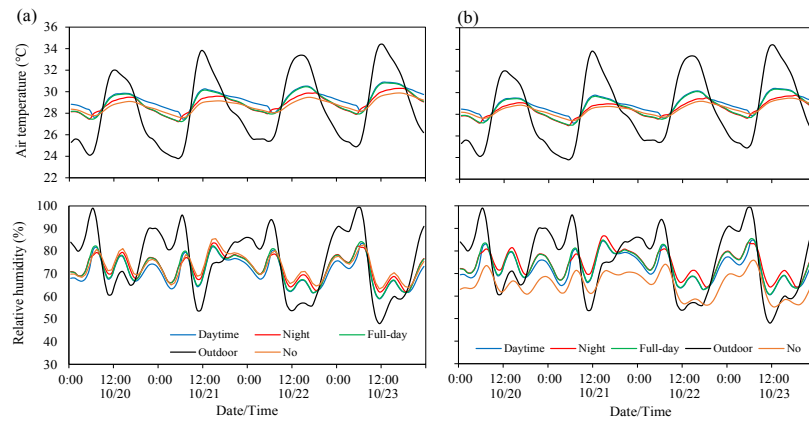


Figure 3.48. Simulation results of indoor thermal environments of master bedroom in the old public apartment under different ventilation conditions for (a) east-facing and (b) north-facing orientations.

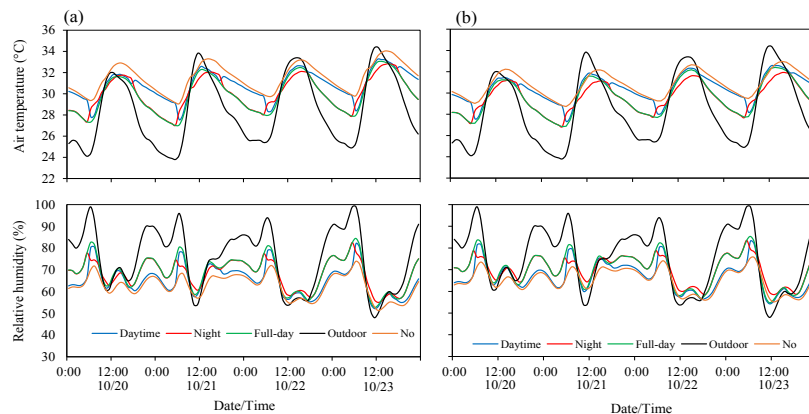


Figure 3.49. Simulation results of indoor thermal environments of master bedroom in the new public apartment under different ventilation conditions for (a) east-facing and (b) north-facing orientations.

up to 34.5°C and 34.1°C respectively; these values are 0.5-0.8°C and 0.6-1.0°C higher than those of north- and south-facing unit respectively (Figure 3.47bc). As shown in Figure 3.47, unit facing north is considered of having similar air temperatures profile as south-facing unit while west-facing unit has similar profiles as east-facing unit, although very small differences can be seen there. Therefore, in the next investigation, east-facing unit and north-facing were be used to evaluate indoor air temperatures under different ventilation conditions.

Figures 4.48-50 present the simulation results for indoor the three apartments under different ventilation conditions in the east- and north-facing orientations respectively. As shown, at the daytime, profiles of air temperatures in the old public apartment when applying daytime and full-day ventilations are similar, but those are different at the night-time regardless the orientations. As the field measurement results, it confirms that building

structures are not cooled by the nocturnal ventilative cooling when the daytime ventilation is applied. When the night ventilation is applied, the maximum indoor air temperatures reduce by 0.4-0.5°C compared to those when daytime or full-day ventilation applied. Unlike the field measurement results, no ventilation condition received the lowest values at the daytime regardless orientations. Nevertheless, north-facing unit has lower statistical values than the east-facing unit regardless ventilation conditions, with the differences averagely of 0.2-0.4°C (see Figure 3.51).

Unlike in the old public apartment, the profiles of air temperatures during the no ventilation condition in the new public apartment and middle-class high-rise apartment are higher than those of other ventilation conditions, regardless orientation. These results confirm the result of field measurement. During the peak hours, night ventilation in the new public apartment obtains lower indoor air temperatures compared to other ventilation conditions regardless

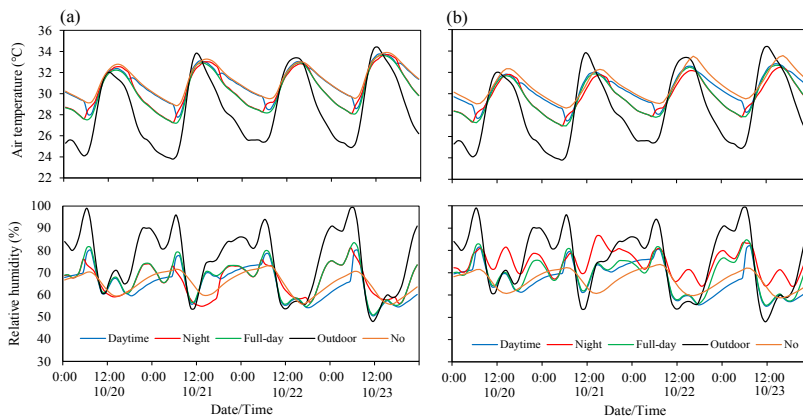


Figure 3.50. Simulation results of indoor thermal environments of master bedroom in the middle-class high-rise apartment under different ventilation conditions for (a) east-facing and (b) north-facing orientations.

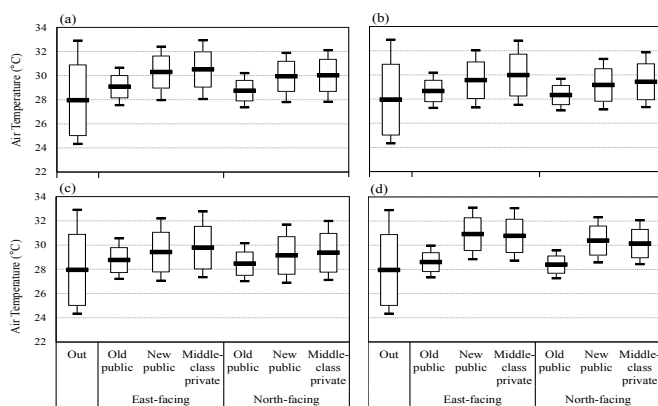


Figure 3.51. Statistical summary (5th and 95th percentile, mean and \pm one standard deviation) of indoor and outdoor air temperatures of master bedrooms in in the three apartments under (a) daytime ventilation, (b) night ventilation, (c) full-day ventilation and (c) no ventilation.

orientations, although the differences are relatively small (Figure 3.49). The simulation results obtained the lower values than the field measurement results because the field measurement was carried out on the top floor of the unit. Meanwhile, the simulation results in the middle-class high-rise apartment showed that there is almost no difference of indoor air temperature amongst the ventilation conditions regardless the orientations (Figure 3.50). If compared to the field measurement results, the simulation results are 0.3-0.9°C lower in terms of air temperatures regardless ventilation conditions. As previously shown, the RMSE for validation of master bedroom is around of 0.51°C, and it is lower than the measured experiment data (see Figure 3.43a and Table 3.9). Nevertheless, units that facing north (or south) in both apartments have relatively lower indoor air temperatures than those of facing east (or west). The differences between them are averagely around of 0.3-0.5°C for the new public apartment and 0.4-0.6°C for the middle-class high-rise apartment (Figure 3.51).

3.4.2.3 Indoor thermal comfort

Evaluation of thermal comfort in the master bedrooms was carried out by using the adaptive comfort equation, which was developed for the use in hot-humid climatic regions (Toe and Kubota 2013). Evaluation was conducted under daytime and night ventilation conditions in different orientations (i.e. facing east and north). Figures 3.52-53 show the evaluation of thermal comfort using the 80% upper comfortable limits based on the simulation results of operative temperatures in the three apartments. As shown, the indoor operative temperatures in all the three apartments exceeded the 80% upper comfortable limits for the whole daytime periods when the daytime ventilation are applied regardless the ventilation conditions and orientations (Figure 3.52a). In the case of new public apartment and middle-class high-rise

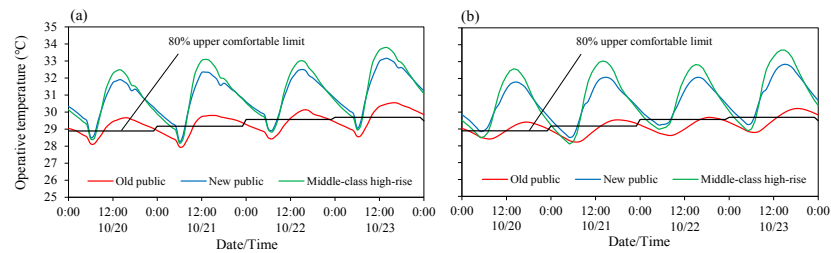


Figure 3.52. Thermal comfort evaluation in the three apartments in east-facing unit under (a) daytime ventilation and (b) night ventilation conditions based on computer simulation.

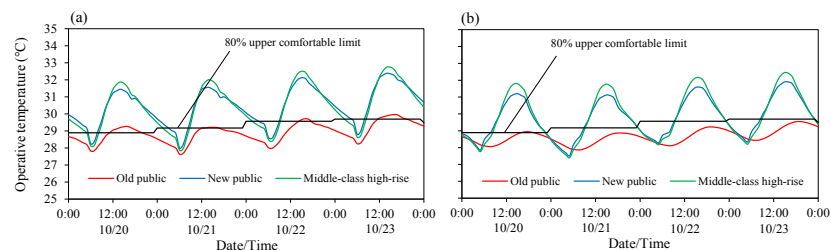


Figure 3.53. Thermal comfort evaluation in the three apartments in north-facing unit under (a) daytime ventilation and (b) night ventilation conditions based on computer simulation.

Table 3.10. Results of adaptive thermal comfort evaluation in the master bedroom under different ventilation conditions based on the simulation results.

Type of apartment	Orientation	Ventilation conditions	Deviation of OT and 80% upper comfortable limit		Exceeding period (%)
			Daily min. (°C)	Daily max. (°C)	
Old public apartment	East-facing	Daytime	0.0 to -2.0	-0.2 to 1.8	57.1
		Night	-1.8 to 0.5	-0.5 to 1.5	47.8
		Full-day	-1.9 to 0.4	-0.4 to 1.5	51.2
		No	-	-	-
	North-facing	Daytime	-2.2 to -0.5	-0.5 to 1.1	34.3
		Night	-2.0 to -0.1	-0.8 to 0.8	20.5
		Full-day	-2.0 to -0.1	-0.7 to 0.9	23.8
		No	-	-	-
New public apartment	East-facing	Daytime	-2.3 to 0.1	1.6 to 3.7	86.6
		Night	-1.8 to 0.5	1.4 to 3.5	83.6
		Full-day	-2.0 to 0.2	1.3 to 3.4	79.9
		No	-	-	-
	North-facing	Daytime	-2.3 to -0.1	1.4 to 3.1	81.2
		Night	-2.3 to -0.3	1.1 to 2.7	59.7
		Full-day	-2.0 to 0.0	1.2 to 2.7	70.8
		No	-	-	-
Middle-class private apartment	East-facing	Daytime	-1.8 to 0.0	1.8 to 4.4	85.5
		Night	-1.9 to 0.2	1.8 to 4.4	76.7
		Full-day	-2.0 to 0.0	1.7 to 4.3	74.4
		No	-	-	-
	North-facing	Daytime	-1.9 to -0.3	1.7 to 3.4	76.9
		Night	-2.4 to -0.4	1.6 to 3.2	58.8
		Full-day	-2.4 to -0.5	1.6 to 3.3	58.0
		No	-	-	-

apartment, the operative temperatures exceeded the 80% upper comfortable limits almost throughout the days particularly when the unit is facing east (Figure 3.52b). During the daytime ventilation condition, maximum indoor operative temperature in the old public apartment, new public apartment and middle-class high-rise apartment are 28.5-30.9°C, 30.1-33.2°C and 30.3-33.8°C respectively. The deviation of operative temperature from the upper limit in the master bedroom was 0.3-1.8°C for the old public apartment, 1.6-3.7°C for the new public apartment and 1.8-4.4°C for the middle-class high-rise apartment (Figure 3.52a). When night ventilation is applied, the maximum operative temperatures reduce 0.1-0.3°C, 0.2-0.3°C and 0.1°C compared to those of daytime ventilation (Figure 3.52b). Furthermore, old public apartment received the lowest exceeding periods of 80% upper comfortable limits, which is around of 57.1%, while those in the new public apartment and middle-class high-rise apartment are around of 86.6% and 85.5% respectively. When the night ventilation is applied, the exceeding periods in the three apartments reduce by 9.3%, 2.9% and 8.8% respectively.

Compared to the east-facing unit, north-facing units obtained lower operative temperatures regardless ventilation conditions. When the daytime ventilation is applied, the maximum operative temperatures of the master bedroom in the respective old public apartment, new public apartment and middle-class high-rise apartment were around 28.3-30.5°C, 30.0-32.4°C and 30.2-32.7°C; or around 0.2-0.5°C, 0.1-0.8°C and 0.2-1.0°C lower than those in east-facing unit (Figure 3.53). The exceeding periods in these units were also lower than those in the east-facing unit, which is around 34.3%, 81.2% and 76.9% respectively. When night ventilation is applied in this north-facing unit, the maximum operative temperatures as well as exceeding periods in the three apartments further reduced by 13.7%, 21.5% and 18.1% respectively (Table 3.10).

Table 3.11. Profile of measured units

Type of apartment	Unit No	Floor level	Floor area (m ²)	Number of occupants	Unit orientation	Number of fan
Old public apartment	N208	2	21	4	North	2
	S212	2	21	1	South	1
	S214	2	21	2	South	2
	N304	3	21	1	North	1
	N306	3	21	4	North	2
	S312	3	21	5	South	2
	N401	4	21	1	North	-
	S415	4	21	5	South	1
	W302	3	18	4	West	2
	N304	3	18	5	North	1
	S216	2	18	2	South	2
	W419	4	18	3	West	2
	N305	3	21	1	North	2
	S210	2	21	3	South	2
	S503	5	21	3	South	2
New public apartment	W203	2	24	2	West	1
	E216	2	24	2	East	1
	W301	3	24	5	West	2
	E313	3	24	3	East	2
	W407	4	24	1	West	2
	E420	4	24	2	East	1
	W507	5	24	3	West	1
	E515	5	24	2	East	2
	S308	3	24	2	South	1
	E203	2	24	3	East	2
	E305	3	24	4	East	1
	W419	4	24	4	West	2
	W513	5	24	4	West	0
	W119	1	32	4	West	2
	E203	2	32	2	East	1
	W419	4	32	3	West	1
	E305	3	32	4	East	2

3.5 Thermal comfort in occupied units

3.5.1. Field investigation of indoor thermal environments.

The field measurement in occupied units was conducted in 15 units in old public apartment, 17 units in new public apartment and 10 middle-class high-rise apartment units. Units of middle-class high-rise apartment were excluded for further analysis because they used air-conditioner(s). Table 3.11 presents the profile of measured units and drawings of floor plan in the measured units were shown in Appendix B. As shown in Table 3.11, average of occupancy level in the old public apartment was 3-4 persons in 18-21m² of unit area.

Figures 3.54-55 present daily mean temporal variations of air temperatures in the occupied units of the public apartments under daytime ventilation and night/full-day ventilation. Overall, the profiles of indoor air temperatures are not significantly different regardless ventilation conditions. The daily maximum air temperatures in the top floor units of the old public apartment were around of was 30.4-30.9°C, or around of 1.6-2.1°C lower than the corresponding outdoors regardless ventilation conditions employed. These air temperatures reached its peaks at the daytime. Meanwhile, the daily maximum air temperatures in the intermediate floor units were about of 29.6-31.8°C and it reached the peak at the night-time (around of 4.3-5.4°C higher than corresponding outdoors) (Figure 3.54). In the top floor units, the units receive heat from the roof at the daytime and re-radiate to the sky at the night-time (radiant cooling). The higher indoor air temperatures in the other units (i.e. intermediate floor units) at the night-time most probably due to the heat gain from occupancy level and other heat gain sources (such as from electronic devices, etc.).

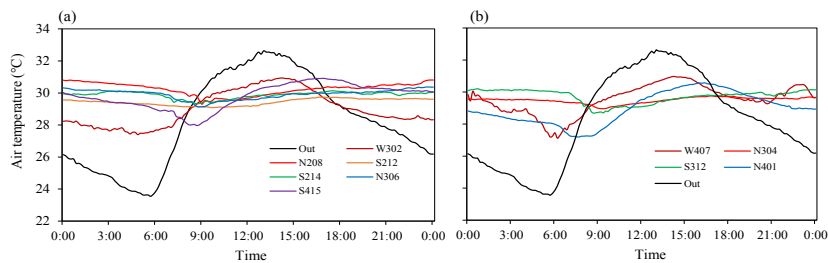


Figure 3.54. Mean temporal variation of air temperature in the old public apartment in (a) daytime ventilated units and (b) night-ventilated and full-day ventilated units.

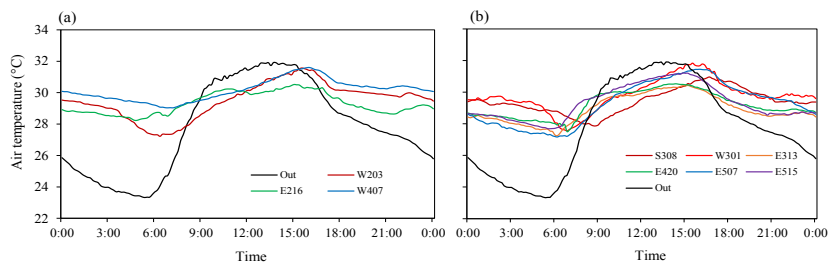


Figure 3.55. Mean temporal variation of air temperature in the new public apartment in (a) daytime ventilated units and (b) night-ventilated and full-day ventilated units.

Table 3.12. Summary of household size and indoor air temperatures (descending order of mean indoor air temperature).

	Unit No	W302	N208	S214	N306	N415	S312	W407	S212	N304	N401
Old public apart.	Household size	4	4	2	4	5	5	5	1	1	1
	Max. AT (°C)	31.8	30.8	30.8	30.7	31.4	30.9	31.3	30.1	30.0	31.2
	Avg. AT (°C)	31.3	30.3	29.9	29.9	29.8	29.7	29.5	29.4	29.5	29.0
	Unit No	W407	W301	W203	S308	E420	W507	E515	E216	E313	
New public apart.	Household size	1	5	2	2	2	3	2	2	3	
	Max. AT (°C)	31.6	31.5	31.6	32.4	31.8	31.5	31.4	31.8	31.4	
	Avg. AT (°C)	30.0	29.8	29.6	29.5	29.3	29.3	29.3	29.1	29.0	

Note:

Red color indicates hottest peak is at daytime;

Blue color indicates the hottest peak is at night-time

In the new public apartment, the mean indoor temperature was around of 29.1°C and the differences between the indoor air temperature in the top floor and intermediate floor could not be seen clearly. The daily maximum air temperatures in the west-facing units at the peak hours (around 4:00 pm) were around of 0.4-1.6°C higher than those in east-facing units (Figure 3.55). This is due to the direct solar radiation and heat emitted from the human body. The nocturnal indoor air temperatures were recorded relatively high because a lot of occupants staying in the living room from evening to the morning time. Further, Table 3.12 presents the summary of household size and indoor air temperatures in the both public apartments. As shown, there is positive correlation between the household size and the indoor air temperatures in the old public apartment. The larger household size, the higher daily maximum and average air temperature. It is noted that the heat radiated from the human body significantly affect the indoor air temperatures, mainly due to the high occupancy density. As previously described, the single room with total area of 18-21m² in this apartment was occupied by averagely 3-4 persons. Further, the unit orientation does not significantly affect the indoor air temperatures.

3.5.2 Thermal comfort evaluation

Thermal comfort was evaluated using the same adaptive comfort equation as previous sections (see Section 3.4.1.5 and 3.4.2.3). The operative temperature was calculated by assuming that indoor wind speed is 0.1 m/s throughout the day, because wind speed measurement was not carried out during this field measurement. Figure 3.56 presents the results of thermal comfort evaluation using adaptive comfort equation in the public apartments.

As shown, the operative temperatures in occupied units in both public apartments exceeded the 80% of upper comfortable limits during the daytime. The top floor units obtained the lowest operative temperatures at the night-time most probably due to the radiant cooling during the night-time. Internal heat gain from the human body also increased the operative temperature particularly during the night-time. Exceeding periods in the units with household size more than four persons (i.e. N208, W302, N306, S312, W407, and S415) were relatively larger (averagely of 60.5%) than those in the smaller household size (averagely of 37.8%)

regardless ventilation conditions. In the other hand, exceeding periods in the new public apartment was averagely of 53.9%. The average exceeding periods in the top floor units obtained relatively shorter than those in the middle floor units (top floor: 41%, intermediate floors: 56%). In addition, the average exceeding periods in east-facing units and south-facing units obtained slightly shorter than those in the west-facing units (east- and south-facing: 49%, west-facing: 56%). As previously discussed, the west-facing units received more direct solar than east-facing units, since the measurement sensors were installed in the living room. Furthermore, night and full-day ventilation conditions obtained 10% shorter of exceeding periods than the daytime ventilation.

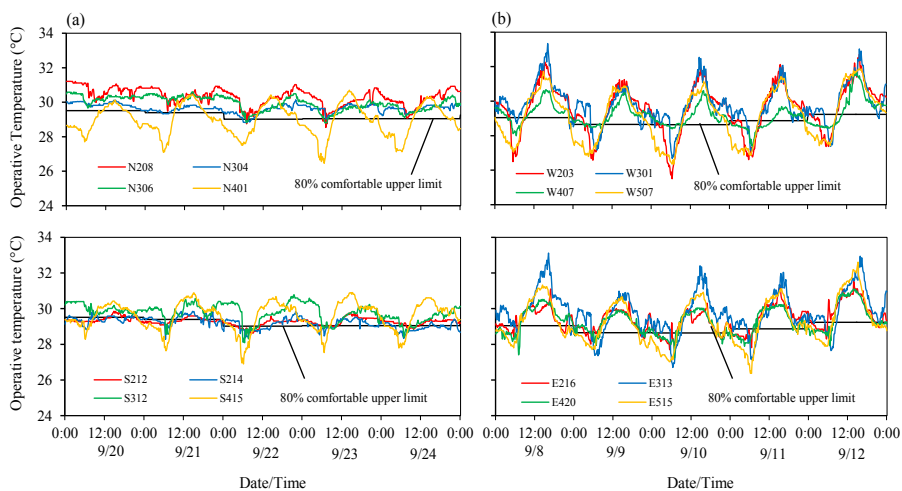


Figure 3.56. Thermal comfort evaluation using adaptive comfort equation in (a) old public apartment and (b) new public apartment under occupied condition.

3.5.3 Factors influencing thermal conditions.

Multiple regression analysis was carried out to further investigate the factors influencing indoor air temperatures in the naturally ventilated apartments (i.e. old public and new public apartments). Several independent variables were developed based on the thermal conditions (e.g. outdoor air temperature, solar radiation), physical conditions of apartment (e.g. orientation, floor level, area, etc.) and occupants' behavior on opening windows/doors (e.g. opening back windows, opening front windows, etc.). Table 3.13 summarizes the independent variables used for this analysis. The total of 32 data sets which consist of 15 data sets from old public apartment and 17 data sets from new public apartment were used. Furthermore, this analysis was conducted for target dependent variable: indoor air temperature (InAT).

The step-wise method with pairwise deletion and enter methods were utilized based on the hourly data to determine the factors which best explain the indoor air temperatures of the occupied units in the public apartments. Multicollinearity problems in this analysis were addressed by:

- 1) Merge several possible variables which has high inter-collinearity, i.e. front openings (merge from front door and front window) and back openings (merge from back door and back window).
- 2) Removing variables with high inter-collinearity ($r \geq \pm 0.7$) from correlation tables and $VIF > 10$ from coefficient tables.
- 3) Removing and control particular outliers.

Table 3.14 present the results of multiple regression analysis for the indoor air temperatures using step-wise method. As shown, outdoor air temperature is the main factor influencing the indoor air temperatures throughout the day (with high correlation from 0.435** to 0.803***). During the night-time (19:00-07:00), high correlations were presented by opening behavior of the occupants (i.e. opening back windows/doors only, openings front windows/doors only, and opening front and back windows/doors) and the household size in some occasions (at 23:00 pm). For instance, from 19:00 to 22:00, cross ventilation (i.e. open both front and back openings) is important in influencing the indoor air temperature while open the rear windows/doors only is important after 23:00 with the correlation of -0.349*-

Table 3.13. Variables used in Multiple Regression Analysis (MRA).

No	Variables	Remarks
1	OutAT	Outdoor air temperature
2	SolRad	Solar radiation
3	Dum_N	Dummy variable for orientation facing north
4	Dum_S	Dummy variable for orientation facing south
5	Dum_EW	Dummy variable for orientation facing east or west
6	FloorLevel	Location of the unit (floor level)
7	Dum_Corner	Dummy variable for location of unit in the corner
8	Area	Total area of the unit (m ²)
9	ThermalMass	Thermal mass of the unit (kg/m ³)
10	WWR	Window to wall ratio
11	Dum_RoomBetween	Dummy variable for the existence of the room between measured room and the outdoor
12	BalconyAreaRatio	Ratio of Balcony Area to the total area of unit
13	CorWidth	Width of the corridor space (m)
14	Dum_WinTopHung	Dummy variable for the existence of top hung window
15	Dum_VentHole	Dummy variable for the existence of permanent ventilation hole in the unit
16	DoorArea	Total area of the doors in the unit (m ²)
17	Dum_Shading	Dummy variable for the existence of shading devices (internal or external shading devices)
18	Dum_OpenCor	Dummy variable for the existence of the open corridor space
19	HouseholdSize	Household size (persons) at particular time
20	Occupancy	Occupancy at particular time
21	Opening_F	Opening the front windows only
22	Opening_B	Opening the back windows only
23	Opening_FandB	Opening the front and back windows at the same time
24	ApartType	Apartment type (0: old public apartment; 1: new public apartment)

Table 3.14. Results of multiple regression analysis for indoor air temperature using step-wise method (n=32)

Time	R ²	Adj. R ²	Independent variable	β		r	
0:00	0.530*	0.497***	Outdoor air temperature	0.621	**	0.654	**
			Open back openings	-0.306	*	-0.374	*
1:00	0.541*	0.510*	Outdoor air temperature	0.650	**	0.677	**
			Open back openings	-0.290	*	-0.349	*
2:00	0.422**	0.403**	Outdoor air temperature	0.650	**	0.650	**
3:00	0.411**	0.391**	Outdoor air temperature	0.641	**	0.641	**
4:00	0.378**	0.357**	Outdoor air temperature	0.615	**	0.615	**
5:00	0.335**	0.312**	Outdoor air temperature	0.579	**	0.579	**
6:00	0.325**	0.302**	Outdoor air temperature	0.570	**	0.570	**
7:00	0.347*	0.302*	Outdoor air temperature	0.435	*	0.435	**
8:00 – 11:00			<i>No equation</i>				
12:00	0.536*	0.486*	Outdoor air temperature	0.595	**	0.516	**
			Facing east/west orientation	0.358	**	0.362	*
			Floor level	0.345	*	0.289	
13:00	0.723**	0.692**	Outdoor air temperature	1.070	**	0.625	**
			Window to wall ratio	0.534	**	-0.135	
			Floor level	0.366	**	0.343	*
14:00	0.700**	0.667*	Outdoor air temperature	0.867	**	0.678	**
			Floor level	0.366	**	0.361	*
			Window to wall ratio	0.288	*	-0.067	
15:00	0.591*	0.562*	Outdoor air temperature	0.677	**	0.654	**
			Floor level	0.405	**	0.365	*
16:00	0.545*	0.513*	Outdoor air temperature	0.677	**	0.663	**
			Floor level	0.325	*	0.297	
17:00	0.546*	0.514*	Outdoor air temperature	0.701	**	0.690	**
			Floor level	0.263	*	0.235	
18:00	0.644**	0.632**	Outdoor air temperature	0.803	**	0.803	**
19:00	0.692*	0.670*	Outdoor air temperature	0.609	**	0.801	**
			Open front & back openings	-0.294	*	-0.692	**
20:00	0.791*	0.759*	Outdoor air temperature	0.726	**	0.800	**
			Open front & back openings	-0.462	**	-0.668	**
			Open front openings	-0.357	**	0.193	
			Open back openings	-0.263	*	0.112	
21:00	0.669*	0.645*	Outdoor air temperature	0.568	**	0.763	**
			Open front & back openings	-0.353	*	-0.667	**
22:00	0.600**	0.572*	Outdoor air temperature	0.515	**	0.697	**
			Open front & back openings	-0.385	**	-0.628	**
23:00	0.581*	0.534*	Outdoor air temperature	0.602	**	0.627	**
			Open back openings	-0.308	*	-0.352	*
			Household Size	0.269	*	0.353	*

0.374*). Rear windows/doors connect the indoor space with the outdoors. Since the direction is negative, it implies that the indoor air temperature at the night-time tend to be lower when the windows/doors are open during that period.

During the daytime, open the windows/doors is no longer influence the indoor air temperature. In addition to outdoor air temperature, some variables such as orientation

(0.362*), floor level (0.235-0.365*), window to wall ratio (-0.135) influence the indoor air temperatures. The results imply that units facing east or west tend to have higher indoor air temperatures during the daytime because of the direct solar radiation effects. In addition, the higher unit location from the ground floor, the indoor air temperatures also tend to be higher. Air infiltration during the daytime is also affecting the indoor air temperatures. This means that the smaller window to wall ratio, the lower indoor air temperatures would be.

Further analyses of factors influencing indoor air temperatures in the naturally ventilated apartments were carried using enter method. In this method, all independent variables were entered into the equation after reducing all possible variables (see Table 3.13) to those that necessary to predict the equation. Selection was conducted by firstly enter all the independent variables into the equation and then each variable is deleted at a time if they did not significantly providing contribution to the equation. Through above processes, 10 variables were selected and entered into the equation, they are: outdoor air temperature (OutAT), solar radiation (SolRad), east- or west-facing orientation (Dum_EW), floor level (FloorLevel), window to wall ratio (WWR), household size (HouseholdSize), occupancy level (Occupancy), opening front windows/doors (Opening_F), opening back windows/doors (Opening_B) and opening both front and back windows/doors (Opening FandB).

The results of coefficient of correlation (R^2) for single regression of each variables is shown in Figure 3.57 and the complete results of enter method are presented in Appendix E. As shown, outdoor air temperature is the main predictor of the indoor air temperature for almost throughout the day, except in the early morning time (08:00-10:00). The coefficient of correlation (R^2) of outdoor air temperatures obtained relatively higher which is averagely of above 0.30. As step-wise results, open the both front and back windows (i.e. cross ventilation) can be considered as the factor influencing indoor air temperatures at the night-time (after 20:00 pm). Meanwhile, open the rear windows/doors as well as front windows/doors, solar radiation, occupancy level and east- or west-facing unit have shown slightly higher correlation (R^2) during the daytime. It is obtained that the correlation of those variables are around of 0.14-0.21, 0.10-0.12, 0.12-0.18, 0.14-0.18 and 0.12-0.16 respectively. These results overall confirm the results of using step-wise method.

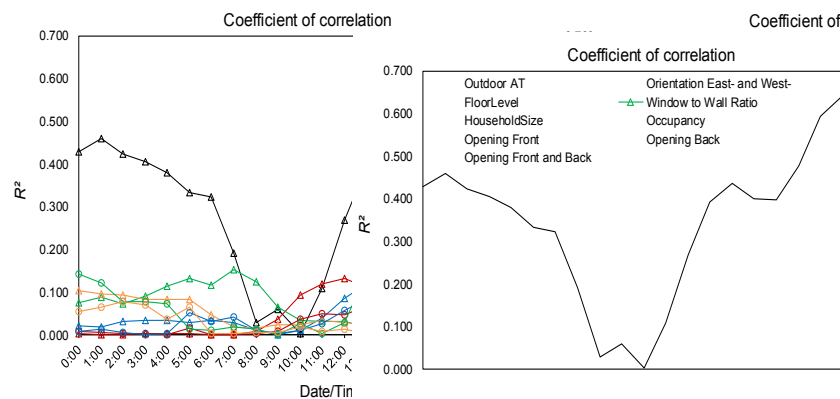


Figure 3.57. Results of multiple regression analysis for indoor air temperature using enter method.

3.6 Discussion

3.6.1. Current problems of design of apartments in Indonesia

The daytime ventilation represents the current practice of most of the occupants in the apartments of Indonesia. As previously described, daytime indoor air temperature in the old public apartment was lower than the corresponding outdoor air temperature during the peak hours, whereas the nocturnal indoor air temperature was approximately 5.0°C higher than the outdoors (Figures 3.14). The average indoor air temperature in the master bedroom of the old public apartment was nearly the same as the outdoors with the difference of only 0.1-0.5°C regardless of the ventilation conditions. In the old public apartment, indoor air temperature is well stabilized due to the relatively high thermal mass, which was calculated of 2,031 kg/m². In fact, although the large corridor space was well ventilated during the daytime as shown in the wind speed measurements, the corresponding air temperature maintained lower values than the outdoors. The other reason for relatively lower indoor air temperature in the old public apartment is the building orientation (south-facing) so that the indoor space did not receive the direct solar radiation during the measurement. Furthermore, the corridor space and balcony with a shading device played a role as a thermal buffer in reducing the heat gains. The average air temperatures in the corridor space and balcony were slightly lower than the outdoors. However, the effects of night ventilation in the old public apartment were not as high as expected due to the higher air infiltration rate although windows were closed (see Tables 3.6-7). The permanent ventilation holes were exist in this apartment.

In the case of new public, indoor air temperatures in the master bedrooms were higher than the outdoor air temperature during most of the hours (Figures 3.15). The average air temperatures in the rooms and the corridors in new public were generally higher than the outdoors. Unlike the old public apartment, the master bedroom of new public apartment did not have a balcony. During the peak hours, indoor air temperature in the master bedroom were up to 2.7°C higher than the corresponding outdoor air temperature. The sharp peaks of indoor air temperatures observed during the afternoon were mainly due to the building orientation (facing west). Moreover, the unit of the new public apartment received direct solar radiation in both living room and master bedroom. The existing external shading device was not sufficient to avoid the direct solar radiation (see Figure 3.20b). Furthermore, the corridor space in the new public apartment was semi-opened and therefore the air temperature in the space followed the outdoor temperature particularly during the daytime. In this circumstance, even if the living rooms do not receive any direct solar radiation, the daytime indoor air temperature would not become the same level as the outdoors because of the higher air temperature in the corridor space. It is important to maintain lower air temperature in the adjacent corridor spaces for lowering indoor air temperature through natural ventilation. In the other hand, the average air temperatures in the living room of the new public apartment were approximately 0.8-1.5°C lower than those in the master bedroom. This also indicates the effectiveness of buffer space such as veranda/corridor space to provide the shading for indoor spaces.

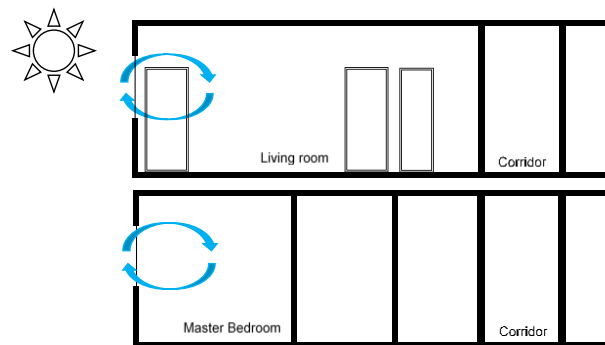


Figure 3.58. Problem of single-sided ventilation in the middle-class private apartment.

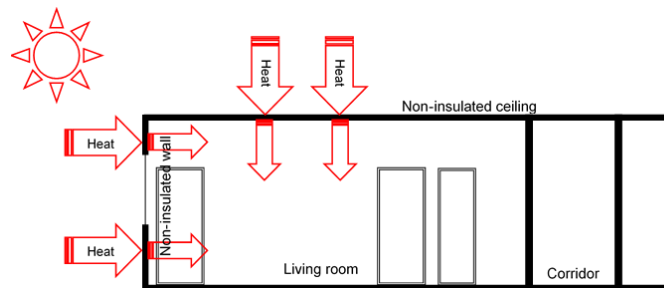


Figure 3.59. Problem of uninsulated external wall for the middle-class private apartment.

As shown in the simulation results, building orientation does not significantly affect the indoor air temperatures of master bedroom in the old public apartment under no ventilation condition due to the presence of balcony. In terms of thermal comfort, the indoor operative temperatures in both public apartments exceeded the 80% upper comfortable limits for the whole daytime periods when the daytime ventilation are applied regardless orientations (Figure 3.52a). During the daytime ventilation condition, maximum indoor operative temperature in the old public apartment, new public apartment and middle-class high-rise apartment are 28.5-30.9°C and 30.1-33.2°C respectively. Simulation results showed that night ventilation and full-day ventilation improved thermal condition in the old public and new public apartments respectively. Night ventilation would improve thermal comfort in the old public apartment by 9.3% while full day ventilation improved thermal comfort in the new public apartment by 3.0%, compared to those of daytime ventilation (Figure 3.52b). Thermal comfort would further improve in both old public and new public apartments by 13.8% and 21.5% respectively when the unit is facing south or north. Through simulation, Nguyen and Reiter (2012) found that full-day ventilation was the most sufficient ventilation strategies for the low-cost naturally ventilated apartments in hot-humid Vietnam. Under south orientation condition, this strategies obtained 68.4% of comfort zones using standard as proposed by ASHRAE-55 while night ventilation obtained 65.8% of comfort. However applying night ventilation may increase the humidity level during the daytime, as noticed by Kubota *et al.* (2009) and therefore could cause some negative effects such as molds, and so on.

In the case middle-class high-rise apartment, indoor air temperatures in the master bedroom were higher than the outdoor air temperature during most of the hours (Figures 3.16). Like the new public apartment, the master bedroom of middle-class high-rise apartments did not have a balcony, and also was not equipped with external shading device (see Figure 3.21). During the peak hours, indoor air temperature in the master bedroom of both apartments were up to 1.8°C higher than the corresponding outdoor air temperature mainly due to the building orientation (west-facing). The living room received the direct solar radiation during the peak hours, thus the peak indoor air temperatures were increased to the same levels as master bedroom. However, indoor wind speeds in the middle-class high-rise apartment were relatively low (although the higher outdoor wind speed) due to the single-sided ventilation (Figure 3.58). On the other hand, the corridor space in the middle-class high-rise apartment was enclosed and therefore the air temperature in the space was quite stable and generally high. Therefore, even if the living room do not receive any direct solar radiation, the daytime indoor air temperature would not become the same level as the outdoors due to the same reasons as that in the case of new public apartment.

Simulation results showed that indoor operative temperatures in the middle-class high-rise apartments exceeded the 80% upper comfortable limits for the whole daytime periods even when the night ventilation is applied. Full-day ventilation is found to be the most effective ventilation strategies in achieving thermal comfort in this apartment. At the east-facing orientation, maximum indoor operative temperature the daytime ventilation in this apartment were around of 30.3-33.8°C with the deviation of operative temperature from the 80% upper limit was around of 1.8-4.4°C and received the exceeding periods of averagely of 85.5%. When the full-day ventilation is applied, the thermal comfort in this apartment improved by 10.8% of comfort under same orientation. Compared to the east-facing unit, north-facing units obtained lower operative temperatures regardless ventilation conditions. Under this condition, thermal comfort for daytime ventilation condition would improve 8.6% and would further improve to 27.5%.

From the measurement of vertical distribution of temperature and surface temperature, it reveals that thermal insulation was not applied to the roof and ceiling particularly in the new public apartment and middle-class high-rise apartment. In the case of middle-class high-rise apartment, the surface temperatures of the external wall (west wall) varied largely (from 25.3 to 38.6°C) and recorded the highest values during the peak hours (Figures 3.34-35). This is mainly because of thin wall structure (80mm) with relatively low thermal capacity used, and not well insulated (Figure 3.59). It was found from the CO₂ concentration measurement that the unit in the middle-class high-rise apartment had relatively high air tightness compared to the other two types of apartment. It implies that the newly constructed middle-class high-rise apartment are designed on the premise of using air-conditioning.

Simulation results confirm the results of field measurements. As shown in Figure 3.60a, the heat flow from solar radiation in the old public apartment is not exist although it facing east. In contrast, the heat flow from solar radiation is higher in the new public apartment (Figure 3.60b); and these values are higher than those in middle-class high-rise apartment. This is because window area in the former was larger than that in the latter. In the case of middle-class high-rise apartment, the largest heat flow come from the external wall. This result clarifies the previous finding from the fields measurement. Furthermore, based on the simulation results, night ventilation reduces maximum daytime indoor air temperature

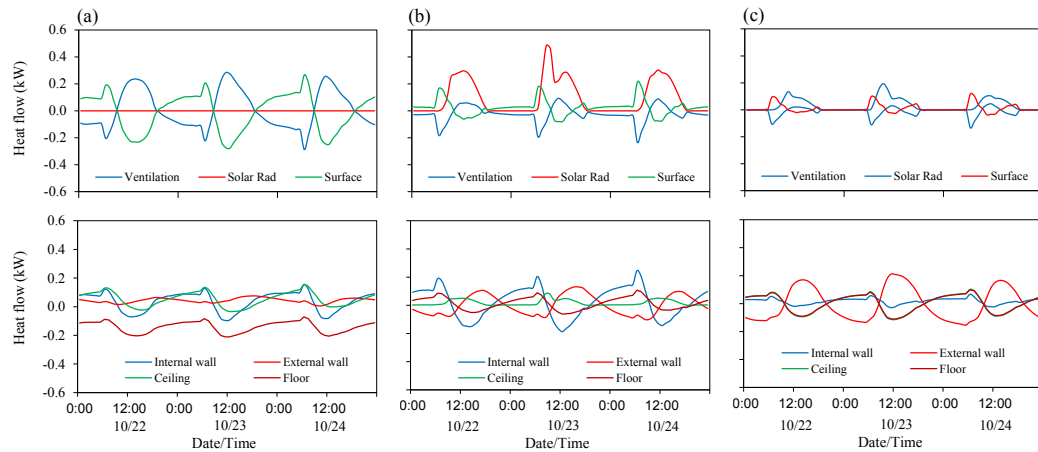


Figure 3.60. Heat flow in the three apartments based on the simulation results under daytime ventilation condition at east-facing unit in (a) old public apartment, (b) new public apartment and (c) middle-class private apartment.

compared to that of daytime ventilation. North-facing orientation reduces more the maximum daytime indoor air temperature than the base condition (i.e. east-facing and daytime ventilation). The complete results of

Under occupied condition, the profiles of indoor air temperatures were different from those of unoccupied unit. Nocturnal indoor air temperatures obtained relatively higher than the daytime indoor air temperature in the old public apartment (see Figure 3.54), most probably due to the internal heat gain from human body and the electronic devices during the night-time. In the case of new public apartment, the lowest nocturnal air temperatures were received by the units located on the top floor most probably due to the radiant cooling to the sky during the night-time.

Analysis of multiple regression analysis reveals that outdoor air temperatures is the main factor influencing the indoor air temperature throughout the days. During the night-time, opening both front and back windows/doors, opening front windows/doors only, opening back windows/doors only, and the household size were considered as predictor variables for the indoor air temperatures. Meanwhile, some variables such as orientation, floor level, window to wall ratio, were considered as factors influencing the indoor air temperatures during the daytime (see Table 3.14).

Evaluation of thermal comfort reveals the indoor operative temperatures in all the three apartments exceeded the 80% upper limits for the whole daytime periods. The deviation in the master bedroom was much larger than that in the living room in the case of new public apartment simply because of the intense direct solar radiation. As shown in Table 3.8, full-day ventilation presents relatively shorter exceeding periods than the others in the cases of the old public and new public apartments, while night ventilation obtained the shortest exceeding period in the middle-class high-rise apartment. It should be noted that thermal comfort cannot be achieved throughout the day in all the apartments if all the windows and doors are closed (i.e., no ventilation condition). However, the effects of nocturnal ventilative cooling were cut

off by the strong direct solar radiation particularly in the new public apartment and middle-class high-rise apartment. These results clearly indicate that it is very difficult to achieve thermal comfort particularly in both new public and middle-class high-rise apartments by means of natural ventilation alone, particularly when the units are facing west.

3.6.2 Potential passive cooling techniques

Based on the field measurement results, several potential passive cooling strategies can be suggested particularly for the apartments targeting the newly emerging middle-class. First of all, proper external and/or internal shading devices are necessary to avoid the direct solar radiation. Building orientation is also one of the important aspects for avoiding the excessive solar incidence into the rooms. Thermal mass can be considered as passive cooling techniques to modulate heat transmitted into the indoor space. In addition, external walls and ceilings should be insulated to reduce the heat gain through the building fabric. Appropriate thermal buffer zones (such as a balcony and corridor space) should also be considered. The corridor space should be kept at lower air temperature for lowering indoor air temperature through natural ventilation. Night ventilation would be more effective in these apartments if the above techniques are properly adopted.

3.7 Summary

Field measurements were been conducted under unoccupied and occupied conditions in the three types of apartments of Indonesia. In the naturally ventilated apartments, under unoccupied condition, the old public apartment unit showed better thermal environments compared to those in the other two apartments. During daytime ventilation condition, indoor air temperature in the old public apartment was lower than the outdoors during peak hours, while those in the new public and middle-class high-rise apartments were equal or even higher than the corresponding outdoor air temperatures. Several problems particularly in the middle-class high-rise apartment were addressed. Building orientation, insufficient shading devices and building materials (thermal property) were suggested as some of the factors causing hot conditions particularly in the newly emerging middle-class apartments. Middle-class high-rise apartments are design on premise of using air-conditioning system. In contrast, under occupied condition, nocturnal indoor air temperatures in the old public apartment were higher than the daytime indoor air temperature most probably due to the occupancy level and heat gains from the electronic devices.

Factors influencing indoor air temperatures in the naturally ventilated apartment were investigated and discussed in this chapter. In addition to outdoor air temperatures, windows/doors opening behavior (i.e. opening front and back windows/doors, opening front windows/doors only and opening back windows/doors) have become predictor of indoor air temperatures during the nigh-time. Meanwhile, some physical conditions such as solar radiation, unit orientation (i.e. east- or west-facing unit), floor level and window to wall ration are some factors influencing indoor air temperatures during the daytime.

Evaluation of thermal comfort using the adaptive comfort equation showed that thermal comfort can be achieved over 52-66% of the day only in the old public apartment under full-

day ventilation and night ventilation conditions. It was difficult to achieve thermal comfort without relying on air-conditioning in both new public and middle-class high-rise apartments. The results of computer simulation under different conditions (i.e. orientation and natural ventilation conditions) confirmed the results of field measurement. Several potential passive cooling strategies were suggested based on the results. Particularly for west-facing units, proper external and/or internal shading devices are necessary to avoid intense solar radiation in the tropics. Design of thermal buffer zones such as balcony and corridor was also recommended. To reduce the heat gains through building fabric, external walls and ceilings should be insulated. Night ventilation would be more effective in these apartments if the above techniques are properly adopted.

4

Field Investigation of Indoor Thermal Environments in Dutch Colonial Buildings

The Dutch colonial building is considered to be one of the vernacular architecture that still exists until today in Indonesia. Colonial building is a building typology that can be seen in every European colonial town, whether in Africa, Asia and America. Nearly everywhere, in the early days of the colonization, Europeans brought and applied building technologies, materials and design of their home countries to the new areas where they colonized. Sometimes what was brought was not in accordance with the local conditions including culture and climate, and thus, over time Europeans adapted their technologies, materials and design to fit to the localities without any exceptions including those in Indonesia. The presence of hundreds of years of colonial buildings have also undergone significant developments associated with the style and adjustment to the local conditions.

This chapter aims to evaluate indoor thermal environments in the three selected Dutch colonial buildings in the city of Bandung, Indonesia and to find out their cooling strategies that are worthwhile of applying to the modern high-rise apartments. This chapter begins with the history and description of Dutch colonial buildings in Indonesia (Section 4.1), and then selection of the case study buildings are discussed in the Section 4.2. Further, Section 3.3 presents the methods of field experiments to investigate the indoor thermal environments of the selected Dutch buildings. The results of field investigations are discussed in Sections 4.4-4.6, for respective case study building.

4.1 Introduction

There are several definition for the colonial building. Colonial architecture might refer to architecture from the past, constructed in former Western colonies now independent now independent for decades, (Passchier, 2007), and in this chapter, colonial buildings follow this definition. Colonial buildings in Indonesia evolved since the arrival of Europeans into the

archipelago. It can be characterized by the presence of *Verenigde Oostindische Compagnie* (VOC) in several port cities, such as Batavia, Semarang and Surabaya. The initial period of the presence of colonial buildings can be associated with the construction of the castle buildings in those cities at the beginning of the 15th century.

Over time, the fortress cities then developed and expanded to the surrounding areas. Widening areas of VOC, which were later taken over by the Netherlands East Indies Government in 1800 due to bankruptcy, significantly increased the number of the buildings with European architectural styles. In addition to the port cities, which were the entry points of the Europeans, the government established new *gementee* in inland regions, such as Bandung, Cimahi, Magelang and Malang.

The Dutch colonial buildings in Indonesia can be broadly classified into the following four periods, they are early period (1600-1800), the second period (1800-1900), the third/transition period (1900-1920s) and the modern period (1920s-1940s) (Handinoto, 2010). They were strongly associated with periodization and the influence of building style in other parts of the world, especially Europe and America (Figure 4.1).

In general, the colonial buildings in the early period were mimic to those in their home country. At this periods, the Europe's four-season architectural typology and design were transplanted directly into the tropical landscape (Widodo, 2007), for example *Stadhuis van Batavia* (Fatahillah Museum) that was built in 1707-1710 closely resemble to the *Koninklijk Paleis Amsterdam* in Netherlands and Fort Rotterdam of Makassar in South Sulawesi. The earliest structures of these buildings exemplifying the typology of trading posts, military forts and fortified towns (Widodo, 2007).

During the second period (1800-1900), the Indies Style Empire flourished in the early 19th century after the colonized areas were taken over by the Netherlands East Indies Government. The building style was inspired by the Neo-Classic style. The buildings in this era usually had a wide front and back porches with typical Greece pillars such as Doric, Ionic and Corinthian. This style of buildings was not only found in formal buildings, but also in residential buildings with large yard, various materials and roof shape adjustments. During this period, the Dutch colonial buildings gradually adapted to the hot-humid climatic condition, and characterized by larger windows area to allow natural ventilation, new design of roof and building façade, including utilization of large corridor, and the use of louver windows/doors to ensure cross ventilation (Widodo, 2007; Passchier, 2007; Handinoto, 2010).

The New Indies style was developed in the early 20th century (1900-1920s) as a form of adaptation to the tropical climate of Indonesia. The use of corridor space and shading devices instead of large corridor becoming more common during this period. As recorded by Barbieri and van Duin, (2003), at the same period, the Dutch buildings in the mainland (the Netherland) were typically not equipped with large verandas or corridor spaces. This building typology was commonly found in the Netherland not only in the public buildings such as schools, city hall, etc., but also in the residential buildings including apartments. In addition, Neo-Gothic Style was also evolved in this period marked by the construction of *De Kerk van Onze Lieve Vrouwe ten Hemelopneming* (Jakarta Cathedral Church) in Batavia (completed in 1901).

And in the last stage of development of Dutch colonial buildings, the Art-Deco Style spread in the 1920s to the 1940s in various colonial cities, particularly in Bandung as planned to be the new capital city of the Netherlands East Indies Government. The Art-Deco style itself was promoted at the *Exposition Internationale des Arts Décoratifs et Industriels Modernes*

(International Exposition of Modern Decorative and Industrial Arts) in Paris in 1925. In Bandung, this style then evolved into *Nieuwe Bouwen*/International Style with more streamlined design. In the midst of a wide variety of styles, the Neo-Gothic Style was still applied in church design in Bandung (Voskuil, 1996). Further adaptation during this period was further carried out by embracing local architectural elements (such as *pendopo*) and local spatial concept (Widodo, 2007).

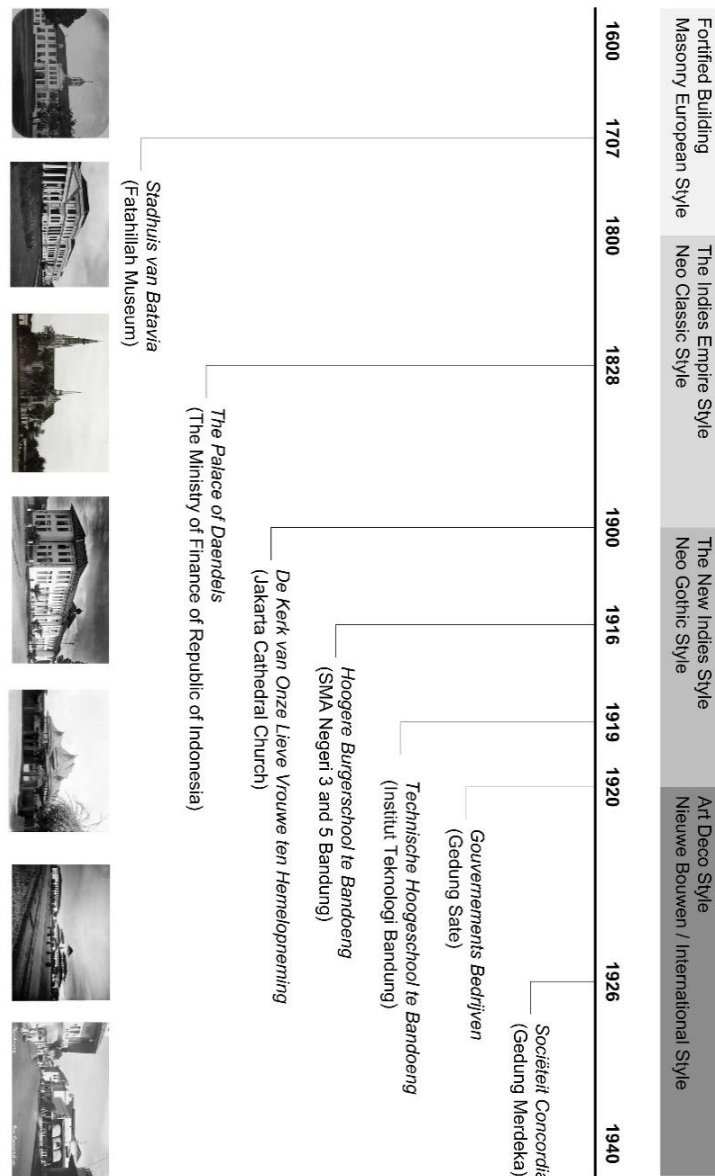


Figure 4.1. Timeline of colonial architecture in Indonesia (Collection Nationaal Museum van Wereldculturen).

4.2 Case study buildings in Bandung

Bandung was developed as a new city in the early 20th century. In 1906, the Netherlands East Indies Government promoted Bandung as *gemeente*, an autonomy city government (Kunto, 1986). The city is also known as one of the cities passed by *De Grootte Postweg* (the Great Post Road), which is one of the most important colonial cities in Indonesia that maintain colonial buildings. Several Dutch architects, such as Henri Maclaine Pont, Herman Thomas Karsten, C.P. Wolff Schoemaker, C. Citroen and *Algemeen Ingenieurs en Architecten* (A.I.A), delivered their projects in Bandung. Many of their works are buildings that contributed to the development of the identity of Bandung, including Ceremonial Hall of *Technische Hoogeschool te Bandoeng* (Institut Teknologi Bandung/ITB), *Gouvernements Bedrijven* (Gedung Sate), *Sociëteit Concordia* (Gedung Merdeka), Churches, Schools, and others. Van Dullemen (2012) presented the detailed information of Schoemaker's works particularly in Bandung.

Bandung is the capital of West Java province with the total population of 2.5 million and the population density was 14,768 people/km² as of 2014 (BPS, 2015). Since Bandung is located on the highland (approximately 760m above sea level), the climate is relatively cool. The monthly average temperature is 22.5-24.2°C, while the monthly average relative humidity ranges from 53-83%. Since its establishment in 1811, many buildings with various architectural styles were built by Dutch in the city of Bandung. In particular, these Dutch colonial buildings were constructed during the periods of New Indies Style (1900s-1920s), followed by Art-Deco Style and *Nieuwe Bouwen* Style (1920s-1940s). It is reported that approximately 1,500 Dutch colonial buildings still exist in Bandung alone and many of them are well conserved (Nurfindarti and Zulkaidi, 2015).

Selection of the case study Dutch colonial buildings was carried out through several steps. First of all, residential buildings, special buildings (such as military building, hospital, etc.) and buildings that are not occupied by the people (such as power plant, swimming pool, etc.) were removed from the list of Dutch colonial buildings in Bandung (around of 374 lists). After removing those categories, obtained around of 108 lists of buildings. These lists then grouped into two major groups, they are building forms (i.e. type of roof, existing towers, shape of building, function and type of openings) and the existence of the semi-outdoor spaces (convex roof, concave balcony and concave entrance). Further field observation was also conducted to take their environmental designs into account in the selection. The air-conditioned buildings were removed from the selection. As a result, the three colonial buildings, which are currently used as schools and office, were chosen as case study buildings, hereafter namely Case study 1, Case study 2 and Case study 3.

Case study 1 is the two-storey school building constructed with timber for the main structure and brick and lime cement for the walls (approximately 40cm thick). It was firstly built in 1916 as school building (i.e. *Hogere Burgerschool te Bandung*) and classified in the third period's colonial building (Figure 4.2a). Currently, this building is used for Senior High School, namely SMAN 3 Bandung and SMAN 5 Bandung. The front façade is facing the north, whereas a large corridor (3.35m width) is located in the southern side. On the ground floor, the corridor is enclosed while it is semi-open on the first floor. In addition, windows and doors

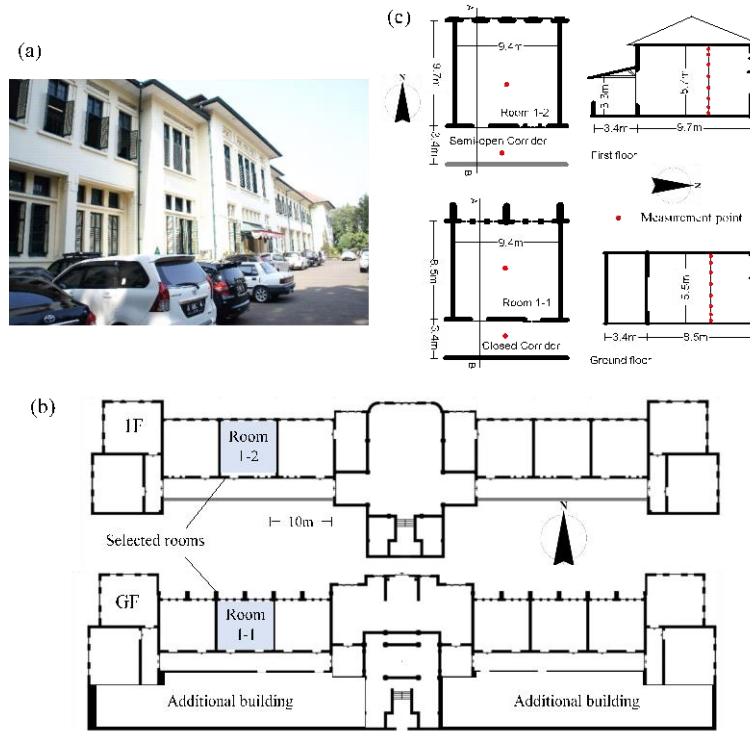


Figure 4.2. Case study buildings: (a) Views of Case study 1, (b) Floor plan of Case study 1 and (c) Floor plan and section of selected rooms (Room 1-1 and Room 1-2).



Figure 4.3 Louver windows and ventilation openings above windows/door.

in the Case study 1 were permanently open-grill while the ventilation holes were exist at above the windows/doors in all the rooms (Figure 4.3).

Meanwhile, Case study 2 is the single-storey school building with large corridors on both sides (Figure 4.4a). Like the Case study 1, it was built in 1920 as junior high school (i.e. *Meer Uitgebreid Lager Onderwijs*) and been considered as the transition architecture from the third

period to the modern period. Currently, Case study 2 is used for Junior High School, namely SMPN 5 Bandung. The original building (Dutch building) had L-form and the courtyard was exist next to the main building. The main structure of Case study 2 was concrete, and brick and lime cement were used for the walls (approximately 28cm thick). It has pitched roof with the clay roof-tile as roof cover. The width of both corridors was 3.0m and they were well shaded by long eaves. Unlike Case study 1, windows and doors in this building were not louver doors nor louver windows, but permanently ventilation holes were exist closely below ceiling (above windows/doors) (Figure 4.4b).

Case study 3 is an unoccupied two-storey office building located in the city center of Bandung (Figure 4.5a). This building was built during the last period of building colonial in 1930 and used to be utilize as Dutch's gas company (*N.V. Nederlandsch-Indische Gasmatschappij*). Currently, this building belongs to national gas company (PT. Gas Negara) and remain empty. The main structure of the building was concrete with brick and lime cement walls (approximately 35cm thick). It was a square form building with a relatively large void space at the center with less opening ventilation holes and a skylight window above it (Figure 4.5bc). It has flat room constructed from the black-painted solid concrete. The front façade was facing west and the windows were placed on one side only. As the Case study 1, the windows consist of two layers, which is the inside layer was glazing window and the outside layer was the louver window. In addition, permanently ventilation holes also existed above those windows. The corridor was situated inside the building between the rooms and void space on the first floor (Figure 4.5c).

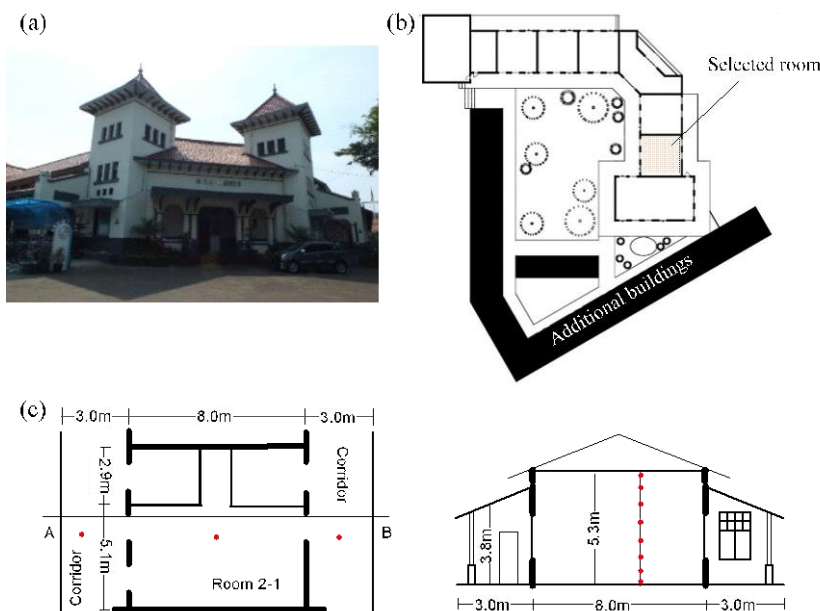


Figure 4.4. Case study buildings: (a) Views of Case study 2, (b) Floor plan of Case study 2 and (c) Floor plan and section of selected room (Room 2-1).



Figure 4.5. Case study buildings: (a) Views of Case study 3, (b) Floor plan of Case study 3 and (c) Floor plan and section of selected rooms (Room 3-1 and 3-2).

4.3 Methods

4.3.1 Field measurement

Field measurements were conducted during the hottest period of dry season from August to October 2015. In Case study 1, the measurements were conducted in two class rooms (Rooms 1-1 and 1-2). These rooms were located at the same position between the north-facing front façade and the rear corridor, but on the different floor (Room 1-1: ground floor, Room 1-2: first floor) (Figure 4.2b). Room 1-1 was slightly smaller than Room 1-2 in size (80m² and 91m², respectively). Both of the rooms have high ceilings (5.5m and 5.7m) with large windows on both sides of the rooms (Figure 4.2c). Meanwhile, the measurement in Case study 2 was carried out in one of the office rooms (Room 2-1) located in between the two corridors (east- and west-facing). Room 2-1 has a floor area of 64m² with the ceiling of 5.3m height (Figure 4.4c). In Case study 3, the field measurement was conducted in two office rooms (Rooms 3-1 and 3-2) facing south. As in Case study 1, the two rooms were located at the same position but on the different floor (Room 3-1: ground floor/GF, Room 3-2: first floor/1F). Both rooms had floor area of 32m² each and ceiling height of 5.7m (Figure 4.5bc).

Major thermal parameters including air temperature, relative humidity, wind speeds and globe temperature were measured at 1.1m above floor in the center of rooms and corridors of

the buildings respectively (Figure 4.5ab). The vertical distributions of air temperature were also measured at the same points. These distributions of the indoor space in Case study 1 were measured at 0.1m, 0.6m, 1.1m, 1.8m, 2.4 m, 3.0m, 3.6m, 4.2m, 4.8m and 5.7m (5.4m in the case of 1F) above floor level, while those in the Case study 2 were measured at 0.1m, 0.6m,

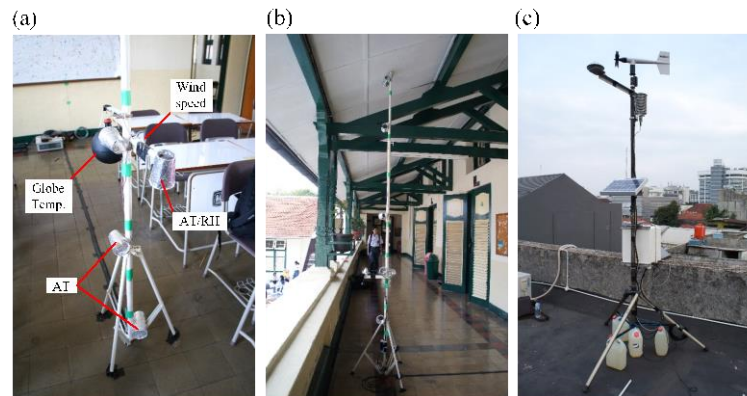


Figure 4.6. Measurement setting in (a) class room, (b) corridor space and (c) outdoor.

Table 4.1. Description of measurement instruments used in the selected rooms.

Measured variable	Instrument model	Accuracy
<i>Indoor spaces (Rooms 1-1, 1-2, 2-1 and 3-2)</i>		
Air temperature and RH	Vaisala HMP155	$\pm 0.10^{\circ}\text{C}$; $\pm 1.0\%$ RH at 0-75% RH
Globe temperature	Thermocouple type T inside 150mm black globe	$\pm 0.1\% + 0.5^{\circ}\text{C}$ plus $\pm 0.5^{\circ}\text{C}$ for cold junction compensation
Wind speed	Kanomax probe 0965-03	± 0.15 m/s at 0.1 – 4.99 m/s
<i>Indoor space (Room 3-1)</i>		
Air temperature and RH	T&D TR-72U	$\pm 0.3^{\circ}\text{C}$; $\pm 5\%$ RH
Globe temperature	Thermocouple type T black ping-pong globe	$\pm 0.1\% + 0.5^{\circ}\text{C}$ plus $\pm 0.5^{\circ}\text{C}$ for cold junction compensation
Wind speed	Kanomax probe 0965-03	± 0.15 m/s at 0.1 – 4.99 m/s
<i>Corridor spaces (Buildings 1 and 2)</i>		
Air temperature and RH	T&D TR-72U	$\pm 0.3^{\circ}\text{C}$; $\pm 5\%$ RH
Globe temperature	T&D TR-52i inside 75mm black globe	$\pm 0.1\% + 0.5^{\circ}\text{C}$ plus $\pm 0.5^{\circ}\text{C}$ for cold junction compensation
Wind speed	Kanomax probe 0965-03	± 0.15 m/s at 0.1 – 4.99 m/s
<i>Void space</i>		
Air temperature	Thermocouple type T	$\pm 0.1\% + 0.5^{\circ}\text{C}$ plus $\pm 0.5^{\circ}\text{C}$ for cold junction compensation
<i>Weather Station</i>		
Air temperature and RH	Vaisala HMP155A	$\pm 0.3^{\circ}\text{C}$; $\pm 5\%$ RH
Wind speed and wind direction	Young 05103	± 0.3 m/s or 1% of reading; $\pm 3^{\circ}$ for wind direction
Global horizontal solar radiation	Hukseflux SR20	± 2 W/m ²

1.1m, 1.7m, 2.6 m, 3.7m, 4.7m, 5.2m, and 5.2m. In Case study 3, vertical distribution of air temperatures was measured in the void space instead of corridor space at every 1.0 meter above floor level (i.e. 1.1m, 2.0m, 3.0m, 4.0m, 5.0m, 6.0m, 7.1m, 8.0m, 9.0m, 10.0m and 11.0m). In Buildings 1 and 2, the measurements were conducted under occupied conditions, while that in Case study 3 was done under unoccupied condition. Occupancy and window/door opening conditions were recorded. Different ventilation conditions were applied during the measurements, they are daytime ventilation, night ventilation, full-day ventilation and no ventilation. For the daytime ventilation, windows and all other openings were opened from 6:00 to 18:00. In contrast, all of them were opened from 18:00 to 6:00 during the night ventilation condition. Meanwhile, outdoor thermal conditions were recorded by a weather station located on the roof top in the measurement site (Figure 4.5c). All measurements were logged automatically at 10-minute intervals. Table 4.1 presents the measurement instruments used during the field measurements. Some variables such as mean radiant temperature and operative temperature, are calculated using Equations 3.4-3.8 as presented in Chapter 3.

4.3.2 Questionnaires

The field survey through questionnaires was conducted at the same time as the field measurements conducted. Questionnaires were distributed to the occupants (i.e. students and teachers) in Rooms 1-1 and 1-2 respectively during the same measurement period to investigate their perceived thermal comfort conditions. Thermal sensation, thermal preference, and thermal comfort, etc. during morning class time (08:00-11:00) and afternoon class time (12:00-15:00) were asked using a questionnaire form at the ends of the respective periods. A 7-scale of thermal sensation was used to evaluate thermal sensation (from -3 for cold to 3 for hot) and a 5-scale was used to evaluate humidity and wind speed sensations (i.e. from -2 for too dry to 2 for too humid and from -2 for too still to 2 for too breezy). Meanwhile, a 3-scale of preference was used to assess the occupants' preference for thermal, humidity and wind speed condition (i.e. -1 for cooler/lower humidity/less air flow to 1 for warmer/higher humidity/more air flow). 4-scales of thermal comfort (from 1 for very uncomfortable to 4 for comfortable). Moreover, during field survey, clothing values and the seating position relative to windows were evaluated. The detail of questionnaire is attached in the Appendix F.

4.4 Case study 1

4.4.1 Indoor thermal environments in different natural ventilation conditions

During the field measurements, outdoor air temperature ranged from 18.1 to 32.4°C with the average of 24.7°C, while the outdoor relative humidity ranged from 18 to 96% during the measurement periods. The daily global horizontal solar radiation measured at 11.2-26.0 MJ/m². Average outdoor wind speeds measured at 12.6m were approximately 1.1 m/s. Figure 4.7 presents the temporal variations of measured thermal parameters in the rooms, corridors and outdoors in the Case study 1, while Figure 4.8 shows the statistical summaries of air temperature measurements under different ventilation conditions. As shown, daytime ventilation was adopted during weekdays while night/full-day ventilation was applied during

weekends. Rooms 1-1 and 1-2 were occupied with about 30-35 students during the school time (07:00-15:00).

Figures 4.7-8 showed that indoor air temperature profiles are largely different between the floor levels (i.e., between Rooms 1-1 and 1-2) rather than the differences caused by various ventilation conditions. As shown, indoor air temperature profiles were not significantly different amongst different ventilation conditions. For instance, the maximum indoor air temperatures in the ground floor during daytime ventilation were averagely 4.5°C lower than the outdoors while those during night ventilation conditions (around of 4.3°C lower). The daytime indoor air temperatures on the ground floor (Rooms 1-1) obtained lower values (2.4-6.2°C lower than the outdoors) than those of the first floor (0.2-4.1°C lower) regardless of the ventilation conditions. Meanwhile, nocturnal indoor air temperature profiles show the opposite patterns; indoor air temperatures on the ground floor are rather higher than those of the first floor. The maximum nocturnal indoor air temperatures in the ground floor were slightly higher

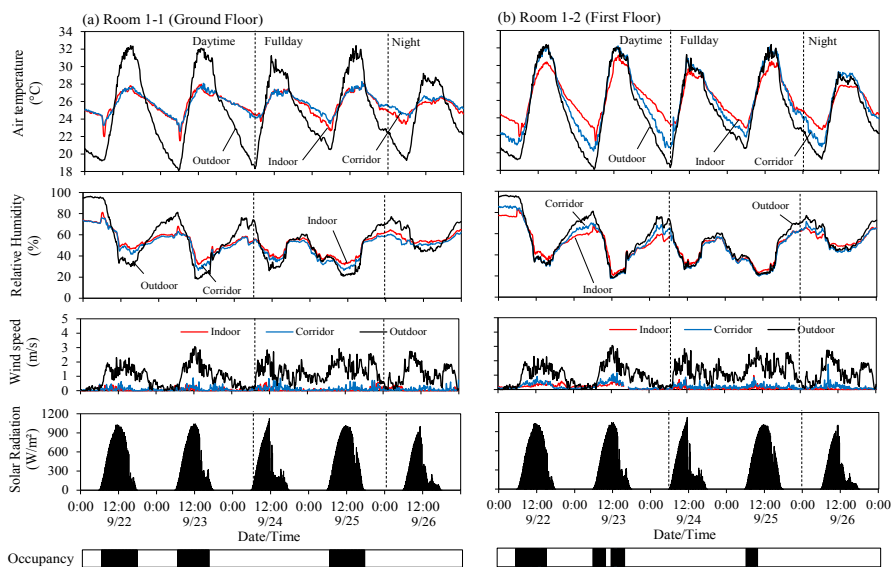


Figure 4.7 Temporal variations of thermal parameters in Case study 1 (a) Room 1-1 (ground floor) and (b) Room 1-2 (first floor).

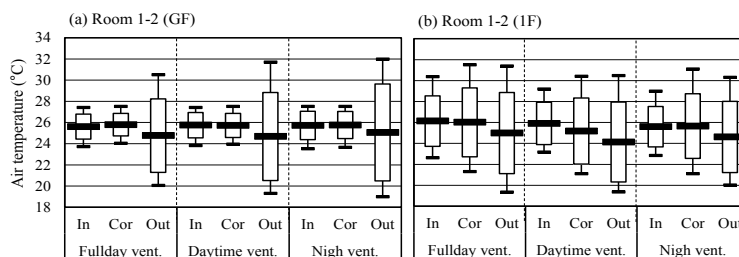


Figure 4.8. Statistical summary (5% percentile, average, 95 percentile and average \pm standard deviation) of air temperatures in (a) Room 1-1 and (b) Room 1-2 under different ventilation conditions.

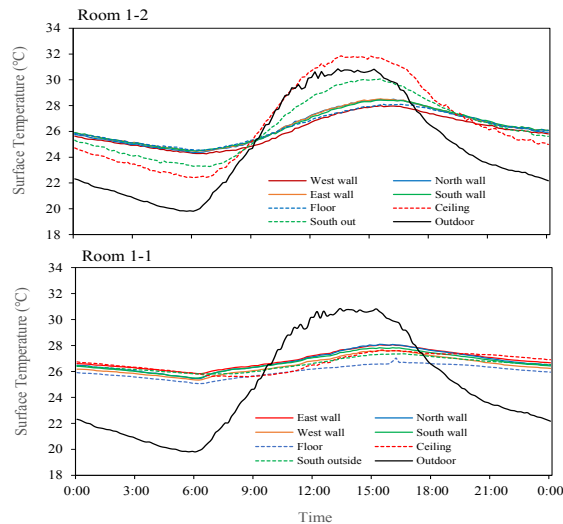


Figure 4.9. Surface temperature of walls, floor and ceiling in the Case study 1

(0.4-0.5°C higher) than those in the first floor, which are recorded at 21.5-23.8°C and 21.1-23.3°C respectively. These differences are not only due to the floor levels but also due to the difference in the corridor types (enclosed/semi-open corridors). Moreover, the nocturnal indoor air temperatures during the night-time were higher than the outdoors due to the thermal mass effect, which is accounted for 3.479 kg/m³ (in the ground floor) and 2.919 kg/m³ (in the first floor). Overall, indoor air temperatures in the rooms adjacent to enclosed corridor spaces (i.e., Room 1-1) maintained narrow diurnal temperature ranges compared to the outdoor temperatures even when the windows/doors were opened all the day (i.e., full-day ventilation).

As indicated in Figure 4.7, the measured wind speeds in corridors and Room 1-1 were slightly lower (up to 0.2m/s and 0.3m/s, respectively) than those Room 1-2 (up to 0.6m/s and 0.5m/s, respectively) during the daytime. The enclosed adjacent corridor spaces discouraged the cross ventilation in the rooms. On the other hand, air temperatures in the semi-open corridors situated adjacent to the room (Room 1-2) closely followed the outdoor air temperatures. The cooling effect of nocturnal ventilation is narrowly seen in some cases. On average, the indoor-outdoor difference of air temperatures in the ground floor became smaller at night (0.9°C to 2.9°C) when the windows/doors were opened (i.e., night ventilation and full-day ventilation) than those when windows/doors were closed (i.e., daytime ventilation) (1.1°C to 4.3°C).

Figure 4.9 shows the profile of surface temperatures of walls, floor and ceiling in respective rooms of the Case study 1. As indicated, those profiles are quite stable and almost the same amongst surfaces, except ceiling in the first floor (Room 1-2). This is most probably due the thickness of the wall, which is around 40 cm, and therefore the heat stored in the structure rather than emitted to the indoor space. It is recorded that the range of surface temperature in the first floor (24.3-28.5°C) was larger than that in the ground floor (25.3-28.1°C). This slightly difference not only due to the floor level but also due to the type of corridor space. As shown,

outside surface temperature of south wall (corridor-side) in the enclosed corridor space (Room 1-1) was lower than that in the semi-open corridor space (Room 1-2). As previously described, since the roof was uninsulated, then the roof received heat from direct solar radiation and transmitted it to the indoor space through the ceiling. Therefore, the surface temperature of the ceiling was relatively higher compared to other surfaces.

Figure 4.10 shows the correlations between indoor, corridor and outdoor air temperatures in all the rooms under the different ventilation conditions. As shown, air temperature profiles are almost the same between indoor and corridor in Rooms 1-1 (enclosed corridors) regardless of ventilation conditions, while those profiles are slightly different in Room 1-2 (semi-open corridor). It indicates that the enclosed corridor space plays a role as a thermal buffer space.

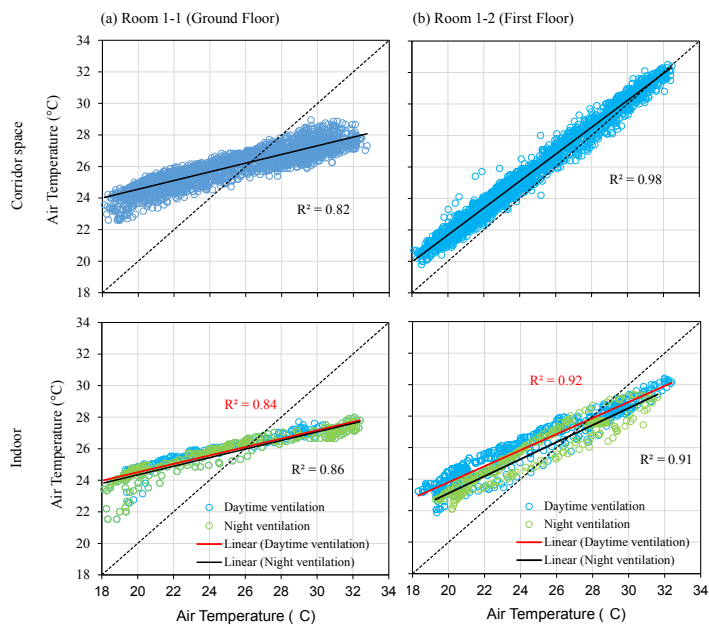


Figure 4.10 Correlation of indoor, corridor space and outdoor air temperature in Case study 1 for (a) ground floor (Room 1-1) and (b) first floor (Room 1-2).

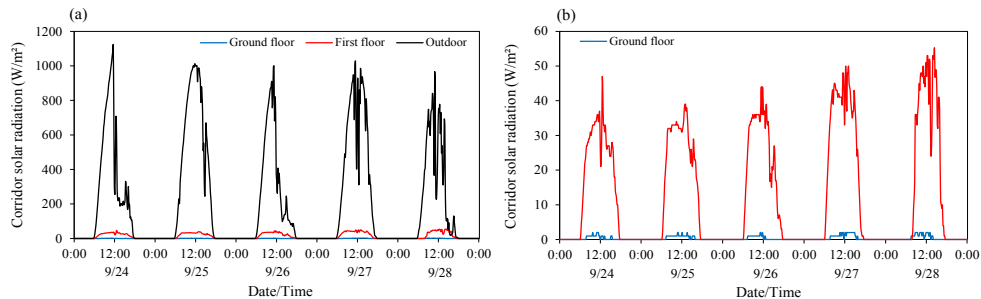


Figure 4.11. Solar radiation of the ground floor and the first floor in the Case study 1, (a) including outdoor solar radiation and (b) excluding outdoor solar radiation.

As indicated in Figure 4.11, even the semi-open corridor space cut off the solar radiation by 95% (under north-facing orientation) (Figure 4.11a). It is recorded that the maximum solar radiation recorded in the enclosed corridor space was 2.0 W/m^2 , while that in the semi-open corridor space was $39\text{-}55 \text{ W/m}^2$ (Figure 4.11b). Nevertheless, enclosed corridor space was particularly effective during the daytime, although it prevented the heat from releasing during the night-time when it was enclosed. However, even if it is a semi-open corridor space such as those for Room 2-1, the indoor air temperature adjacent to the corridor was not as low as the outdoors at night due primarily to the thermal mass effect.

The effect of night ventilation was slightly observed in Rooms 1-2. In general, its cooling effect was diminished mainly because of the permanently-open ventilation openings and louver doors. These openings allowed natural ventilation even when the main windows/doors were closed. Cross ventilation was ensured in Room 1-2 even when windows and doors were closed during the daytime (i.e., night ventilation) due to the ventilation openings and louver windows/doors. Therefore, temperature profiles in this room are almost the same among different ventilation conditions.

4.4.2 Vertical distribution of air temperatures

Figure 4.12 shows vertical distributions of air temperatures in the Case study 1 under daytime and night ventilation conditions. Overall, the ceiling surface temperatures during the daytime in Room 1-2 obtained higher values than those in Room 1-1 simply because the former was situated below roofs. Both roof and ceiling were not insulated and heat was transmitted to the room below. As previously discussed, permanently-open ventilation openings and louver doors allow the natural ventilation flowing indoor space even the windows/doors closed. It is also confirmed by the profiles of vertical distribution of indoor air temperatures particularly in Room 1-2. The vertical temperature gradients are evident even in Room 1-1. The

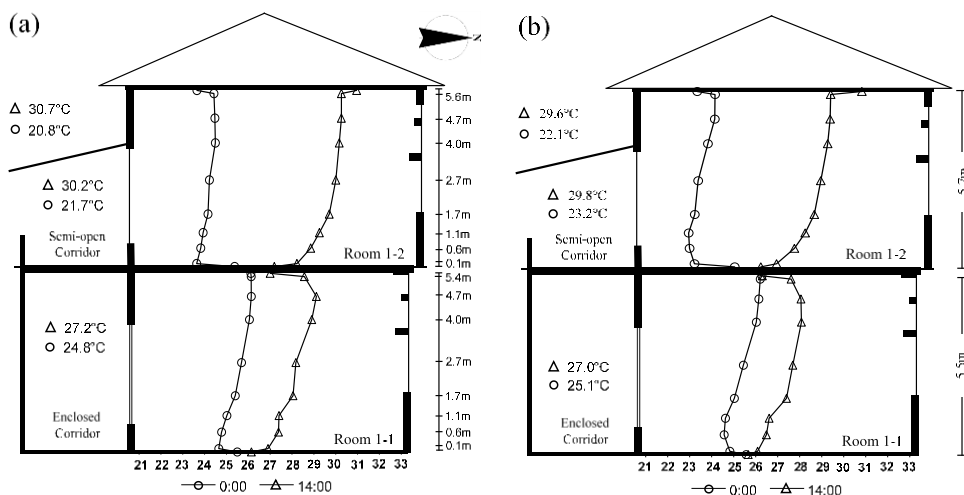


Figure 4.12. Vertical distribution of indoor air temperature in Case study 1 under (a) daytime ventilation and (b) night ventilation conditions.

temperature gradients seen in these rooms are attributed not only to the transmitted heat from the ceilings, but also to the high ceilings (5.5-5.7m). It should be noted that indoor air temperatures at the occupied level (around 1.1m above floor) maintained relatively lower values even when windows and doors were opened during daytime. As shown, the daytime indoor air temperatures at occupied level were 1.0-1.7°C lower than those at upper levels, regardless of ventilation conditions. This implies that a high ceiling would contribute to maintain relatively lower daytime air temperature even when daytime ventilation is adopted in the hot-humid outdoor conditions.

4.4.3. Thermal comfort evaluation

For this analysis, indoor thermal comfort was indexed by using the operative temperature (OT) and SET*. Operative temperatures were calculated using Equations 3.4-3.5 in Chapter 3, while thermal comfort was assessed using Adaptive Comfort Equation (ACE) as proposed by Toe and Kubota (2013) for operative temperature. Table 4.2 presents the summary of indoor thermal environments during the thermal comfort survey while Figure 4.13 shows the evaluation results of indoor thermal comfort in all rooms by the two indices, respectively. As shown, in most of the periods, operative temperature in Room 1-1 does not exceed the 80% upper comfortable limit regardless of ventilation conditions. Exceeding periods of operative temperatures in Room 1-1 during daytime ventilation, night ventilation and full-day ventilation were recorded at 16%, 13% and 15%, respectively (Table 4.3). Meanwhile, most of the daytime periods in Room 1-2 exceeded the 80% upper comfortable limits. It is recorded that during the daytime ventilation, the exceeding period was 30% while that of during night ventilation and full-day ventilation were 26% and 32% respectively. It is found that night ventilation obtained the shortest exceeding period rather than other ventilation conditions. Nevertheless, if the evaporative cooling effects are taken into account by using SET*, the resulting SET* values in Rooms 1-2 were 3.4-6.3°C lower than the operative temperature while those in Room 1-1 were 2.4-3.0°C lower than the operative temperature. As previously described, Room 1-2 received slightly higher wind speed particularly during the daytime. This means that indoor thermal comfort was considered to be achieved in the rooms throughout the day if evaporative cooling effects are considered.

Table 4.2. Summary of indoor thermal environments in Case study 1 during thermal comfort survey.

Room		Morning (08:00-12:00)			Afternoon (12:00-15:00)		
		AT (°C)	RH (%)	Wind speed (m/s)	AT (°C)	RH (%)	Wind speed (m/s)
Room 1-1 (Ground floor)	Minimum	24.8	44	0.00	26.7	42	0.00
	Maximum	27.3	58	0.35	27.9	50	0.35
	Average	26.1	52	0.10	27.1	47	0.06
	Std.Dev.	0.8	3.9	0.09	0.4	2.3	0.09
Room 1-2 (First floor)	Minimum	23.6	40	0.08	27.8	28	0.12
	Maximum	28.8	63	0.46	29.6	46	0.46
	Average	26.2	52	0.18	29.0	43	0.24
	Std.Dev.	1.7	7.3	0.09	0.5	2.3	0.10

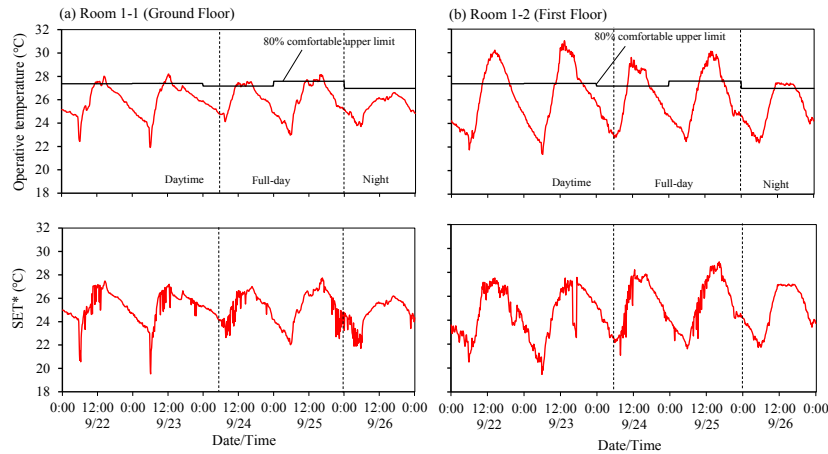


Figure 4.13. Thermal comfort evaluation using adaptive comfort evaluation and SET* in (a) Room 1-1 (ground floor) and (b) Room 1-2 (first floor).

Table 4.3. Results of adaptive comfort evaluation in Case study 1 building under different ventilation conditions.

Ventilation conditions	Room	Deviation of OT and 80% upper comfortable limit		Exceeding period (%)
		Daily min. (°C)	Daily max. (°C)	
Daytime ventilation	Room 1-1	-3.9 to -5.5	0.6 to 0.9	16
	Room 1-2	-4.4 to -5.6	1.6 to 2.8	30
Night ventilation	Room 1-1	-4.9 to -5.5	0.6 to 0.8	13
	Room 1-2	-4.6 to -5.3	0.5 to 1.7	26
Full-day ventilation	Room 1-1	-2.2 to -4.9	-0.4 to 1.3	15
	Room 1-2	-4.1 to -6.1	1.5 to 3.9	32
No ventilation	Room 1-1	-	-	-
	Room 1-2	-4.6	0.5	29

From thermal comfort survey, total of 287 respondents with total of 360 thermal responses were obtained mostly from the students; 240 thermal responses from the ground floor and 120 thermal responses from the second floor. The respondents aged between 16-17 years old with the number of female respondents (56.8%) were higher than that of male respondents (around of 43.2%). By using standard clothing values from ISO 7730, the clothing values of the respondents were observed. It is recorded that the clothing values of the male students were around 0.51-0.63 while those of the female students were around of 0.46-0.71. Meanwhile, clothing values for male teachers were averagely of 0.58 while those for female teachers were around of 0.61-0.71.

Figure 4.14 presents the results of thermal comfort survey in the both rooms during field measurement in both rooms. Other results of surveys are presented in Appendix G. Based on

the questionnaires, it is found that there is no significant difference in the thermal responses of the occupants between Rooms 1-1 and 1-2. Most of students in both rooms tend to feel “slightly cool” and “cool” during morning time. As shown, more than half of respondents (around 55.1%) of the ground floor were feel slightly cool. These numbers decreased at afternoon by around 14%. Meanwhile, those who feel neutral and slightly warm dramatically increased by more than doubled from 15.0% to 31.2% and from 2.0% to 12.9% respectively. In the case of first floor (Room 1-2), most of the respondents tend to feel cool and slightly cool (47.5% and 32.2%, respectively). At the afternoon, those who vote neutral doubled from

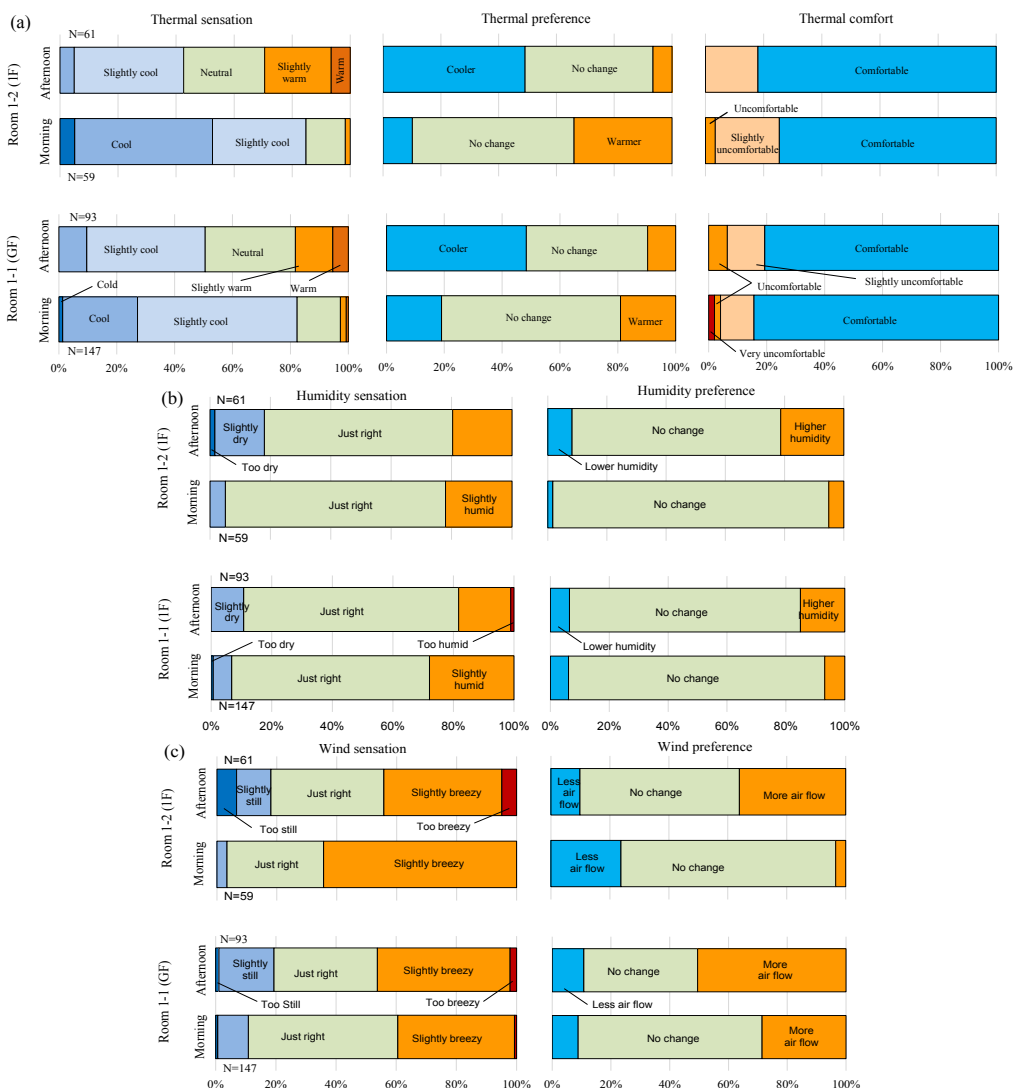


Figure 4.14 Results of thermal comfort survey in Case study 1, (a) Thermal perception, (b) Humidity perception and (c) Wind speed perception.

(a) **Test Statistics^a**

	ThermalSens	ThermalPref	ThermalComf	Hum Sens	HumPref	WindSens	WindPref
Mann-Whitney U	14266.500	13890.000	13858.000	13580.500	13788.000	12629.500	11534.000
Wilcoxon W	43186.500	42810.000	21118.000	20840.500	42708.000	41549.500	18794.000
Z	-.152	-.605	-.861	-1.068	-1.008	-2.072	-3.474
Asymp. Sig. (2-tailed)	.879	.545	.389	.286	.313	.038	.001

a. Grouping Variable: FloorLevel

(b) **Test Statistics^a**

	ThermalSens	ThermalPref	ThermalComf	Hum Sens	HumPref	WindSens	WindPref
Mann-Whitney U	3321.000	3503.500	3937.500	4155.000	4227.500	3193.500	2880.000
Wilcoxon W	5091.000	14381.500	5707.500	5925.000	15105.500	14071.500	4650.000
Z	-2.848	-2.463	-1.530	-.571	-.516	-3.279	-4.480
Asymp. Sig. (2-tailed)	.004	.014	.126	.568	.606	.001	.000

(c) **Test Statistics^a**

	ThermalSens	ThermalPref	ThermalComf	HumSens	HumPref	WindSens	WindPref
Mann-Whitney U	2460.000	2770.500	2766.000	2692.000	2712.500	2818.500	2483.000
Wilcoxon W	6831.000	4661.500	7137.000	4583.000	7083.500	4709.500	4374.000
Z	-1.461	-.272	-.383	-.646	-.608	-.071	-1.443
Asymp. Sig. (2-tailed)	.144	.786	.702	.519	.543	.943	.149

a. Grouping Variable: GFa1Fa

(d) **Test Statistics^a**

	ThermalSens	ThermalPref	ThermalComf	HumSens	Hum Pref	WindSens	WindPref
Mann-Whitney U	4128.500	4693.500	6576.000	6054.000	6327.000	6735.500	5560.000
Wilcoxon W	15006.500	9064.500	10947.000	10425.000	17205.000	17613.500	16438.000
Z	-5.568	-4.544	-.757	-1.811	-1.513	-.208	-2.728
Asymp. Sig. (2-tailed)	.000	.000	.449	.070	.130	.836	.006

a. Grouping Variable: Time

(e) **Test Statistics^a**

	ThermalSens	ThermalPref	ThermalComf	HumSens	HumPref	WindSens	WindPref
Mann-Whitney U	643.500	893.500	1655.500	1576.000	1623.500	1408.500	1109.500
Wilcoxon W	2413.500	2784.500	3425.500	3467.000	3393.500	3299.500	2879.500
Z	-6.296	-5.189	-1.057	-1.420	-1.373	-2.268	-4.230
Asymp. Sig. (2-tailed)	.000	.000	.290	.155	.170	.023	.000

a. Grouping Variable: Time

Figure 4.15. Mann-Whitney U test results for comparing the significant difference between (a) GF and 1F, (b) GF-Morning and 1F-Morning, (c) GF-Afternoon and 1F-Afternoon, (d) GF-Morning and GF-Afternoon and (e) 1F-Morning and 1F-Afternoon.

13.6% to 27.9% while those who feel slightly warm dramatically increased from 1.7% to 23.0% (Figure 4.14a). Although those who select “slightly warm” increased in the afternoon, but mostly still feel “slightly cool” and “neutral”. Under these circumstances, most of the respondents prefer no change in the morning time while at the afternoon, those who prefer cooler and no change were significantly not different regardless of location (i.e. ground floor and first floor). Most of respondents in both rooms feel comfortable (more than 70%) even during the afternoon. Interestingly, those who feel comfortable at afternoon in Room 1-2 were higher than those at morning. In contrast, different responses can be seen in Room 1-1. In terms of relative humidity, the response of the respondents in both room was the same regardless of the time (i.e. morning and afternoon). Most of the respondents tend to feel just

right and prefer no change. Furthermore, slightly differences can be found in wind speed response. In Room 1-1, majority of the students (49.6%) tend to feel just right at morning time but those students (44.1%) tend to feel slightly breezy at the afternoon. In contrast, slightly breezy were chosen by majority of the students at both the morning time and afternoon, although the number decreasing (from 64.4% to 39.3%).

To compare two sample means from the same population, and to test whether two sample means are equal or not, Mann-Whitney U test was used. This test was employed since the data collected during the field survey were ordinal data. Basically, The Mann-Whitney U is a non-parametric test used to evaluate the significant differences in a scale or ordinal dependent variables by a single dichotomous independent variable. The comparison was conducted to compare the condition between floor levels (i.e. ground floor and first floor) and between survey times (i.e. morning and afternoon). And finally, cross-tabulation between thermal sensation vote and wind speed sensation was carried out to see the relationship between two variables.

Figure 4.15 presents the statistical results of Mann-Whitney U test for the different conditions (i.e. floor levels and times) in the Case study 1 while Figure 4.16 relationships between a 5-scales of wind sensation (from -2 for too still to 2 for too breezy) and a 7-scales of thermal sensation in Rooms 1 and 2 respectively. As shown in Figure 4.15, wind sensation and wind preference were statistically significant difference between ground floor and first floor ($p < 0.05$). In general, there are no significant different between two floors in terms of thermal perceptions (i.e. thermal sensation, thermal preference and thermal comfort). These perceptions are significantly different between two rooms only at the morning time while all variables are not statistically significant different at the afternoon (Figure 4.15abc). This means that relatively large differences observed between the two rooms in terms of air temperature and operative temperature do not cause significant differences in their thermal sensation and preference. In the other hand, thermal sensation, thermal preference and wind preference were

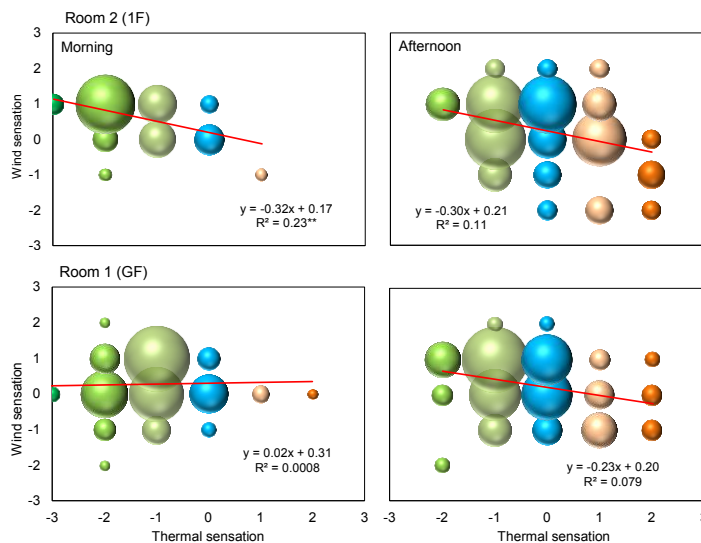


Figure 4.16. Relationship between thermal sensation and wind sensation in Rooms 1-1 and 1-2.

statistically significant different between morning time and afternoon in both ground floor and the first floor ($p < 0.05$) (Figure 4.15de). In addition, wind speed sensation also significantly different in the first floor at the afternoon. These results indicate that thermal perceptions and wind perceptions (particularly wind speed preference) are statistically significant different between two times (i.e. morning and afternoon). This is most probably that the students expected more wind speed at afternoon due to the increasing indoor air temperature to cooling themselves. As shown in Figure 4.16, during both periods, significant relationships can be seen only in Room 1-2 (adjacent to the semi-open corridor). As the wind sensation increases (when they feel stronger winds), they tend to feel cooler. As previously discussed herein, this result also proves that thermal comfort in Room 1-2 was improved by the increased wind speed due primarily to the cross ventilation improved by the semi-open corridor space. The corridor space plays an important role to improve the cross ventilation and thus indoor thermal comfort.

4.5. Case study 2

4.5.1. Indoor thermal environments in different natural ventilation conditions.

During the field measurements, outdoor air temperature ranged from 19.6 to 33.7°C with the average of 26.0 °C, while the outdoor relative humidity ranged from 18 to 96% during the measurement periods. The daily global horizontal solar radiation measured at 11.6-26.3 MJ/m². Average outdoor wind speeds in the three cases were approximately 1.1 m/s (measured at 12.6m). Room 2-1 was occupied by less than 10 office workers (staffs and teachers) during the school time (07:00-15:00). Daytime ventilation was adopted during weekdays while night/full-day ventilation was applied during weekends. Figure 4.17 presents the temporal

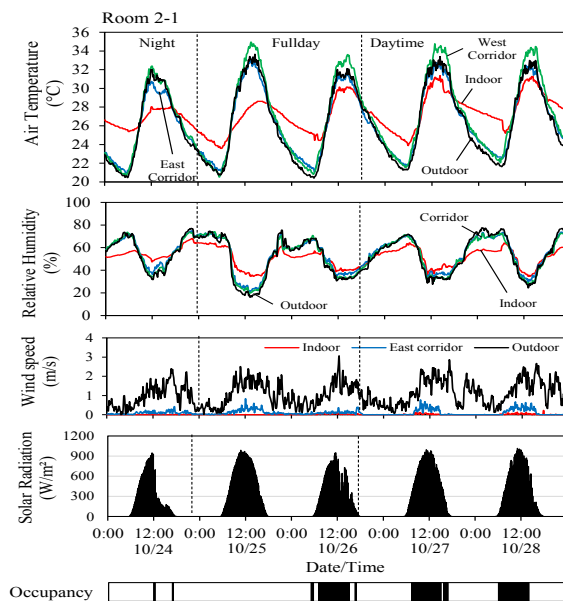


Figure 4.17. Temporal variations of thermal parameters in Case study 2 (Room 2-1).

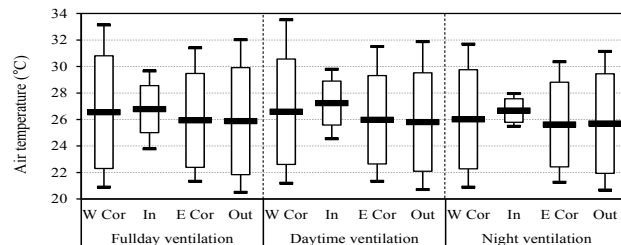


Figure 4.18. Statistical summary (5% percentile, average, 95 percentile and average \pm standard deviation) of air temperatures in Case study 2 (Room 2-1) under different ventilation conditions.

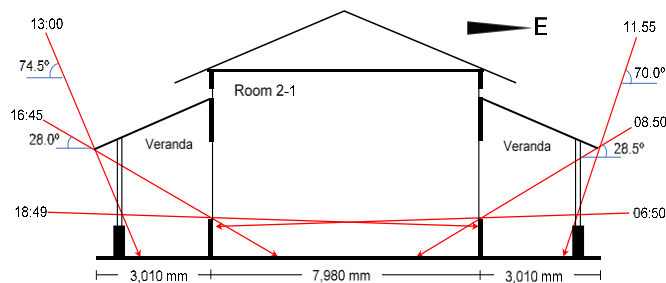


Figure 4.19. Illustration of solar radiation through the window in Case study 2 (Room 2-1).

variations of measured thermal parameters in the rooms, corridors and outdoors in the Case study 2, while Figure 4.18 shows the statistical summaries of air temperature measurements under different ventilation conditions.

Figures 4.17-18 showed that indoor air temperature profiles during daytime ventilation condition are largely different from those of other ventilation conditions. As shown, maximum daytime indoor air temperatures during the daytime ventilation were around of 29.8-31.4°C, or 1.4-3.0°C lower than the outdoors, while those during night and full-day ventilation condition were 4.0°C and 2.2-5.5°C lower than the outdoors, respectively. Meanwhile, nocturnal indoor air temperature profiles show the opposite patterns; higher than the outdoors. On the other hand, both corridor spaces are semi-open corridor space and therefore, the air temperature profiles tend to follow the outdoor air temperature. Moreover, the west corridor space had relatively higher air temperature during the peak hours than the east corridor space mainly due to the direct solar radiation from west-side and also reflected solar radiation from the pavement. As Room 1-2, air temperatures in the semi-open corridors situated adjacent to the rooms (Room 2-1) followed the outdoor air temperatures (see Figure 4.7). Cross ventilation was ensured in Room 2-1 even when windows and doors were closed during the daytime (i.e., night ventilation) due to the ventilation openings.

It is found that the cooling effect of nocturnal ventilation is narrowly seen. On average, the indoor-outdoor difference of air temperatures became smaller at night (0.9°C to 2.9°C) when the windows/doors were opened (i.e., night ventilation and full-day ventilation) than those when windows/doors were closed (i.e., daytime ventilation) (1.1°C to 4.3°C). Unlike Room 1-

2, this cooling effect was not diminished due to the permanently-open ventilation openings. Nevertheless, it is important to be noted that measurement period for night ventilation was very short, only one day measurement. The diurnal ranges of indoor air temperatures were narrower than those of the outdoors mainly due to the effects of high thermal mass of the buildings, which is calculated at 2,685 kg/m². Wind speeds were recorded quite low during field measurement (averagely of 0.1 m/s), although the windows were open throughout the days (i.e. full-day ventilation).

Although Room 2-1 is facing both east and west, the long eaves of corridor spaces prevent solar radiation from entering indoor spaces, and thus the indoor air temperatures maintained relatively lower values than the outdoors even during daytime. As shown in Figure 4.19, the Room 2-1 received the direct solar radiation through the windows for about two hours during the morning period (6:50-8:50) and for about two hours during the afternoon period (16:45-18:49). Figure 4.20 confirmed the role of the corridor space in cutting off the solar radiation before entering indoor space. It is recorded that solar radiation in the east corridor space ranged from 5 to 6 W/m² while that in the west corridor space ranged from 14 to 23 W/m². The west corridor space obtained the higher solar radiation than the east corridor space simply because the former had no obstruction to the outdoor rather than the latter (see Figure 4.4b).

Since west corridor space received more solar radiation, the west wall surface also received more heat from the outdoor than the east wall surface. As shown in Figure 4.21, the maximum surface temperature of west wall was 1.4°C higher than that of east wall. As that in Room 1-2 of Case study 1, then the roof received heat from direct solar radiation and transmitted it to the

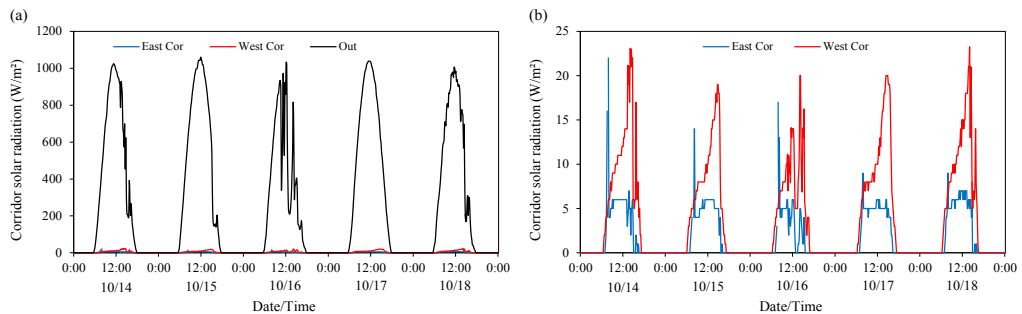


Figure 4.20. Solar radiation of the ground floor and the first floor in the Case study 2, (a) including outdoor solar radiation and (b) excluding outdoor solar radiation.

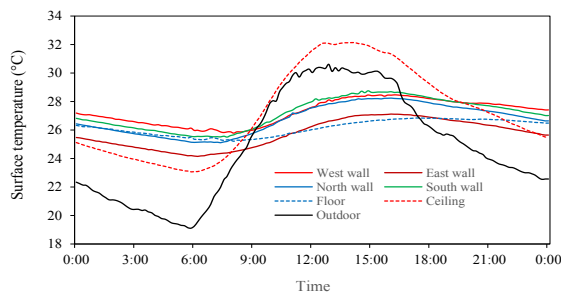


Figure 4.21. Surface temperature of walls, floor and ceiling in the Case study 2 (Room 2-1).

indoor space through the ceiling. Therefore, the surface temperature of the ceiling was relatively higher compared to other surfaces.

Figure 4.22 shows the correlations between indoor, corridor and outdoor air temperatures in Room 2-1 under the different ventilation conditions. As previous room adjacent semi-open corridor space (Room 1-2), air temperature profiles are almost different between indoor and corridor in Rooms 1-2. Furthermore, the night cooling effects can be seen in this room, although it should be noted that the measurement period under this condition was quite short (one day measurement). It is expected that daytime indoor air temperature would be further reduced if night ventilation is applied. As previously described, the diurnal ranges of indoor air temperatures in Room 2-1 were narrower than those of the outdoors mainly due to the effects of high thermal mass of the buildings.

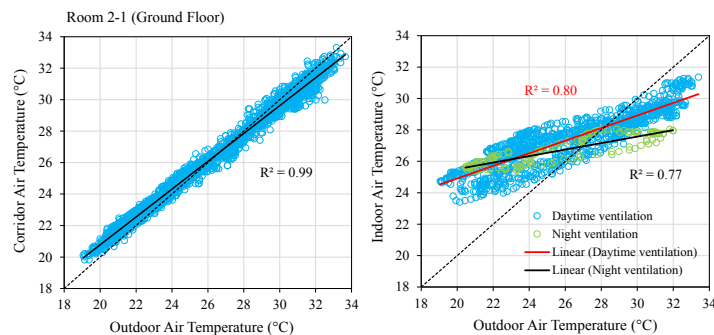


Figure 4.22. Solar radiation of the ground floor and the first floor in the Case study 2, (a) including outdoor solar radiation and (b) excluding outdoor solar radiation.

4.5.2. Vertical distribution of air temperature

Figure 4.23 shows vertical distributions of air temperatures in Room 2-1 under the different ventilation conditions. Overall, the ceiling surface temperatures during the daytime obtained higher values simply because the former was situated below roofs. Both roofs and ceilings were not insulated in the three buildings and heat was transmitted to the rooms below. The vertical temperature gradients can be seen clearly particularly during the peak hours (14:00), due to the high ceilings (5.3m). Moreover, the steeper gradient can be seen when night ventilation was applied. It is found that indoor air temperature at the occupied levels (1.1 m above floor) when night ventilation is applied was 3.3°C lower than those of when daytime ventilation is applied. In addition, indoor air temperatures at the same level maintained relatively lower values even when windows and doors were opened during daytime. It is recorded that the indoor air temperature of this level 2.5-5.8°C lower than the upper levels (above 1.7m above floor level). This implies that a high ceiling would contribute to maintain relatively lower daytime air temperature even when daytime ventilation is adopted in the hot-humid outdoor conditions. However, during peak hours, the surface temperatures of ceiling in Rooms 2-1 were 5.5 to 5.8°C higher than those of floor. This might cause local discomfort due to the radiant temperature asymmetry between ceiling and floor.

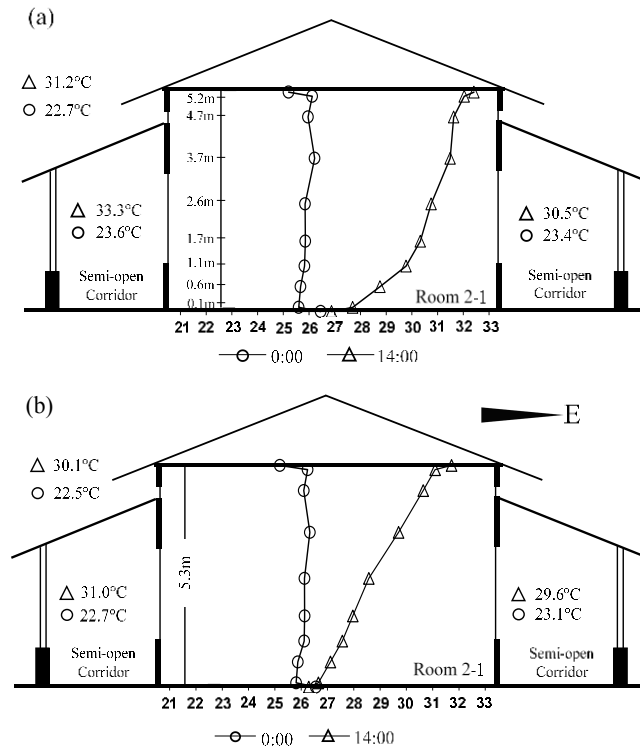


Figure 4.23. Vertical distribution of indoor air temperatures in Case study 2 for (a) daytime ventilation and (b) night ventilation conditions.

4.5.3 Thermal comfort evaluation

As previous Sections, indoor thermal comfort was indexed by using the operative temperature (OT) and SET*, was evaluated using Adaptive Comfort Equation (ACE) for operative temperature. Figure 4.24 presents the evaluation results of indoor thermal comfort in Room 2-1 by the two indices, respectively. As shown, operative temperature in Room 2-1 does not exceed the 80% upper comfortable limits in most of the periods particularly when daytime ventilation is applied. It is found that night ventilation obtained the shortest exceeding period rather than other ventilation conditions. It is recorded that during the daytime ventilation, the exceeding period was 45.2% while that of during night ventilation and full-day ventilation were 28.5% and 39.3%, respectively (Table 4.4). Nevertheless, if the evaporative cooling effects are taken into account by using SET*, the resulting SET* values in Rooms 2-1 were 1.3-1.9°C lower than the operative temperature regardless of ventilation conditions. This means that indoor thermal comfort was considered to be achieved in the rooms if evaporative cooling effects are considered.

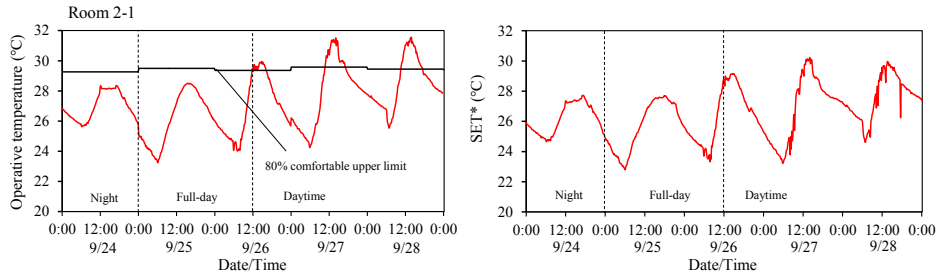


Figure 4.24. Thermal comfort evaluation using adaptive comfort evaluation and SET* in the Case study 2 (Room 2-1).

Table 4.4. Results of adaptive comfort evaluation in Case study 2 building under different ventilation conditions.

Ventilation conditions	Deviation of OT and 80% upper comfortable limit		Exceeding period (%)
	Daily min. (°C)	Daily max. (°C)	
Daytime ventilation	-2.5 to -4.1	1.4 to 3.5	45
Night ventilation	-2.1	0.6	28
Full-day ventilation	-3.2 to -4.2	0.8 to 2.5	39
No ventilation	-1.5 to -2.1	0.8 to 1.2	38

4.6. Case study 3

4.6.1. Indoor thermal environments in different natural ventilation conditions.

During the field measurements, outdoor air temperature ranged from 19.0 to 33.7°C with the average of 25.6°C, while the outdoor relative humidity ranged from 16 to 93% during the measurement periods. The daily global horizontal solar radiation measured at 11.6-26.3 MJ/m². Average outdoor wind speeds in the three cases were approximately 1.1 m/s (measured at 13.2m). Since Case study 3 was unoccupied during field measurement, different ventilation conditions were applied. During field measurements, other windows and doors (in other rooms) including entrance doors and main windows in first floor were closed. Figure 4.25 presents the temporal variations of measured thermal parameters in the rooms, corridors and outdoors in the Case study 3 under different ventilation conditions and Figure 4.26 shows the statistical summaries of air temperature measurements under different ventilation conditions. It should be noted that wind speeds were not measured in the Room 3-1, and therefore thermal comfort was not evaluated in this room.

Generally, indoor thermal environments in Case study 3 were not as good as the previous two case study buildings. As shown, indoor air temperature profiles are largely different between the floor levels (i.e., between Rooms 3-1 and 3-2) rather than the differences caused by various ventilation conditions. Overall, indoor thermal air temperatures in Room 3-2 were

relatively higher than the corresponding outdoors during the peak hours regardless of ventilation conditions. Indoor air temperatures in Room 3-2 were averagely 1.2-4.4°C higher than those in Room 3-1, regardless of the ventilation conditions. Room 3-2 received more heat than in the Room 3-1. In addition, these differences were likely also influenced by the void space. As shown, air temperatures of corresponding void space at height level 1.1m (adjacent

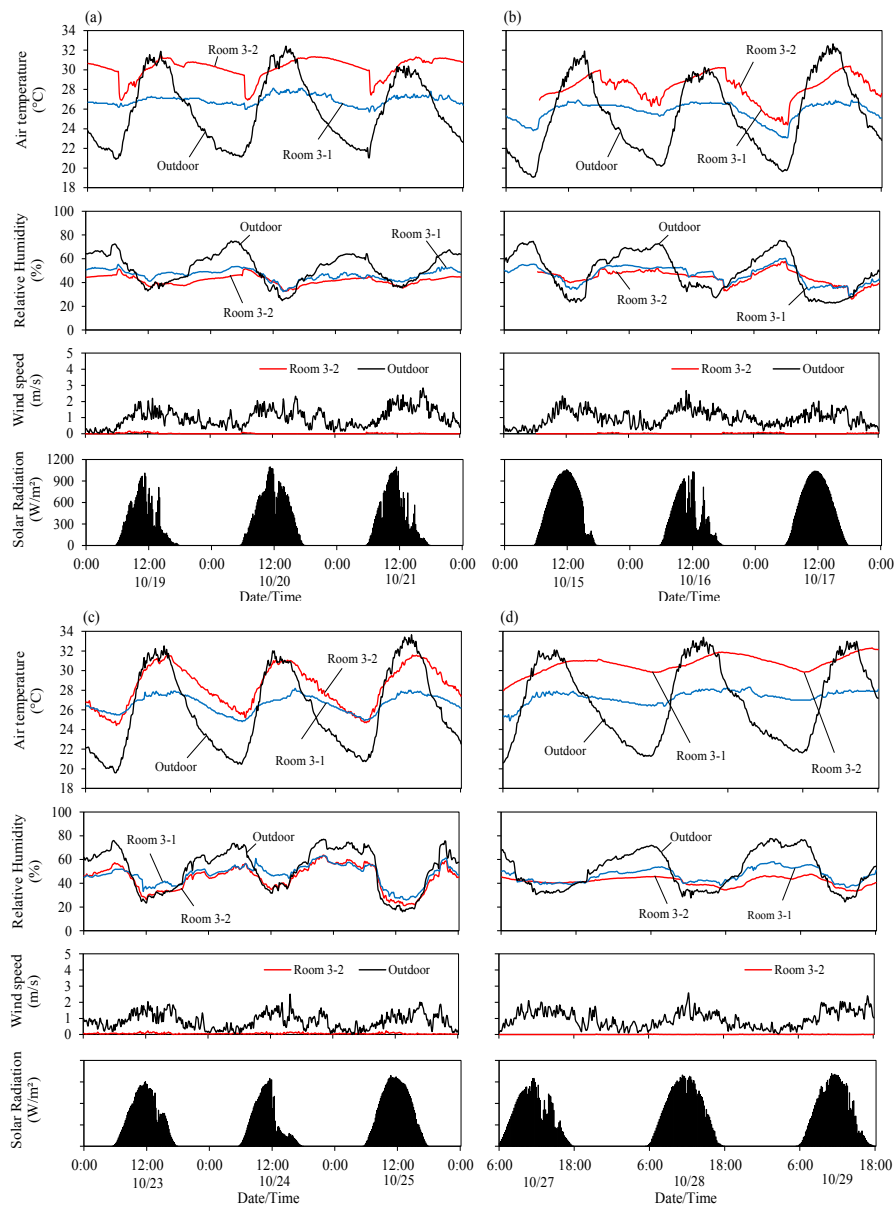


Figure 4.25. Temporal variations of thermal parameters in Case study 3 under (a) daytime ventilation, (b) night ventilation, (c) full-day ventilation and (d) no ventilation.

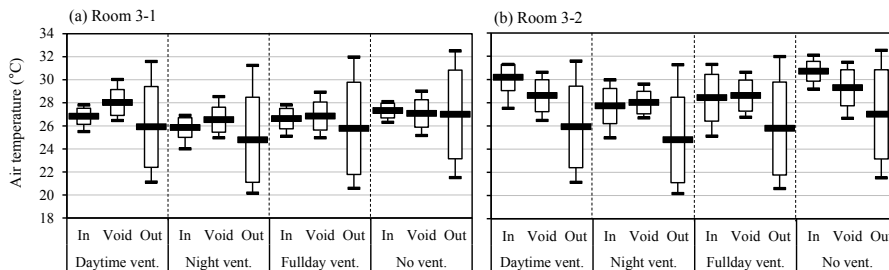


Figure 4.26. Statistical summary (5% percentile, average, 95 percentile and average \pm standard deviation) of air temperatures in Case study 3, (a) Room 3-1 and (b) Room 3-2, under different ventilation conditions.

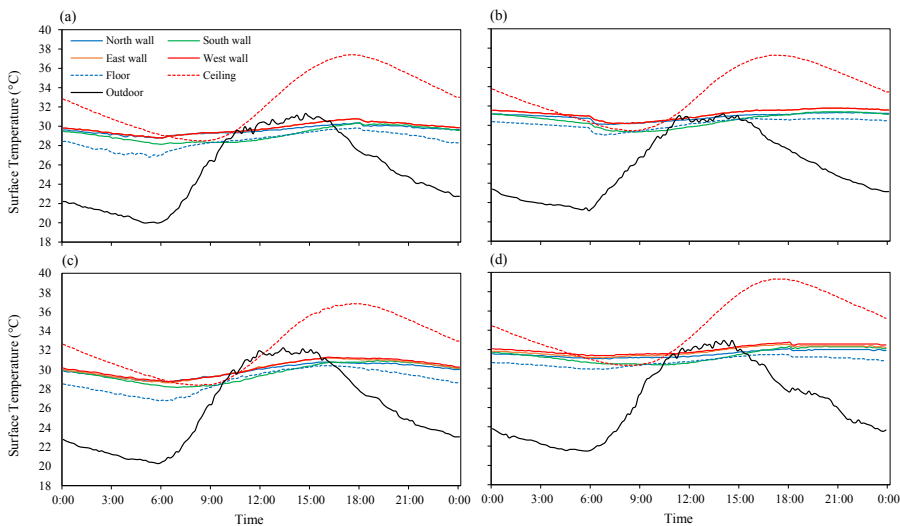


Figure 4.27. Surface temperatures of walls, floor and ceiling in the Room 3-2 under (a) night ventilation, (b) daytime ventilation, (c) full-day ventilation and (d) no ventilation conditions.

to Room 3-1) and at 7.1m (adjacent to Room 3-2) were largely different, which is 2.2-2.8°C in differences (Figures 4.25-26).

Meanwhile, the indoor air temperature profiles were also different amongst different ventilation conditions. The cooling effect of nocturnal ventilation is seen particularly in Room 3-2. On average, the indoor-outdoor difference of air temperatures became smaller at night (24.2-24.7°C). Moreover, when night ventilation was applied, daytime indoor air temperatures were 1.4-2.4°C lower than those when the windows opened during the daytime (i.e. daytime ventilation and full-day ventilation). However, nocturnal indoor air temperature profiles show higher values than the outdoors due to the thermal mass effect. The diurnal ranges of indoor air temperature of both rooms during no ventilation condition were the narrowest compared to other ventilation conditions. Although both windows and doors were open, the ventilation rates in Room 3-2 were relatively low. It is recorded that the maximum indoor wind speeds during field measurement were around 0.1-0.2 m/s, regardless of ventilation conditions. This most

probably due to the surrounding building obstructed the outdoor wind speed flowing into the room, as well as due to the enclosed void space (see Figure 4.5c). The enclosed adjacent void space discouraged the cross ventilation in the rooms.

Figure 4.27 shows the profiles of surface temperatures in the walls, floor and ceiling in Room 3-2 of Case study 3 building under different ventilation conditions. As shown, the profiles of surface temperatures are almost the same regardless of ventilation conditions. Ceiling surface temperatures were higher simply because the roof (i.e. concrete) was uninsulated and therefore it received heat from direct solar radiation. Even during the nighttime, it still higher due to the thickness of the roof, therefore it capable of storing heat longer.

Figure 4.28 shows the correlations between indoor, corresponding void space and outdoor air temperatures in all the rooms under the different ventilation conditions. As previously described, air temperature profiles of corresponding void spaces to indoor rooms are largely different. As shown, air temperature profiles are almost the same amongst different ventilation condition in Room 3-1 regardless of ventilation conditions, while those profiles are different particularly in Room 3-2. This is mainly due to the high thermal mass effect in Room 3-1 while at the same time, this room do not receive much heat from the outdoor. In contrast, even Room 3-2 also has high thermal mass, but it receives more heat than Room 3-1. The effect of night cooling was observed in Room 3-2. When night ventilation was applied, the daytime indoor air temperatures were lower than those when the windows/doors open during the daytime (i.e. full-day ventilation and daytime ventilation). It should be noted that the nocturnal indoor air temperatures under full-day and night ventilation conditions were almost the same.

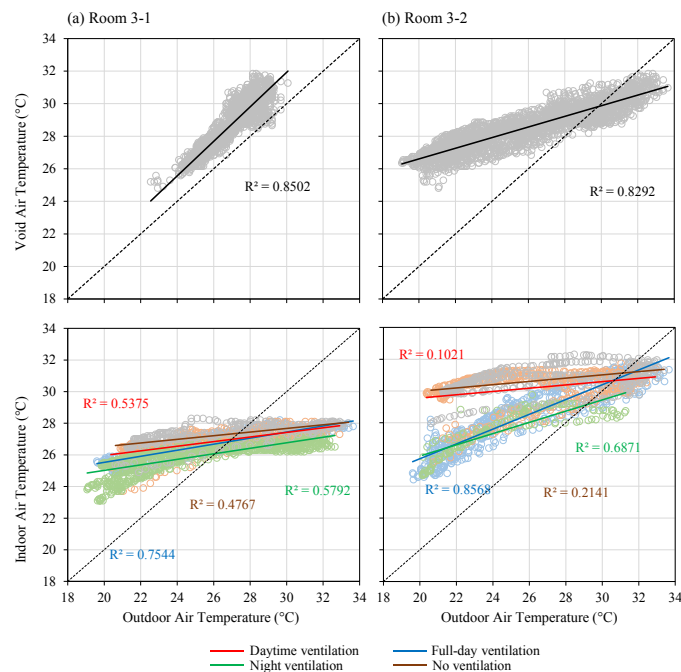


Figure 4.28. Correlation between corridor space, indoor and outdoor air temperatures in (a) Room 3-1 and (b) Room 3-2 under different ventilation conditions.

4.6.2. Vertical distribution of air temperature

Figure 4.29 shows vertical distributions of air temperatures in Case study 3 under daytime and night ventilation conditions. The ceiling surface temperatures during the daytime in Room 3-2 obtained high values simply because the former was situated below roofs. The ceiling surface temperature reached up to 37-38°C in Room 3-2 because of the absence of attic space. This roof was not insulated and therefore, heat was transmitted to the rooms below. Meanwhile, the cooling effect of nocturnal ventilation can be seen clearly in Room 3-2. The vertical temperature gradients are evident particularly in night ventilated Room 3-2. It is expected that daytime indoor air temperature would be further reduced if night ventilation is applied. The temperature gradients seen in these rooms are attributed not only to the transmitted heat from the ceilings, but also to the high ceilings (5.7m). Meanwhile, the temperature gradient still could be found in the case of daytime ventilation, even with small different from the above level (around of 0.3-2.1°C). This implies that a high ceiling would contribute to maintain relatively lower daytime air temperature even when windows and doors were opened during daytime. However, during peak hours, the surface temperatures of ceiling in Room 3-2 were 5.1 to 5.8°C higher than those of floor. This could cause local discomfort due to the radiant temperature asymmetry between ceiling and floor. Meanwhile, the air temperatures in the upper part of void space (7m and above) were overheated and averagely higher than the outdoors during the daytime. This potentially provided stack effect ventilation, although the effect was considered small because there were only small openings on the top of the void space.

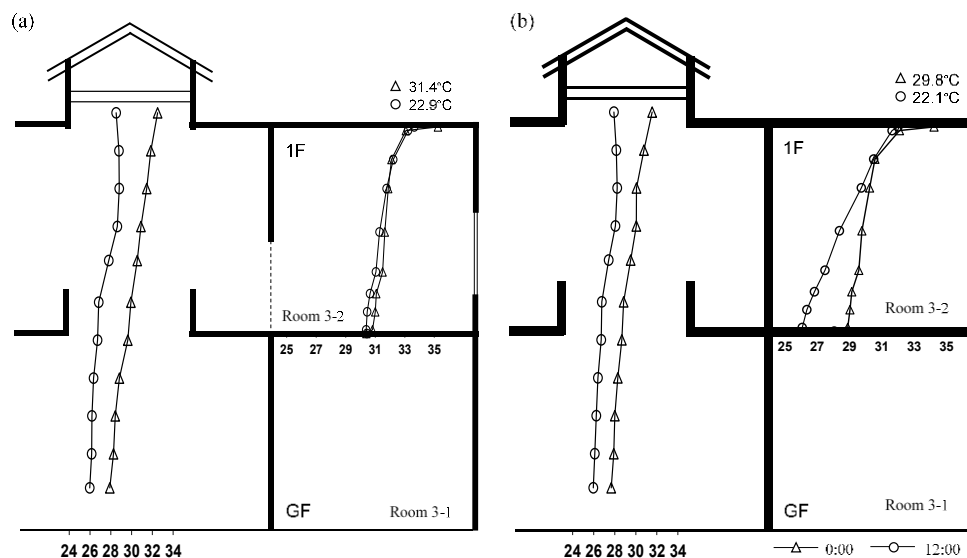


Figure 4.29. Vertical distribution of indoor air temperatures in Case study 3 building under (a) daytime ventilation and (b) night ventilation conditions.

4.6.3 Thermal comfort evaluation

Figure 4.30 presents the results of thermal comfort evaluation using adaptive comfort equation in Room 3-2 of Case study 3, while Table 4.5 summarizes the results of thermal comfort evaluation. As previous Sections, indoor thermal comfort was indexed by using the operative temperature (OT) and SET*, was evaluated using Adaptive Comfort Equation (ACE) for operative temperature. Evaluation of thermal comfort only conducted in Room 3-2 only since wind speed was not measured in Room 3-1 during field measurement. As shown, the operative temperatures in occupied units in both public apartments exceeded the 80% of upper comfortable limits during the daytime. It is found that thermal comfort cannot be achieved during the daytime particularly when daytime ventilation and no ventilation condition are applied. As indicated, the exceeding periods for above ventilation conditions were above 90% (95-99%, respectively). When the windows/doors opened during the nighttime (i.e. night ventilation and full-day ventilation), the exceeding periods reduced by more than 30% (around 61%, respectively). However, if the evaporative cooling effects are taken into account by using SET*, the resulting SET* values in Room 3-2 were lower than the

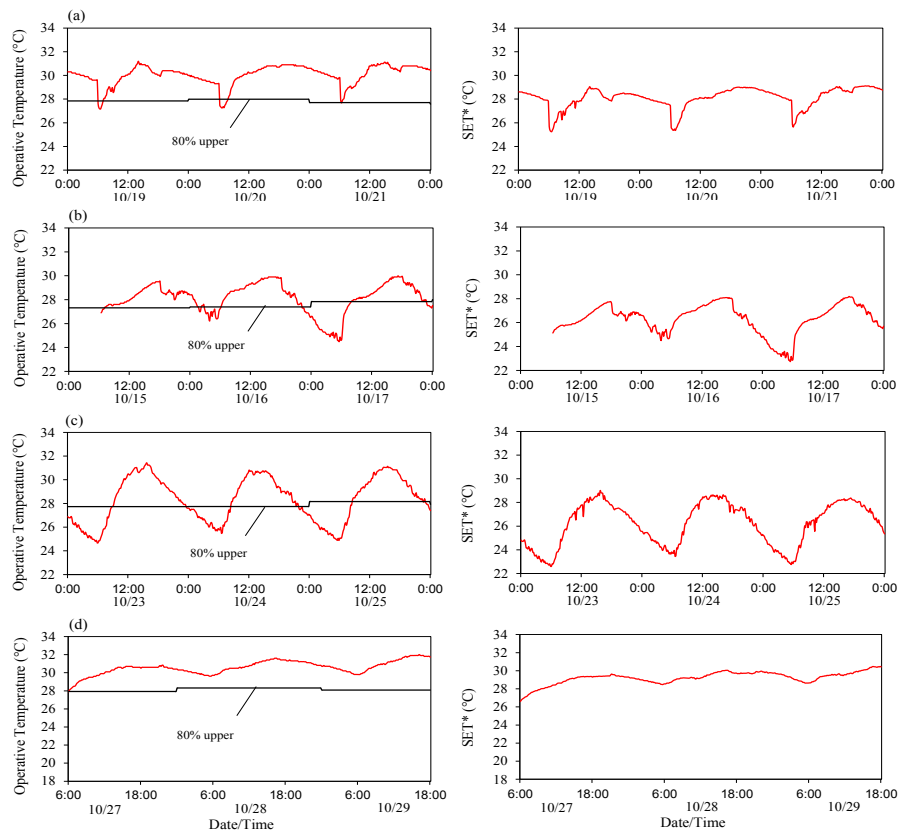


Figure 4.30. Thermal comfort evaluation using adaptive comfort evaluation and SET* in Case study 3 building under (a) daytime ventilation, (b) night ventilation, (c) full-day ventilation and (d) no ventilation conditions.

Table 4.5. Results of adaptive comfort evaluation in Case study 3 building under different ventilation conditions.

Ventilation conditions	Deviation of OT and 80% upper comfortable limit		Exceeding period (%)
	Daily min. (°C)	Daily max. (°C)	
Daytime ventilation	-0.7 to 2.0	2.8 to 3.4	95
Night ventilation	-0.4 to -3.3	1.3 to 2.5	61
Full-day ventilation	-1.2 to -3.3	3.0 to 3.7	61
No ventilation	-0.2 to 1.7	2.9 to 3.9	99

operative temperature. It is recorded that the SET* values were 1.7-2.0°C when night ventilation is applied. Meanwhile, during the daytime ventilation and no ventilation conditions, the SET* values were 1.6-2.7°C and 1.0-1.9°C lower than the corresponding operative temperature respectively. This means that indoor thermal comfort was considered to be achieved in the rooms if evaporative cooling effects are considered.

4.7 Discussion

4.7.1. The effects of corridor spaces on indoor thermal environments.

From the field measurements, it is found that corridor spaces played important roles as the thermal buffer zones. As indicated in the Figures 4.9, the air temperature profiles between enclosed corridor and indoor spaces are almost the same: relatively lower than the corresponding outdoors during the daytime but higher during the night-time, regardless of ventilation conditions. This type of corridor space is effective in lowering indoor air temperature during the daytime although it prevents heat to release during the night-time. In the other hand, the indoor air temperatures adjacent to the semi-open corridor spaces (Rooms 1-2 and 2-1) are not as low as those in Room adjacent enclosed corridor space (Room 1-1). The temperature of semi-open space follows the corresponding outdoors particularly during the daytime. Although the indoor temperatures of Rooms 1-2 and 2-1 are lower than those of Room 1-1 during night-time, but these temperature could not as low as the outdoors mainly due to thermal mass effect as well as the semi-open corridor space. As shown in Figures 4.7 and 4.17, temperatures of semi-open corridor spaces during night-time are slightly higher than the corresponding outdoors.

In addition to thermal buffer zones, corridor space also played significant roles in cutting off the effects of direct solar radiation, particularly to the building facing west or east, as illustrated in Figure 4.19. As shown, although Room 2-1 is facing east and west, the indoor air temperatures during the daytime maintain relatively lower than the corresponding outdoors thanks to long eaves of the corridor spaces. These long eaves helped preventing direct solar radiation to penetrate indoor spaces. Therefore, the heat gain from the solar radiation can be minimized by the corridor spaces functioned as a shading devices. Nevertheless, the semi-open corridor is effective to improve cross-ventilation while shading the indoor spaces. As shown in Figure 4.31, the average wind speeds during daytime and night-time in Room 1-2

were relatively higher than those in Room 1-1. Cross ventilation was ensured by the semi-open corridor in Room 1-2, even when windows/doors were closed during the daytime, due to the permanent ventilation openings and louver doors above the doors.

Study on the studies of thermal performance in colonial buildings particularly in the tropics are rarely found. Several studies on the function of veranda in vernacular architecture emphasized on semi-open corridor space rather than enclosed corridor space. The effects of enclosed corridor spaces as found in this case study building are still rarely discussed. Shading devices are very prominent and important techniques in vernacular buildings of hot-humid climatic regions to cut direct solar radiation (Chandel *et al.*, 2016; Toe and Kubota, 2015). These techniques originally employed by tropical traditional houses and then were adopted by colonial buildings in order to cope with the severe conditions of tropics. Ardiyanto, *et al.* (2015) mentioned that the corridor spaces are part of adopted passive techniques to the local hot-humid climate as shading devices without further investigate their thermal performance. Kowaltowski *et al.* (2007) found that semi-open veranda has become important element of hot-humid vernacular buildings in Brazil influenced by Portuguese colonial architecture. However, the study did not elaborate further quantitatively the roles of this corridor spaces.

Thermal function of semi-open veranda space was confirmed by Dili *et al.* (2010) in warm-humid vernacular buildings of Kerala, India. In their study, semi-open corridor space in traditional vernacular buildings of Kerala were 4.0°C lower than the outdoor, corresponding to the lower part of courtyard next to veranda space. This results correspond with our finding, where corridor space with courtyard lower the air temperature than the corridor space without courtyard (see Figure 4.15). Nguyen *et al.* (2011) found that semi open corridor spaces adjacent to the courtyard act as wind tunnel which induced more wind into the courtyard. Their study included several vernacular building types such as traditional and French colonial buildings in hot-humid Vietnam.

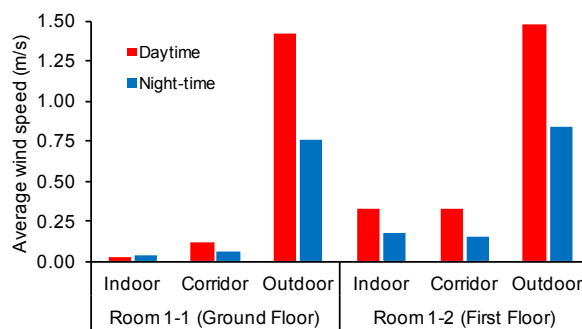


Figure 4.31. Average wind speeds of indoor, corridor and outdoor spaces at daytime and night-time in Case study 1.

4.7.2. The effects of ceiling height.

The profiles of vertical distribution of air temperatures in all above case study buildings confirmed that ceiling height important for the occupied level (around 1.1m above floor) to

maintain relatively lower values even when windows and doors were opened during daytime. The temperature gradients can easily be seen in the case of Dutch colonial buildings, attributed not only to the transmitted heat from the ceilings, but also to the high ceilings (5.5-5.7m). Even in Case study 3, which is its indoor thermal environments are generally worse, the temperature gradients are evident in Room 3-2. In the high ceiling as found in Dutch colonial buildings, heat flowing upper part of indoor space and maintaining lower part cooler than the upper. It is recorded that the indoor air temperature of this level 2.5-6.2°C lower than the upper levels (above 1.7m above floor level). However, during peak hours, the surface temperatures of ceiling particularly in Rooms 2-1 and 3-2 were above 5.0°C higher than those of floor (around 5.1-5.8°C). This might cause local discomfort due to the radiant temperature asymmetry between ceiling and floor. It is important to insulate the ceiling so that the temperature difference between ceiling and floor can be reduced.

In the case of Case study 3, high void space (around 12m height) potentially provided stack effect ventilation. During the peak hours, the upper parts of void (7m and above) are overheated and there are small temperature differences between those parts and the outdoors, which is around 0.3-1.2°C. Nonetheless, this effect is considered relatively small due to small openings on the top of void space. If those openings were wider, and the windows/doors in buildings were open, it is expected that the building enjoy the better stack effect ventilation.

In addition to high thermal mass, ceiling height is might be can be considered as a unique feature of the colonial buildings compared to other vernacular buildings. Colonial buildings have relatively high ceiling, as found in this study (around 5.3-5.7m). Several studies also reported that colonial buildings have relatively higher ceiling height than the other vernacular buildings (i.e. traditional buildings), such as reported by Kowaltowski *et al.* (2007) in hot-humid Brazil and by Nguyen *et al.* (2011) in hot-humid Vietnam. Traditional Malay houses and Chinese shop-house of Malaysia are reported have ceiling height of around 2.75-2.95m and 3.5-4.0m, respectively (Toe and Kubota, 2015). This study indicates that temperature difference between the occupied level and the upper levels are not as large as those found in the colonial buildings. In another study, vernacular buildings in hot-humid Kerala have been reported to have ceiling height of 2.5m (Shanthi Priya *et al.*, 2012), but further investigation on this were not carried out.

4.7.3. Comfort ventilation in Dutch colonial buildings.

Results of the field measurement revealed that temperature profiles in these buildings are almost the same among different ventilation conditions. It implies that the effects of structural cooling (i.e., night ventilation) diminished due to the ventilation openings and louver windows/doors, as can be seen in Case studies 1 and 3. These openings allowed natural ventilation even when the main windows/doors are closed. Particularly in Room 1-2, cross ventilation was ensured as indicated by relatively higher average indoor wind speeds than those in Room 1-1 even when windows and doors were closed during the daytime (i.e., night ventilation).

If these increasing wind speeds are taken into account to assess thermal comfort indexed by SET*, the evaluation showed that SET* values are lower than the operative temperature. The results of thermal comfort survey confirmed that this wind speed important to achieve

thermal comfort particularly when the indoor air temperatures are high. As previously discussed, thermal sensation between the occupants in Rooms 1-1 and 1-2 during the daytime are significantly not different although the former has relatively lower indoor air temperature than the latter (Room 1-2). On the other hand, wind speed responses are significantly different between two rooms. It is found that there is strong relationship between thermal sensation and wind speed sensation. The higher wind speed (breezier) perceived by the respondents, the cooler thermal conditions perceived. These findings implies that evaporative cooling effects by increasing wind speeds are considered to be important for achieving thermal comfort. Similar techniques were employed in the other vernacular buildings. For example, Malay traditional houses apply large window openings with grills and wood carving decorations to let the fresh air to come inside the house (Hoseini, *et al.*, 2014).

4.7.4. Cooling strategies employed in the Dutch colonial buildings: Recommendation for modern houses.

Based on the field measurement results, it is found that there are some cooling strategies employed in the selected Dutch colonial buildings. First of all, high thermal mass (more than 2,600 kg/m²) can be used to modulate heat so that indoor air temperature maintain lower values than the corresponding outdoors during the daytime although it increases nocturnal indoor air temperature. Nevertheless, it should be further consider if it will be applied to the modern houses, particularly in terms of structural load and cost. Moreover, it was found that corridor spaces played significant roles for the indoor thermal environments. They play a role as a thermal buffer space particularly when the corridor was enclosed, and as a shading device on the other hand. It was particularly effective during the daytime, though it prevented the heat from releasing during the night-time if it is enclosed. If the adjacent corridors in the modern houses (or apartments) can be designed to be enclosed spaces during the daytime and to be semi-open spaces during the night-time, then the thermal benefits of corridors can be obtained during day and night. The enclosed void space may be consider to generate stack effect ventilation, but it should be designed appropriately to avoid overheating during daytime as well as to ensure sufficient ventilation rate. Meanwhile, night ventilation was found to be more effective in reducing indoor air temperatures compared to other natural ventilation conditions in most cases.

The thermal comfort evaluation results showed that indoor thermal comfort was improved by increasing wind speeds during daytime although open windows may increase indoor air temperatures. Thermal comfort survey revealed that comfort ventilation is important to achieve thermal comfort. Therefore, permanent openings and louver doors/windows are important to let winds enter the rooms and ensure cross ventilation even during daytime. Furthermore, a high ceiling can be one of the options to maintain relatively lower air temperature at the occupied level in the modern houses while allowing natural ventilation during daytime. Nevertheless, the local discomfort due to the vertical air temperature difference and radiant temperature asymmetry should be further considered. To avoid that, roof and ceiling should be well insulated.

4.8. Summary

Field measurement in Dutch colonial buildings in Indonesia has been done to investigate indoor thermal environments and find out cooling strategies employed to those buildings. The measurement results showed that the selected Dutch colonial buildings, particularly those building that come from the second and third period (i.e. Buildings 1 and 2) maintained relatively low daytime indoor air temperatures compared to the corresponding outdoor temperatures mainly because of the thermal mass effect. In contrast, building from the last period (Case study 3) overall has relatively higher daytime indoor air temperature than the outdoors. Roofs and ceilings in all selected buildings were not insulated and therefore the rooms located on the top floor observed relatively higher air temperatures. Thermal comfort is achieved in the ground floor while that in the top floor exceeded 80% of comfortable limit during the daytime. Nevertheless, thermal comfort in the rooms on the top floor was improved due to the increased indoor air speeds.

Cooling strategies found from the present measurements include high thermal mass effect, night ventilation, appropriate design of corridor spaces, high ceiling and permanent openings above windows/doors (for comfort ventilation). Those above cooling strategies are worthwhile of applying to the modern houses including high-rise apartment buildings. However, these techniques should be reevaluated with the aim of applying to modern houses by considering the fact that Bandung experiences relatively cool climate. Therefore, it is important to examine the vernacular cooling techniques in different cities of Indonesia, particularly those with the hotter condition (such as Jakarta or Surabaya).

5

Parametric Study of Cooling Strategies for High-Rise Apartments

5.1 Introduction

In parallel with the previous chapters, computer simulations were performed to examine the effects of the selected cooling techniques, as found in the existing apartments of Indonesia (see Chapter 3) as well as in Dutch colonial buildings (see Chapter 4), on indoor thermal environments of the middle-class high-rise apartments. The objectives of these computer simulations have been explained in the Chapter 1. These simulations basically are to initiate a base model that will be used for further simulation studies in the future research. In addition to TRNSYS-COMIS, Computational Fluid Dynamics (CFD) was used for this simulation. The reason of using TRNSYS-COMIS was explained in the previous chapter (see Chapter 3). Description of the simulation programs particularly CFD is described in the Section 5.2. Details of the base model of the middle-class high-rise apartment unit and its validity are given in this section as well. Several simulation test cases are considered in Section 5.3 while the simulation results are discussed in Section 5.4. They include the effects of respective strategies as well as combination of those techniques.

5.2 Methods

In this chapter, computer simulations were divided into two parts. First part evaluates the indoor thermal environments of middle-class private apartment under naturally ventilated condition focusing in the living room. In this part, simulation evaluates the effect of structural cooling and comfort ventilation in the living room. Meanwhile, the second part investigated the indoor thermal environments in master bedroom under air-conditioned conditions while the living room maintain under naturally ventilated condition. The objective of this simulation is to investigate the means to reduce the cooling load in the master bedroom. To achieve above mentioned targets, two different simulation software are used, they are TRNSYS-COMIS and Computational Fluid Dynamics (CFD) STREAM.

5.2.1 TRNSYS and COMIS

Detail information of TRNSYS and COMIS were explained in Chapter 3 (Section 3.3.3). Further explanations of this software are not necessary in this chapter.

5.2.2 Computational Fluid Dynamic (CFD): STREAM

Computational Fluid Dynamics or CFD is the analysis of systems involving fluid flow, heat transfer and associated phenomena such as chemical reactions by means of computer based simulation (Versteeg and Malalasekera, 2007). CFD modelling is the process of representing a fluid flow problems by mathematical equations based on the fundamental laws of physics, and solving those equations to predict the variation of the relevant parameters within the flow field, such as velocity, pressure and temperature, and other variables such as turbulence, and so on (Jones and Whittle, 1992). The fundamental principles of computational fluid dynamics is given by Versteeg and Malalasekera (2007). CFD is very powerful and spans a wide range of industrial and non-industrial application areas such as aerodynamics of aircraft and vehicles, hydrodynamics of ship, power plant, food industry, and so on. CFD has been applied in the research of ventilation and room air distribution for almost 50 years (Nielsen, 2015) and it widely used in the building application, mainly to predict indoor and outdoor airflow, pressure, temperature, humidity and chemical species distribution (Wang and Zhai, 2016). Baskaran and Kashef (1996), for instance, used CFD for modelling wind environmental conditions around a variety of building configuration. Other application of CFD in simulating airflows in building can be seen in D'Agostino and Congedo (2014), Yang *et al.* (2015), Ramponi and Blocken (2012), Pere *et al.* (2015).

Since the movement of air in and around buildings has a major influence on thermal comfort and on the efficiency of space cooling/heating and ventilation, CFD is more suitable to investigate indoor thermal environment related to the air movement. Compared to the multi-zone approach (i.e. TRNSYS-COMIS), CFD is better-suited method to predict airflows in large indoor spaces than are the zonal method for isothermal airflow (Wang and Zhai, 2016). However, simulation using CFD takes huge computational time than using multi-zone approach. In addition, CFD simulation has some uncertainties in reproducing complex turbulent flows, and therefore it need to be verified and validated against field experimental data (Omrani *et al.*, 2017). Nevertheless, it is quite difficult to use CFD without previous knowledge on fluid dynamics and software (Fouquier *et al.*, 2013).

STREAM is the thermal fluid analysis software developed by Software Cradle Co., Ltd. This software can solve the thermal fluid problems consider heat transfer, mass diffusion, chemical reaction and so on. Basically, as the other SFD programs, STREAM consists of three sets of programs, they are Preprocessor (*STpre*), Solver (*STsolver*) and Postprocessor (*STpost*) (Figure 5.1). Preprocessor helps create input data; Solver loads the input data, executes calculation and output results; and Postprocessor loads the output results and visualize the results.

Theoretically, there are two basic kinds of thermodynamics systems: closed systems and control volume. A closed system refers to a fixed quantity of matter whereas a control volume

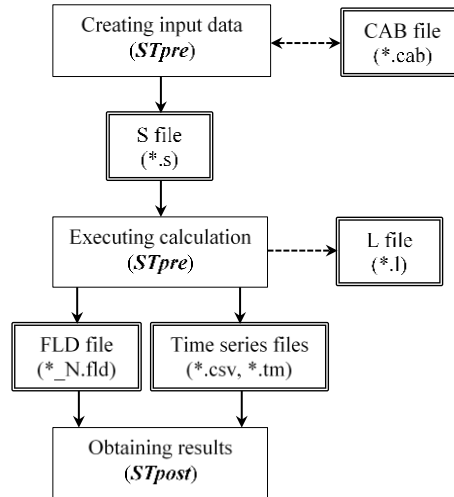


Figure 5.1. Main components and structures of the CFD STREAM (Cradle, 2015)

is a region of space through which mass may flow cross the boundary of a thermal system (Moran *et al.*, 2011). In order to solve the problems of thermal fluid analysis in CFD, some fundamental equations that govern the physical problems under given boundary conditions and initial conditions are necessary. Governing equations in this thermo-fluid analysis are consider to momentum conservation equations (the Navier-Stokes equations), continuity equation, energy conservation equation and model equations to represent turbulent transport. The finite volume method is used in this software to solve the equations by converting above equations into an integral conservation form that is expressed on each fractional unit of decomposed elements (control volume). In the finite volume method, each equation is solved separately for the whole field so that in one iteration, equations are assembled and solutions obtained for each velocity component, pressure, temperature and turbulent quantities (Patankar in Jones and Whittle, 1992).

For the simulation analysis, incompressible air is used as main component of fluid. Density of incompressible fluid (air) is assumed to be constant, and is determined by the equation of state in compressible analysis. In a control volume, there may be several locations on the boundary through which mass enters or exits. For incompressible fluids, mass conservation, momentum conservation, energy conservation and turbulent kinetic energy and its dissipation rate are governed using following equations (Equations 5.1-4) respectively:

$$\frac{\partial v_i}{\partial x_i} = 0 \quad (5.1)$$

$$\frac{\partial \rho v_i}{\partial t} + \frac{\partial v_j \rho u_i}{\partial x_j} = -\frac{\partial p}{\partial x_i} + \frac{\partial}{\partial x_j} \mu \frac{\partial v_i}{\partial x_j} - \rho g_i \beta (T - T_o) \quad (5.2)$$

$$\frac{\partial \rho C_p T}{\partial t} + \frac{\partial v_j \rho C_p T}{\partial x_j} = \frac{\partial}{\partial x_j} K \frac{\partial T}{\partial x_j} + \dot{q} \quad (5.3)$$

$$\frac{\partial \rho k}{\partial t} + \frac{\partial v_i \rho k}{\partial x_i} = \frac{\partial}{\partial x_i} \left(\frac{\mu_t}{\sigma_k} \frac{\partial k}{\partial x_i} \right) + G_s + G_T - \rho \epsilon \quad (5.4)$$

where v_i is velocity of flow in x_i - direction (m/s); x_i is coordinates (m); ρ is density of fluid or solid/material (kg/m³); t is time (s); p is pressure of fluid (N/m²); μ is viscosity of a fluid (kg/m.s); g_i is gravity (m/s²); β is thermal expansion coefficient (1/K); T is temperature of a fluid or solid (K); T_o is reference temperature of fluid (K); C_p is specific heat at constant pressure (J/kg.K); K is thermal conductivity (J/m.s.K); \dot{q} is heat source (J/m³.s); and k is turbulent kinetic energy (m²/s²).

Preprocessor (*STpre*)

Figure 5.2 illustrates the flowchart of simulation process in STREAM. Basically, Preprocessor (*STpre*) comprises all necessary procedures in setting the model before executing it in the Solver (*STsolver*). *STpre* prepares all information to analyze fluid flows such as mesh division, material properties, boundary conditions, initial conditions, and so on (Cradle, 2015). In STREAM, 3D model can be directly developed in the Preprocessor (*STpre*) or imported from the other CAD data after previously converted into allowable file format (for example XT file, STEP file, DXF file, IDF file, etc.). Before making 3D model, computational domain should be determined (see Figure 5.3).

Setting of boundary condition is the most important part for CFD simulation besides meshing generation. The boundary where flow goes in or out is referred to as inflow and outflow boundary. As previously described, all mathematical calculations on physical transfer (i.e. mass, momentum, energy and continuity) in this simulation caused by the flow is referred to as advection. Inflow and outflow boundary conditions can be specified only at the interfaces between the fluid and the outside of computational domain. In STREAM, four types of inflow and outflow boundary are available, they are: conditions to specify flow velocity, conditions to specify pressure, conditions to specify both flow velocity and pressure and conditions not to specify anything (Cradle, 2015).

Wall boundary conditions are important to calculate momentum conservation equations. Wall boundary conditions directly have influence on the equations for energy and momentum conservation, as well as diffusive species through the boundary surface. Wall boundary conditions of momentum equations are referred to as wall stress conditions. They determine the friction stress (σ_{ij}) of the interface between fluid and walls. These conditions can be set on the interfaces between fluid and non-fluid material (such as solid) (Cradle, 2015). Thermal boundaries setting is necessary to calculate the heat transfer between fluid and solid, or between solid and solid. Heat transfer coefficient need to be specified, with refer to the specified literature such as ASHRAE (2013). Solar radiation setting (absorbance of surface material) as well as radiation setting (emission of material) are other important setting for heat boundary conditions. Method of humidity transfer (from outdoor to indoor and vice versa), also determined in this simulation.

There are two calculation methods for simulation using CFD STREAM: steady state and transient. Steady state means that temperatures and heat flow rates are independent of time (Hens, 2012). A system is at steady state if none of its properties change with time, or variations with the time are small enough to ignore (Moran *et al.*, 2011). In contrast, transient

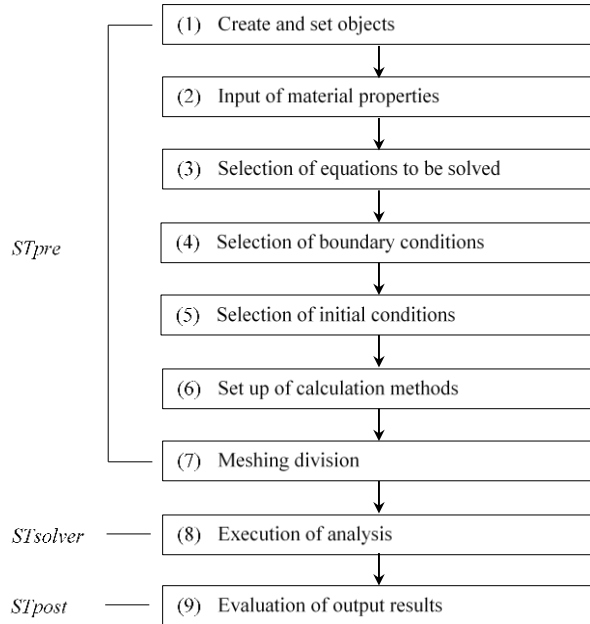


Figure 5.2. Flowchart of simulation in the CFD STREAM (source: Cradle, 2015)

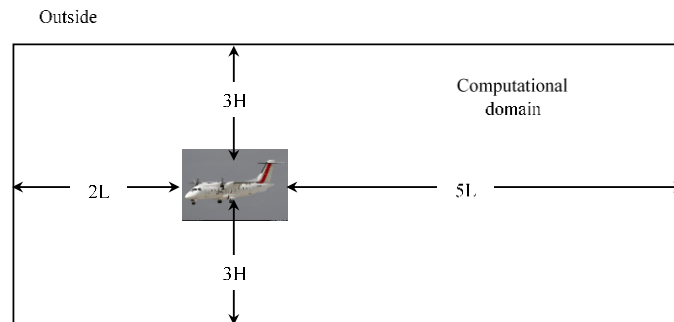


Figure 5.3. Computational domain for CFD simulation.

means that temperatures and flow rates change with time (Hens, 2012). Therefore, transient method should be used when the properties varying and change with time. Another important variable in calculation method is courant number, particularly for transient analysis method. The Courant number can be considered to be a parameter that avoids wrong prediction so that a time step size (Δt) is maintained within a proper range (Cradle, 2015). The time step for given Courant number is computed using following equation:

$$\Delta t = \frac{\Delta L}{v} C \quad (5.5)$$

where Δt is time step (s), ΔL is element size (m), v is wind speed (m/s) and C is Courant number.

For better accuracy of calculation, time step should satisfy condition of $C \leq 1$. Users may specify time step sizes throughout the calculation without using the Courant number. In this case, the time step size should satisfy the same Courant number condition (Cradle, 2015). Equation 5.5 indicate that the element size is important in order to obtain optimum time step for better accuracy, and therefore, meshing size is very important in simulation. A consideration of the grid or mesh upon which a calculation is performed is fundamental to the application of CFD. In a CFD application, the solution domain is defined by a grid of cells where the number and size of cells represent the level of resolution that the calculation can achieve (Jones and Whittle, 1992). Meshing size should be generate as small as possible, and for reasons of resolution and accuracy of solution, the cells should be concentrated predominantly in the region adjacent to the air inlet and near to the walls. It should be noted to maintain ratio of grid of 1:1.2 in order to maintain high accuracy of calculation. Output file to be executed in the Solver (*STsolver*) is S file (*.s) (see Figure 5.1). The S file is a medium to communicate information from *STpre* to *STsolver*. Information necessary for *STpre* is saved in another file namely CAB file.

Solver (*STsolver*)

On loading the S file in *STsolver*, a simulation for a fluid flow with or without heat and mass transfer is carried out on the basis of input information from the S file. *STsolver* input consists of data type specification, file specification, initial settings and commands. A situation for the simulation can be confirmed by way of a log file called L file. *STsolver* sometimes needs a huge amount of time to simulate flows, and hence may not be able to finish the simulation at one time. If the simulation is divided into more than two steps, the simulation

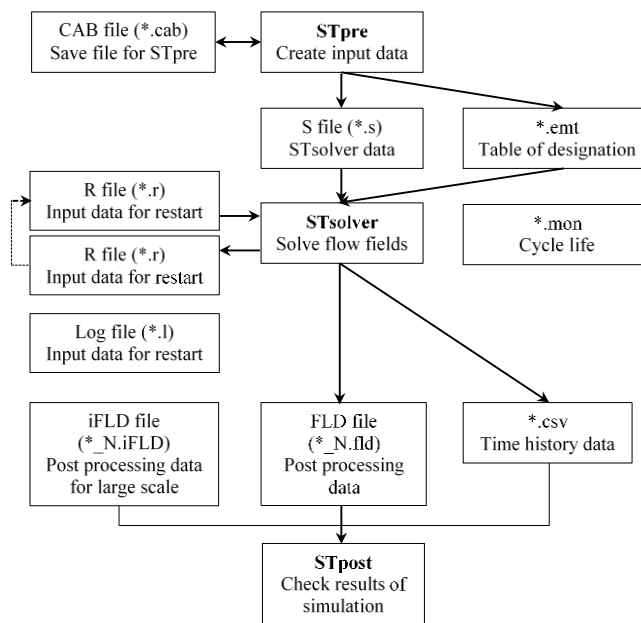


Figure 5.4. Flowchart of *STsolver* in STREAM.

after the second step is called restart simulation (or restart calculation). For the purpose of the restart simulation, a restart file called R file, which only includes data obtained from *STsolver* at the final cycle, is used. The R file is saved at the first step calculation, and then is loaded to continue the simulation using information at the final cycle of the previous simulation. If the simulation is needed to be repeated, the R file must be saved again (Cradle, 2015). Figure 5.4 presents the flowchart of calculation method in *STsolver*.

Postprocessor (*STpost*)

STpost visualizes FLD drawing files. It can handle a single or multiple FLD files at a time. The results of an analysis are evaluated in detail by creating a drawing canvas with various functions such as a cross sectional plan or an iso-surface for each FLD file. Local coordinate systems and a global coordinate system are used on a case by case in *STpost*. Local coordinate systems are created for each FLD file loaded to *STpost*. Each object is classified into FLD object or global object by the coordinate system of the object. FLD objects hold the information of the FLD file and local coordinate systems (Cradle, 2015).

5.2.3 Validation: Model specifications and simulation conditions.

In this section, validation will focus on the validation of middle-class high-rise apartment for CFD STREAM. Validation of the base model was carried out by comparing the simulation results with the field experiment data. This validation was conducted on the master bedroom, living room and corridor space, under different ventilation conditions, i.e. no ventilation, full-day ventilation and night ventilation conditions. Definition of each ventilation conditions refer to the previous chapters (Chapters 3 and 4). Meanwhile, validation of the base model for air-conditioned conditions of master bedroom (i.e. using TRNSYS-COMIS) have already conducted (please refer to Chapter 3: Section 3.4.2.1). As previously discussed, the results of validation for the middle-class high-rise apartment using TRNSYS-COMIS are generally satisfy in describing the thermal behavior of the apartment buildings.

Basic Setting

Middle-class high-rise apartment so called *Rusunami* that used to be performed in the field measurements was modelled for the purpose of this simulation in order to validate the model based on the field experiment data. The apartment models for this simulation were modelled in three dimensions directly using the Preprocessor (*STpre*). The apartment models were developed based on the actual conditions (see Figure 3.8b). Figure 5.5 illustrates the 3D model of the middle-class private apartment used in *STpre*. A single west-facing unit located at the eight floor was modelled in this simulation. In addition, the length of the corridor spaces in this model was model shortened whilst maintaining the ratio of openings to total floor since it is open corridor spaces. Thermal properties of building materials that were assigned to the model refer to Table 5.1.

Computational domain for this simulation was determined following ideal computational domain suggested by the developer (Figure 5.3), and incompressible air was set for this domain.

Turbulent flow (standard k- ϵ model) was used in this simulation because this is the most fundamental model and widely used to predict various types of turbulent flows regardless of compressibility or incompressibility of fluids. Heat, humidity, solar radiation and radiation were analyzed. View Factor (VF) method for radiation analysis was used in this simulation since this method is suitable for relatively low-temperature phenomena that involve no radiant gas such as air-conditioner and thermal design of other electronics (Cradle, 2015). Meanwhile, diffusion coefficient for humidity was set on fixed value at 2.77×10^{-5} (m²/s). This value was calculated based on Equation 5.6 with the temperature reference at room temperature (27°C) and pressure of 1 atm. The reason for setting 1 atm for the pressure is because the absolute humidity of saturated air is determined from the value of 1 atm in a physical property table.

$$\text{HDIF} = \frac{2.311 \times 10^{-5}}{P} \left(\frac{T_a}{273} \right)^{1.8} \quad (5.6)$$

where HDIF is humidity diffusion coefficient (m²/s), P and T_a are air pressure (atm) and air temperature (°C), respectively.

In this simulation, equations for solving flow (heat, humidity and wind flow) were selected. Since turbulent flow predominantly used to explain the behavior of the flow in practical engineering, this type of flow was employed. In this model, the three dimensional incompressible flow of Newtonian fluid is governed by the mass conservation and the Navier-Stokes equations. This model is well known and most commonly used in engineering

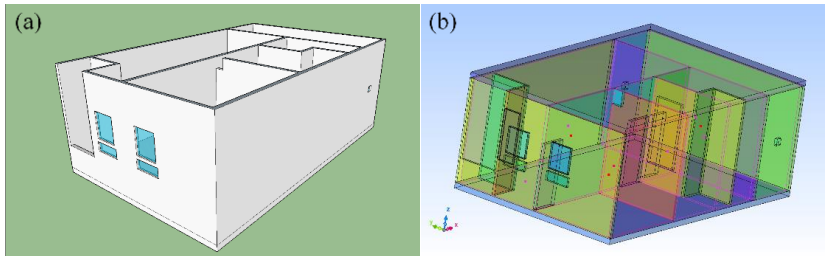


Figure 5.5. Model of middle-class apartment for CFD simulation in (a) Google SketchUp and (b) Preprocessor (*STPre*).

Table 5.1. Thermal properties of the building materials in the base models.

Material	Density (kg/m ³)	Specific heat capacity (J/kgK)	Thermal conductivity (kJ/hmK)	Thermal resistance (hm ² K/kJ)
Aerated light concrete	780	920	0.536	n/a
Cement board	550	960	1.843	n/a
Cement plaster	1250	840	2.595	n/a
Concrete slab	2400	880	6.264	n/a
Ceramic tile	2022	1250	3.987	n/a
Precast concrete	2100	840	5.040	n/a
PVC door pane	1200	1000	0.540	n/a
Timber (door)	620	1300	0.497	n/a

applications (Veersteeg and Malalsekera, 1995). For building applications it is the standard k- ε model which finds most current favor, being as it is a compromise between level of sophistication and computational efficiency (Jones and Whittle, 1992). The standard k- ε model for incompressible fluids are usually expressed by following equations (Cradle, 2015).

$$\frac{\partial \rho k}{\partial t} + \frac{\partial v_i \rho k}{\partial x_i} = \frac{\partial}{\partial x_i} \left(\frac{\mu_t}{\sigma_k} \frac{\partial k}{\partial x_i} \right) + G_S + G_T - \rho \varepsilon \quad (5.7)$$

$$\frac{\partial \rho \varepsilon}{\partial t} + \frac{\partial v_i \rho \varepsilon}{\partial x_i} = \frac{\partial}{\partial x_i} \left(\frac{\mu_t}{\sigma_\varepsilon} \frac{\partial \varepsilon}{\partial x_i} \right) + C_1 \frac{\varepsilon}{k} (G_S + G_T) (1 + C_3 R_f) - C_2 \frac{\rho \varepsilon^2}{k} \quad (5.8)$$

where:

$$G_S = \mu_t \left(\frac{\partial v_i}{\partial x_j} + \frac{\partial v_j}{\partial x_i} \right) \frac{\partial v_i}{\partial x_j};$$

$$G_T = g_i \beta \frac{\mu_t}{Pr_t} \frac{\partial T}{\partial x_i};$$

$$R_f = -\frac{G_T}{G_S + G_T}$$

and k is turbulent kinetic energy (Joule), ε is dissipation rate (m^2/s^3), v is air velocity (m/s), β is thermal expansion coefficient (1/K), μ is viscosity of fluids (kg/m.s) and ρ is density of fluids (kg/m^3).

Since property values, work and heat transfer rates, and mass flow rates may vary with time during transient operation, then the steady-state assumption is not appropriate when analyzing such cases. In this case, transient analysis was used to validate indoor thermal behavior of middle-class apartment. Initial condition for each elements (i.e. condition regions, solid, parts) refer to the field experiment data. For example, initial conditions for air temperature and relative humidity of master bedroom, living room and corridor space were set based on the field measurement data.

Boundary conditions

As previously described, flow boundary conditions can be specified only at the interfaces between the fluid and the outside of computational domain (X_{min} , X_{max} , Y_{min} , Y_{max} , Z_{min} , Z_{max}). In these interfaces, inflow boundary was set come from X_{min} (for flow direction toward x-axis or eastward) and Y_{min} (for flow direction toward y-axis or northward). For inflow boundary, fixed velocity was employed as input. Since the transient analysis was used, table of outdoor wind speeds in specified direction developed from field experiments was used as input. Meanwhile, fixed total pressure (i.e., 0 Pa) was set as outflow condition. In STREAM, fixed total pressure is valid only for incompressible flow.

Heat boundary conditions were specified at each building elements such as wall, floor, ceiling, doors, windows and glasses. Heat transfer between a fluid and a solid wall is calculated based on the Equation 5.9 as follow, while heat transfer coefficients in different position and form of surface are presented in Table 5.2 (ASHRAE, 2013). Heat transfer coefficients were specified to each surface of building envelopes, which is depend on the position of the surface.

$$\dot{Q} = h_t (T_W - T) A \quad (5.9)$$

where q is transferred heat energy (W), h is heat transfer coefficient (W/m²K), T_W is wall surface temperature (K), T is characteristic temperature of fluid (K) and A is sectional area (m²).

Turbulent kinetic energy and turbulent dissipation rate were suggested to 0.0001 m²/s², respectively. Absorbance of material referred to the available literature (such as Szokolay, 2004), while the absorbance of the surface were set at 0.4 for bright and light color of wall surface (Szokolay, 2004). Diffusion coefficient of water vapor as described by Equation 5.6 was used for humidity transfer boundary. Each sides of main object (except back-side and front-side) were assumed to be adiabatic, i.e. no heat transfer between the walls or floor/ceiling surfaces and the fluid. The geographical location of the base model followed that of the actual apartments, i.e. latitude 7.37°S and 112.77°E (longitude at standard time 105).

Weather data (including air temperature, relative humidity, wind speed and solar radiation)

Table 5.2. Surface film coefficient (ASHRAE, 2013)

Position of surface	Direction of heat flow	Surface emittance, ε (W/m ² K)		
		Non-reflective ($\varepsilon=0.90$)	Reflective $\varepsilon=0.20$	Reflective $\varepsilon=0.05$
<i>Indoor</i>				
Horizontal	Upward	9.26	5.17	4.32
Horizontal	Downward	6.13	2.10	1.25
Vertical	Horizontal	8.29	4.20	3.35
Slope at 45°	Upward	9.09	5.00	4.15
Slope at 45°	Downward	7.50	3.41	2.56
<i>Outdoor</i>				
Wind (for winter) at 6.7 m/s	Any	34.0		
Wind (for summer) at 3.4 m/s	Any	22.7		

Table 5.3 Typical values of ground reflectance of foreground surfaces (ASHRAE, 2013)

Foreground surfaces	Reflectance (σ)
Water (near normal incidences)	0.07
Coniferous forest (winter)	0.07
Asphalt, new	0.05
Asphalt, weathered	0.10
Bituminous and gravel roof	0.13
Dry bare ground	0.20
Weathered concrete	0.20 to 0.30
Green grass	0.26
Dry grassland	0.20 to 0.30
Desert sand	0.40
Light building surfaces	0.60
Snow covered surfaces:	
- Typical city center	0.20
- Typical urban site	0.40
- Typical rural site	0.50
- Isolated rural site	0.70

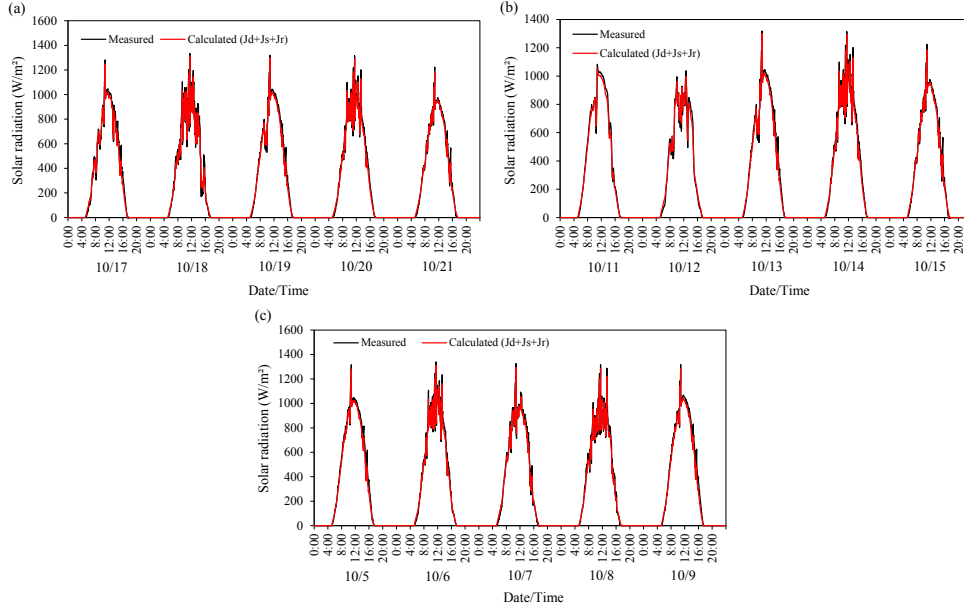


Figure 5.6. Comparison between the measured and calculated global horizontal solar radiation under (a) no ventilation, (b) full-day ventilation and (c) night ventilation conditions.

that was measured on site throughout the field experiment periods, i.e. 11-16 October for full-day ventilation condition and 17-22 October for no ventilation condition, were used. Since the measured solar radiation was the global horizontal solar radiation, then input for solar radiation was distinguished into its components. The global horizontal solar radiation (J_t) is sum of its components, direct solar radiation (J_d), sky solar radiation (J_s), reflected solar radiation (J_r) and solar radiation from cloud (J_c), and calculated using Equation 5.10. *STsolver* supports the three components of global solar radiation, i.e. direct solar radiation, sky solar radiation and reflected solar radiation, but not solar radiation from cloud.

$$J_t = J_d + J_s + J_r + J_c \quad (5.10)$$

Component of direct solar radiation (J_d) and sky solar radiation (J_s) were calculated using Bouguer's equation and Berglarge's equation, respectively, as shown in Equations 5.11-12.

$$J_d = J_0 P^{\frac{1}{\sin(h)}} \quad (5.11)$$

$$J_s = \frac{1}{2} J_0 \sin(h) \frac{1 - P^{\frac{1}{\sin(h)}}}{1 - 1.4 \ln(P)} \quad (5.12)$$

where J_0 is solar constant ($1,330 \text{ W/m}^2 \cdot \text{K}$), h is the sun altitude (rad), and P is atmospheric transmissivity (dimensionless), which is depend on the specific location.

Atmospheric transmissivity (P) was obtained by derived Equations 5.11 and 5.12, and the results is shown in Equation 5.14.

$$P = \text{EXP} \left(\frac{\left(-1.4 \ln \left(\frac{J_t}{J_0} \right) - \sqrt{\left(1.4 \ln \left(\frac{J_t}{J_0} \right) \right)^2 - \frac{5.6 J_t}{\sin(h) J_0}} \right) \sin(h)}{2.8} \right) \quad (5.13)$$

Meanwhile, the reflected solar radiation (J_r) was calculated using following equation:

$$J_r = \sigma_r J_s \quad (5.14)$$

where σ is reflectance of ground of foreground surface (dimensionless). These values referred to ASHRAE (2013) as summarized in Table 5.3.

The comparison between the measured and calculated global horizontal solar radiation is shown in Figure 5.6. As shown, the calculated solar radiation had almost the same values as the measured solar radiation. The MBE and RMSE for the calculated results under no ventilation condition were $-8.54 \text{ W/m}^2\text{K}$ and $24.86 \text{ W/m}^2\text{K}$, respectively. Meanwhile, those statistical errors (i.e., MBE and RMSE) for the full-day ventilation condition were $-7.36 \text{ W/m}^2\text{K}$ and $22.40 \text{ W/m}^2\text{K}$, respectively and those for night ventilation condition were $-10.98 \text{ W/m}^2\text{K}$ and $25.28 \text{ W/m}^2\text{K}$, respectively. The coefficient of correlation (R^2) between the measured and calculated for respective ventilation conditions was 0.997.

Calculation method

As previously described, transient analysis was used in this simulation. The simulation time step of 1 minute was set to coincide with the weather data at 10-minute intervals. Total of 7,200 cycles including 2,880 cycles for spin up period was set to represent three or four day simulation. In order to shorten the calculation time without sacrificing the accuracy of

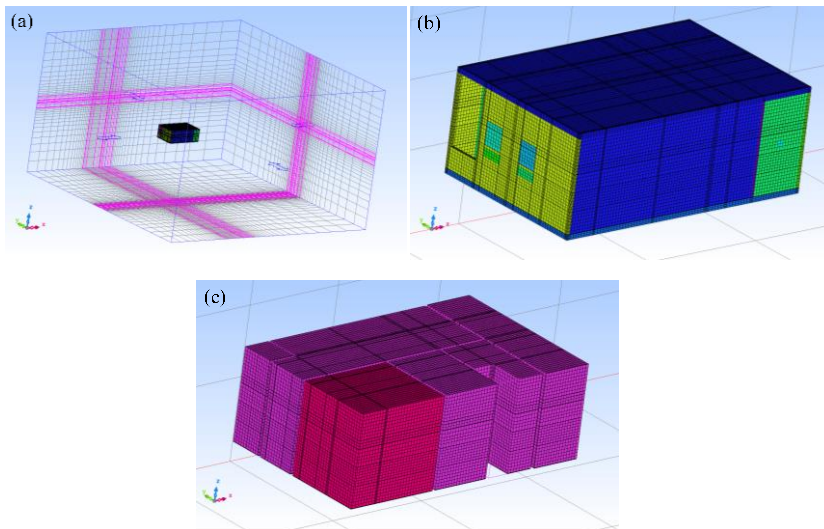


Figure 5.7. View of meshing division in (a) object and computational domain, (b) middle-class private apartment model and (c) connected regions in model.

calculation, solving flow velocities discontinuously was set with time duration to solve the flow field continuously 1 seconds at time interval 60 second (1 minute). Calculation of radiation view factor and thermos-fluid analysis were executed simultaneously in this simulation. Heat balance equation was corrected by assuming difference in thermal conductivity for different materials. Fixed pressure was computed after a pressure correction equation is solved. Meshing divisions for the validation are shown in Figure 5.7. A 200mm rough meshing was employed, and detailed meshing was applied in the specific locations particularly those near the wall surface to represent the temperature gradient and to accurately estimate the amount of heat transfer.

Two statistical error tests, the mean bias error (MBE) and the root mean square error (RMSE), are used to validate this model through checking the deviations of simulation results from actual measurement data. These two error test are calculated using Equations 3.12 and 3.13. The validation of building energy simulation models is currently based on a models compliance with standard criteria for MBE, as used by ASHRAE Guideline 24 (Coakley *et al.*, 2014), which is around 10%.

Validation Results

Figures 5.8-9 present the validation results of indoor air temperature, relative humidity and wind speed under no ventilation condition in respective rooms (i.e. master bedroom, living room and corridor space), while Tables 5.4 summarizes the statistical error test of the model. As indicated, the MBE values for air temperature in the master bedroom, living room and corridor space are 0.14, -0.13 and -0.07, respectively. Meanwhile, the RMSE values are calculated at 0.38, 0.28 and 0.34, respectively. Corridor space had relatively lower coefficient of correlation (R^2) compared to other rooms, which is around of 0.64 (see Table 5.4). As shown in Figure 5.8c, there are small time lag at the peak hours between the simulated values and the measured values. In contrast, corridor space has the highest R^2 value of the relative humidity (0.97) while the living room had lowest ($R^2=0.64$). The MBE values are -1.72 for master bedroom, -0.28 for the living room and 0.87 for the corridor space. However, the profiles of the simulated values were similar and tend to follow the profiles of the measured values.

Figure 5.9 demonstrated that wind speeds in respective room were difficult to be simulated and fit the measured wind speed. It should be noted that the simulated wind speeds are average value from several simulation points. In case of master bedroom and living room, this is most likely due to the low value of measured wind speeds, which is less than 0.1 m/s. However, the simulated wind speed in the living room has the almost same pattern as the measured wind speed although its values were overestimate. In case of corridor space, wind speed was difficult to be simulated because corridor space in the simulation model does not reflect the actual condition of corridor space.

Figures 5.10-11 present the validation results of indoor air temperature, relative humidity and wind speed under full-day ventilation condition in master bedroom, living room and corridor space. As shown, the profiles of simulated air temperature and relative humidity in the respective rooms follow the profiles of measured air temperature and relative humidity (Figure 5.10). The values of MBE and RMSE of respective rooms are presented in Table 5.4.

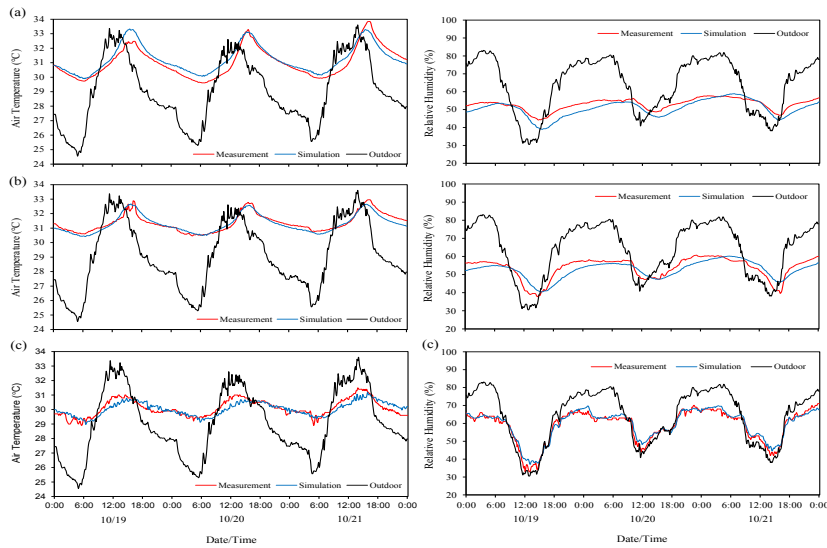


Figure 5.8 Validation results of indoor air temperature and relative humidity in (a) master bedroom, (b) living room and (c) corridor space under no ventilation condition.

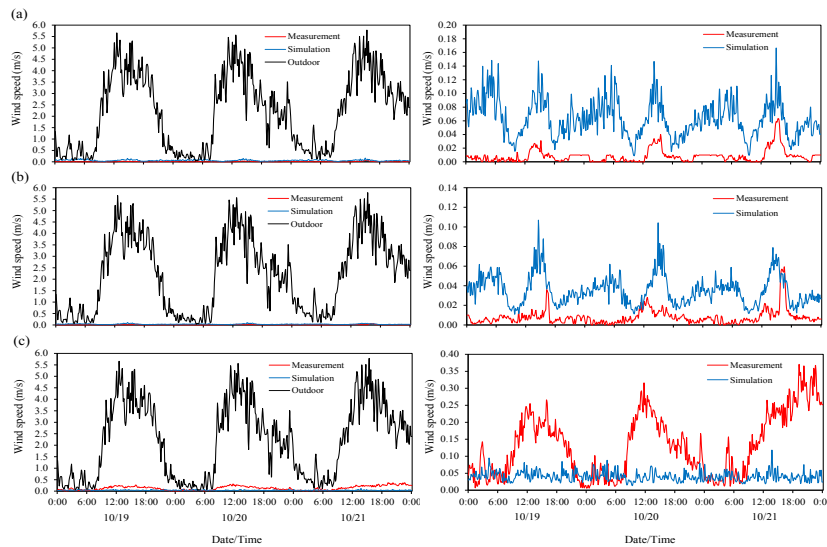


Figure 5.9 Validation results of indoor wind speed including and excluding outdoor wind speed in (a) master bedroom, (b) living room and (c) corridor space under no ventilation condition.

Coefficient of determination (R^2) for indoor air temperature in master bedroom revealed higher values than those of other rooms, while in the other side, MBE and RMSE values in corridor space were smaller as well as its R^2 value (0.45). This lower R^2 value is mainly due to small time lag at the peak hours between the simulated values and the measured values, as indicated in Figure 5.10c. Meanwhile, the R^2 values for relative humidity in the respective rooms showed

relatively higher, which is around 0.89-0.95 (see Table 5.4). Unlike no ventilation condition, the simulated wind speed under full-day ventilation condition showed closer values as well as its patterns to the measured wind speed except those in the living room, where the simulated wind speed at night-time were higher than the measured (Figure 5.11). Nevertheless, it implies that these results satisfy to explain the wind speed behavior of the model.

In STREAM, simulation for night ventilation condition is carried out by using restart method. In this method, simulation is conducted in two different conditions; open the window

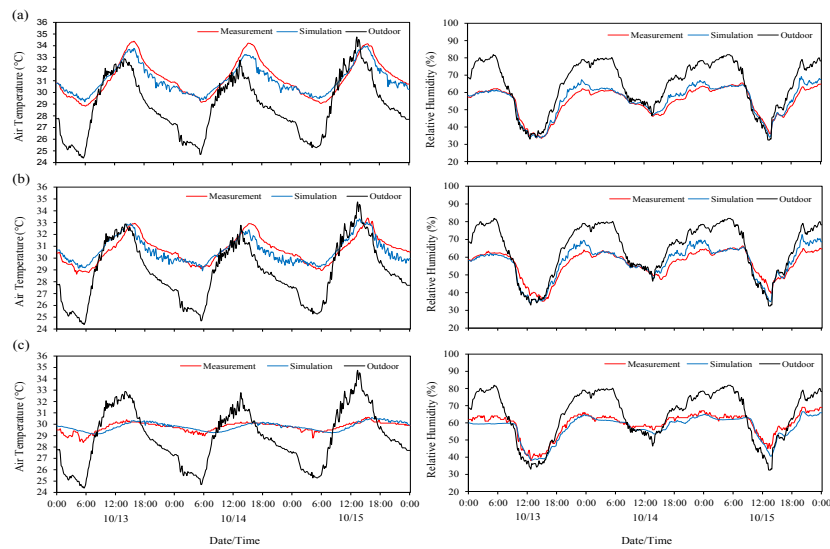


Figure 5.10 Validation results of indoor air temperature and relative humidity in (a) master bedroom, (b) living room and (c) corridor space under full-day ventilation condition.

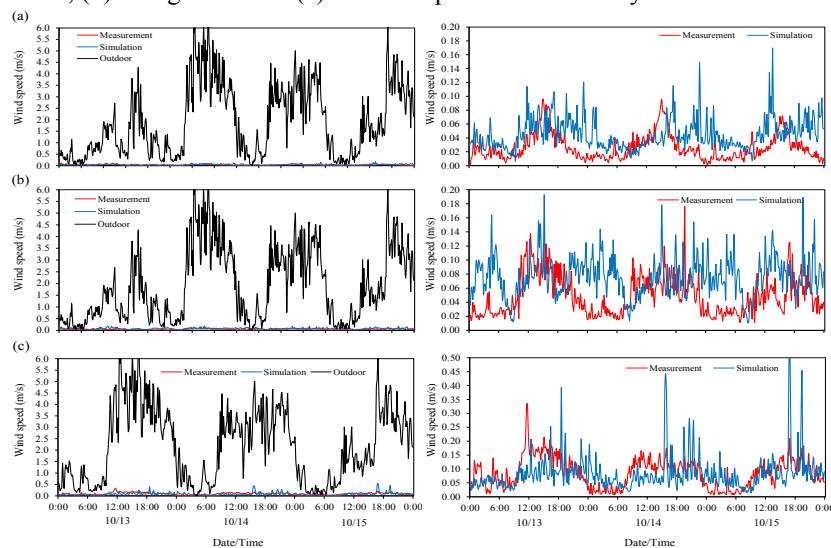


Figure 5.11 Validation results of indoor wind speed including and excluding outdoor wind speed in (a) master bedroom, (b) living room and (c) corridor space under full-day ventilation condition.

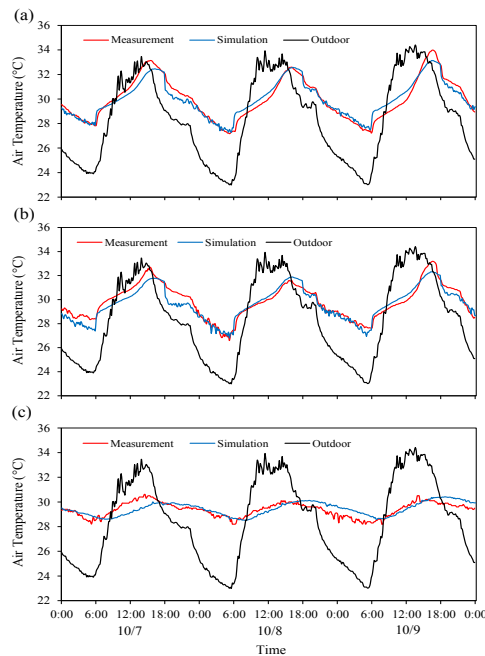


Figure 5.12 Validation results of indoor air temperature and relative humidity in (a) master bedroom, (b) living room and (c) corridor space under night ventilation condition.

during the night-time (18:00-06:00) and closed the window during the daytime (06:00-18:00). First step, window is set as condition region to represent open condition, then run simulation under specific number of cycles. After finishing first step, modify the model by setting the window as solid (glass) to represent closed condition. Then, restart method is employed by to proceed the previous simulation by applying new cycles number. These procedures continuously and alternately run until final cycle is approached. One of the disadvantages of this method, and also the limitation of this software, is that this method validly simulated only heat flow and air flow, while relative humidity cannot and impossible to be simulated (Kota, 2017).

The validation results under night ventilation condition in the respective rooms are shown in Figures 5.12-13 and Table 5.4. Figure 5.12 showed that the profiles of simulated air temperature in the respective rooms follow the profiles of measured air temperature and relative humidity (Figure 5.12). As indicated, the MBE values of the respective rooms, i.e., master bedroom, living room and corridor space are -0.02, -0.20 and 0.97, respectively. Meanwhile, the RMSE values are 0.47, 0.50 and 1.07 respectively. Coefficient of determination (R^2) for indoor air temperature in master bedroom showed higher values than those of other rooms, those in the corridor space were the smallest ($R^2=0.45$). As the previous cases (e.g., no ventilation and full-day ventilation conditions), this lower R^2 value is mainly due to small time lag at the peak hours between the simulated values and the measured values (Figure 5.12c). The simulated wind speeds under night ventilation condition in master bedroom and living room showed the similar pattern as the measured wind speed, but the

values were overestimated (Figure 5.13ab); the presence of wind speed during the night-time and the absence during the daytime. In the other side, wind speed was difficult to be simulated in the corridor space since the corridor space in the simulation model does not reflect the actual condition of corridor space. Nevertheless, it implies that these results satisfy to explain the wind speed behavior of the model. In general, the results indicated that the MBE values in respective rooms under different ventilation conditions fulfilled the requirements of ASHRAE Guideline 24, and therefore satisfactorily describing thermal behavior and air flow behavior of the model.

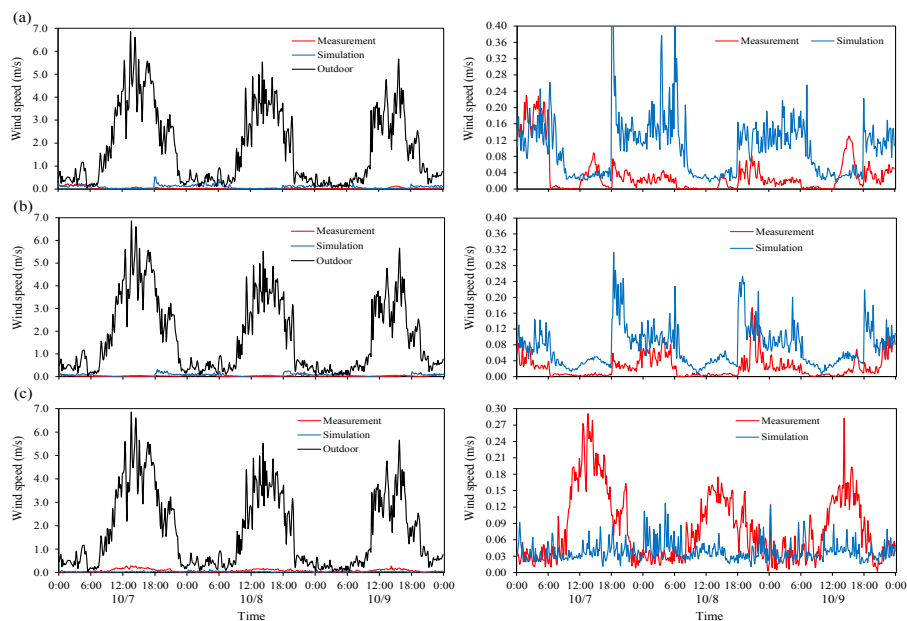


Figure 5.13 Validation results of indoor wind speed including and excluding outdoor wind speed in (a) master bedroom, (b) living room and (c) corridor space under night ventilation condition.

Table 5.4 Summary of statistical error tests of the validation results.

Ventilation conditions	Room	Air temperature			Relative humidity		
		MBE (°C)	RMSE (°C)	R ²	MBE (°C)	RMSE (°C)	R ²
No ventilation	MB	0.14	0.38	0.88	-1.72	3.03	0.82
	LR	-0.13	0.28	0.83	-0.28	3.55	0.69
	Corridor	-0.07	0.34	0.64	0.87	1.94	0.97
Full-day ventilation	MB	-0.02	0.51	0.93	0.75	2.14	0.95
	LR	0.04	0.58	0.79	0.56	3.39	0.89
Night ventilation	Corridor	-0.01	0.34	0.45	-2.24	3.13	0.91
	MB	-0.02	0.47	0.93	n/a	n/a	n/a
	LR	-0.20	0.50	0.89	n/a	n/a	n/a
	Corridor	0.97	1.07	0.44	n/a	n/a	n/a

5.3 Base model and simulation test cases

5.3.1 Base model and simulation test cases for CFD STREAM

Figure 5.14 illustrates the 3D model of base model for the middle-class private apartment used for the CFD simulation. The simulated room focus on the living room since the simulation investigates the effect of structural cooling and comfort ventilation in the living room. The dimension of living room reflects the actual size of that of measured apartment (6.40m x 2.8m) with some modifications were made differently from the actual situations. Additional windows and permanently opening holes were added in the back-side to ensure cross ventilation (Figure 5.14a). As previous findings (see Chapter 3), balcony is important as thermal buffer zone, therefore additional balcony was added in the front-side of the model (Figure 5.14b) with the width of 1.5m. To simulate the wind flow particularly turbulent flow around the building, additional blocks considered as obstacle were added surrounding the main object (Figure 5.14cd).

Weather data including air temperature, relative humidity, wind speed and solar radiation, that was measured on site throughout the field experiment period, i.e. 1-27 October, was used. As validation process, different components of global solar radiation excluding solar radiation from the cloud (i.e. direct solar radiation, sky solar radiation and reflected solar radiation) were employed as input for solar radiation. Meanwhile, the measured wind speed was modified based on its direction using simple trigonometry equation. Then, the input for wind speed was set following the orientation of the model. For instance, if the model is south-facing orientation, then the north-ward wind speed is set for the model. The simulation time step was set to 20 second in order to obtain more accurate calculation results as well as to reduce Courant number as required ($C \leq 1$). Therefore, total of 12,960 cycles including 4,320 cycles for spin up period was set to represent three days simulation. Thermal properties of materials that used for the base model were refer those as used in the validation process (see Table 5.1) and so as for the boundary conditions (i.e. flow boundary condition, thermal boundary condition and humidity boundary condition). Each sides of main object (except back-side and front-side) that interfaced with the additional blocks were assumed to be adiabatic, i.e. no heat transfer between the walls and the blocks (obstacles). Meshing division of the base model are shown in Figure 5.15. Initial air temperature and relative humidity both inside the room (i.e. living room) and balcony were set at 25.0°C and 50%, respectively.

Table 5.5 summarizes the simulation test cases and their test condition for naturally ventilated condition in living room. The simulation test cases mainly focus on parameters for generalization of indoor thermal environments under naturally ventilated condition in the living room, and parameters for improvement of energy usage under air-conditioned master bedroom (while maintaining living room naturally ventilated). In the case of structural cooling, the purpose is mainly to obtain the benefit of cooling the structure (such as wall, floor and ceiling) and therefore, night ventilation was applied to the living room; the windows are open from 18:00 to 06:00 and closed from 06:00 to 18:00. The effects of thermal mass and the ratio of windows area to total floor area were investigated in this case. Thermal mass is considered as the one of passive cooling techniques for heat modulation (Givoni, 1994; Santamouris, 2007; Geetha and Velraj, 2012). Meanwhile, windows area closely related to the air infiltration

rates into the indoor space (Awbi, 2003, ASHRAE, 2017). The ventilation rates depend not only on the windows area but also on the design of windows, whether or not it enables to ensure cross ventilation (Swami and Chandra, 1987). The target of varying these parameters is to investigate the cooling effects of nocturnal ventilative cooling and combination of passive strategies, i.e. thermal mass and air flow rates, which is represented by the ratio of windows area to total floor area, to the thermal environments. Windows position employed in this simulation cases was different; central window and upper/lower window

As previously mentioned, comfort ventilation is important for hot-humid climatic regions. Thermal comfort can be achieved by increasing wind speed by opening the windows although it increases indoor air temperature. The main purpose of this simulation is to reduce the SET* in the living room. Thus, full-day ventilation was applied (i.e. open windows for 24 hours)

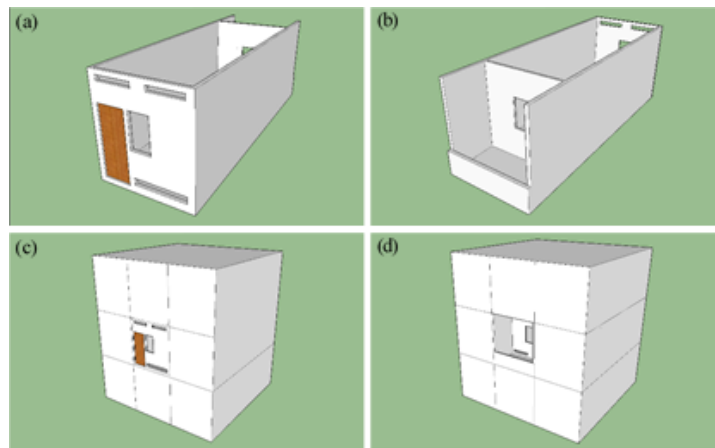


Figure 5.14. 3D model for simulation, (a) front view, (b) front view with the surrounding, (c) back view and (d) back view with the surrounding.

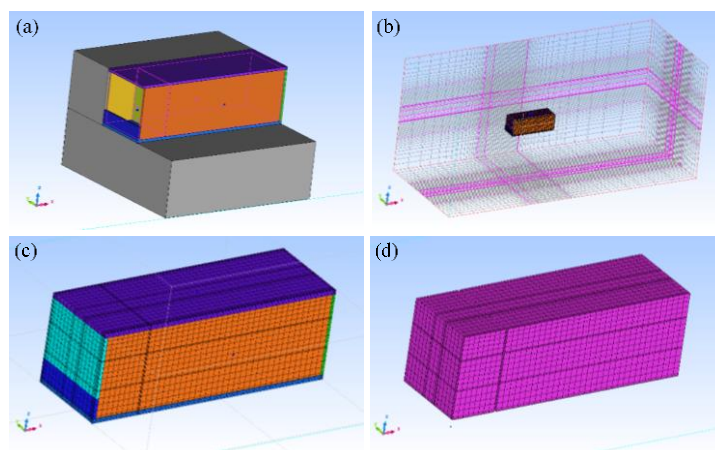


Figure 5.15. (a) 3D view of base model in Preprocessor, (b) meshing division of object and computational domain, (c) meshing division of the model and (d) meshing division of connected regions of the model.

Table 5.5 Case designs for CFD simulation for naturally ventilated living room

Parameters	Test conditions	
<i>Structural cooling (living room)</i>		
Ventilation conditions	Night ventilation	
Orientation (external-wall)	South-facing	
Thermal mass (kg/m ²)	1,000	2,000
Ratio of opening area to floor area	0.05	0.15
Ceiling height (m)	3.0	5.0
Opening position	Central	Upper + Lower
<i>Comfort ventilation (living room)</i>		
Ventilation conditions	Full-day ventilation	
Orientation (external-wall)	South facing	
Thermal mass (kg/m ²)		
Ratio of opening area to floor area	0.05	0.10
Ceiling height (m)	3.0	5.0
Opening position	Central	Upper + Lower

with the changing of air flow that represented by the ratio of openings area to total floor area. In this simulation, the previous results (i.e. structural cooling simulation) particularly the optimum thermal mass, were used as input for the full-day ventilation simulation. Those values were combined with the different ceiling heights and the opening ratios. As previously discussed, ceiling height plays important roles in maintaining the occupied level lower than the upper part (see Chapter 4). As those in structural cooling, the windows positions employed were different; central window and upper/lower window. In the simulation cases, central window maintained no change on the back side while the window position switched between central window and upper/lower window on the front-side (balcony-side) only (see Figure 5.14ab). Additional cases were put on the simulation cases regarding the window position by adding another upper/lower window type and placed them on the front side of the unit model. The detailed information of the test cases will be given in the next Sections (see Sections 5.4.1 and 5.4.2)

5.3.2 Base model and simulation test cases for TRNSYS-COMIS

Base model of middle-class private apartment for simulating air-conditioned master bedroom using TRNSYS-COMIS as well as the settings of simulation, are refer to the previous chapter (Chapter 3, Section 3.3.3.2). The 3D model is presented in Figure 3.13. The base case for this simulation was determined by finding the optimum combination of ventilation conditions between master bedroom and living room. Air conditioner was assumed to be operated during the night-time only (from 18:00 to 06:00). Total of eight cases of ventilation conditions in both rooms are presented in Table 5.6. This simulation was carried out at west-facing orientation, represent the actual condition of field experiment data.

Table 5.6 Case designs for ventilation conditions in the master bedroom

Case	Room	Ventilation condition
Case 1	Master bedroom	Daytime ventilation
	Living room	Daytime ventilation
Case 2	Master bedroom	No ventilation
	Living room	Daytime ventilation
Case 3	Master bedroom	Daytime ventilation
	Living room	Full-day ventilation
Case 4	Master bedroom	No ventilation
	Living room	Full-day ventilation
Case 5	Master bedroom	Daytime ventilation
	Living room	Night ventilation
Case 6	Master bedroom	No ventilation
	Living room	Night ventilation
Case 7	Master bedroom	Daytime ventilation
	Living room	No ventilation
Case 8	Master bedroom	No ventilation
	Living room	No ventilation

Table 5.7 Case designs for simulation of the air-conditioned master bedroom

Parameters	Test conditions			
Ventilation condition for MB	Daytime	Night	Full-day	No
Ventilation condition for LR	Daytime	Night	Full-day	No
Orientation (external wall)	North	South	West	East
Insulation	Internal	External		
Ceiling height (m)	2.2	2.5	2.8	

As for simulation test cases of the air-conditioned condition, the simulation focusing on the ceiling height and insulation of master bedroom (see Table 5.7). Further simulations were conducted by varying selected base case to the different orientations (i.e. North, South, West and East). The test cases related to the insulation applied thermal insulation internally and externally in master bedroom, with the value of thermal conductivity applied was 0.03 W/m²K. Meanwhile, those related to ceiling height employed different ceiling height in the master bedroom.

5.4 Results: Naturally ventilated conditions

As previously described, the simulations of the naturally ventilated living room were carried under two different conditions, i.e. structural cooling and comfort ventilation. This section summarizes and discusses the results of simulation by using CFD STREAM.

Table 5.8 Simulation cases for structural cooling in the living room

Simulation Cases	Thermal mass (kg/m ²)	Ratio of window area to floor area	Ceiling height (m)	Windows position	
				Front-side	Back-side
Case 01	1,000	0.05	3.0	Central	Central
Case 02	2,000	0.05	3.0	Central	Central
Case 03	1,000	0.05	3.0	Central	Upper/Lower
Case 04	2,000	0.05	3.0	Central	Upper/Lower
Case 05	1,000	0.15	3.0	Central	Central
Case 06	2,000	0.15	3.0	Central	Central
Case 07	1,000	0.15	3.0	Central	Upper/Lower
Case 08	2,000	0.15	3.0	Central	Upper/Lower
Case 09	1,000	0.05	5.0	Central	Central
Case 10	2,000	0.05	5.0	Central	Central
Case 11	1,000	0.05	5.0	Central	Upper/Lower
Case 12	2,000	0.05	5.0	Central	Upper/Lower
Case 13	1,000	0.15	5.0	Central	Central
Case 14	2,000	0.15	5.0	Central	Central
Case 15	1,000	0.15	5.0	Central	Upper/Lower
Case 16	2,000	0.15	5.0	Central	Upper/Lower

5.4.1 Structural cooling in the living room

At first step, the effects of thermal mass is evaluated in this Section. Consecutively, the effects of ratio of opening area to total floor area that represent the ventilation rate, ceiling height and window position were further investigated. The optimum combination of above parameters in reducing indoor air temperature are then proposed. The total number of cases for structural cooling is 16 cases, and the detail are presented in Table 5.8. As previously described, additional simulation cases were put on the case designs regarding window position, as presented by Cases 17-24 (see Table 5.9). The aims of this additional cases was to further investigate the effects of different window positions to indoor space under night ventilation condition.

5.4.1.1 The effects of thermal mass

Figure 5.16 presents the profiles of indoor air temperature for different thermal mass (i.e. 1,000 kg/m² and 2,000 kg/m²). As shown in Figure 5.16, when thermal mass applied is higher (i.e. 2,000 kg/m²), the daytime indoor air temperature obtained lower value than that of smaller thermal mass (1,000 kg/m²) applied regardless of ratio of window area to floor area, ceiling height and window position. In contrast, its nocturnal indoor air temperature was relatively higher. As indicated, Figure 5.16a compared of indoor air temperature under different thermal mass and same window position (i.e. front-side: central window and back-side: central window) and Figure 5.16c compared the indoor air temperature under different thermal mass

and same ratio of opening area to floor area (0.15). From the simulation results, it is obtained that the maximum indoor air temperature at thermal mass of 1,000 kg/m² was ranged from 30.9°C to 31.2°C with average of 29.8-30.3°C while that at thermal mass of 2,000 kg/m² was ranged from 30.2°C to 30.7°C with average of 29.2-29.9°C. It is clearly seen that when thermal mass is increasing, the maximum indoor air temperature is decreasing by maximum of 0.5-0.7°C or by averagely of 0.4-0.6°C. At the other sides, the higher thermal mass caused the nocturnal indoor air temperature increased. It is obtained that average night-time indoor air temperatures at thermal mass of 1,000 kg/m² and 2,000 kg/m² were ranged at 27.1-28.4°C and 27.2-28.7°C, respectively. This increasing is not as large as the decreasing of daytime indoor air temperature, which is around of 0.1-0.3°C.

The highest maximum indoor air temperature was obtained when central window on the both sides were applied, i.e. Case 1, Case 5, Case 9 and Case 13. Although those cases have different ratio of opening area to floor area (i.e. 0.05 and 0.15), the maximum indoor air temperatures in those cases were exactly same, which is 31.2°C. It should be noted that even though they have the same value of maximum indoor air temperature, nocturnal indoor air temperature of those with the larger opening ratio and higher ceiling height (i.e. Cases 5 and 13) was averagely 0.5-0.6°C lower than those with the smaller opening ratio and lower ceiling height (i.e. Cases 1 and 9). This is most probably because the sky solar radiation entering the room with larger opening ratio were larger than that of with smaller ratio, and therefore it

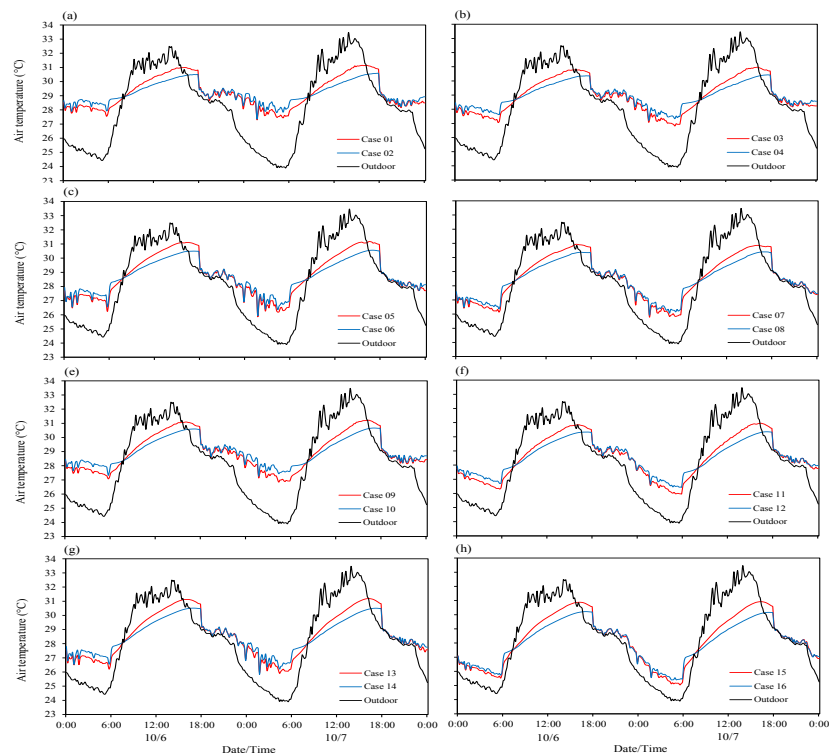


Figure 5.16. Comparison of simulation results of indoor air temperature at 1.1m above floor under different thermal masses.

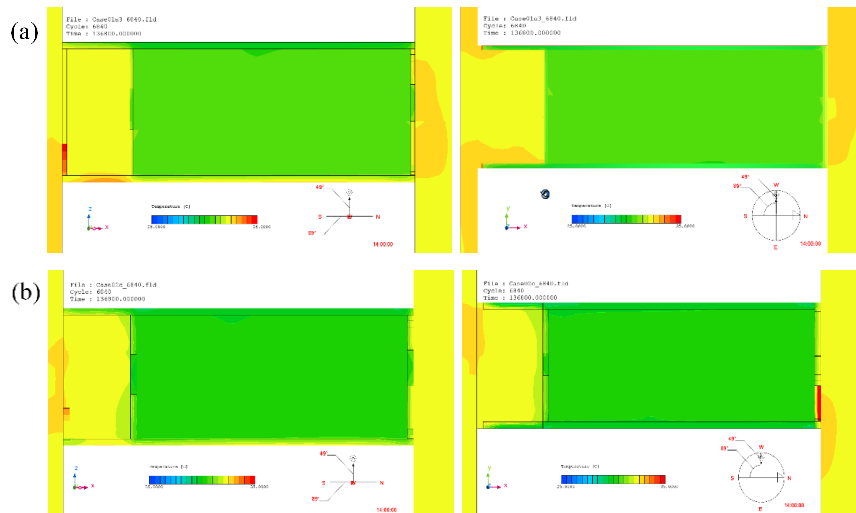


Figure 5.17. View of distribution of indoor air temperature (left: y-axis at 1.4m, right: z-axis at 1.1m) at thermal mass of (a) 1,000 kg/m² and (b) 2,000 kg/m² during daytime (14:00).

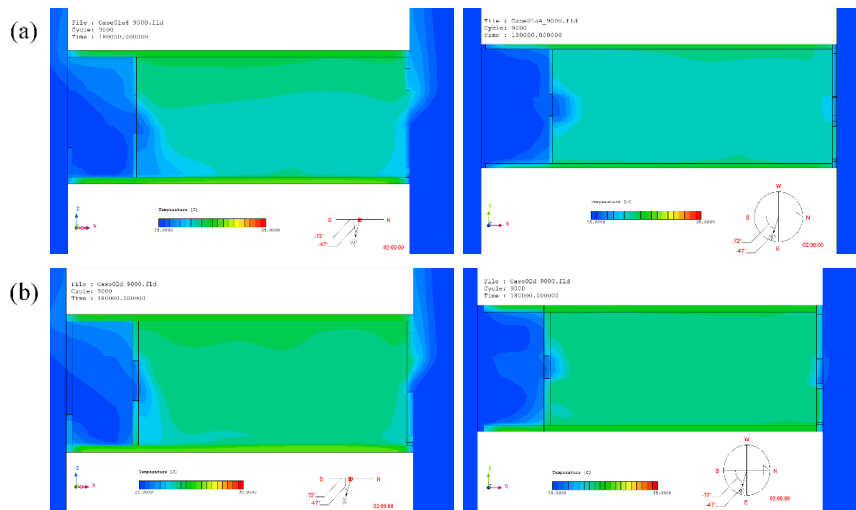


Figure 5.18. View of distribution of indoor air temperature (left: y-axis at 1.4m, right: z-axis at 1.1m) at thermal mass of (a) 1,000 kg/m² and (b) 2,000 kg/m² during night-time (02:00).

traded off the nocturnal ventilative cooling effects by the larger opening ratio. In addition, the lowest indoor air temperature (25.0°C) was obtained when thermal mass is 1,000 kg/m² combined with opening ratio of 0.15 and ceiling height of 5.0m (i.e. Case 15). The increasing of thermal mass under same conditions (i.e. Case 16) increased the night-time indoor air temperature by averagely of 0.1°C only (see Figure 5.16h). It clearly indicated that ratio of opening area largely affect the nocturnal indoor air temperature rather than thermal mass.

Further discussion on the effects of ratio of opening area to floor area are presented in Subsection 5.4.1.2.

Figures 5.17-18 present visualization of indoor air temperature distribution in the room under different thermal masses during the daytime and night-time, respectively. As shown, indoor air temperatures during the peak hours (14:00) between two thermal masses have identical patterns (Figure 5.17). Meanwhile, the slightly different can be seen during the night-time between the two cases. There are larger cool air layered at the lower area of the unit with thermal mass of 1,000 kg/m² rather than at the unit of thermal mass of 2,000 kg/m² (see Figure 5.18ab at y-axis). Warmer air, however, existed in both cases at the upper area. A relatively thick layer of warmer air can be seen at the upper area of unit with thermal mass of 2,000 kg/m². This is most probably due to the heat emitted from thermal mass at the night-time.

Figure 5.19 shows the comparison of indoor wind speed profiles under different thermal masses. As shown, there is almost no difference of indoor wind speed between two cases under different thermal masses. When the windows opened at 18:00, indoor wind speed showed relatively high value and its pattern tend to follow the corresponding outdoor wind speed. The profiles of wind speed are closely related to difference of the ratio of opening area to floor area rather than the difference of thermal masses (see Figures 5.19a and 5.19c for instance). When the ratio of opening area to floor area is 0.05, the maximum indoor wind speed was around of 1.62-2.50 m/s, while when the ratio increasing to 0.15, the maximum indoor wind speed

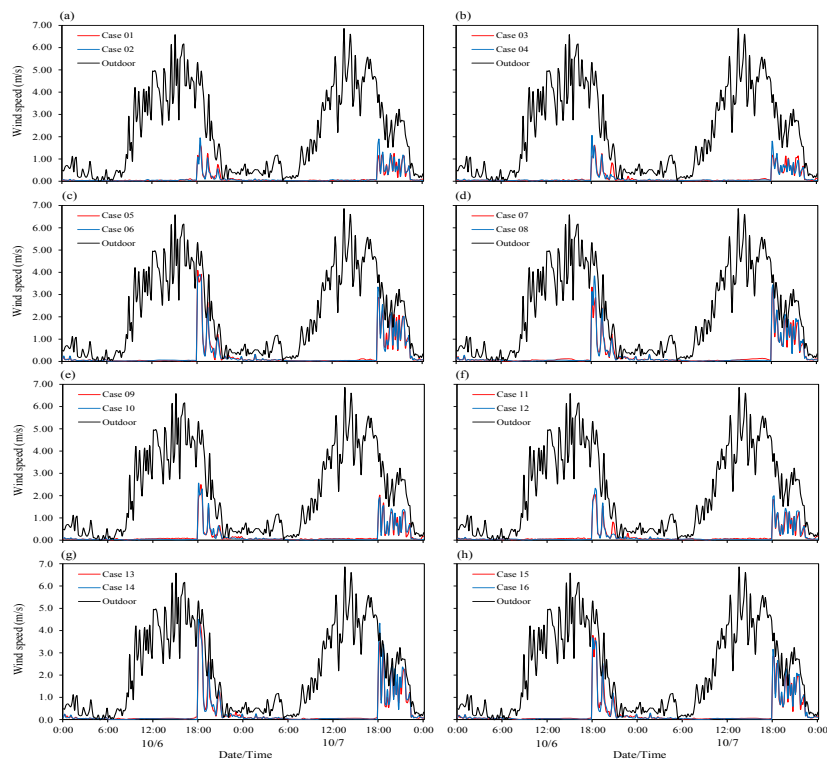


Figure 5.19. Comparison of simulation results of indoor wind speed at 1.1m above floor under different thermal masses.

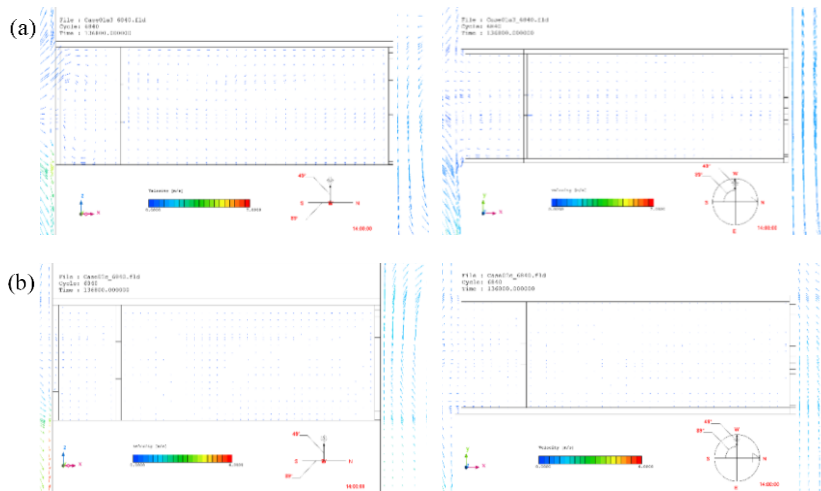


Figure 5.20. View of distribution of indoor wind speed (left: y-axis, right: z-axis) at thermal mass of (a) 1,000 kg/m² and (b) 2,000 kg/m² during daytime (14:00).

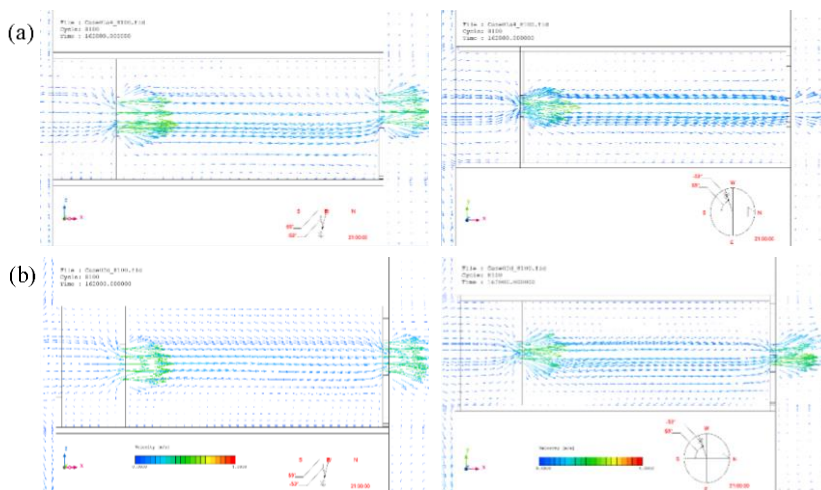


Figure 5.21. View of distribution of indoor wind speed (left: y-axis, right: z-axis) at thermal mass of (a) 1,000 kg/m² and (b) 2,000 kg/m² during night-time (21:00)

increased almost double to 3.36-4.49 m/s. Figures 5.20-21 illustrate the wind flow under different thermal masses during the daytime and night-time respectively. As indicated, between two cases, there are no difference in the profile of wind flow inside the room during daytime and night-time. Cross ventilation occurred particularly when the central windows at both sides are open (see Figure 5.21). Further discussion on the effects of ratio of opening area to floor area are presented in Subsection 5.4.1.2.

Figures 5.22 and 5.23 present the comparison of simulation results of surface temperature of walls, floor and ceiling under different thermal mass at ceiling height of 3.0m and 5.0m respectively. As implied, the profiles of surface temperature of walls, floor and ceiling have

similar pattern regardless of ratio of opening area to floor area, window position and ceiling height. As indoor air temperature, the surface temperatures of walls, floor and ceiling at 2,000 kg/m²-thermal mass unit were generally lower during the daytime and higher during the nighttime than those at unit with thermal mass of 1,000 kg/m². It is also found that the range of surface temperature at thermal mass of 2,000 kg/m² was narrower. It means that the higher thermal mass stabilizes the temperature of surfaces. At south- and north-wall, the range of surface temperature was relatively larger compared to other surfaces simply because those walls exposed to the outdoor. Furthermore, the profiles of surface temperature at south-side wall showed slightly lower than or almost the same as those at north-side due to the presence of balcony at the south-side that play role as thermal buffer zone. When the thermal mass increased, this difference between two sides become larger particularly when the ceiling height is 3.0m (see Figure 5.22). Nevertheless, when the ceiling height is 5.0m, this difference was not as large as that in 3.0m-ceiling height unit (see Figure 5.23). This is probably because the lower density of building materials (for walls, floor/ceiling) due to the higher ceiling height (or larger volume) in order to maintain thermal mass at 2,000 kg/m².

Unlike south- and north-wall, east- and west-wall had relatively narrower range of surface temperature. This is simply because east- and west-wall did not expose to the outdoor. It is found that there is almost no difference on the profile of both surface temperatures at thermal mass of 1,000 kg/m². When thermal mass increased to 2,000 kg/m², the west-wall had

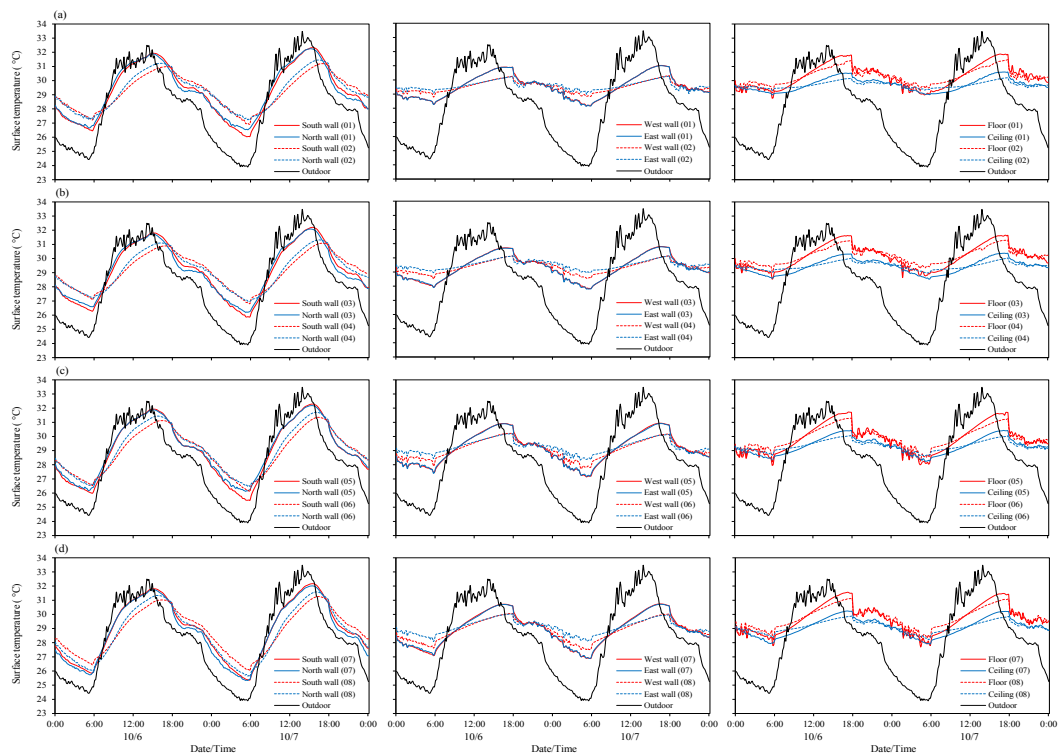


Figure 5.22. Comparison of surface temperature of walls, floor and ceiling under different thermal masses at ceiling height of 3.0m.

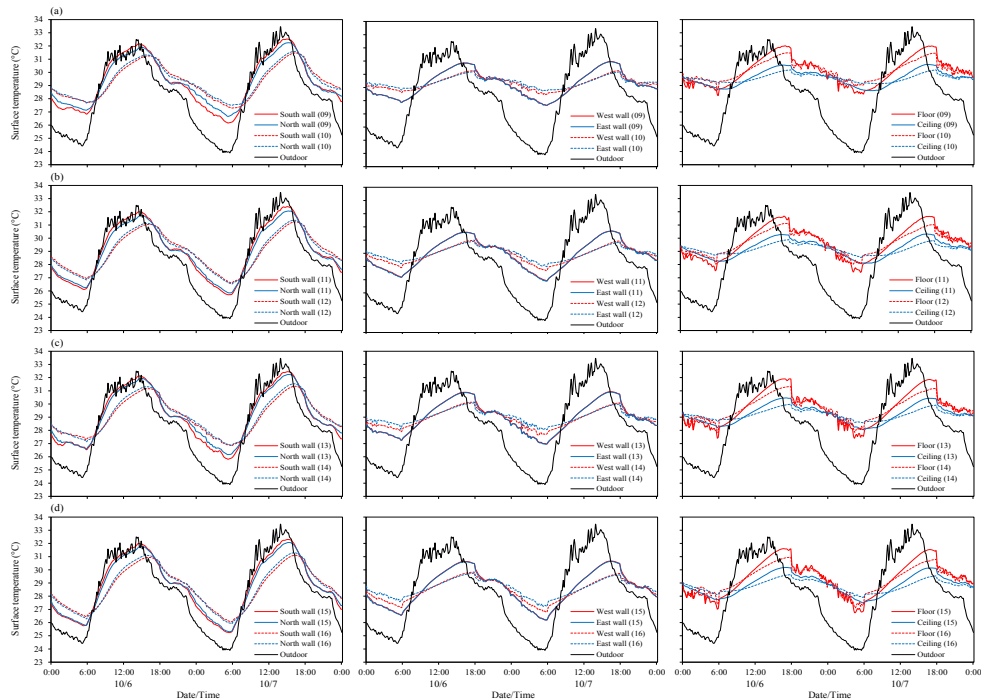


Figure 5.23. Comparison of surface temperature of walls, floor and ceiling under different thermal mass at ceiling height of 5.0m.

relatively higher surface temperature than the east-wall particularly during the night-time. This is most probably because the east wall received more heat from direct solar radiation that conductively transferred through balcony wall during the afternoon, stored it and then released it at the night-time into indoor space. The higher thermal mass, the higher capacity of structure in storing heat. Nevertheless, this difference is decreasing for the same reason as previous surfaces (i.e. south- and north-wall); lower material density due to the higher ceiling height. In addition, surface temperature of floor showed relatively higher than the ceiling's particularly during the daytime because the floor received sky solar radiation through the openings area (i.e. central window). View of the surface temperature at different thermal mass during daytime and night-time respectively, are visualized in Figures 5.24-25. During the daytime, external walls (south- and north-wall) of 1,000 kg/m²-thermal mass unit showed higher surface temperature than those of 2,000 kg/m²-thermal mass unit. As the consequences, the surface temperature of internal side of external wall obtained the higher values as well (Figure 5.24). At the night-time, the surface temperature of these walls lowered faster and therefore internal side of external walls and other walls (such as east- and west-wall) showed lower values as well (Figure 5.25).

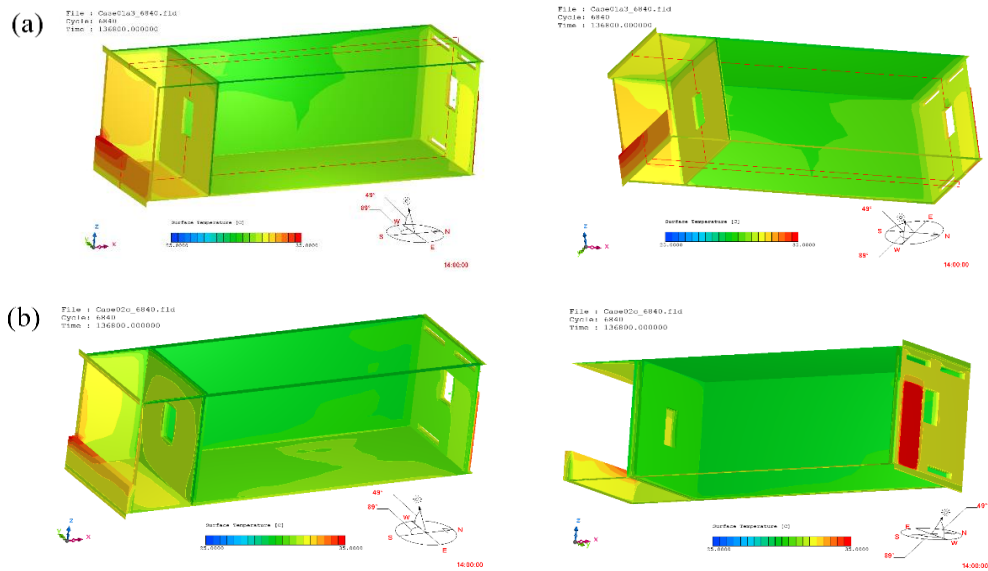


Figure 5.24. View of surface temperature of walls, floor and ceiling during at the peak hour (14:00) at thermal mass of (a) 1,000 kg/m² and (b) 2,000 kg/m².

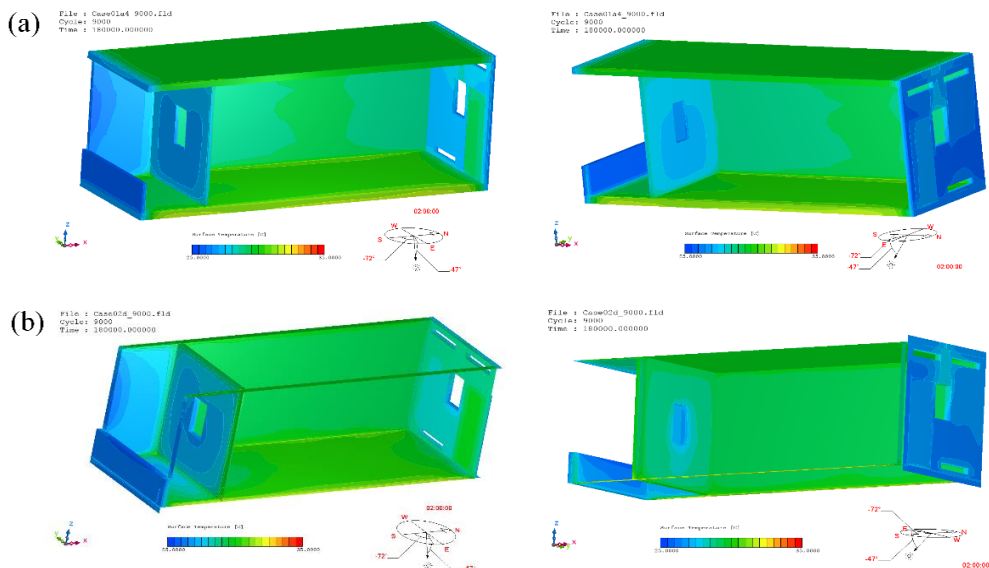


Figure 5.25. View of surface temperature of walls, floor and ceiling at the night-time (02:00) at thermal mass of (a) 1,000 kg/m² and (b) 2,000 kg/m².

5.4.1.2 The effects of ratio of windows area to floor area

Figure 5.26 presents comparison of indoor air temperature at 1.1m above floor level under different ratio of opening area to floor area. As shown, the increasing of opening ratio caused the night-time indoor air temperature decreasing regardless of thermal mass, ceiling height and window position. It is found that the night-time indoor air temperatures reduced by 0.9-1.5°C when the ratio of opening area to floor area is increasing. Meanwhile, the profiles of daytime indoor air temperature showed almost the same values between both ratios (i.e. 0.05 and 0.15). As previously described, the effects of nocturnal ventilative cooling by larger ratio of opening area to floor area were diminished by the larger amount of sky solar radiation received by the indoor space through the opening. Moreover, slightly difference can be seen at unit with thermal mass of 2,000 kg/m² and ceiling height of 5.0m (Figures 5.26f and 5.26h). Under those circumstances, the increasing of ratio generally lowered indoor air temperature throughout the day. Compared to Figures 5.26b and 5.26d, it is clearly implied that the increasing of ratio would affect in lowering the daytime indoor air temperature at unit with thermal mass of 2,000 kg/m² and ceiling height of 5.0m.

Figures 5.27-28 visualize the profile of indoor air temperature under different ratio of opening area to floor area at daytime and night-time respectively. As shown, during the peak hours, indoor air temperature profiles between two opening ratios (see Figures 5.27) are not

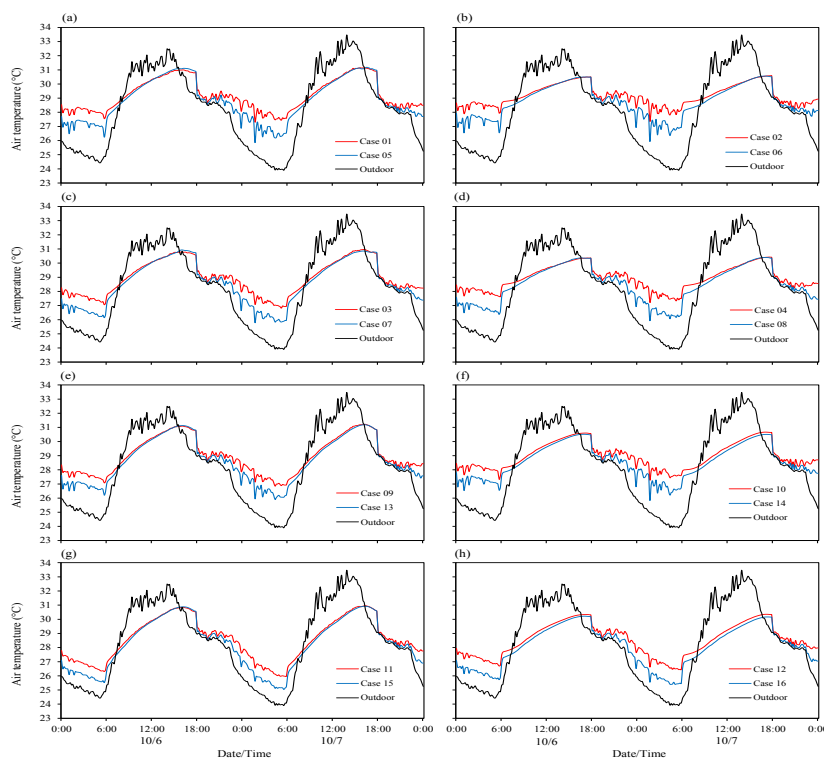


Figure 5.26. Comparison of simulation results of indoor air temperature at 1.1m above floor under different ratio of opening area to floor area.

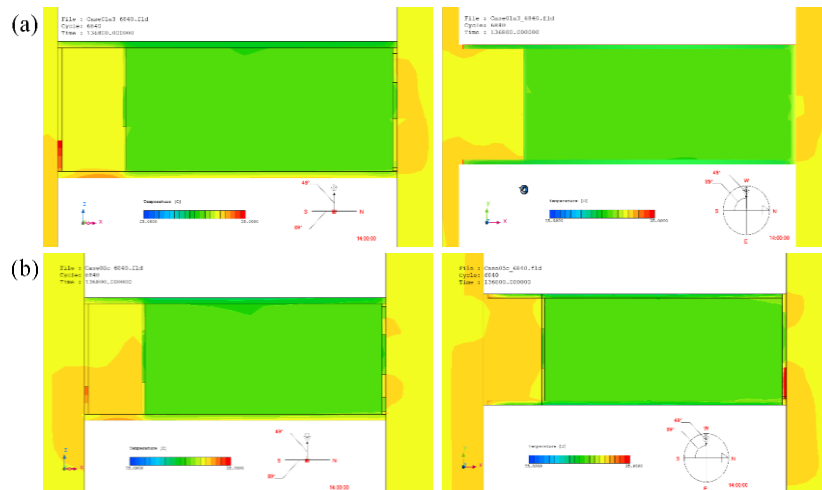


Figure 5.27. View of distribution of indoor air temperature (left: y-axis at 1.4m, right: z-axis at 1.1m above floor) at opening ratio of (a) 0.05 and (b) 0.15 during daytime (14:00).

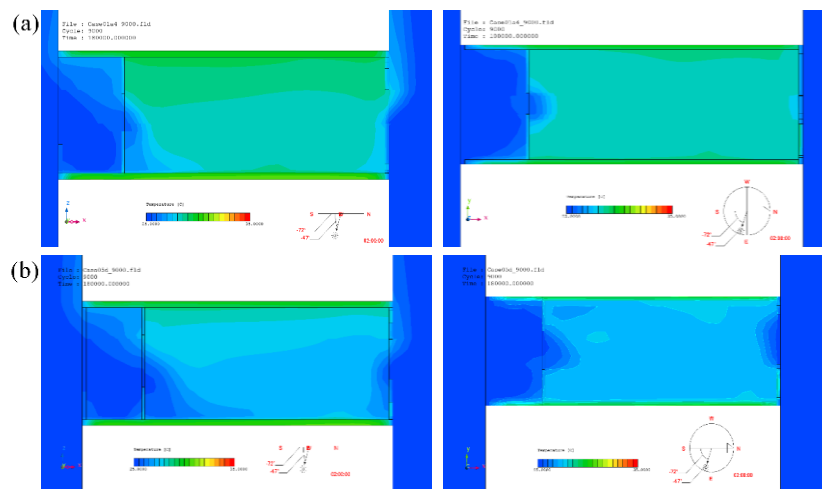


Figure 5.28. View of distribution of indoor air temperature (left: y-axis at 1.4m, right: z-axis at 1.1m above floor) at opening ratio of (a) 0.05 and (b) 0.15 during night-time (02:00).

significantly different. The indoor air temperature evenly distributed in y-axis and z-axis. Slightly difference is found in the balcony area, whereas warmer air was formed around the larger window area rather than at the smaller window area. During the night-time, the outdoor air temperature overwhelmingly enter the indoor space with the larger opening ratio rather than that with smaller ratio (Figure 5.28). It creates the layer of cool air at the lower part of indoor space while maintaining warmer air at the upper part of space. This cool air also distributed evenly throughout the space at the occupied level, or at 1.1m above floor level (see

Figure 5.28b). At the same time, unit with opening ratio of 0.05 had slightly higher indoor air temperature although thermal stratification could be seen there.

Figure 5.29 shows the comparison of the profile of indoor wind speed at 1.1m above floor level under different ratio of opening area to floor area. It should be noted that the outdoor wind speed was measured at height of 26m above the ground and therefore, the wind speeds

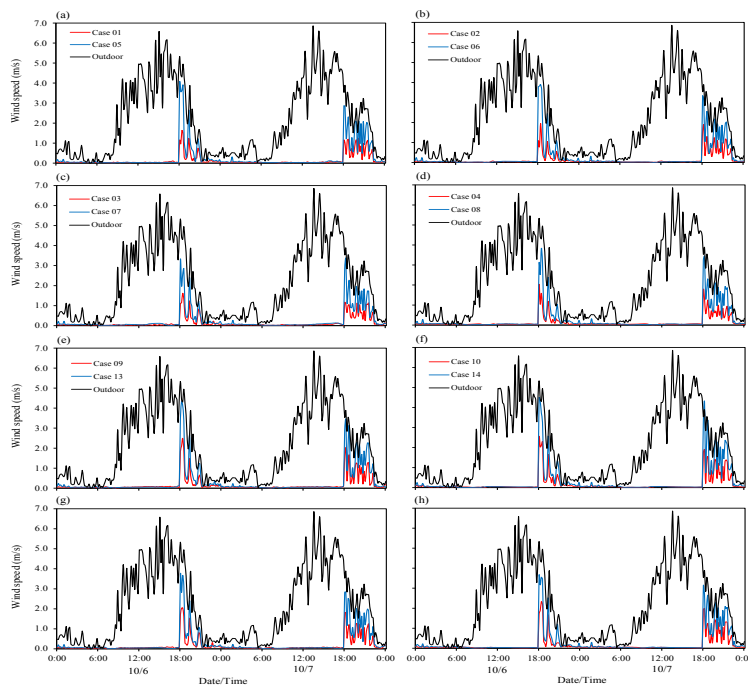


Figure 5.29. Comparison of simulation results of indoor wind speed at 1.1m above floor under different ratios of opening area to floor area.

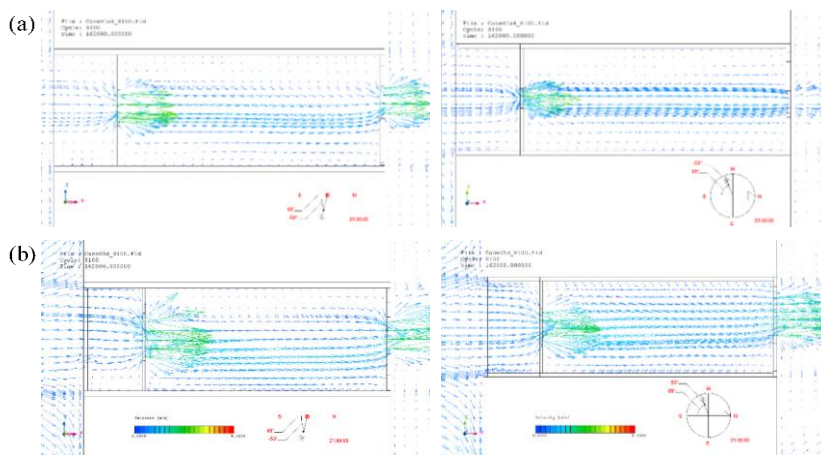


Figure 5.30. View of distribution of indoor wind speed (left: y-axis, right: z-axis) at opening ratio of (a) 0.05 and (b) 0.15 during night-time (21:00).

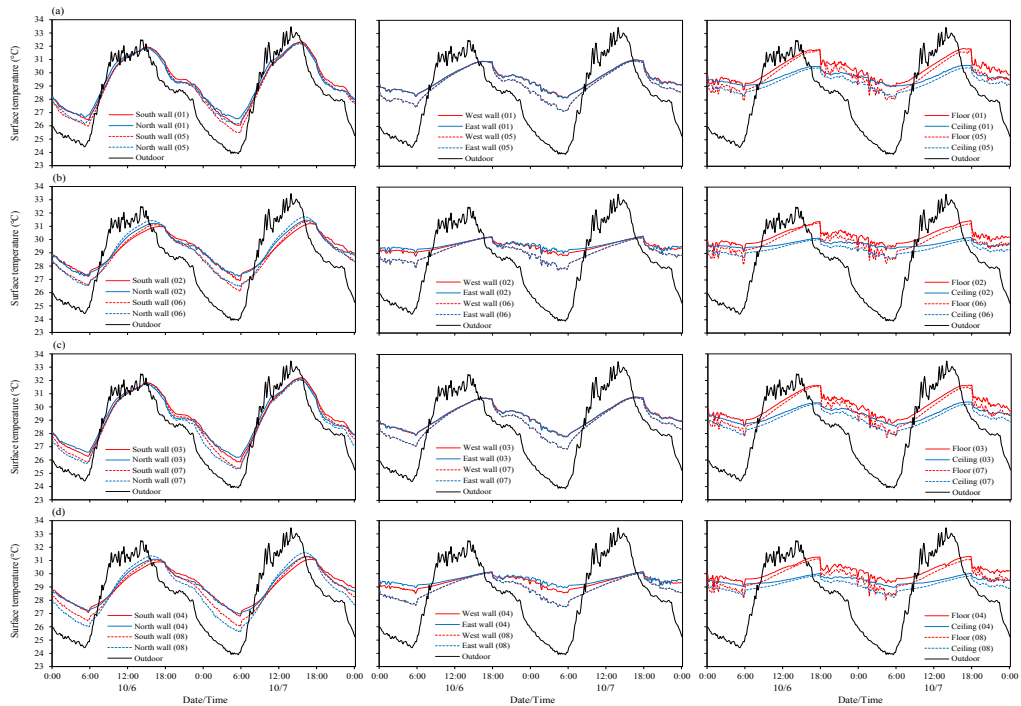


Figure 5.31. Comparison of surface temperature of walls, floor and ceiling under different ratios of opening area to floor area at ceiling height of 3.0m.

recorded relatively high value with the maximum wind speed of 6.8 m/s. As previously mentioned, the maximum indoor wind speed would increase by almost two times when the ratio of opening area to floor area is increasing from 0.05 to 0.15. As shown, when the windows are open, the indoor wind speeds at the opening ratio of 0.15 were averagely 1.74-1.99 m/s higher than those at the ratio of 0.05 regardless of thermal mass, ceiling height and windows position (see Figures 5.29a and 5.29b or Figures 5.29a and 5.29c, for instance). The indoor wind speeds obtained relatively high values due to the cross ventilation occurred in the unit (Figure 5.30). Since the window closed during the daytime, air flow is not flowing into the indoor space. As can be seen in Figure 5.14, the position of front- and back-side windows was perpendicular to each other. Further discussions on the effects of window position are discussed in the next Subsection (Subsection 5.4.1.4).

Figures 5.31 shows the surface temperature of walls, floor and ceiling under different ratio of opening area to floor area at 3.0m-ceiling height unit. As shown, the profiles of surface temperatures of walls, floor and ceiling are follow to the profiles of indoor air temperature; lower at the night-time at the larger opening ratio regardless of window position, thermal mass and ceiling height. At the daytime, the profiles of the surface temperature are almost the same as particularly when the opening ratio is 0.05. At thermal mass of 1,000 kg/m², the increasing of ratio of opening area to floor area would not change the surface temperature of east- and west-walls (see Figures 5.31a, 5.31c). Furthermore, when thermal mass of 2,000 kg/m²

applied, the increasing of opening ratio caused the difference of surface temperature in south- and north-walls become larger during the night-time (see Figure 5.31b, 5.31d). It implies that the increasing of opening ratio would effectively cool the structure through night ventilation particularly when thermal mass of 2,000 kg/m² is applied. As previously described, since floor received sky solar radiation from the outdoor, its surface temperature showed relatively higher than ceiling during the daytime.

Figures 5.32-33 illustrate the distribution of surface temperature of walls, floor and ceiling during the daytime and night-time under different ratio of opening area to floor area, respectively. As indicated, it is found that the distribution of surface temperature in the two units with the different opening ratios are not significantly different, both during the daytime and night-time (see Figures 5.32-33). It indicates that the ratio of opening area to floor area did not significantly affected to the surface temperature of building envelope.

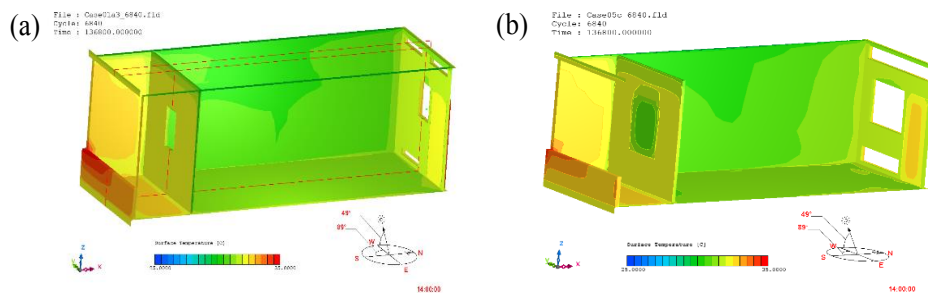


Figure 5.32. View of surface temperature of walls, floor and ceiling during the daytime (14:00) at opening ratios of (a) 0.05 and (b) 0.15.

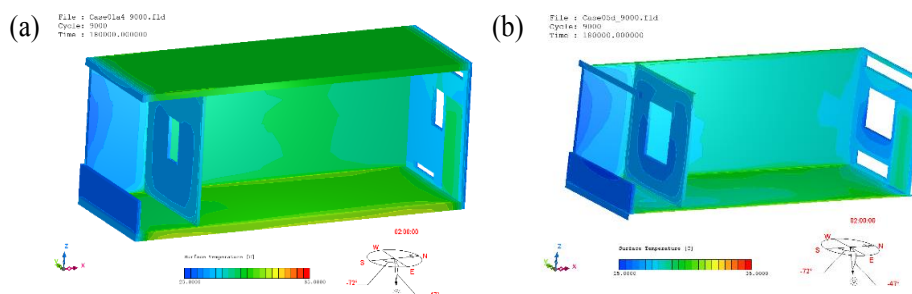


Figure 5.33. View of surface temperature of walls, floor and ceiling during the night-time (02:00) at opening ratio of area to floor area of (a) 0.05 and (b) 0.15.

5.4.1.3 The effects of ceiling height

Comparisons of indoor air temperature at 1.1m above floor are presented in Figure 5.34. It should be noticed that the comparison was carried out under same thermal mass, ratio of opening area to floor area and window position. When the unit ceiling height is 5.0m, indoor air temperature at that point was tend to lower than that when the ceiling height is 3.0m, even

during the daytime. Gradually, this indoor air temperature increased and reached the same values as that in ceiling height of 3.0m particularly at the peak hours (around of 14:00-18:00). This is because at that time, this point (i.e. 1.1m above floor) in both cases received the same amount of heat emitted by the surrounding building structures such as east-wall, west-wall, and floor (see Figure 5.41). In addition, this is most probably also due to the same amount of sky solar radiation received by that point. Furthermore, further reduction of indoor air temperature was obtained when the upper/lower windows are applied, under same thermal mass and ratio of opening area to floor area (see Figures 5.34a and 5.34c, or Figures 5.34e and 5.34g, for comparison). Further discussion on the effects of window position are discussed in Subsection 5.4.1.4.

Interestingly, air temperature stratification could not be seen even when the ceiling height of 5.0m is applied. Based on the previous findings (see Chapter 4), it is found that ceiling height played important role in maintaining indoor air temperature at occupied level (1.1m above floor level) lower even during peak hours. As shown in Figure 5.35, indoor air temperatures profile at peak hours for ceiling height of 5.0m was same as that for the ceiling height of 3.0m. This results confirmed the results as presented in Figure 5.34. This is most probably because the volume of unit is not sufficient to maintain temperature gradient due to the ceiling height. However, at the 5.0m-ceiling height unit, thermal stratification could be seen before the peak hours (14:00-18:00). Meanwhile, during the night-time, thermal

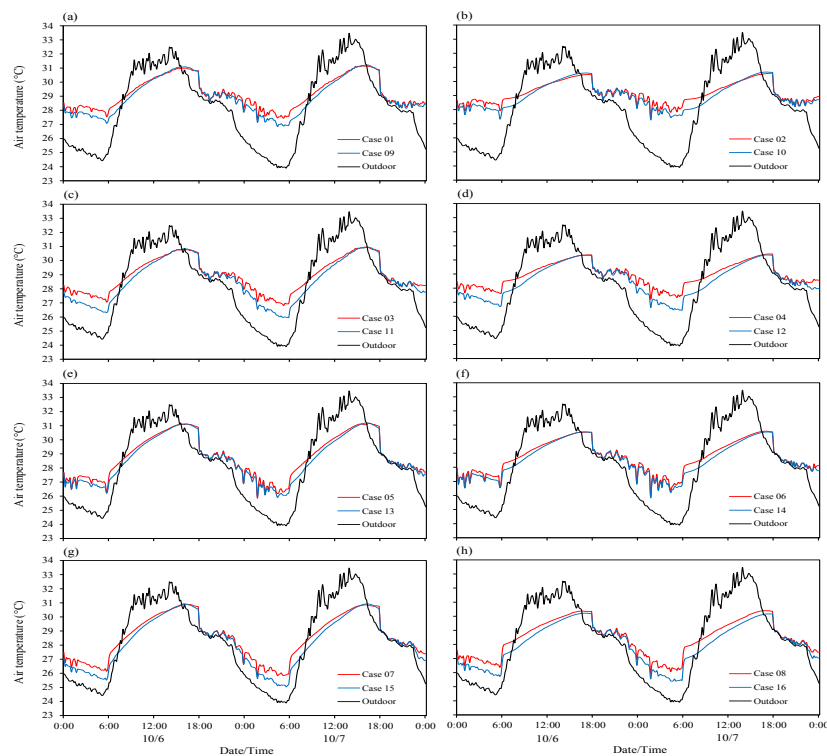


Figure 5.34. Comparison of simulation results of indoor air temperature at 1.1m above floor under different ceiling height.

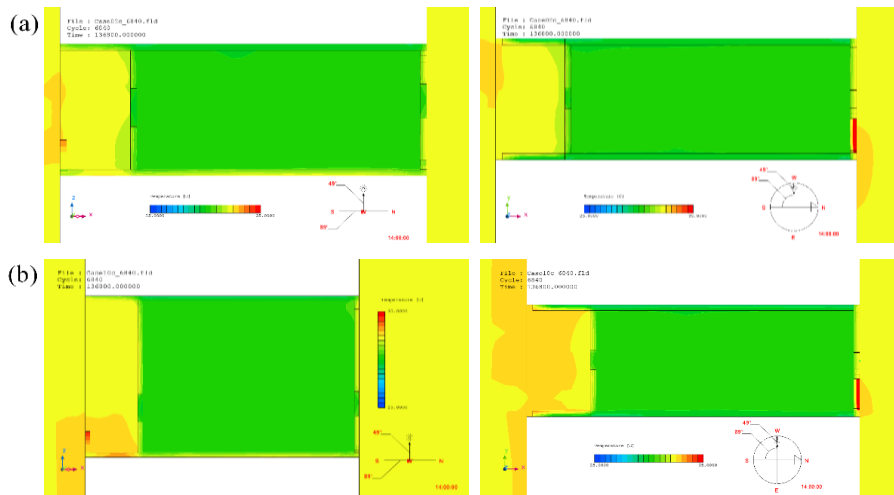


Figure 5.35. View of distribution of indoor air temperature (left: y-axis at 1.4m, right: z-axis at 1.1m above floor) at the ceiling heights of (a) 3.0m and (b) 5.0m at the peak hour (14:00).

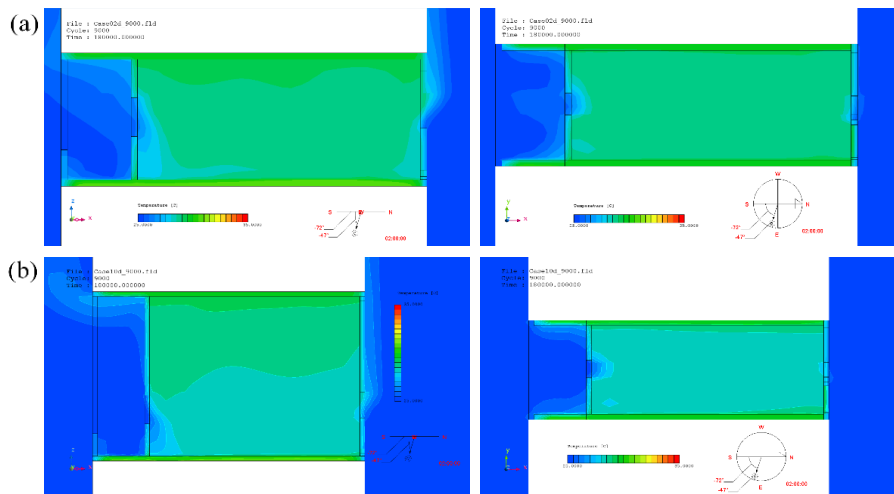


Figure 5.36. View of distribution of indoor air temperature (left: y-axis at 1.4m, right: z-axis at 1.1m above floor) at the ceiling heights of (a) 3.0m and (b) 5.0m during daytime (14:00).

stratification could be seen in both cases (Figure 5.36). It is shown that at the night-time, the area of cooler air at the occupied level were larger in the 5.0m-ceiling height unit rather than in the 3.0m-ceiling height unit. It clearly indicates that ceiling height particularly would effectively lowering lower indoor air temperature at nighttime rather than at daytime under night ventilation condition.

Meanwhile, indoor wind speed at 1.1m above floor in 5.0m-ceiling height unit had the same profile as that in 3.0m-ceiling height unit, as can be clearly seen from Figure 5.37. It should be noticed that the comparisons are carried out under same ratio of opening area to floor area

as well as same window position. Since opening ratio and window position are same, the profiles of wind flow at both daytime and nighttime are generally not significantly different compared to other cases, such as cases of different thermal masses (Figures 5.20-21) and different opening ratios (see Figures 5.30). For further comparison, Figures 5.38 visualize the wind flow in the different ceiling heights at the night-time. As previously discussed, the profiles of wind flow pattern during the daytime are likely similar with other cases due to the closed windows.

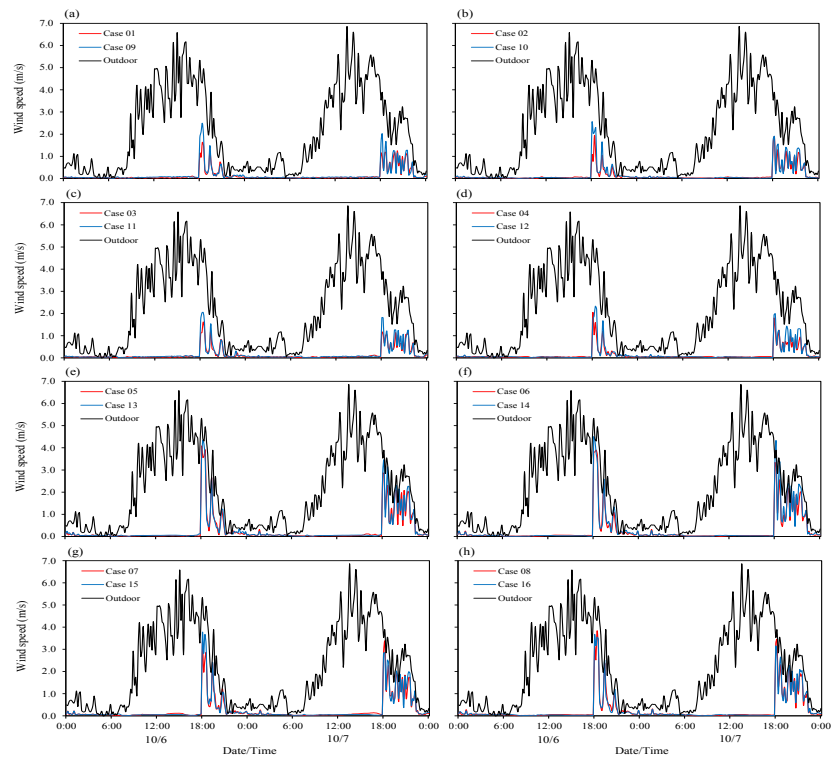


Figure 5.37. Comparison of simulation results of indoor wind speed at 1.1m above floor under different ceiling heights.

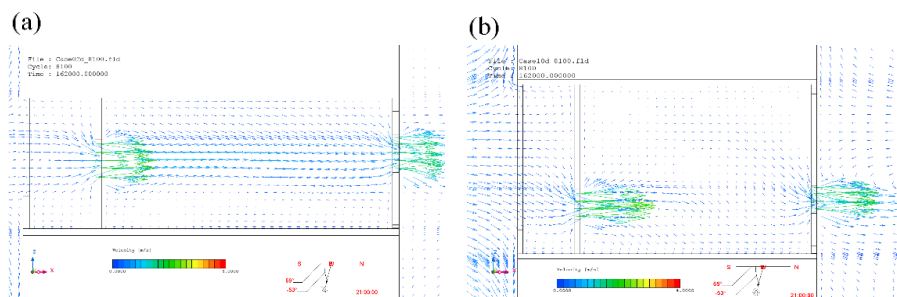


Figure 5.38. View of indoor wind flow (y-axis) at ceiling heights of (a) 0.05 and (b) 0.15 at the night-time (21:00).

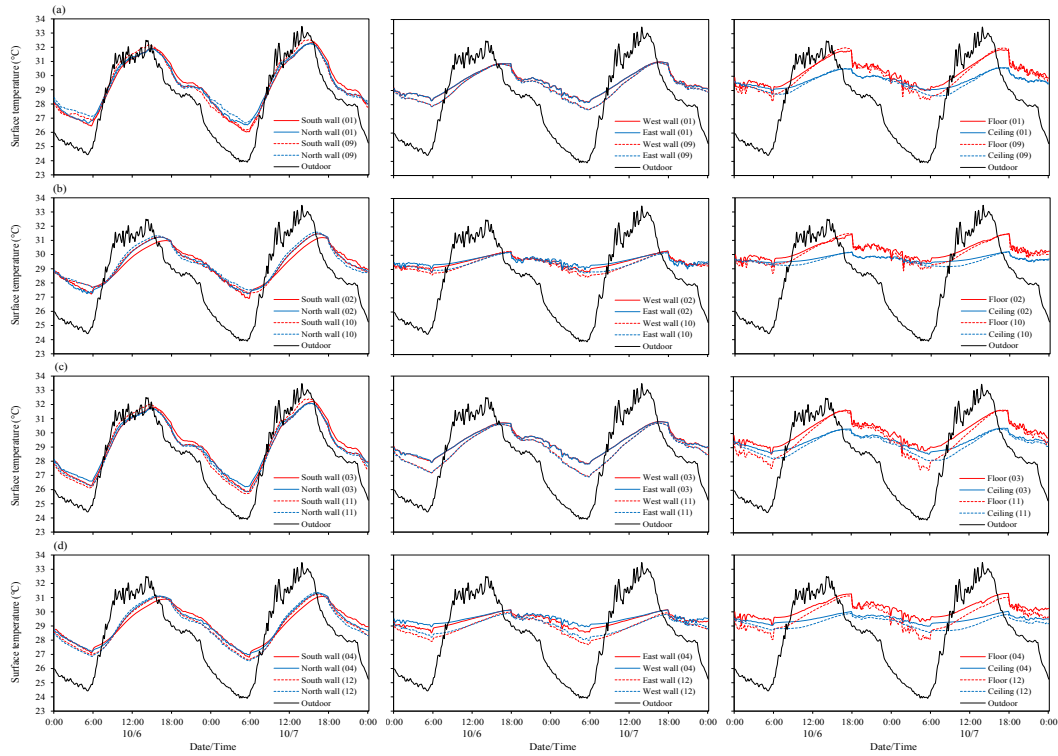


Figure 5.39. Comparison of surface temperature of walls, floor and ceiling under different ceiling heights at ratio of opening area to floor area of 0.05.

Figures 5.39-40 show the comparison of surface temperature of walls, floor and ceilings under different ceiling height at ratios of opening area to floor area of 0.05 and 0.15 respectively. As shown, the profiles of surface temperature were not significantly different between the two external walls (i.e. south- and north-walls) mainly because both walls exposed to the outdoors. In contrary, different phenomena can be seen in other surfaces such as east-wall, west-wall, floor and ceiling. In those surfaces, the higher ceiling height would lower the surface temperature particularly during the night-time. As the profiles of indoor air temperature, the temperatures of those surfaces at peak hours in 5.0m-ceiling height unit approached the same value as those in 3.0m-ceiling height unit. The detailed profiles of surface temperature under different ceiling height are visualized in Figures 5.41-42.

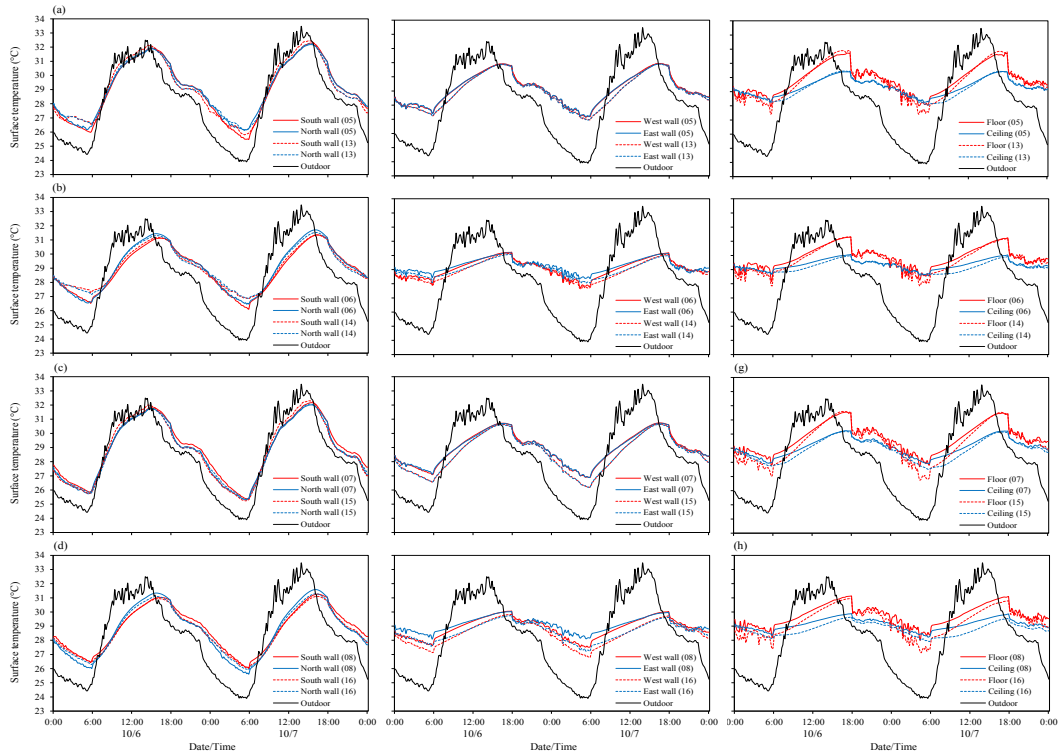


Figure 5.40. Comparison of surface temperature of walls, floor and ceiling under different ceiling heights at ratio of opening area to floor area of 0.15.

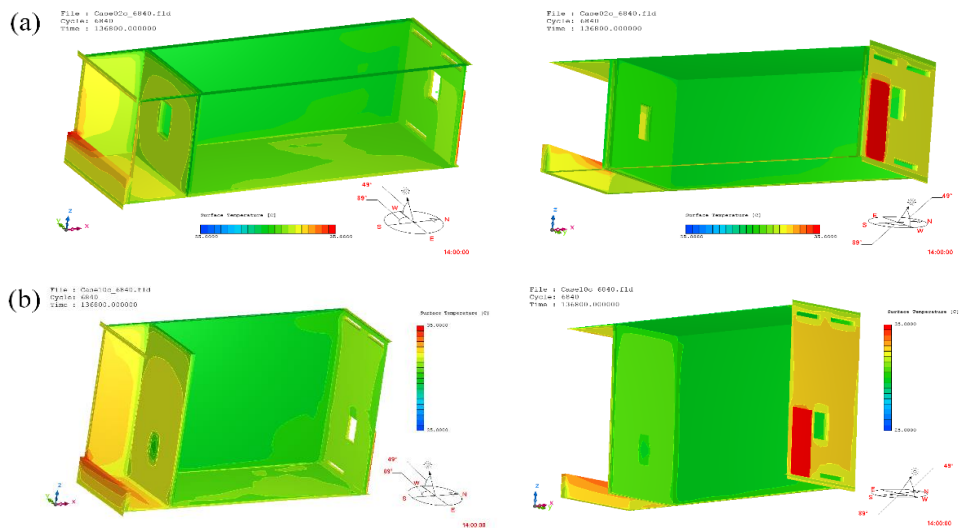


Figure 5.41. View of surface temperature of walls, floor and ceiling at the ceiling heights of (a) 3.0m and (b) 5.0m during daytime (14:00).

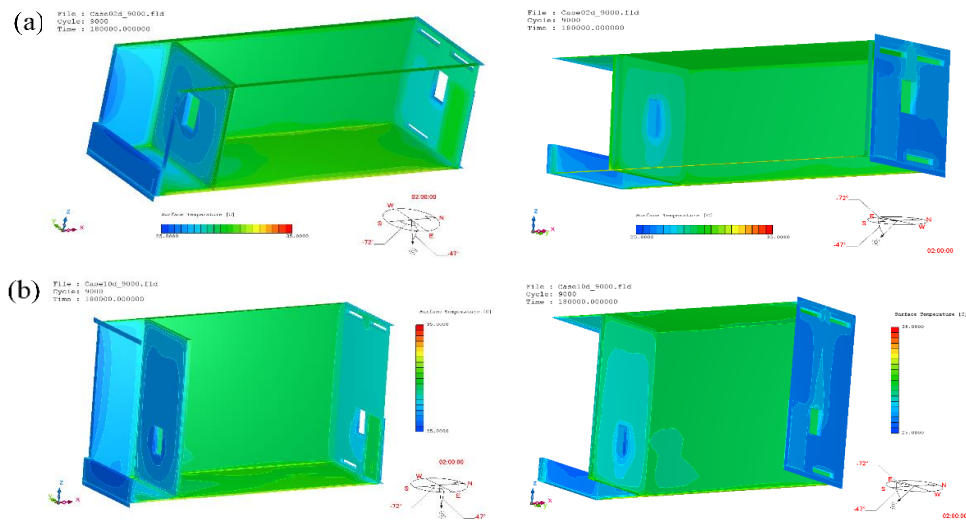


Figure 5.42. View of surface temperature of walls, floor and ceiling at the ceiling heights of (a) 3.0m and (b) 5.0m during night-time (02:00).

5.4.1.4 The effects of opening position

The effects of window positions on the profile of indoor air temperature are presented in Figure 5.43, which shows the comparison between indoor air temperatures in the room applying central windows at both sides and applying upper and lower at the back side (balcony-side). It is found that applying upper and lower windows in the back side for night ventilation generally reduced indoor air temperature rather than when central windows are applied at the both sides. It is shown that during the daytime, room with upper and lower windows had 0.2–0.3°C indoor air temperatures lower compared to that with central windows. Furthermore, applying upper/lower windows would further decrease the indoor air temperature up to 0.9°C during the night-time. It is also found that by increasing the ceiling height at the same time, applying upper and lower windows would further decrease indoor air temperature during both daytime and night-time although its reduction was relatively small (up to 0.1°C).

Figures 5.44–45 show the view of profile of indoor air temperature (y -axis) using *STPost* at the daytime and night-time respectively. As indicated, layer of cooler air was formed in the half lower part (or at occupied level) of the unit with upper and lower windows (Figure 5.44b), while this air was not formed in the other unit. A slightly higher indoor air temperature was evenly distributed inside the room with central windows (Figure 5.44a). This is most probably because cool air that enter the room during the night-time remain in the room even during the daytime. As shown in Figure 5.45b, the cool air from the outdoor that enter the indoor space mostly went to the lower part of the unit and created layers of cool air there, and therefore it cooled the floor. In addition, the unit with upper and lower window remove the hot air in the room through lower window rather than through upper window. In the other word, upper/lower window is more effective in removing the hot air inside the room during the night-time, as

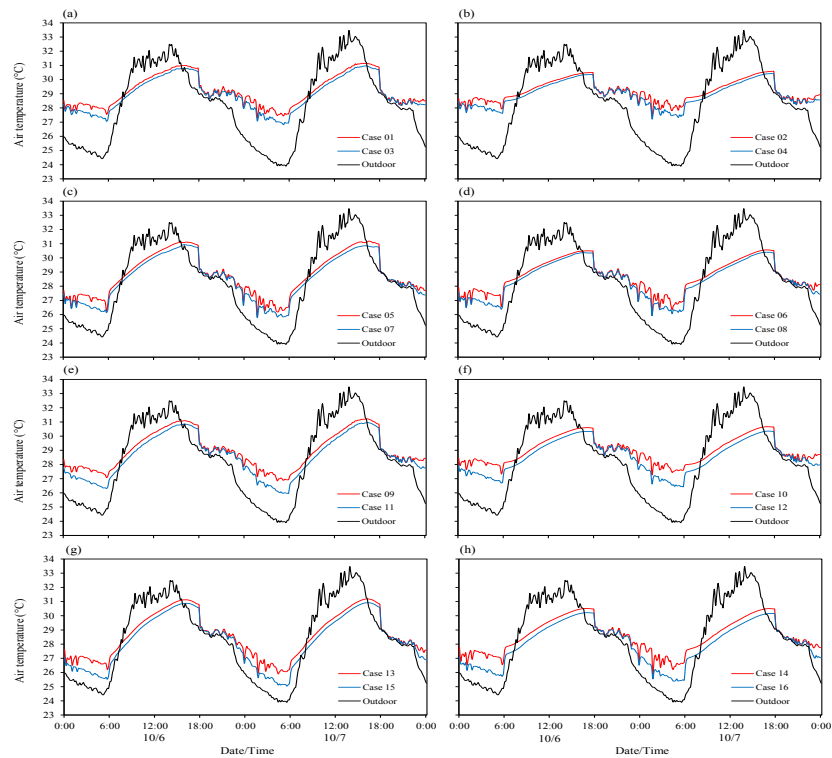


Figure 5.43. Comparison of simulation results of indoor air temperature at 1.1m above floor under different window positions.

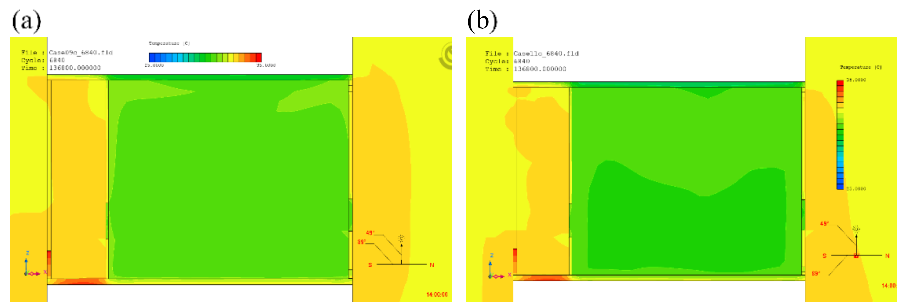


Figure 5.44. View of indoor air temperature (y-axis) at the peak hour (14:00) in the unit applying (a) central window and (b) upper and lower window at back-side.

well as cool the structure particularly the floor. It should be noted that floor received more heat compared to the ceiling during the daytime.

The profiles of indoor wind speeds in the units with different opening positions are not significantly different. Figure 5.46 show the profile of wind speed under different window positions. It should be noted that comparisons are conducted under same ratio of opening area to floor area. It is shown that although upper/lower windows were applied at the opposite side of wind-ward, the indoor wind speed at 1.1m above floor level was almost the same as that of

unit applying central windows on the both sides. This is mainly due to the cross ventilation occurred in the both cases. In addition, at both cases, front side (or balcony side) applied the same window (i.e. central windows) and therefore, the wind flowed directly to the indoor space through that front window before going out of the space through back side. As for unit applying upper/lower windows, the air tend to flow out through the lower window (Figure 5.47b). As the previous cases, the wind barely enter the indoor space because of closed window during the daytime.

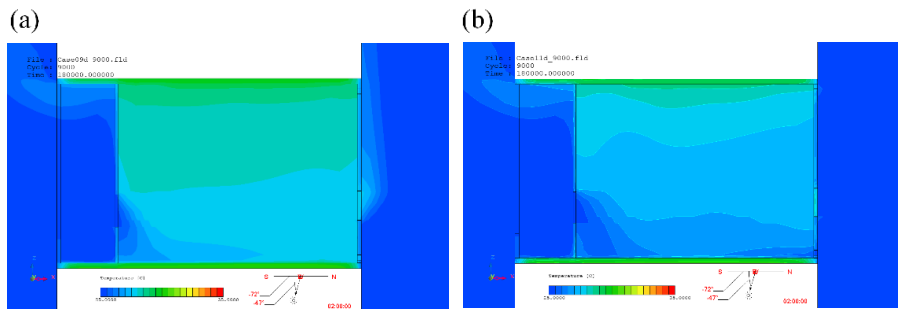


Figure 5.45. View of indoor air temperature (y-axis) at the night-time (02:00) in the unit applying (a) central window and (b) upper and lower window at back-side.

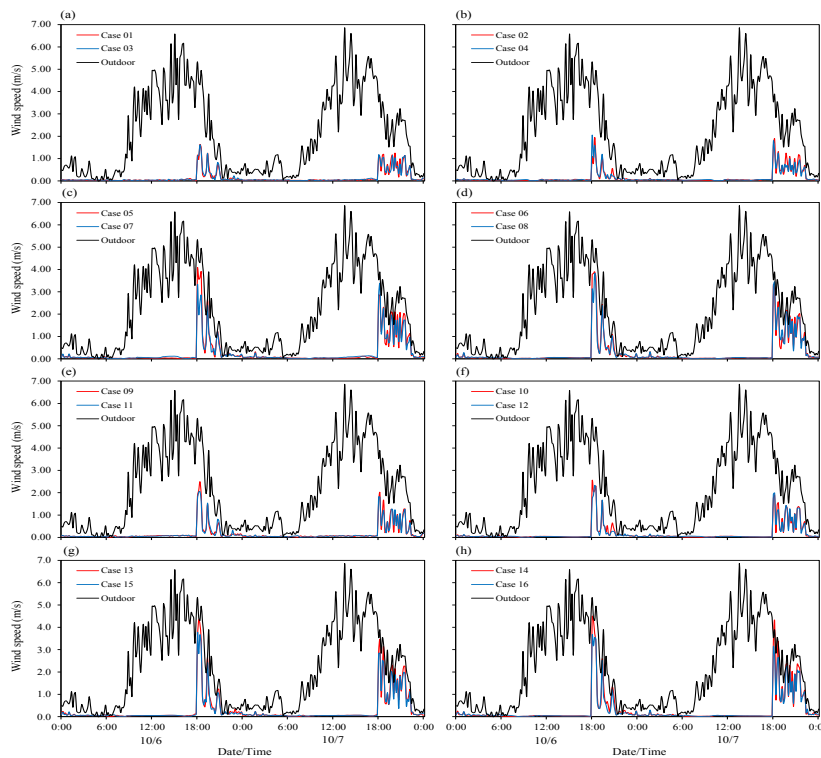


Figure 5.46. Comparison of simulation results of indoor wind speed at 1.1m above floor under different window positions.

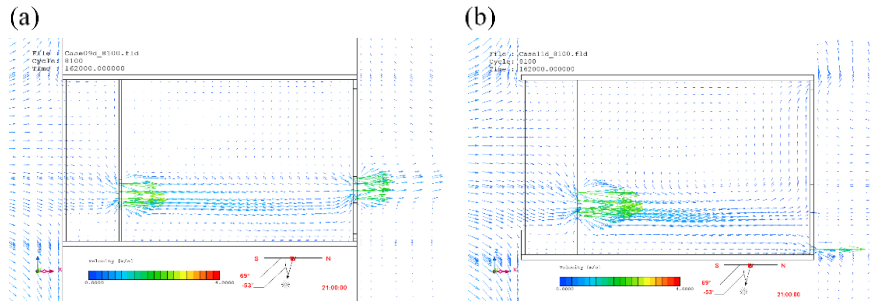


Figure 5.47. View of indoor wind speed pattern (y-axis) at the unit with (a) central windows and (b) upper/lower windows at the night-time (21:00).

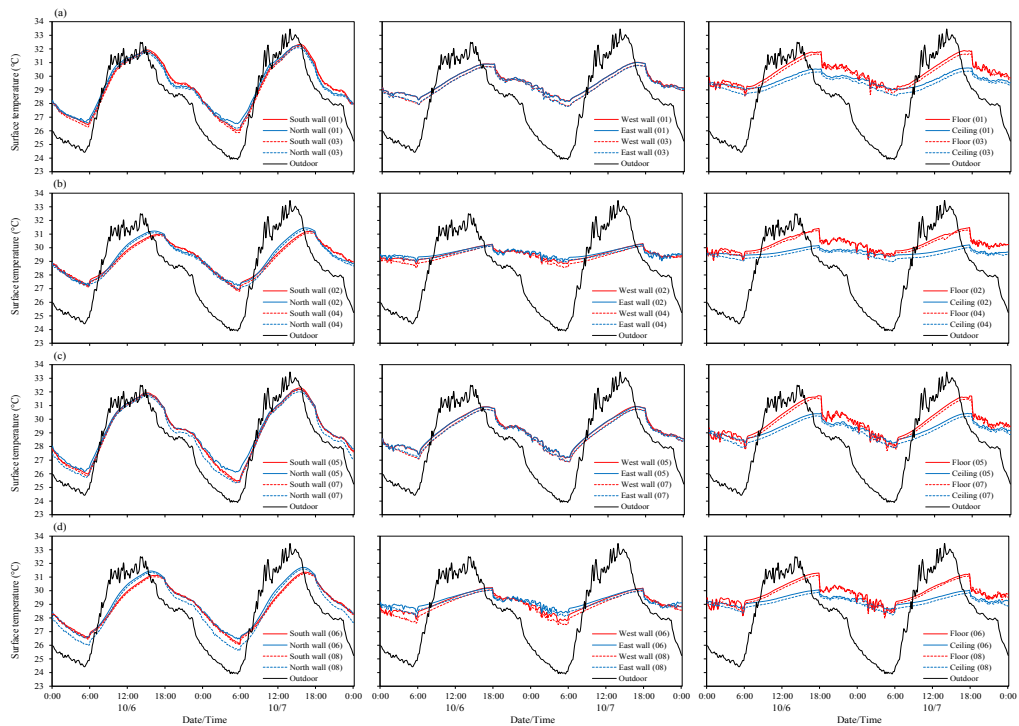


Figure 5.48. Comparison of surface temperature of walls, floor and ceiling under different window position at ceiling height of 3.0m.

Comparison of the profiles of surface temperature between in the unit applying central windows and upper/lower windows are shown in Figures 5.48-49, for ceiling height of 3.0m and 5.0m respectively. Generally, the profile of surface temperature of both south- and north-wall in the two units with different window positions are not significantly different. As previously discussed, this is simply because these walls functioned as external wall and exposed to the outdoors. However, surface temperatures of those walls in 5.0m-ceiling height unit become lower during the night-time compared to those in the of 3.0m-ceiling height unit

(see Figure 5.49). Moreover, applying upper and lower windows caused the other surfaces (i.e. east-wall, west-wall, floor and ceiling) relatively lower even during the daytime regardless of thermal mass and ceiling height. As shown in Figure 5.50b, all the west-wall surface in unit with upper/lower windows had the uniform temperature and it relatively lower. Moreover, all the surfaces at upper/lower windows unit obtained lower values than those at central windows (Figure 5.51). It clearly implies that window position largely affecting the performance of the structural cooling under night ventilation condition.

Further simulations were conducted to figure out the effects of different window positions on the indoor thermal environments. Additional simulations were carried out by adding other cases regarding window position. In previous simulations, window position referred to the two different positions, i.e. applying central windows at both sides and using upper and lower windows at back side while maintaining central windows at front-side. In the additional simulations, 8 additional simulation test cases due the different window positions were added (see Table 5.9). As summary, these additional simulation cases comprises two types of window positions, they are: applying upper and lower windows at front-side and central window at back-side; and applying upper and lower at both sides. The additional simulations carried out under same thermal mass of 1,000 kg/m² but different ratio of opening area to floor area.

Figure 5.52 shows the results of additional simulations and its comparisons to the corresponding cases. Compared to unit with central windows at both sides (i.e. Cases 01, 05, 09 and 13), applying of upper and lower window at front side while maintaining central

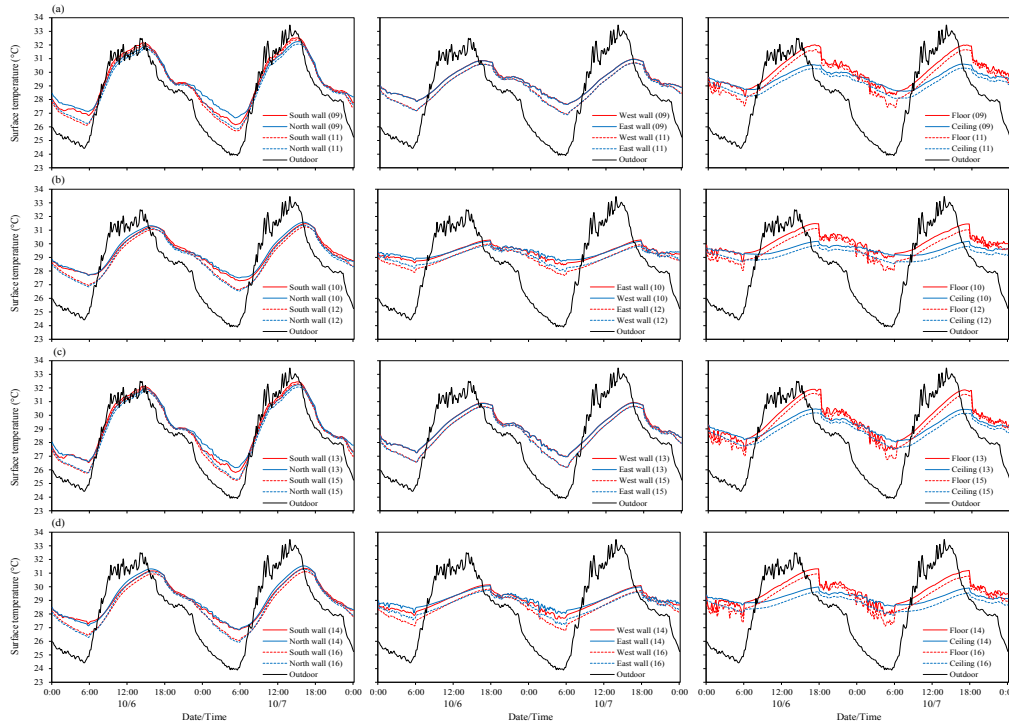


Figure 5.49. Comparison of surface temperature of walls, floor and ceiling under different window position at ceiling height of 5.0m.

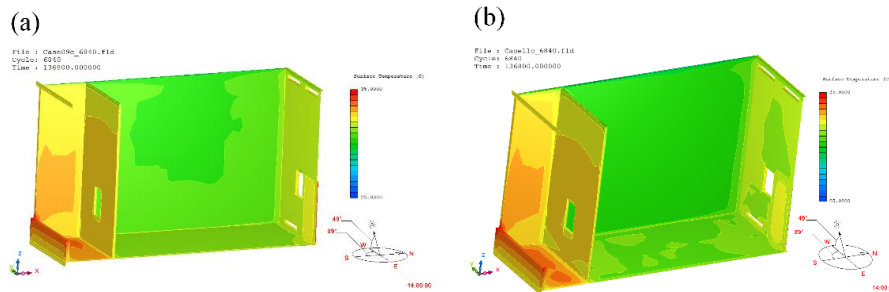


Figure 5.50. View of surface temperature of walls, floor and ceiling in the unit with (a) central window (b) upper and lower window at the peak hour (14:00).

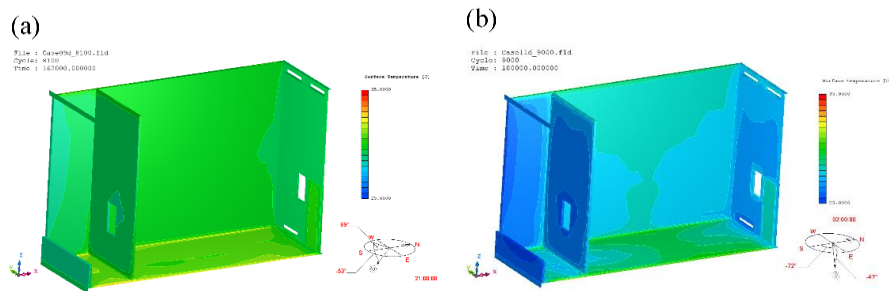


Figure 5.51. View of surface temperature of walls, floor and ceiling in the unit with (a) central window (b) upper and lower window at the night-time (02:00).

Table 5.9. Additional simulation test cases based on the different window positions.

Simulation Cases	Thermal mass (kg/m ²)	Ratio of window area to floor area	Ceiling height (m)	Windows position	
				Front-side	Back-side
Case 17	1,000	0.05	3.0	Upper/lower	Central
Case 18	1,000	0.05	3.0	Upper/lower	Upper/Lower
Case 19	1,000	0.15	3.0	Upper/lower	Central
Case 20	1,000	0.15	3.0	Upper/lower	Upper/Lower
Case 21	1,000	0.05	5.0	Upper/lower	Central
Case 22	1,000	0.05	5.0	Upper/lower	Upper/Lower
Case 23	1,000	0.15	5.0	Upper/lower	Central
Case 24	1,000	0.15	5.0	Upper/lower	Upper/Lower

window at back side would effectively lower indoor air temperature if ceiling height of 5.0m is applied. Other than that, the change of window position would not significantly affect the indoor air temperature. If compared to the unit applying upper and lower window at back side while maintaining central window at front side (i.e. Cases 03, 07, 11 and 15), it would not significantly affect the indoor air temperature except when the ratio of opening area is 0.05 and the ceiling height is 3.0m. Under above circumstances, the amount of cool air entering the

room is less during night-time so that the cooling effect also become less. Therefore, under this condition, applying upper/lower window at front side while using central window at back-side would increase the indoor air temperature throughout the day. In addition, it obviously implies that changing window position diametrically would not significantly affect the indoor air temperature.

Furthermore, when upper and lower windows applied at both sides, the indoor air temperature was significantly lower indoor air temperature even during the daytime compared to that when central windows applied at the both sides. Under condition of opening ratio of

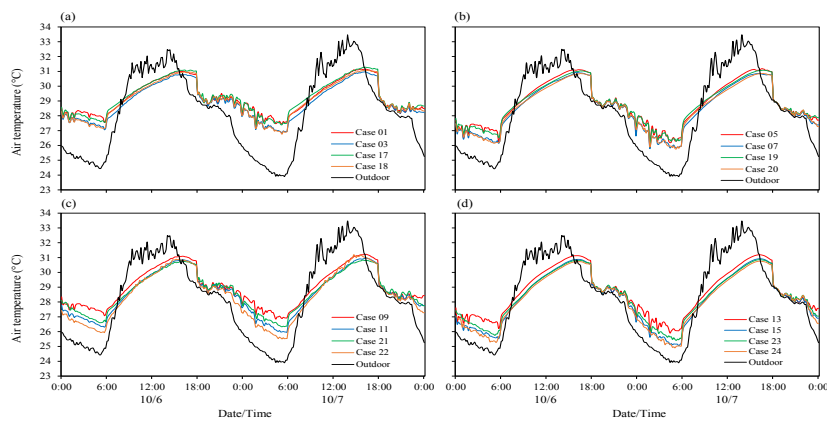


Figure 5.52. Comparison of indoor air temperature in the unit with (a) central windows at both sides, (b) upper/lower windows at back-side, (c) upper/lower windows at front side and (d) upper/lower at both sides.

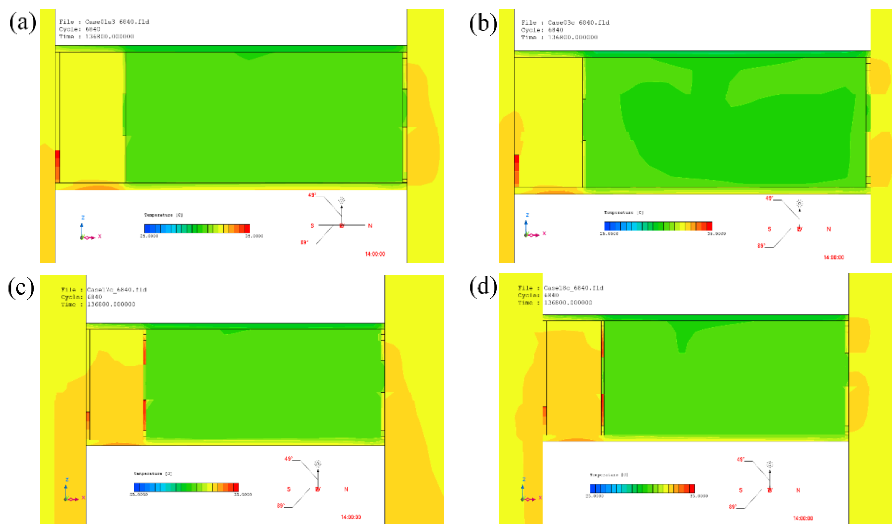


Figure 5.53. View of indoor air temperature profiles (y-axis) at the peak hours (14:00) in the unit with (a) central windows at both sides, (b) upper/lower windows at back-side, (c) upper/lower windows at front side and (d) upper/lower at both sides.

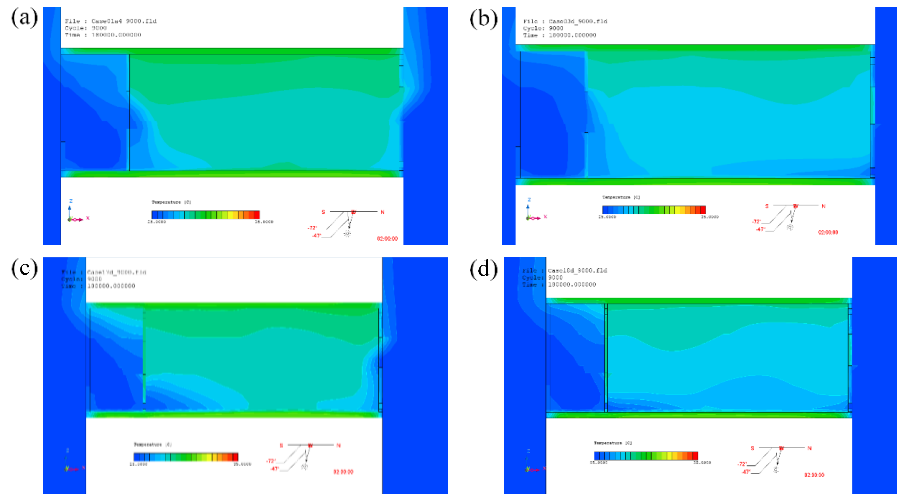


Figure 5.54. View of indoor air temperature profiles (y-axis) at the night-time (02:00) in the unit with (a) central windows at both sides, (b) upper/lower windows at back-side, (c) upper/lower windows at front side and (d) upper/lower at both sides.

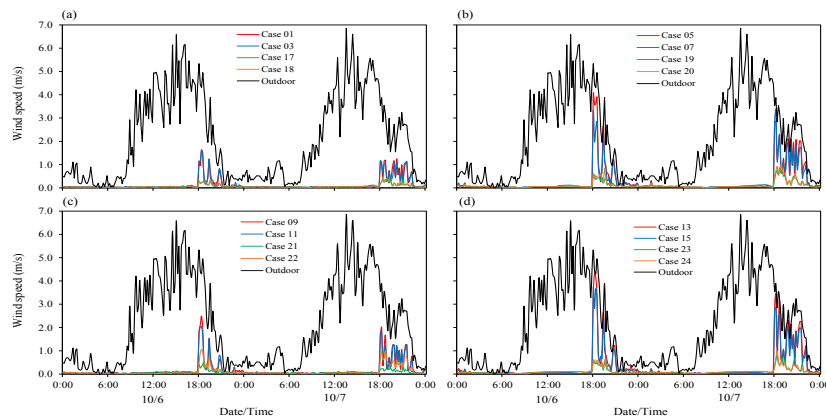


Figure 5.55. Comparison of indoor wind speed in the unit with (a) central windows at both sides, (b) upper/lower windows at back-side, (c) upper/lower windows at front side and (d) upper/lower at both sides.

0.05 and ceiling height of 3.0m, both type of opening positions showed almost same daytime indoor air temperature (see Cases 01 and 18 in Figure 5.52a). When the ratio of opening area increased, the daytime indoor air temperature would reduce 0.3-0.4°C if the upper/lower window at both sides is applied (see Cases 05 and 20 in Figure 5.52b). Furthermore, when the ceiling height is 5.0m, it would further reduce daytime indoor air temperature by averagely of 0.4°C (see Cases 09 and 22 in Figure 5.52c and Cases 13 and 24 in Figure 5.52d). Therefore, it is found that applying upper and lower window at both sides would significantly affect in lowering indoor air temperature when the opening ratio and ceiling height are increasing.

If compared to the unit applying upper and lower window at one side (either front side or back side), the unit that applying upper and lower window at both sides showed almost the same or slightly lower indoor air temperature. The unit with upper/lower windows at both sides obtained the lowest indoor air temperature during the night time compared other window positions, particularly when the opening ratio is 0.05. However, when the opening ratio increased, the profiles of indoor air temperatures amongst them are almost same. The view of profiles of indoor air temperature under these conditions can be further seen in Figures 5.53-54, for daytime and night-time respectively.

Figure 5.55 present the comparison profiles of indoor wind speed under different window position. It is found that applying upper and lower window at windward side (or balcony side/front side) reduced the indoor wind speed during the night time by more than half. At the 3.0m-ceiling height unit, the maximum indoor wind speed at the unit applying upper and lower window at windward side were obtained at levels of 0.43-0.48 m/s. The larger ratio of opening area, the higher maximum indoor wind speed at the same condition, which is calculated around of 0.83-0.98 m/s. When the ceiling height of 5.0m is applied, the maximum indoor wind speed were slightly higher at opening ratio of 0.05, while that at opening ratio of 0.15 were remain same. The difference of wind flow pattern amongst four type of window position particularly at the night-time are presented in Figure 5.56. In particular, Figure 5.56cd shown the wind flow pattern when the upper and lower window are applied at windward side. It also explains the cause of lower wind flow under those conditions. In addition, the profiles of surface temperature under different type of window/opening positions are shown in Figures 5.57-58. As indicated, when the upper and lower windows are applied, either in one side or in both sides, the surface of walls showed relatively lower temperatures.

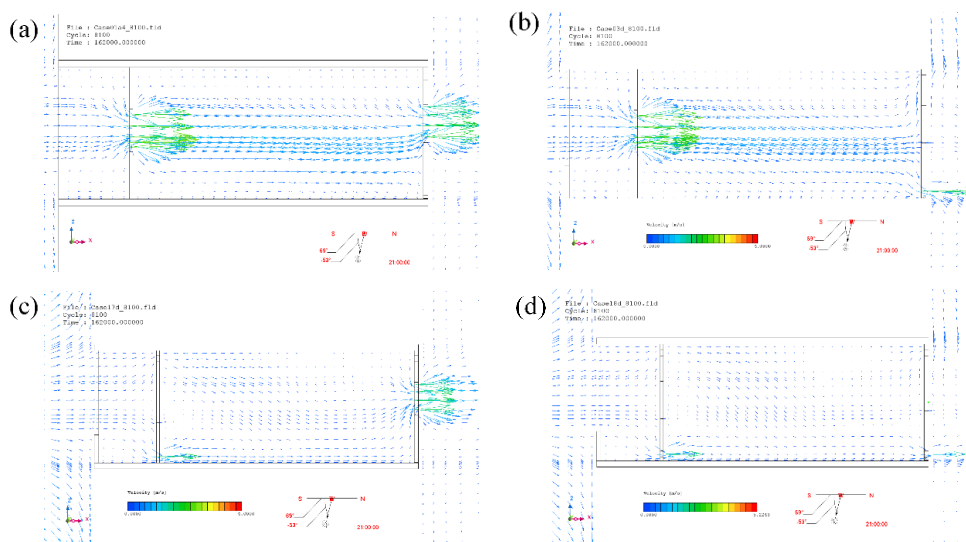


Figure 5.56. View of indoor wind flow pattern at the night-time (21:00) in the unit with (a) central windows at both sides, (b) upper/lower windows at back-side, (c) upper/lower windows at front side and (d) upper/lower at both sides.

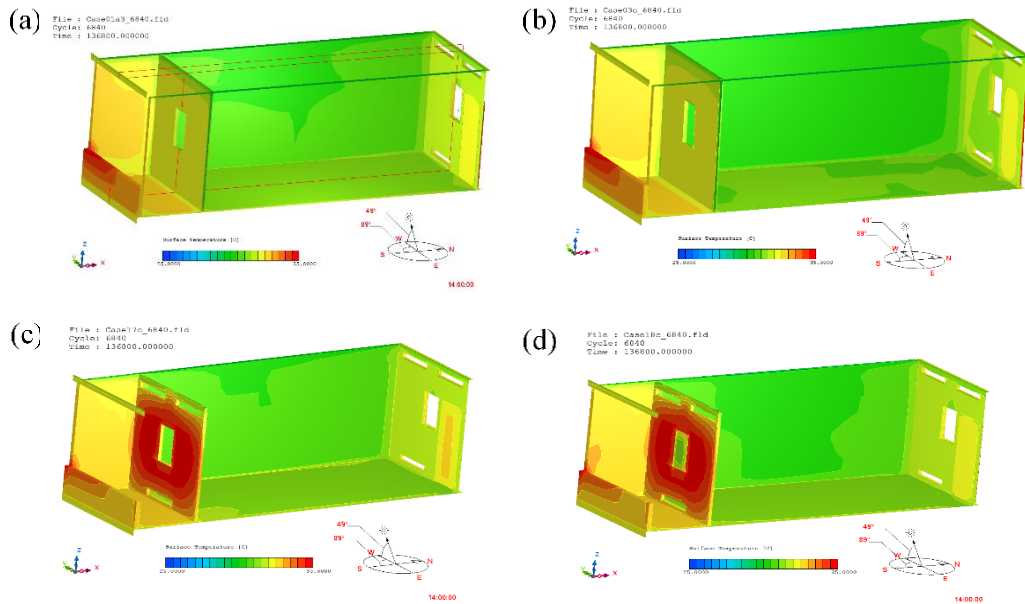


Figure 5.57. View of surface temperatures of walls, floor and ceiling at the peak hour (14:00) in the unit with (a) central windows at both sides, (b) upper/lower windows at back-side, (c) upper/lower windows at front side and (d) upper/lower at both sides.

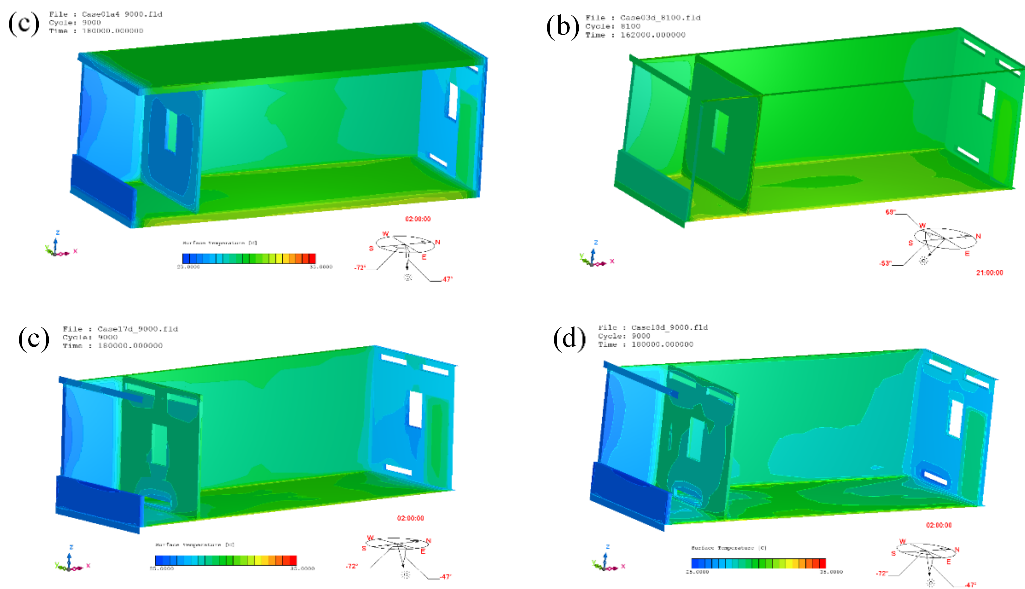


Figure 5.58. View of surface temperatures of walls, floor and ceiling at the night-time (21:00) in the unit with (a) central windows at both sides, (b) upper/lower windows at back-side, (c) upper/lower windows at front side and (d) upper/lower at both sides.

5.4.1.5 Optimum combination

Based on the simulation results, it is found that daytime indoor air temperature would reduce if thermal mass increased (i.e. 2,000 kg/m²). However, the increased thermal mass would raise nocturnal indoor air temperature. To overcome the increased nocturnal indoor air temperature, the ratio of opening area should be enlarged to maximize the amount of cool air from the outdoor enter the indoor space. It is obtained that there is no significant different in daytime indoor air temperature due to the different opening ratios (see Figure 5.26). Nevertheless, the window position should be further considered to reduce more indoor air temperature. As previously discussed, upper and lower window position significantly cool the building structures (i.e. walls, floor and ceiling) and effectively reduce indoor air temperature even during the daytime. As investigated in the additional simulations, changing window position would not significantly affect the indoor air temperature. However, changing window position would reduce indoor wind speed by more than half compared to the previous cases. This is important since some standards such as ASHRAE-55 allowed maximum indoor air

Table 5.10. Summary of the simulation results of indoor air temperatures and wind speeds for structural cooling (night ventilation) in the living room

Simulation cases	Air temperature		Wind speed	
	Daytime (°C)	Night-time (°C)	Daytime (m/s)	Night-time (m/s)
Case 01	31.0-31.2	27.3-27.5	1.14-1.15	0.02-0.03
Case 02	30.5-30.6	27.4-27.9	1.07-1.57	0.03-0.04
Case 03	30.8-31.0	26.8-27.1	1.10-1.16	0.02-0.03
Case 04	30.3-30.4	27.2-27.6	1.74-2.04	0.03-0.04
Case 05	31.1-31.2	25.8-26.2	2.86-4.04	0.03-0.04
Case 06	30.5-30.6	25.9-26.5	3.31-3.78	0.03-0.04
Case 07	30.8-30.9	25.8-26.1	2.83-3.29	0.04-0.05
Case 08	30.4-30.5	25.9-26.4	3.09-3.25	0.05-0.06
Case 09	31.1-31.2	26.8-27.1	1.61-1.83	0.03-0.04
Case 10	30.6-30.7	27.3-27.4	1.75-2.51	0.02-0.03
Case 11	30.8-31.0	26.0-26.3	1.71-1.81	0.02-0.03
Case 12	30.3-30.4	26.4-26.7	1.71-1.93	0.03-0.04
Case 13	31.1-31.2	25.9-26.2	2.89-3.48	0.04-0.05
Case 14	30.5-30.6	25.8-26.5	3.32-4.49	0.03-0.04
Case 15	30.9-31.0	25.0-25.5	2.82-3.69	0.03-0.04
Case 16	30.1-30.2	25.4-25.7	3.10-3.63	0.04-0.05
Case 17	31.1-31.3	27.4-27.6	0.18-0.28	0.02-0.03
Case 18	31.0-31.1	26.8-27.2	0.19-0.28	0.02-0.03
Case 19	31.0-31.1	26.2-26.5	0.36-0.59	0.03-0.04
Case 20	30.9-31.0	25.8-26.2	0.53-0.60	0.03-0.04
Case 21	30.8-30.9	26.3-26.6	0.21-0.40	0.02-0.03
Case 22	30.9-31.2	25.5-25.9	0.45-0.62	0.03-0.04
Case 23	30.8-30.9	25.4-25.7	0.36-0.55	0.03-0.04
Case 24	30.7-30.8	24.9-25.3	0.29-0.61	0.04-0.05

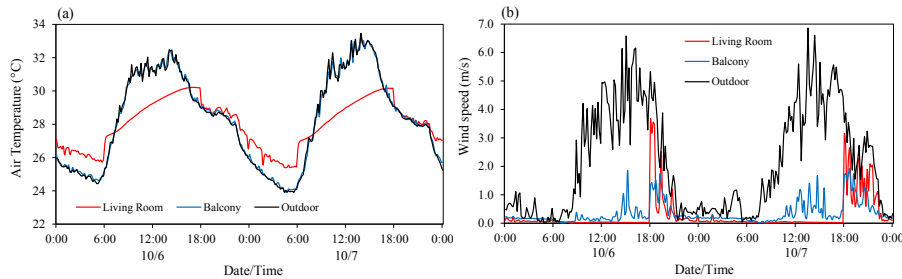


Figure 5.59. Profiles of (a) air temperature and (b) wind speed in indoor space and balcony in Case 16.

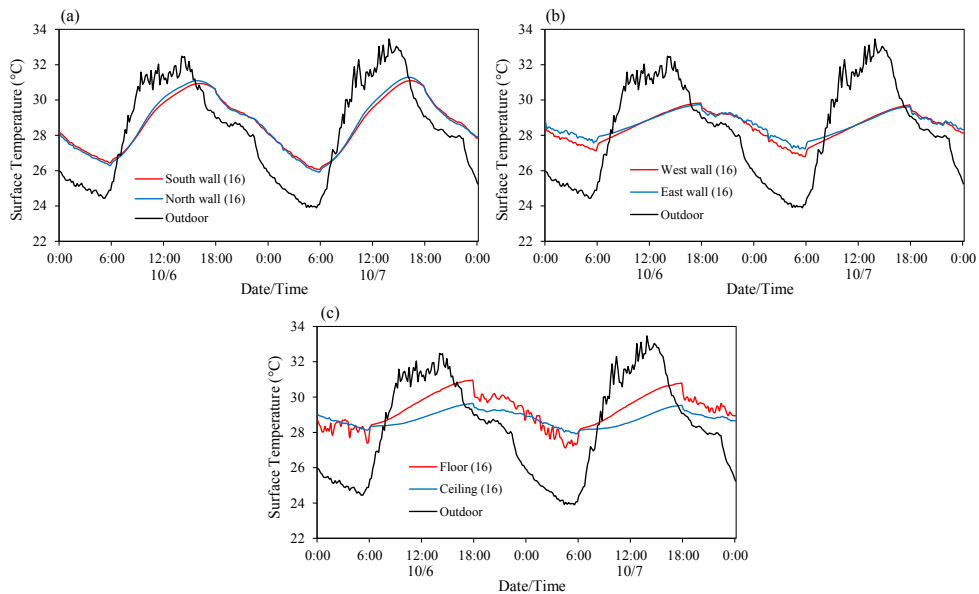


Figure 5.60. Profiles of surface temperatures of (a) south- and north-wall (b) west- and east-wall and (c) floor and ceiling in Case 16.

velocity up to 1.2 m/s. Furthermore, ceiling height should be considered to further optimize the indoor air temperature.

Tables 5.10 summarizes the simulation result of indoor air temperatures and wind speeds for each cases under night ventilation condition. From all the cases, the simulation results showed that Case 16 obtained the optimum results for combination of test cases. As shown in Table 5.8, Case 16 refer to the model applying thermal mass of 2,000 kg/m², ratio of opening area to floor area of 0.15, ceiling height of 5.0m, and upper/lower windows at back-side while maintaining central window at windward side (front-side or balcony side). Profiles of indoor air temperature and wind speed are presented in Figure 5.59, while Figure 5.60 show the profiles of surface temperature of walls, floor and ceiling. It is observed that the maximum indoor air temperature up to 30.1-30.2°C while the lowest indoor air temperature was around

of 25.4°C. Under same conditions (i.e. same opening ratio and thermal mass), these temperatures were slightly lower compared to those in 3.0m unit and central windows unit, which is around 0.3-0.4°C and 0.4°C lower respectively. But if compared to the 1,000-kg/m² unit, these temperatures are 0.8-0.9°C lower under the same conditions. As shown in Table 5.10, the unit with thermal mass of 2,000 kg/m² obtained relatively lower daytime indoor air temperature regardless of opening ratio and ceiling height, which is around 30.1-30.6°C. Moreover, enlarge the opening ratio even three times larger (i.e. 0.15) at thermal mass of 2,000 kg/m² only reduce the daytime indoor by 0.1-0.2°C. It means that thermal mass predominantly affecting the daytime indoor air temperature rather than other parameters. Interestingly, the reduction of daytime indoor air temperatures by the higher ceiling height and upper/lower windows is almost the same (0.2-0.4°C). Nevertheless, combination of those three parameters further reduce daytime indoor air temperature by 0.9-1.1°C. These findings agreed with the findings of Liping and Wong (2007). However, it should be noted that the maximum indoor wind speed when the window open was still quite high, which is around 3.10-3.63 m/s. Therefore, further ventilation strategies particularly window position should be further considered to optimize indoor wind speed into acceptable level of wind speed as required.

5.4.2 Comfort ventilation in the living room

Unlike previous simulation (Subsection 5.4.1), reducing SET* by increasing wind speed is the main objective of this Subsection. Therefore, the effects of ratio of opening area to the total floor area was investigated at the first step. Then, the effects ceiling height and windows position were further investigated under the same thermal mass. It should be noted that thermal mass used in this simulation referred to the previous results of simulation, which is 2,000 kg/m², since the unit with this thermal mass obtained relatively lower daytime indoor air temperature. The optimum combination of above parameters in obtaining optimum SET* are proposed. The total number of cases for comfort ventilation is 8 cases, and the detailed test cases are presented in Table 5.11. For this simulation, full-day ventilation was applied and the unit was facing south. Window position in Table 5.10 refer to the window position on the front-side (or balcony-side), while maintaining central window on the back side.

Table 5.11. Simulation cases for comfort ventilation in the living room

Simulation Cases	Thermal mass (kg/m ²)	Ratio of window area to floor area	Ceiling height (m)	Windows position	
				Front-side	Back-side
Case 25	2,000	0.05	3.0	Central	Central
Case 26	2,000	0.05	3.0	Upper/Lower	Central
Case 27	2,000	0.10	3.0	Central	Central
Case 28	2,000	0.10	3.0	Upper/Lower	Central
Case 29	2,000	0.05	5.0	Central	Central
Case 30	2,000	0.05	5.0	Upper/Lower	Central
Case 31	2,000	0.10	5.0	Central	Central
Case 32	2,000	0.10	5.0	Upper/Lower	Central

5.4.2.1 The effects of ratio of opening area to floor area

Simulation results for indoor air temperature and relative humidity at different ratio of opening area to floor area under full-day ventilation conditions are presented in Figures 5.61-62. As shown, daytime indoor air temperatures between two cases, i.e. ratio of opening area to floor area of 0.05 and 0.10, are almost same as the corresponding outdoor air temperature. This is simply because during the daytime, windows are open and therefore the indoor air temperature follow the outdoors regardless of ratio of opening area to floor area. Meanwhile, during nighttime, the larger opening ratio reduced the nocturnal indoor air temperature. It is observed that the differences of nocturnal indoor air temperature between the two cases were averagely around of 0.6-0.8°C for 3.0 m-ceiling height unit (Figure 5.61ab) and 0.3-0.4°C for 5.0m-ceiling height unit (Figure 5.61cd). In particular, increasing opening ratio would not

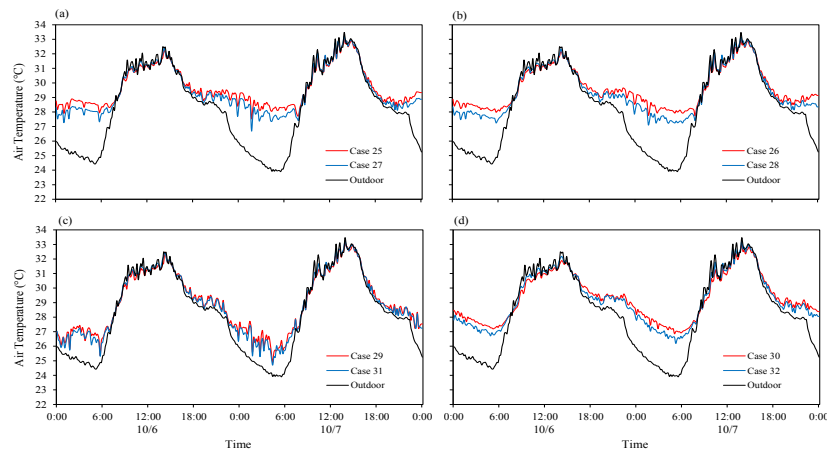


Figure 5.61. Comparison of indoor air temperature under different ratios of opening area to floor area for full-day ventilation condition.

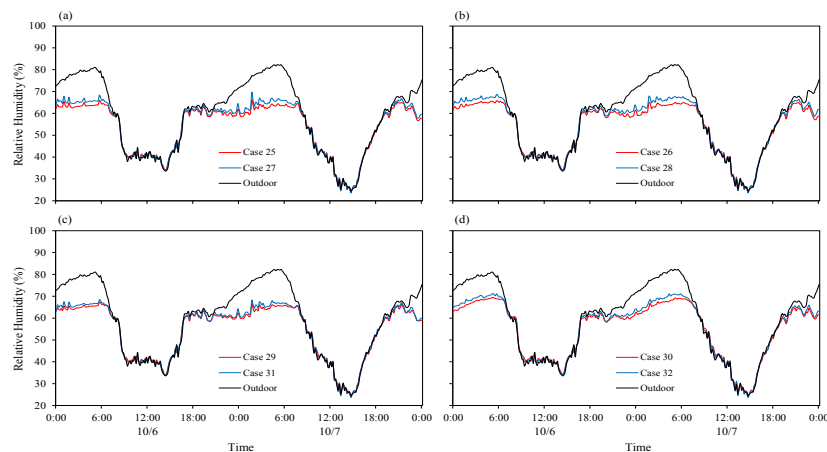


Figure 5.62. Comparison of indoor relative humidity under different ratios of opening area to floor area for full-day ventilation condition.

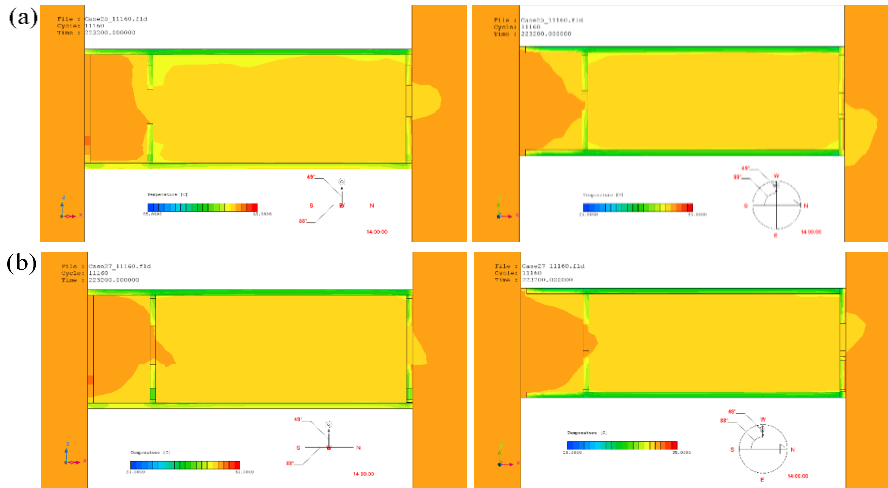


Figure 5.63. View of distribution of indoor air temperature (left: y-axis, right: z-axis at 1.1m) at opening ratios of (a) 0.05 and (b) 0.10 at the peak hour (14:00).

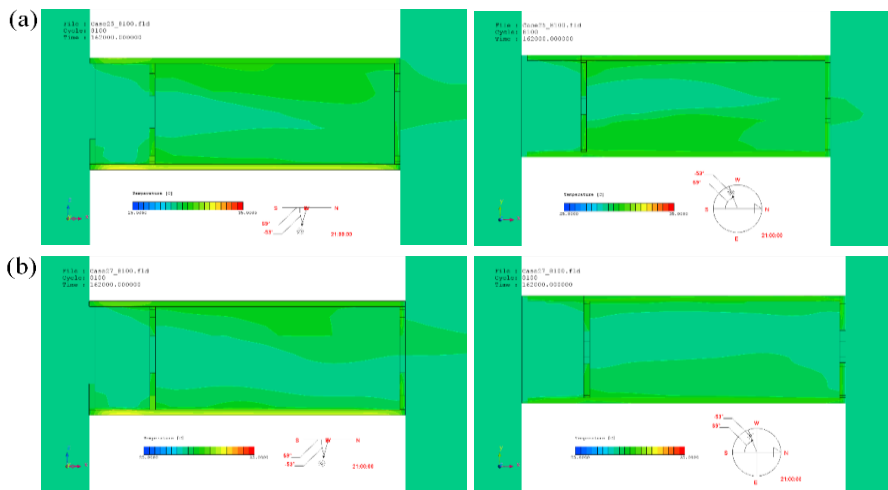


Figure 5.64. View of distribution of indoor air temperature (left: y-axis, right: z-axis at 1.1m) at opening ratios of (a) 0.05 and (b) 0.10 at the night-time (21:00).

significantly affect the indoor air temperature when central windows are used at the both sides and the ceiling height is 5.0m (Figure 5.61c). As can be found in night ventilation results, it is also shown that applying upper/lower window at the same opening ratio (0.10) would further increase this discrepancy (Figure 5.61bd). Further discussions on the effects of window position are presented in the next Subsection. As shown in Figure 5.62, relative humidity between two cases were not significantly different. Regardless of ceiling height, it is obtained that relative humidity at opening ratio of 0.05 was around 24-70% while that at opening ratio of 0.10 was around of 24-71%.

Furthermore, Figures 5.63-64 present view of indoor air temperature profiles for full-day ventilation under different ratio of opening area to floor area at daytime and night-time, respectively. As previously described, the indoor air temperatures during peak hours were not significantly different between two cases. As shown, the distribution of indoor air temperature at y-axis and z-axis between the two cases are almost same. Meanwhile, area with the cooler air was largely seen in the case with larger opening area (Figure 5.64). This cool air was caused by the air movement from the outdoor through the windows. The warmer air was seen around the building envelopes (walls, floor and ceiling) at the both cases.

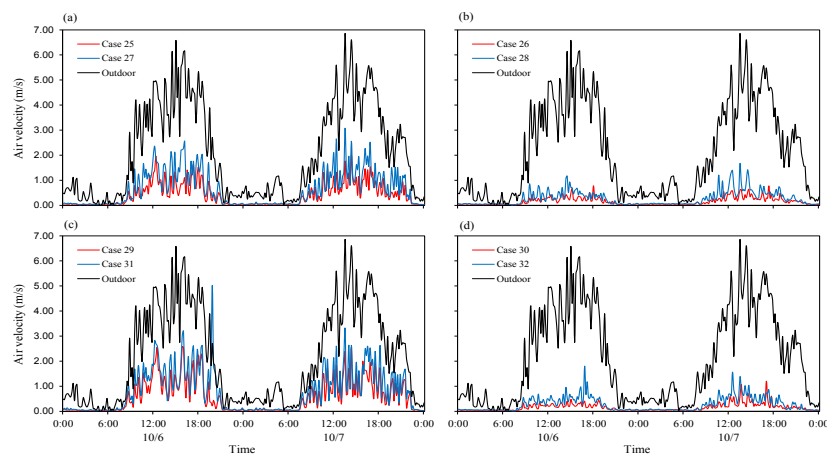


Figure 5.65. Comparison of indoor air temperature under different ratio of opening area to floor area for full-day ventilation condition.

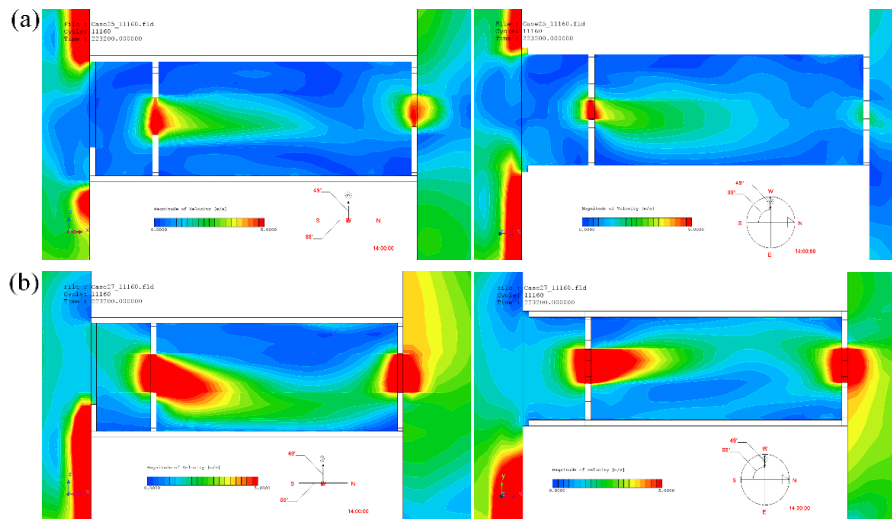


Figure 5.66. View of wind flow pattern (left: y-axis, right: z-axis at 1.1m) at opening ratios of (a) 0.05 and (b) 0.10 at the peak hour (14:00).

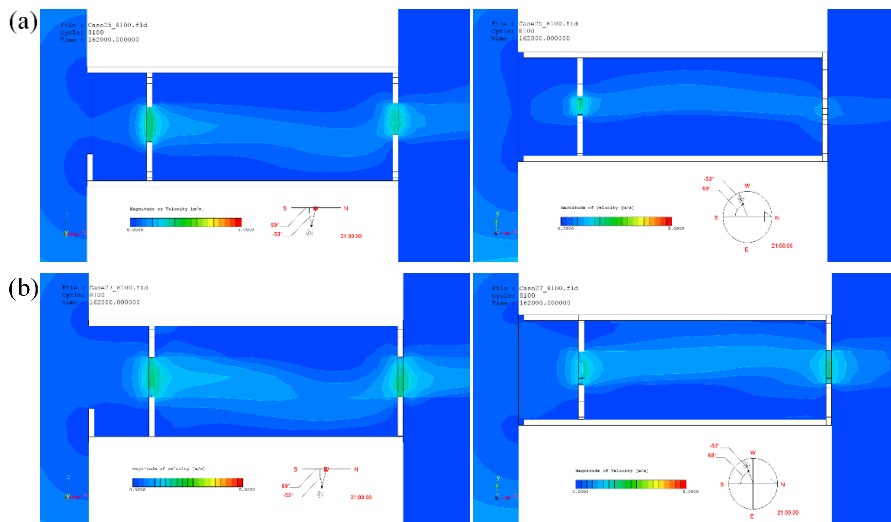


Figure 5.67. View of wind flow pattern (left: y-axis, right: z-axis at 1.1m) at opening ratios of (a) 0.05 and (b) 0.10 during night-time (21:00).

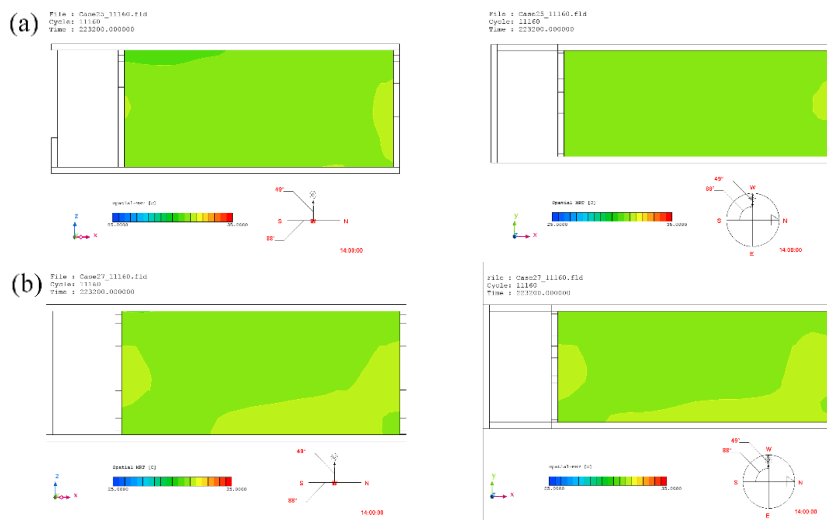


Figure 5.68. View of MRT values (left: y-axis, right: z-axis at 1.1m above floor) at opening ratios of opening area to floor area of (a) 0.05 and (b) 0.10 at the peak hour (14:00).

Figure 5.65 show the indoor wind speed between two cases. As indicated, indoor wind speed profiles at opening ratio of 0.10 was averagely 0.25-0.35 m/s higher than that at opening ratio of 0.05 particularly during the daytime regardless of ceiling height. It is obtained that for applying central windows at both sides, the maximum indoor wind speeds at opening ratio of 0.05 and 0.10 were around of 2.01-2.58 m/s and 3.08-3.30 m/s regardless of ceiling height. This increasing is not as high as that when the opening ratio is 0.15 (see Subsection 5.4.1.2).

Figures 5.66-67 illustrate the distribution of wind speeds (y-axis and z-axis) between the two cases at daytime and night-time respectively. As shown in Figure 5.66, location near the windows showed the higher wind speed rather than other area, and the unit with the larger opening area obtained higher wind speed than that with the smaller opening area. Nevertheless, the wind flow patterns at the two cases were not significantly different during the night-time (see Figure 5.67).

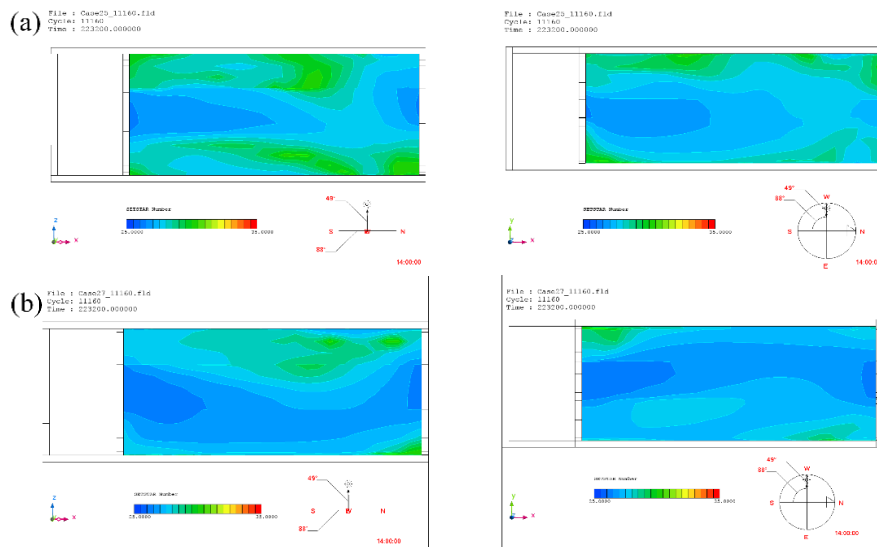


Figure 5.69. View of SET* patterns (left: y-axis, right: z-axis at 1.1m above floor) at opening ratios of (a) 0.05 and (b) 0.10 at the peak hour (14:00).

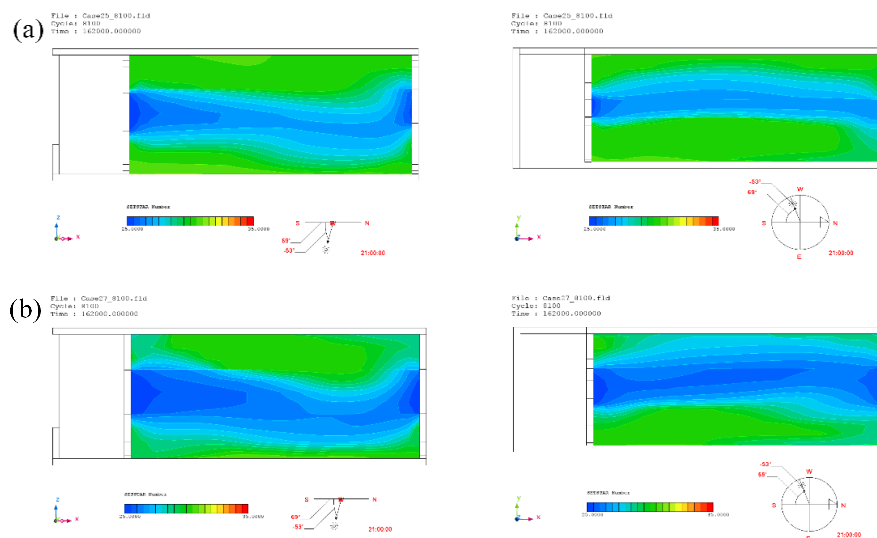


Figure 5.70. View of SET* pattern (left: y-axis, right: z-axis at 1.1m above floor) at ratio of opening area to floor area of (a) 0.05 and (b) 0.10 at the night-time (21:00).

Since the main target of this simulation is to evaluate thermal comfort due to increasing wind speed (i.e. comfort ventilation) particularly during the daytime, then the evaluation of SET* is important. Since the MRT as well as SET* could not output in STREAM as *Time Series*, then the evaluation of SET* was conducted by using two dimensional views of distribution of SET* values. Figure 5.68 shows the profiles of MRTs between two different opening ratio while Figures 5.69-70 present the profiles of SET* values and comparison of them under different opening ratio at daytime and night-time respectively. SET* were calculated under assumption of sedentary work (1 *met*), typical clothing values for tropics which is around of 0.40 (Feriadi, 2004), constant atmospheric pressure of 760 mmHg, and body weight of 70 kg. As shown, MRT in the room with opening ratio of 0.05 during peak hours were ranged from 30.0-31.0°C, and mostly received around of 30.5°C (Figure 5.68a). When the opening ratio increased, the area with higher MRT (31.0°C) increased as well mostly at around the openings (Figure 5.68b). It implies that enlarging opening ration would increase the MRT values as well mostly due to the larger solar radiation enter the room through the openings. Nevertheless, if wind speed is taken into account to thermal comfort evaluation using SET* values, it is obtained that increasing ratio of opening area to floor area would reduce SET* values. It is also found that the area with lower SET* are also found to be larger at room with larger opening ratio (Figure 5.69). Figure 5.69 also showed that that range of SET* values at both cases were relatively same, around 25.5-29.5°C. These values also showed the same as those at the night-time (see Figure 5.70). Compared to the profile of wind flow pattern (Figures 5.66-67), the profile of SET* showed strong correlation with the wind flow. This clearly implies that the higher wind speed, the lower of SET* values would be. The difference lied on the distribution patterns of the SET* in the room.

5.4.2.2 The effects of ceiling height

Simulation results for indoor air temperature and relative humidity under full-day ventilation conditions at different height are presented in Figures 5.71-72. As previous results, daytime indoor air temperatures between two cases showed no significantly difference results due to the air infiltration during the daytime. Meanwhile, during nighttime, the higher ceiling height unit obtained relatively lower indoor air temperature. The discrepancy between two cases increased when the upper and lower windows are applied at the both sides (see Figure 5.71ac). At the 5.0m-ceiling height unit, the minimum indoor air temperature was around of 27.0-27.1°C for applying central windows and 26.3-26.8°C when applying upper/lower windows at front side. This is because more thermal stratification were formed at the higher ceiling height rather than at the lower ceiling height; thus maintained cool air at occupied level (1.1m above floor) and the hot air went to upper part of the unit. However, the effects of ventilative cooling during the night-time diminished by air infiltration during the daytime. Regardless of opening ratio and window position, relative humidity at ceiling height of 3.0m and 5.0m were around 24-70% and 24-71% respectively. Furthermore, Figure 73 shows view of indoor air temperature profiles for full-day ventilation under different ceiling height at daytime. As shown, during the peak hours, the profiles of indoor air temperature at the two cases, i.e. ceiling height of 3.0m and 5.0m, were not significantly different.

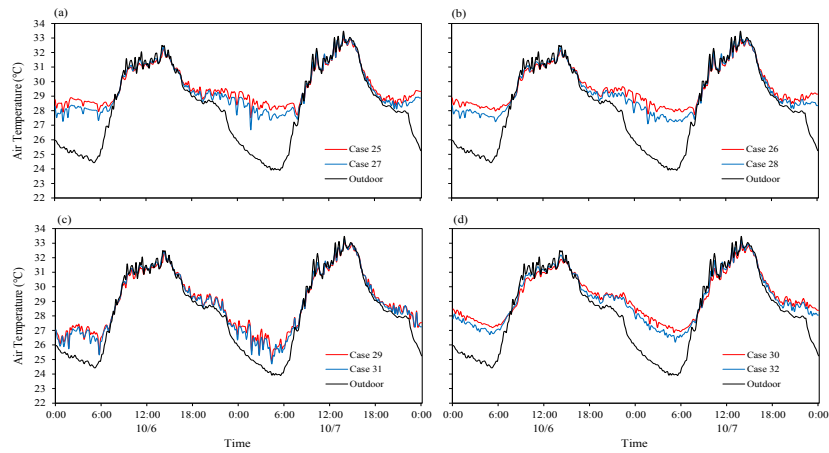


Figure 5.71. Comparison of indoor air temperature under different ceiling heights for full-day ventilation condition.

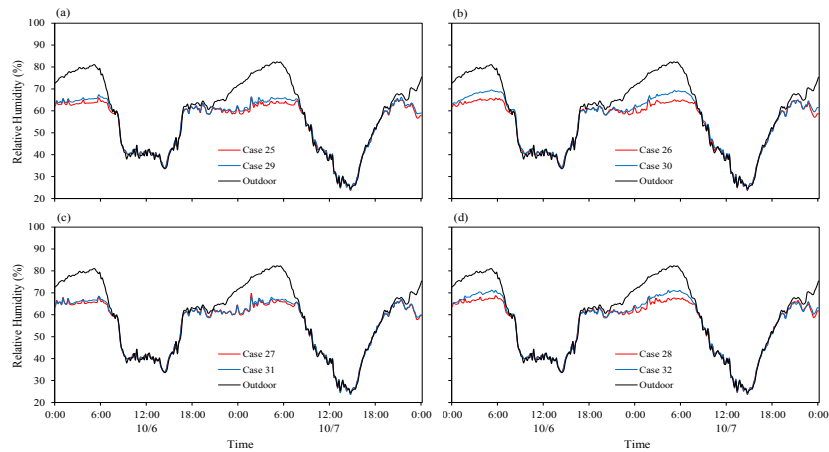


Figure 5.72. Comparison of indoor relative humidity under different ceiling heights for full-day ventilation condition.

Figure 5.74 show the indoor wind speed between two cases during the peak hours. It is shown that indoor wind speed profiles at both cases were not significantly different regardless of window position. The unit with ceiling height of 5.0m obtained averagely of 0.15-0.2 m/s higher wind speed than the 3.0m-ceiling height unit. Maximum indoor wind speed at the 3.0m-ceiling height unit was around of 2.01-3.08 m/s for using central windows at both sides and around of 0.78-1.68 m/s for using upper/lower window at front side. Meanwhile, at the 5.0m-ceiling height unit, the maximum indoor wind speeds were around of 2.58-3.30 m/s and 1.21-1.81 m/s for applying central windows and upper/lower windows respectively. Further profiles of indoor wind speed under different ceiling height at daytime and night-time respectively are shown in Figures 5.75. As indicated, a relatively higher wind speed was seen mainly in

between two openings and situated at the lower part of unit. Unlike the 3.0m-ceiling height unit, the air flow only at the lower part of unit while there is almost no wind flow at the upper part.

Figures 5.76-77 present the profiles of MRT and SET* values and its comparison under different ceiling height at the peak hours. As shown, a relatively large area of higher MRT values (around of 31.0°C) are found around the external wall particularly in the back-side of unit with ceiling height of 5.0m. This is because the external wall received solar radiation from the outdoors, and the higher the ceiling height, the larger area of receiving solar radiation. Moreover, the area with MRT value at back side was larger than that at front side due to the

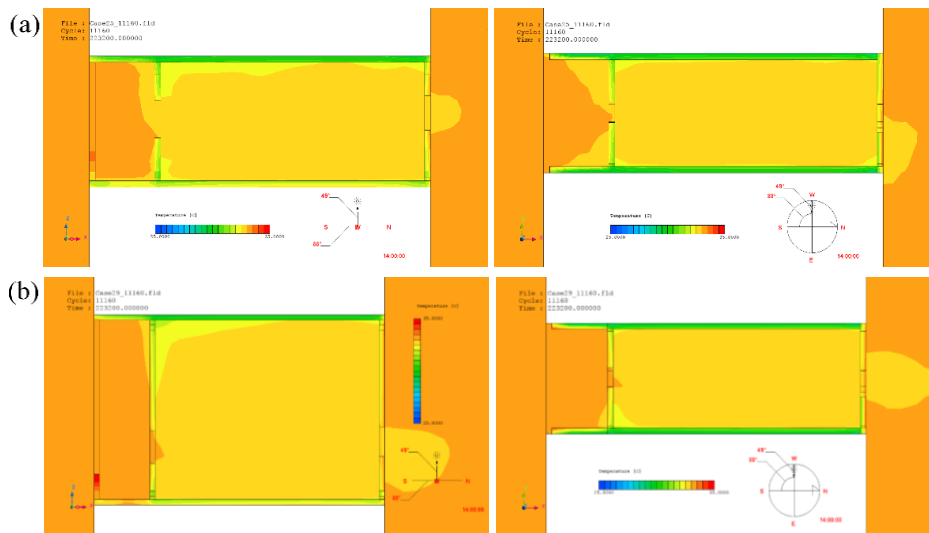


Figure 5.73. View of distribution of indoor air temperature (left: y-axis, right: z-axis at 1.1m) at ceiling heights of (a) 3.0m and (b) 5.0m at the peak hour (14:00).

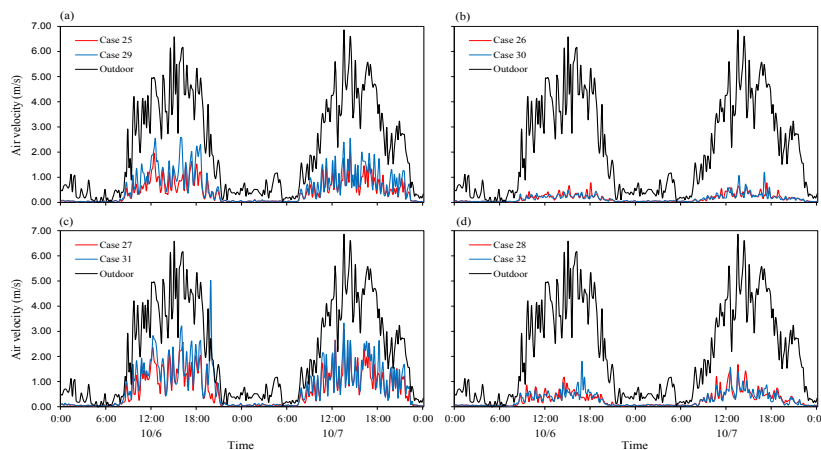


Figure 5.74. Comparison of indoor wind speed under different ceiling heights for full-day ventilation condition.

existence of balcony at the front-side (Figure 5.76b). Nevertheless, the MRT value of 30.5°C occupied the largest portion of area at the both cases. If wind speeds are taken into account for thermal comfort evaluation, it is obtained that at occupied levels, the SET* values ranged from 25.5°C to 27.5°C during the peak hours. Meanwhile, the SET* values at the upper part of unit ranged from 28.0°C to 30.0°C. At the unit with ceiling height of 5.0m, the higher SET* values occupied the larger area (Figure 5.77b). As the previous cases, this results also clarified the strong relationship between wind speed flow pattern and the distribution of SET* values in the room. The stronger wind speed, the SET* values would be lower.

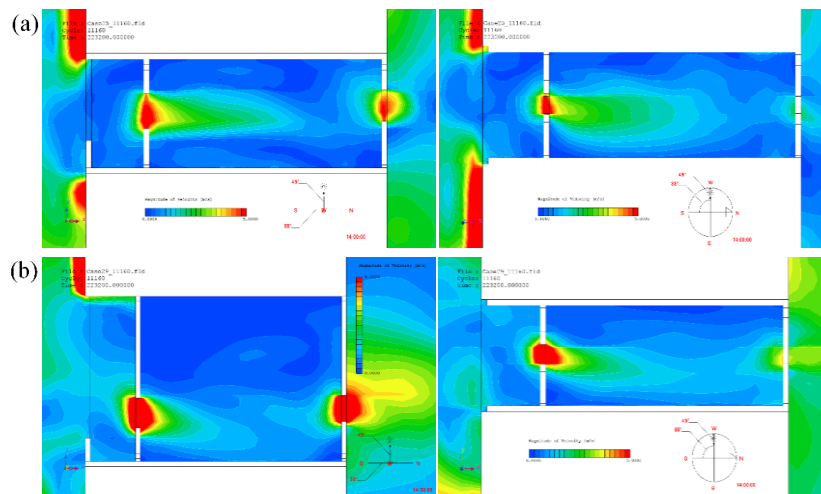


Figure 5.75. View of wind flow pattern (left: y-axis, right: z-axis at 1.1m) at ceiling heights of (a) 3.0m and (b) 5.0m at the peak hour (14:00).

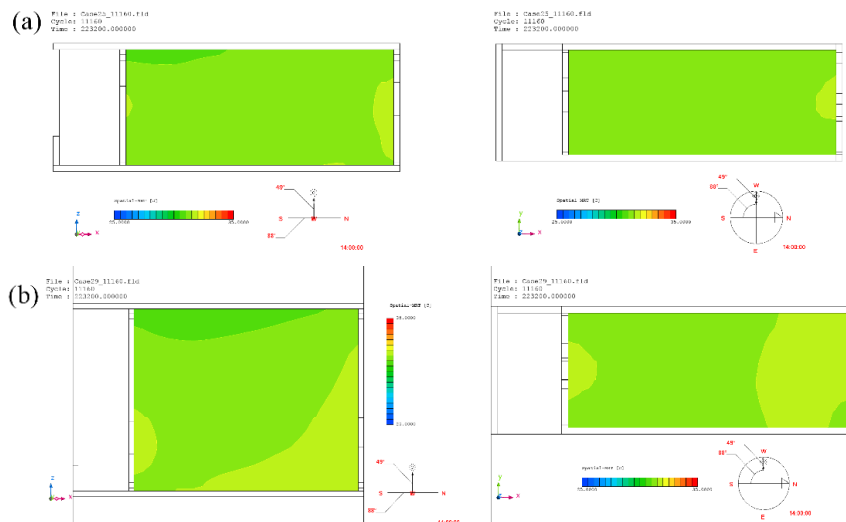


Figure 5.76. View of MRT values (left: y-axis, right: z-axis at 1.1m above floor) at ceiling heights of (a) 3.0m and (b) 5.0m at the peak hour (14:00).

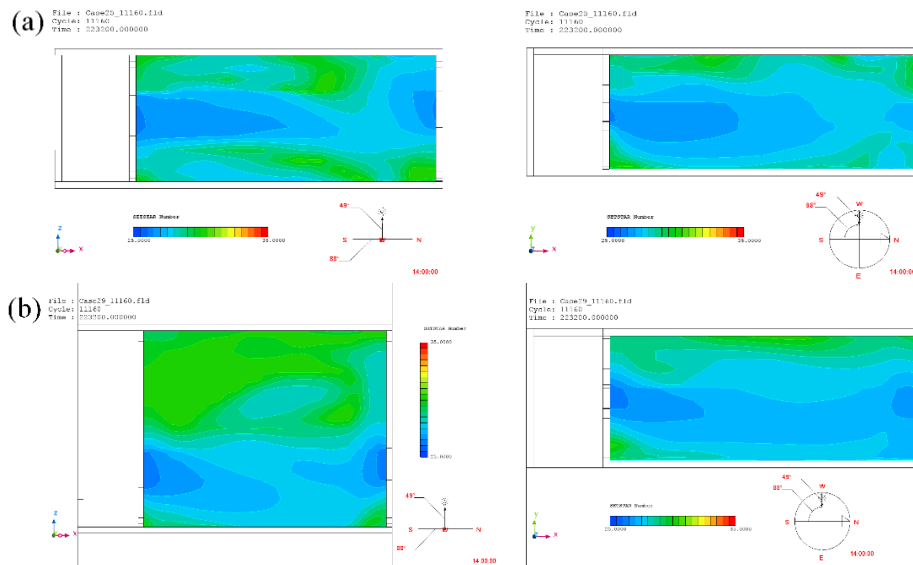


Figure 5.77. View of SET* values (left: y-axis, right: z-axis at 1.1m above floor) at ceiling heights of (a) 3.0m and (b) 5.0m at the peak hour (14:00).

5.4.2.3 The effects of window position

As previous cases, window position was not significantly affecting to indoor air temperature particularly during the daytime (see Figure 5.780) for the same reasons; solar radiation. Meanwhile, slightly difference can be found during night-time. When the ceiling height increased to 5.0m, the discrepancy of nocturnal indoor air temperature between two cases become slightly larger (Figure 5.78ac). Further decreasing was obtained when the ratio of opening area to floor area increased at the same time. As implied, the differences of indoor air temperature between two cases at the night-time for respective ceiling heights (i.e. 3.0m and 5.0m) were around of 0.2-0.3°C and 0.6-0.8°C. Figure 5.79 shows simulation results of indoor relative humidity under different window positions. It is obtained that the relative humidity ranged from 24% to 70% when the central windows are employed at the both sides and ranged from 24% to 73% when upper/lower windows are employed at the front sides. Further presentation of indoor air temperature profiles during the daytime are visualized in Figure 5.80. As shown, the profiles of indoor air temperature distribution between two cases are almost same. At the peak hours (14:00), the largest portion of area was around 33.0°C.

Figure 5.81 show the indoor wind speed between the two different window positions. The relatively large difference in indoor wind speed can be found when the window position is different. When the central windows applied on the both sides, the maximum indoor wind speed reached up to 2.01-3.08 m/s with the average of 0.63-0.99 m/s during the daytime (06:00-18:00). Meanwhile, the indoor wind speed decreased up to 0.78-1.68 m/s at the daytime with the average of 0.18-0.48 m/s. The profiles of indoor wind speed under different opening

positions can be seen further in Figure 5.82. As indicated, largely difference in indoor wind flow pattern could be seen between two cases. Unlike the central windows, distribution of higher wind speed are seen at the upper and lower parts of unit as well as at the back window, while relatively lower wind speed are largely found at the middle of unit.

Figures 5.83-84 present the profiles of respective MRT and SET* values and its comparison under different window positions at the peak hours. Unlike the previous results, the area with higher MRT values are found to be larger at the unit with the central windows rather than at the unit with upper/lower window (see Figure 5.83). As the profiles of wind speed, the SET* values at the occupied level in the unit with upper/lower windows showed relatively higher (Figure 5.84). As shown, the SET* values in the first unit, i.e. unit with central windows, ranged from 25.5-27.5°C, while those in the second unit ranged from 28.0-30.0°C. Moreover, a relatively lower SET* are mostly found at the upper and lower part of the second unit.

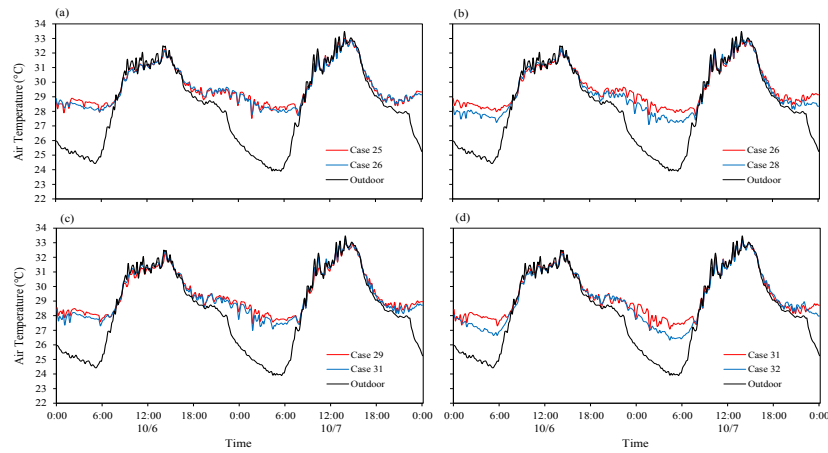


Figure 5.78. Comparison of indoor air temperature under different window positions for full-day ventilation condition.

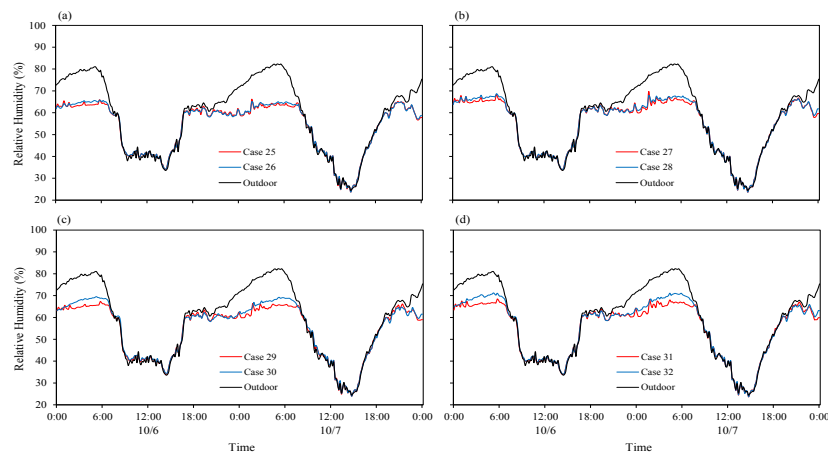


Figure 5.79. Comparison of indoor relative humidity under different window positions for full-day ventilation condition.

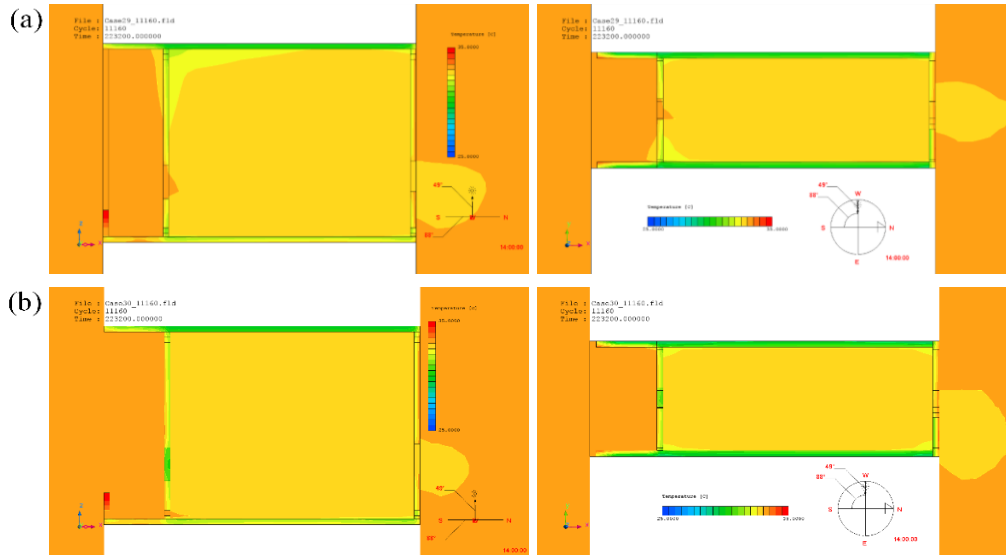


Figure 5.80. View of distribution of indoor air temperature (left: y-axis, right: z-axis at 1.1m) in the unit with (a) central windows and (b) upper/lower windows at the peak hour (14:00).

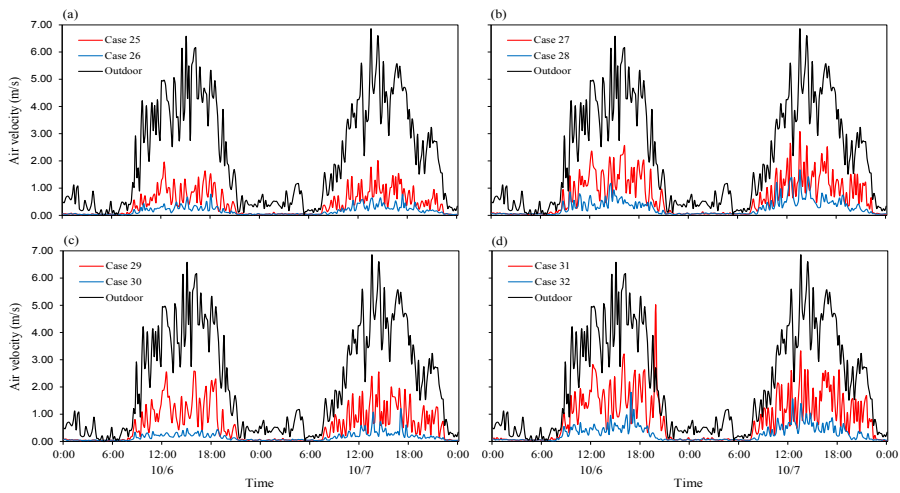


Figure 5.81. Comparison of indoor wind speed under different window positions for full-day ventilation condition.

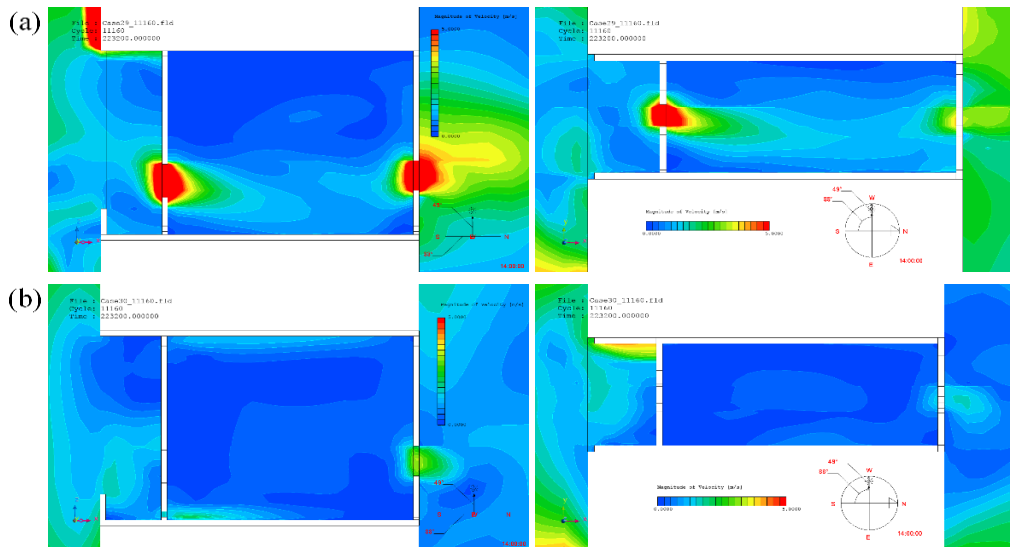


Figure 5.82. View of wind flow pattern (left: y-axis, right: z-axis at 1.1m) in the unit with (a) central windows and (b) upper/lower windows at the peak hour (14:00).

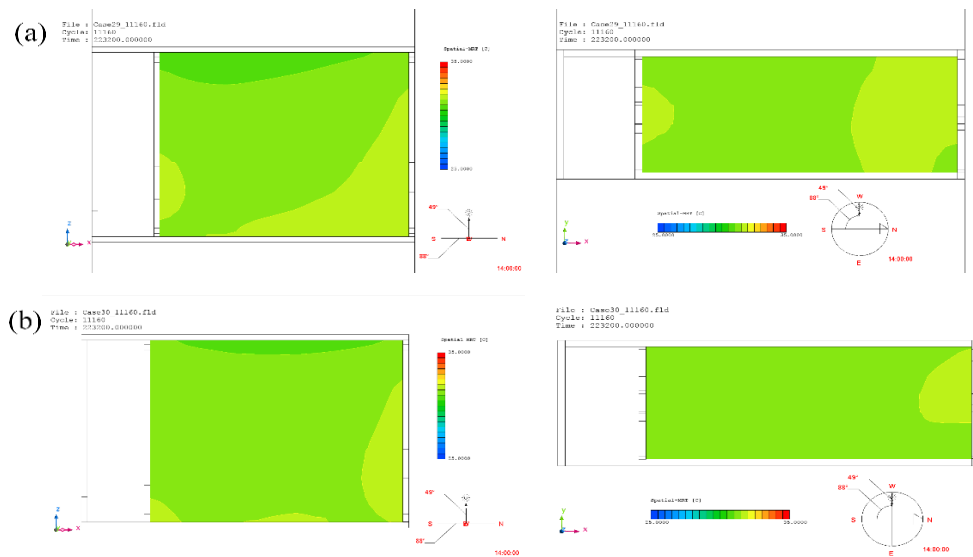


Figure 5.83. View of MRT values (left: y-axis, right: z-axis at 1.1m) in the unit with (a) central windows and (b) upper/lower windows at the peak hour (14:00).

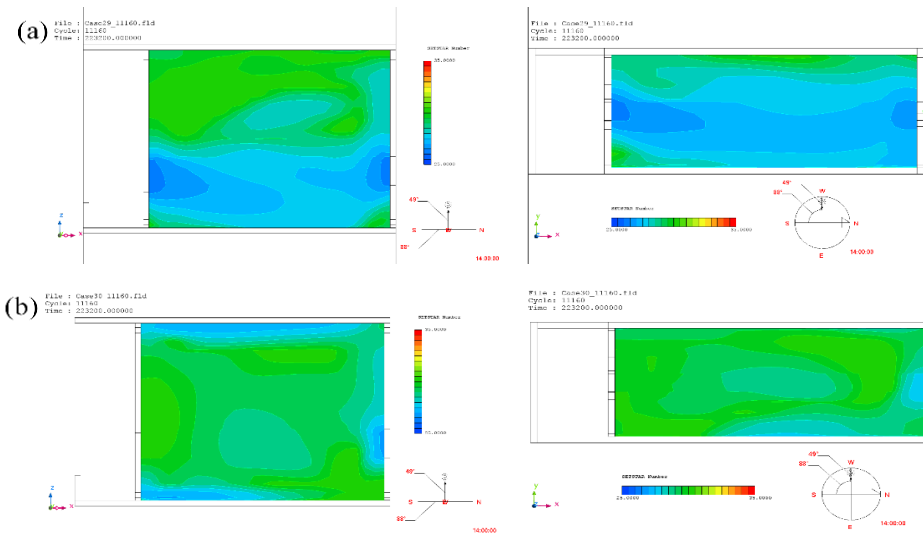


Figure 5.84. View of wind flow pattern (left: y-axis, right: z-axis at 1.1m) in the unit with (a) central windows and (b) upper/lower windows at the peak hour (14:00).

5.4.2.4 Optimum combination

Based on the simulation results, it is obtained that daytime indoor air temperature tend to follow the corresponding outdoors and therefore, had same values as the corresponding outdoor regardless of the ratio of opening area to floor area, ceiling height and window position. It implies that under full-day ventilation condition, applying all the parameters (i.e. opening ratio, ceiling height and window position) did not significantly affect the indoor air temperature at daytime. Moreover, these techniques significantly lower the nocturnal indoor air temperature. However, these effects were diminished by air infiltration during the daytime. Meanwhile, the significant results was found in the profile of wind speed particularly when the different window positions are applied.

Since the main purpose of this evaluation is to obtain optimum SET* value for comfort ventilation, therefore evaluation was carried out by using SET* particularly during the daytime (peak hours). Unfortunately, up to date, the standard of thermal comfort particularly for hot-humid climate regions using SET* values as thermal comfort index are still not exist yet. Gagge *et al.* (1971) for instance, proposed particular thermal conditions (such as comfortable, comfortably cool, comfortably warm, uncomfortable and so on) for particular SET* values. However, this categorization was not used in this evaluation. Nevertheless, based on the simulation results, it is obtained that by employing central windows and increasing window opening ratio to floor area would significantly increase wind speed, and therefore lower the SET* values. Therefore, after comparing the profiles of SET* particularly during peak hours, it is found that the unit with ratio of opening area to floor area of 0.10 and employing central windows at the both sides would enjoy lower SET* values regardless of ceiling height (see Figures 5.69b and 5.85b for comparison).

Table 5.12 Summary of the simulation results of indoor air temperatures, relative humidity and wind speeds for comfort ventilation (full-day ventilation) in the living room.

Simulation cases	Air temperature		Relative Humidity		Wind speed	
	Daytime (°C)	Night-time (°C)	Daytime (%)	Night-time (%)	Daytime (m/s)	Night-time (m/s)
Case 25	32.3-33.0	27.5-27.9	24-34	66-67	1.96-2.01	0.02-0.03
Case 26	32.2-32.9	27.8-28.0	24-34	65-66	0.78-0.79	0.03-0.04
Case 27	32.4-33.2	26.7-27.3	24-34	68-70	2.54-3.08	0.03-0.04
Case 28	32.3-33.2	27.1-27.3	24-34	68-69	1.17-1.68	0.03-0.04
Case 29	32.3-33.0	27.4-27.6	24-34	66-67	2.56-2.58	0.02-0.03
Case 30	32.0-33.0	26.9-27.1	24-34	69-70	0.48-1.21	0.03-0.04
Case 31	32.4-33.3	27.0-27.1	24-34	68-69	3.19-3.30	0.03-0.04
Case 32	32.3-33.2	26.3-26.4	24-34	71-72	1.57-1.81	0.04-0.05

Table 5.13 Summary of the simulation results of indoor MRT, PMV and SET* for comfort ventilation (full-day ventilation) in the living room.

Simulation cases	MRT		PMV		SET*	
	Daytime (°C)	Night-time (°C)	Daytime	Night-time	Daytime (°C)	Night-time (°C)
Case 25	30.5-31.5	30.0-30.5	1.5-2.5	0.5-2.5	26.0-30.0	26.5-30.5
Case 26	30.5-31.0	29.5-30.0	2.0-2.5	1.5-2.5	27.0-30.0	30.0-30.5
Case 27	30.5-31.0	29.5-30.0	2.0-2.5	0.0-1.5	27.0-30.5	26.0-29.5
Case 28	30.0-30.5	30.0	2.0-2.5	0.5-1.5	27.5-30.0	30.0-30.0
Case 29	30.5-31.0	30.0	2.0-2.5	0.5-1.5	26.0-29.0	26.0-30.5
Case 30	31.0-31.5	30.0-30.5	2.0-2.5	1.5-2.5	27.5-30.0	30.0-30.5
Case 31	31.0-32.0	30.0-30.5	2.0-2.5	0.0-1.5	26.5-31.0	26.0-29.5
Case 32	31.0-32.0	30.0-30.5	2.0-2.5	1.0-1.5	27.5-30.0	30.0-31.0

Tables 5.12 summarizes the simulation result of indoor air temperatures, relative humidity and wind speeds for each cases under full-day ventilation condition while Tables 5.13 presents the simulation results of Mean Radiant Temperature (MRT), Predicted Mean Vote (PMV) and Standard Effective Temperature (SET*) under the same ventilation condition. As indicated, daytime indoor air temperatures and relative humidity are generally not difference between cases (Table 5.12). As previously discussed, the wind speed reduced to half during the peak hours when the upper/lower windows are applied in the front-side while maintaining central windows in the rear side. When the ceiling height is 5.0m, these wind speeds even reduced more than half. As shown in Table 5.13, MRT values between daytime and night-time are not significantly difference in all cases. The slightly larger difference could be seen in the unit with thermal mass of 2,000 kg/m² mostly due to the thermal mass effects. Meanwhile, the PMV values at the daytime ranged from 2.0 to 2.5 (or between warm to hot) in all cases. Furthermore, Table 5.13 clearly indicated the effects of wind speed in reducing SET*. When the central windows are applied, the SET* values are almost the same between the daytime and night-time. The difference lies on the distribution pattern of SET* as previously shown.

In contrast, the SET* values at nighttime obtained higher values than those at daytime simply because relatively low wind speed at the night-time.

From all the cases, the simulation results showed that the lowest SET* values obtained when the central windows with larger opening ratio are applied in both sides. It is shown that the SET* values ranged from 26.5°C to 30.0°C. Figure 5.85 illustrates the profiles of SET* values at the 5.0m-ceiling height unit with central windows and opening ratio of 0.10. As indicated in both figures, the lower SET* values occupied larger area in the room particularly at the occupied level (1.1m above floor level). Therefore, during this period, occupants could enjoy evaporative cooling due to the increasing wind speed. Nevertheless, in the case of 5.0m-ceiling height unit, a relatively higher MRT values (around of 33.5°C) could be seen around the back central-window (Figure 5.85a). However, it should be noticed that the wind flowing in to the room at the daytime is still relatively quite high (2.0-3.0 m/s), and therefore it should be further considered in the design of window.

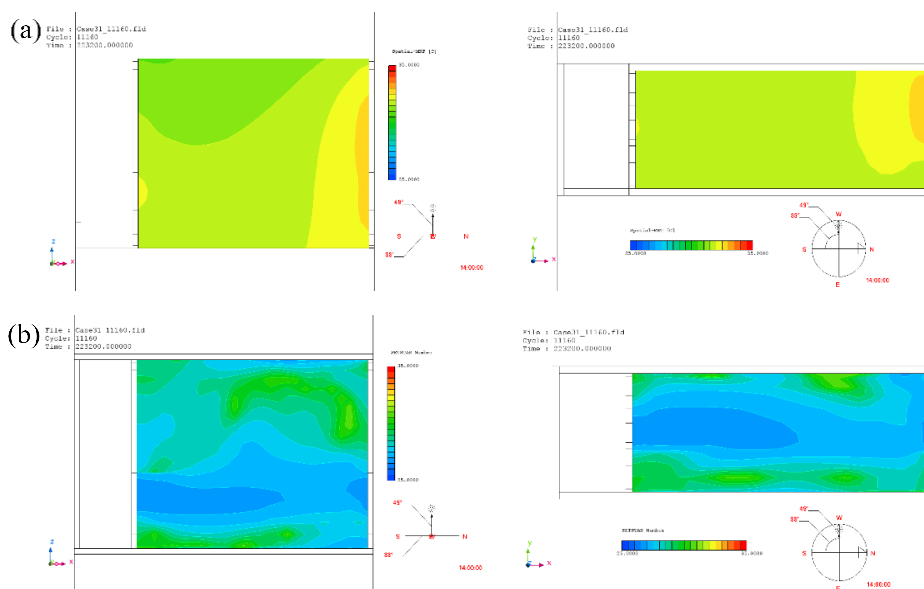


Figure 5.85. Views of (a) MRT and (b) SET* values (left: y-axis, right: z-axis at 1.1m) in the unit with central windows at both sides, opening ratio of 0.10 and ceiling height of 5.0m.

5.5 Results: Air-conditioned conditions

5.5.1 Effect of structural cooling

Figure 5.86 shows simulation results for the cooling load of master bedroom under different combination of ventilation conditions. As previously described, current practices of the occupants in middle-class apartments in Indonesia is applying daytime ventilation for both

master bedroom and living room (Case 1 in Table 5.6). As shown, daily cooling load for current condition was around 11.79 MJ, 0.01 MJ lower than that of when no ventilation applied for both rooms. Among all cases, the relatively lower total cooling loads were obtained when daytime ventilation and no ventilation conditions were applied in the master bedroom, i.e. Cases 3-6, while night cooling (i.e. night ventilation or full-day ventilation) was applied in the adjacent room (living room). These conditions obtained total cooling load around of 11.42-11.51 MJ/day, or 0.28-0.37 MJ/day lower than that of current practices. It should be noted that the difference between daytime and no ventilation conditions in master bedroom were 0.06-0.08 MJ/day.

Moreover, when night ventilation were employed in the living room (Case 5), the difference in cooling load was slightly small, around 0.02 MJ/day lower than that of full-day ventilation (Case 3). This difference due to the sensible cooling load, while latent cooling load remained constant. When night cooling was employed, the sensible cooling loads in master bedroom were much lower (0.26-0.32 MJ/day lower) compared to other ventilation conditions in the living room, i.e. daytime ventilation and no ventilation condition. This implies that applying night cooling in the living room reduces sensible cooling load in master bedroom.

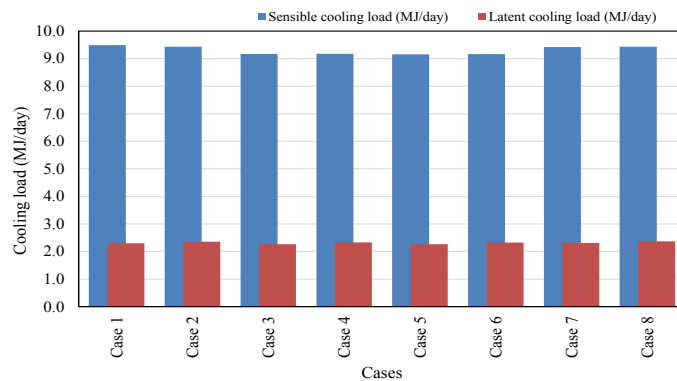


Figure 5.86. Cooling load in master bedroom under different combination of ventilation conditions of master bedroom and living room.

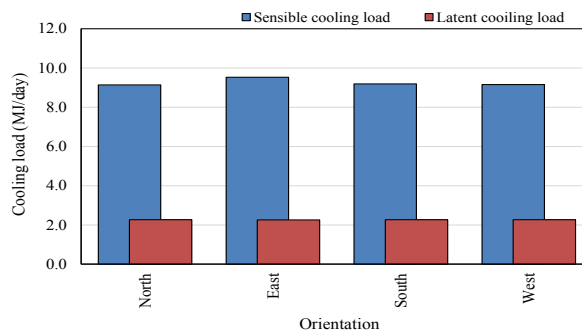


Figure 5.87. Cooling load in master bedroom under different orientations.

Furthermore, compare to above cases (Cases 3 and 5), latent cooling loads in master bedroom increased by 0.6-0.7 MJ/day when no ventilation condition applied in master bedroom (Cases 4 and 6) regardless of ventilation conditions in the living room. This is most probably due to the higher humidity level in the master bedroom rather when no ventilation applied. When daytime ventilation applied in the master bedroom, there is air change between the room and the outdoor at the daytime. Therefore it reduces the humidity although it increases the indoor air temperature as the consequences. This implies that applying daytime ventilation for master bedroom reduces its latent cooling load.

Figure 5.87 presents the simulation results for Case 5 under different orientations. West-facing orientation was the base model. As shown, there is almost no difference between north-facing and the base model. North-facing orientation had 0.01 MJ/day lower total cooling load than the base model. Meanwhile, south-facing orientation obtained the highest total cooling load. Nevertheless, latent cooling load in all orientations were remain no change (2.26 MJ/day). This implies that orientation do not effect on the latent cooling load. The simulation results indicates that Case 5 with north-facing had the lowest cooling load compared to other cases, and therefore, it will be used as base model for the next simulation.

5.5.1.1 Insulation

Insulation was applied internally and externally. Internal insulation was applied in the inside of master bedroom's wall (Figure 5.88a) while the external wall was installed in the outside of external wall of master bedroom (Figure 5.88b). The thermal conductivity of insulation installed was 0.025 W/m.K. Figure 5.89 presents the results of simulation for case application of insulation. As shown, applying insulation material at outside of external wall increased total cooling load by 9.4% compared to base case. Increasing of the latent cooling load was not significant, around 0.01 MJ/day. This increasing is caused by the heat that stored in the building structures through convection during the daytime could not emitted to the outdoor during the night time. Although external insulation prevents heat transfer through

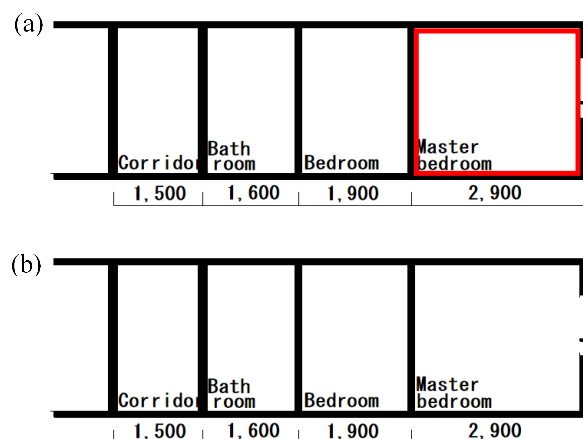


Figure 5.88. Installation of (a) internal insulation and (b) external insulation.

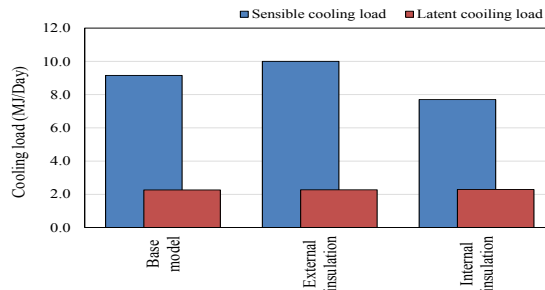


Figure 5.89. Simulation results of cooling load for insulation applications in master bedroom.

conduction during the daytime, but it also prevents heat releasing to the outdoor during night-time. Instead, the heat emitted to the indoor space during the night time and it causes the cooling load increasing during the utilization of air-conditioner.

In contrast, when internal insulation installed, the total cooling load in master bedroom reduced by 12.5% from the base model. Total of cooling load in this case was averagely 9.99 MJ/day. This is because internal insulation prevented heat entering indoor space through conduction and stored in the building structures through convection during the daytime. In addition, by installing insulation materials internally, the heat is enable to be emitted to the outdoors during night-time. Although sensible cooling load decreasing, the latent cooling load was slightly increasing (averagely of 0.02 MJ/day). This is most probably due to the ability moisture absorption by the building structures was reduced by the insulation material.

5.5.1.2 Ceiling height

Figure 5.90 shows the average cooling load of master bedroom under different ceiling heights. Ceiling height of base model was 2.8, while that of the simulated model were 2.2m and 2.5 m. As shown, while the ceiling height reduced to 2.5m, the average cooling load decreased by 13.6% than the base model. The large reduction was found in terms of sensible cooling load, rather than the latent cooling load. It implies that by reducing the volume of room that to be cooled, the cooling load would be decreasing. However, when the ceiling height further reduced (2.2m), the cooling load only reduced by 3.5% from the former (i.e. ceiling height of 2.5m). It indicates that further decreasing in room volume would not significantly reduce the cooling load. This is most probably because the smaller volume of the room, the heat accumulated during the daytime is bigger. The effects of lower ceiling height (i.e., smaller volume) in cooling load were traded off by the larger heat accumulated during the daytime.

5.5.1.3 Optimum combination

Combination of internal insulation and ceiling height of 2.2 was simulated to see the effects to the cooling load of air-conditioned master bedroom. Above techniques were selected since

both reduced the cooling load at the lowest level individually. Figure 5.91 presents the simulation results of cooling load for combination cases. As indicated, compared to other techniques, installing internal insulation was significantly reduced the cooling load and followed by reducing ceiling height. It means that well insulated wall is the most efficient techniques in reducing the cooling load. By combining both techniques, further reduction of the cooling load was obtained. It is found that combination of both techniques reduced by 5.01 MJ/day or around of 43.9% from the base model. As previously discussed, the effects of the lower ceiling height on the cooling load was traded off by the heat accumulated during the daytime. In this case, by applying thermal insulation at the lower ceiling height could reduce the heat gain. Therefore, the cooling load was further reduced when both techniques were applied.

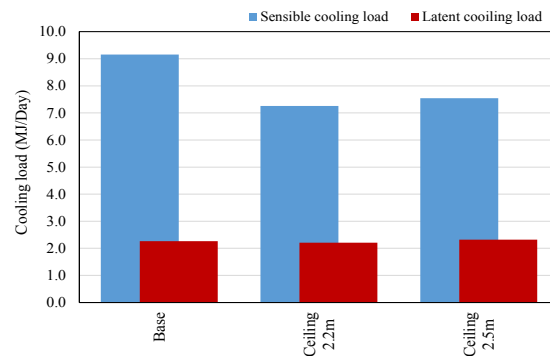


Figure 5.90. Simulation results of cooling load for different ceiling heights in master bedroom.

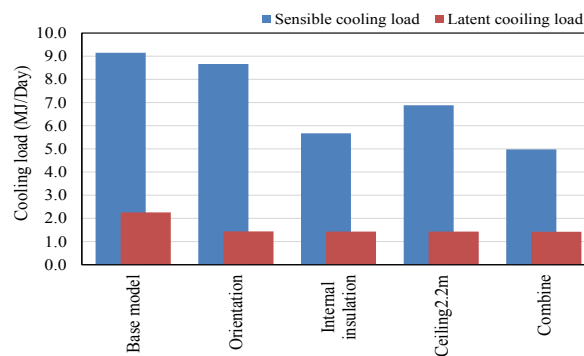


Figure 5.91. Simulation results of cooling load for combined techniques in master bedroom.

5.7 Summary

Simulations to investigate the effects of application of passive cooling strategies in the apartment building have been carried out using CFD STREAM and TRNSYS-COMIS. The validation of both simulation using MBE and RMSE showed that the model satisfactorily

described thermal behavior in the apartment buildings. Based on simulation results, some passive cooling guidelines for high-rise apartments in hot-humid climate of Indonesia are proposed. Orientation, thermal mass, opening area as well as position of the openings, and ceiling height and insulation are some of proposed passive cooling strategies.

Based on the simulation results using CFD STREAM for night ventilation and full-day ventilation conditions, it is found that the optimum indoor air temperature is achieved when the unit employ thermal mass of 2,000 kg/m², ratio of openings area to floor area of 0.15, applying upper and lower window (and it is strongly recommended to use it at both sides) and the ceiling height of 5.0m. Simulation results showed that under these combinations, daytime air temperature was up to 0.7°C lower than that of other cases, and the nocturnal air temperature was lower amongst other cases (25.4°C). Furthermore, simulation on comfort ventilation resulted that using larger ratio of openings area to floor area (i.e. 0.10) and applying central windows on both sides at the same time would lower the SET* values to 25.5-27.5°C. It is found that ceiling height is not significantly affecting on lowering the SET* values in the room. However, it should be noted that the maximum indoor wind speed when the window open was quite high, which is around 3.63 m/s. Therefore, further ventilation strategies should be considered to optimize indoor wind speed as required.

Meanwhile, based on the simulation results using TRNSYS-COMIS, it is found that by applying internal insulation together with ceiling height of 2.2m in the air-conditioned master bedroom obtained the lowest reduction of cooling load almost half from the base model (43.9%). It should be noted that the building unit was facing North/South, and air-conditioning unit used in the night-time only. Meanwhile, daytime ventilation was applied in the master bedroom and the living room applied night ventilation.



6

Recommendations

6.1 Introduction

As a growing country, the development of high-rise apartments is increasing in Indonesia. As introduced previously, comprehensive energy-saving guidelines or standards for the high-rise apartments do not exist to date. The current design guidelines for the high-rise buildings comprise requirements for indoor thermal comfort in terms of air temperature and relative humidity without devising it into specific techniques. This chapter attempts to propose new design guidelines for improving thermal comfort and energy-saving in the high-rise apartments of Indonesia, for naturally ventilated living room and the air-conditioned master bedroom respectively.

6.2 Proposal of design guidelines for high-rise apartments

Based on the simulation for naturally ventilated room (i.e. living room) using CFD STREAM, thermal mass can be used as one of passive cooling strategies for the high-rise apartment buildings. Under night ventilation conditions, it is found that using thermal mass of 2,000 kg/m² reduced indoor air temperature by 0.8-0.9°C compared to that of using thermal mass of 1,000 kg/m². As for current condition, high-rise apartments in Indonesia employed average thermal mass approximately of 1,100 kg/m². In the other hand, increasing thermal mass would increase indoor air temperature at the night-time. Therefore, the ratio of opening area should be enlarged to maximize the amount of cool air from the outdoor enter the indoor space during the night-time. Furthermore, the difference of daytime indoor air temperature between two different opening ratios was not significantly different due to the solar radiation effects. Therefore, ratio of openings area to floor area of 0.15 could be proposed as passive cooling strategies to obtain the benefit of night ventilative cooling. Furthermore, increasing ceiling height (5.0m) could reduce daytime indoor air temperature by 0.3-0.4°C under this condition compared to the lower ceiling height (3.0m).

Furthermore, the window position plays important role in reducing daytime indoor air temperature under night ventilation condition. As found through simulation, upper and lower

window position significantly cooled the building structures (i.e. walls, floor and ceiling) and effectively reduced indoor air temperature even during the daytime. Moreover, changing window position would reduce indoor wind speed by more than half compared to the previous cases. This is important since some standards such as ASHRAE-55 allowed maximum indoor air velocity up to 1.2 m/s. Therefore, the use of upper and lower windows for night ventilation is strongly recommended for structural cooling. In addition, ceiling height should be considered to optimize the indoor air temperature. From the simulation, it is obtained that ceiling height of 5.0m would reduce indoor air temperature particularly when it combined with the larger ratio of openings area to floor area and the position of openings/windows.

For comfort ventilation simulation, i.e. full-day ventilation, the use of central windows at the both sides and the larger ratio of openings area to floor area are recommended. Unlike structural cooling (night-ventilation), the ceiling height is not predominantly affecting evaporative cooling. As found through simulation, the opening ratio of 0.05 is sufficient to

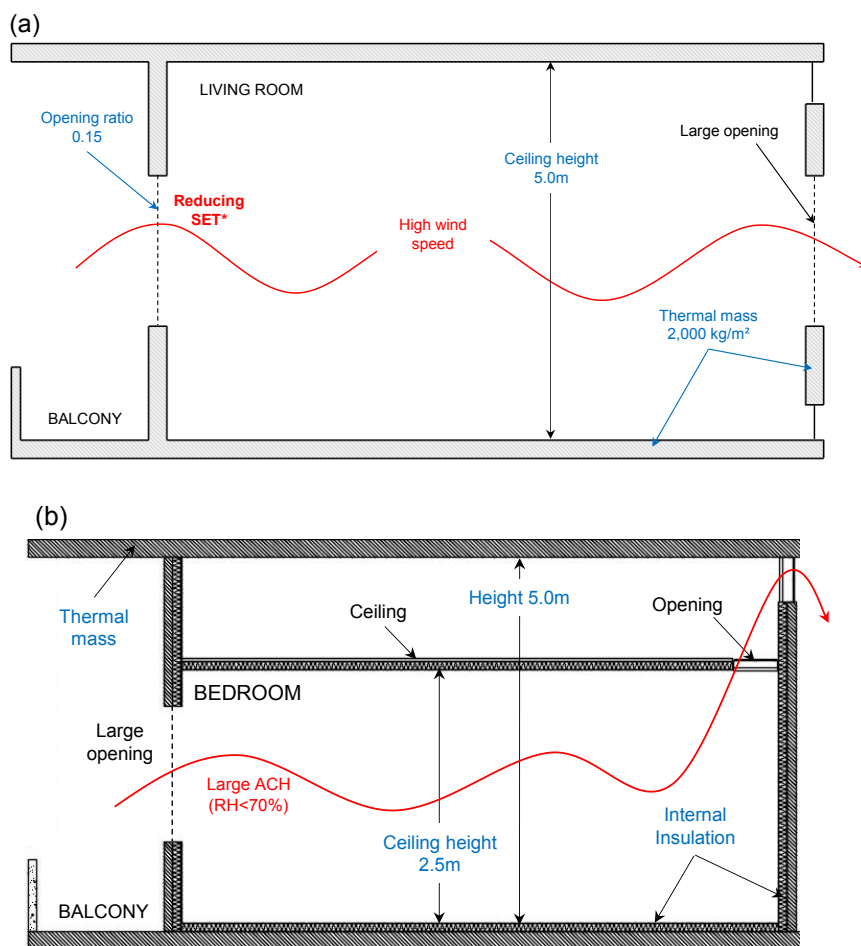


Figure 6.1. Comfort requirements and proposed design guideline for (a) living room and (b) master bedroom during the daytime-time.

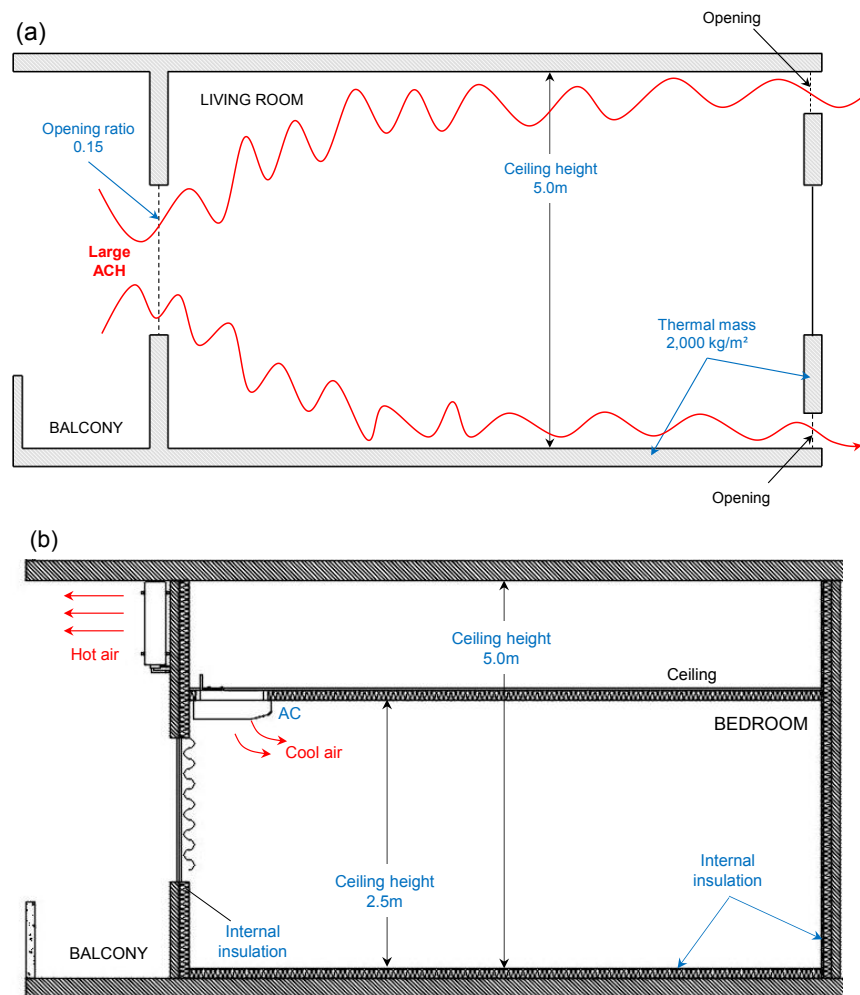


Figure 5.93. Comfort requirements and proposed design guidelines for (a) living room and (b) master bedroom during the daytime.

lower the SET* at the occupied level. Nevertheless, it is important to be noticed that simulation was carried out under condition of actual situation of model, i.e. located at approximately of 26m above ground level and therefore the outdoor wind speed is recorded relatively high. Different ratio of opening area to floor area should be considered to be used for different floor level.

For the air-conditioned room, internal insulation effectively reduced total cooling load by 12.5% from the base model. By reducing ceiling height to 2.5m (from base model 2.8m), the 17.1% of total cooling load are further reduced. However, the reduction was not as significant as expected (only 3.6%). However, when above techniques are combined, the cooling load reduced almost half from the base model (43.9%). Therefore, for air-conditioned room,

applying both techniques are recommended, while maintaining living room (naturally ventilated room) applying nocturnal ventilative cooling (night ventilation). Figures 5.92-93 illustrated the proposed passive cooling guidelines of living room and master bedroom for night-time and daytime respectively, while Table 5.14 summarizes the proposal of design guidelines for high-rise apartment buildings in Indonesia.

Table 6.1 Proposal of design guidelines for high-rise apartment buildings in hot-humid climate of Indonesia.

No	Parameters	Criterion	Notes
1	<i>Naturally ventilated room (living room)</i>		
1.1	Structural cooling (night ventilation)		
a	Orientation	South- or North-facing	
b	Thermal mass (kg/m ²)	2,000	Concrete block with thickness of 120 mm
c	Ratio of openings area to floor area	0.15	Depend on the location of unit. Lower position in the apartment tower may increase the opening ratio
d	Openings position	Upper and lower	For night ventilation, upper and lower window at both sides is strongly recommended.
1.2	Comfort ventilation (full-day ventilation)		
a	Orientation	South- or North-facing	
b	Thermal mass (kg/m ²)	2,000	Concrete block with thickness of 120 mm
c	Ratio of openings area to floor area	0.15	Depend on the location of unit. Lower position of unit in the apartment tower may increase the opening ratio
d	Openings position	Central	Applying central windows at both sides to ensure cross ventilation and increase wind speed
e	Ceiling height (m)	3.0 - 5.0	
2	<i>Air conditioned room (master bedroom)</i>		
a	Orientation	South- or North-facing	
b	Ventilation condition	Daytime ventilation	Apply night ventilation in the living room
c	Insulation (W/mK)	0.03	Installed internally
d	Ceiling height (m)	2.0	

7

Conclusions

The main objective of this thesis was to provide fundamental and comprehensive data and information on newly constructed high-rise apartments, the so-called *Rusunami*, in Indonesia, which are useful in developing new energy-saving guidelines and standards for these apartments. First, this study aimed to understand indoor thermal environments and thermal comfort of the existing apartments in major cities of Indonesia, focusing especially on the high-rise apartments, *Rusunami*. Second, this study investigated the passive cooling techniques embedded in the Dutch colonial buildings located in the city of Bandung with the aim of applying these traditional techniques to the modern houses. Third, the effects of cooling techniques on indoor thermal comfort as well as cooling load reduction in high-rise apartments were analyzed comprehensively through a series of parametric studies using numerical simulations. Fourth, the design guidelines for high-rise apartments towards energy-saving were proposed based on the results of the field measurements and simulations.

6.1 Key findings

Review of passive cooling studies for high-rise apartments

The review mainly focuses on the development of passive cooling strategies for high-rise apartments in the tropics region. The review shows that the number of studies are still lack for hot-humid regions. There are disputes among researchers about the effectiveness of ventilative cooling as well as other passive techniques such as thermal mass and insulation. However, there is still lack of basic field data in many cases so that progress to develop cooling techniques particularly in apartments is difficult to be made. Therefore, both basic and comprehensive studies are necessary to be carried out in these regions. One of the recent interests is to evaluate the thermal performances of vernacular buildings using scientific methods since these buildings are rooted to the local context including the climate conditions. Furthermore, in depth study on thermal performance in the colonial buildings in tropics are hardly found to date. It is derived that the suitable methods for this study would be to conduct

intensive full-scale field measurement in existing buildings, including selected apartments and traditional vernacular houses, then followed by numerical simulation for further tests.

Thermal comfort in the existing apartments

Apartments in Indonesia are broadly divided into four categories, i.e. public apartments (old public and new public apartments), special apartments, state apartments and private apartments. Field measurements were carried out in the public apartments and middle-class high-rise apartments since both apartment types are highly demanded by the middle-class people in major cities of Indonesia. Field survey also was conducted particularly in the public apartments to investigate the factors influencing indoor thermal environments. The key results are as follow:

- Under unoccupied condition, the old public apartment unit showed better thermal environments compared to those in the other two apartments. In contrast, under occupied condition, nocturnal indoor air temperatures in the old public apartment were higher than the daytime indoor air temperature.
- By means of simulation using TRNSYS-COMIS, it is obtained that building orientation does not significantly affecting the indoor air temperatures of master bedroom in the old public apartment due to the existence of balcony as a shading devices as well as thermal buffer zone. In the case of new public apartment and middle-class high-rise apartment, east- and west facing unit show relatively higher indoor air temperatures compared to north- and south-facing unit due to the solar radiation entering the building during the morning time and afternoon.
- Simulation results also found out that night ventilation effectively reduce daytime indoor air temperature in the three types of apartments compared to other ventilation conditions (i.e. daytime and full-day ventilation). When night ventilation applied, the maximum indoor air temperatures reduce by 0.4-0.5°C compared to those of when daytime/full-day ventilation applied. Meanwhile, during the peak hours, night ventilation in the new public apartment obtains lower indoor air temperatures compared to other ventilation conditions regardless orientations although the differences are relatively small. Furthermore, the simulation results in the middle-class high-rise apartment shows that there is almost no difference amongst the ventilation conditions regardless the orientations.
- Based on the simulation results, evaluation of thermal comfort using the adaptive comfort equation showed that thermal comfort is difficult to be achieved without relying on air-conditioning in both new public and middle-class high-rise apartments. Meanwhile, based on the filed measurement, operative temperatures in occupied units in both public apartments exceeded the 80% of upper comfortable limits during the peak hours.
- In the naturally ventilated apartments, i.e. public apartments, physical conditions such as, orientation (i.e. east- or west-facing unit), floor level and window to wall ratio are factors influencing indoor air temperatures at the daytime. In the other hand, windows/doors opening behavior (i.e. opening front and back windows/doors, opening front

windows/doors only and opening back windows/doors) are main factors influencing indoor air temperatures at the night-time.

- Several problems particularly in the middle class high-rise apartment are addressed. Some of them are uninsulated external wall, insufficient ventilation rate due to single sided ventilation, the absence of shading devices. Together with the results of air change rate measurement, it implies that middle-class high-rise apartments are design on premise of using air-conditioning system.
- Several potential cooling strategies were suggested. Particularly for west-facing units, proper external and/or internal shading devices are necessary to avoid intense solar radiation. Design of thermal buffer zones such as balcony and corridor was also recommended. To reduce the heat gains through building fabric, external walls and ceilings should be insulated.

Passive cooling techniques of Dutch colonial buildings

Dutch colonial buildings in Indonesia have long history of development. By the time, this kind of building showed well performance in adaptation to the local hot-humid climatic condition. There are several types of Dutch colonial buildings in Indonesia due to periodization of the development. Nevertheless, they are characterized by high thermal mass, high ceiling height, and large openings as well as corridor spaces. Field measurement was carried out in the three Dutch buildings in Bandung, which is coincidentally represents different period of development, i.e. second period, third period and last (modern period). The main findings of the field measurement are as follow:

- The selected case study buildings showed thermal performances differently. In the first two case studies, i.e. buildings from the second period (Case study 1) and third period (case study 2), indoor air temperatures generally maintained relatively lower compared to the corresponding outdoor. In contrast, building from the last period (Case study 3) overall has relatively higher daytime indoor air temperature than the outdoors.
- Thermal comfort evaluation reveals that thermal comfort is achieved in the ground floor while that in the top floor exceeded 80% of comfortable limit during the daytime. However, thermal comfort in the rooms on the top floor is improving due to the increased indoor air speeds. The questionnaires results in Case study 1 confirmed these results: the occupants (students) expected more wind speed at afternoon due to the increasing indoor air temperature to cooling themselves. As the wind sensation increases (when they feel stronger winds), they tend to feel cooler.
- From the field measurement results, some cooling techniques employed in the Dutch colonial buildings are: relatively higher thermal mass (around 2,685-3,478 kg/m²) to maintain daytime indoor air temperatures lower, proper design of corridor spaces as thermal buffer zones and as shading devices, high ceiling height (5.3-5.7m) to maintain occupied level (1.1m above floor) lower values, and permanent openings above windows/doors and louver windows to ensure cross ventilation throughout the day. Particularly for corridor spaces, if the corridor can be designed to be semi-open at the night-

time and enclosed at the daytime, then thermal benefit from the corridor spaces can be obtained.

Above results obviously indicates that Dutch colonial buildings employed some passive cooling techniques that effectively maintained indoor air temperatures lower than the outdoors during the peak hours. These techniques are worthwhile of implementing in the modern houses. However, these techniques should be reevaluated with the aim of applying to modern houses by considering the fact that Bandung experiences relatively cool climate.

Parametric study of cooling strategies in the high-rise apartment.

Numerical simulations were conducted to investigate the effects of the selected cooling techniques on the indoor thermal environments in the naturally ventilated room as well as on the cooling load in the air-conditioned room. Both multi-zone thermal simulation and Computational Fluid Dynamic (CFD) were used as the main method. To investigate the effects of the selected cooling techniques to indoor thermal environments of naturally ventilated room (living room), Computational Fluid Dynamics (CFD) STREAM was used while TRNSYS and COMIS were used to investigate the effects of passive techniques to cooling loads in the master bedroom of middle-class high-rise apartment. The main findings are:

- Empirical validation of the base model indicates that the model is satisfactorily describing thermal behavior of the naturally ventilated apartments. Mean bias errors (MBE) and Root Mean Square Error (RMSE) for air temperature, relative humidity and absolute humidity can be seen in Table 3.9 and Table 5.4
- Parametric study using CFD STREAM have been carried out for naturally ventilated room (living room), including some parameters such as thermal mass, ratio of opening area to floor area, ceiling height and window position. There are two kind of simulation: structural cooling (night-ventilation) and comfort ventilation (full-day ventilation). The parameter test cases for both simulations are summarized in Tables 5.5 and 5.8 for structural cooling, and Table 5.10 for comfort ventilation.
- From the simulation results of structural cooling, it is found that daytime indoor air temperature would be reduced if thermal mass increased (i.e. 2,000 kg/m²). As the consequences, it raised nocturnal indoor air temperature as well. In this case, the ratio of opening area should be enlarged to maximize the amount of cool air enter the indoor space particularly during the night-time. Moreover, there is no significant different in daytime indoor air temperature between two different opening ratios due to the solar radiation effects. Furthermore, the window position should be considered to reduce more indoor air temperature. Upper and lower window position significantly cooled the building structures and effectively reduced indoor air temperature even during the daytime. Moreover, the changing of window position would reduce indoor wind speed by more than half. This is important since higher wind speed may causes discomfort. Furthermore, ceiling height was found to be important parameters in reducing indoor air temperature.
- Optimum results for structural cooling was obtained when the unit applying thermal mass of 2,000 kg/m², ratio of opening area to floor area of 0.15, ceiling height of 5.0m, and

upper/lower windows at back-side while maintaining central window at windward side (front-side). Under these parameters, the maximum indoor air temperature was recorded up to 30.2°C and the lowest indoor air temperature was around of 25.4°C. However, the maximum indoor wind speed when the window open was quite high, which is around 3.63 m/s. Therefore, further ventilation strategies should be further considered.

- For comfort ventilation, simulation results showed that indoor air temperature during the daytime are not significantly different amongst all cases due to the air infiltration. Instead, applying all parameters (higher opening ratio, higher ceiling height and upper/lower windows) would reduce the nocturnal indoor air temperature. However, these effects were diminished by air infiltration during the daytime. Meanwhile, the significant results was found in the profiles of wind speed particularly when upper and lower windows are applied. It reduced more than half of wind speed compared to that when central windows are applied. It is obtained that the unit employing central windows and increasing window opening ratio to floor area significantly increased wind speed, and therefore lowered the SET* values. Therefore, it is found that the unit with ratio of opening area to floor area of 0.10 and employing central windows at the both sides enjoyed lower SET* values and larger distribution area of these values during the peak hours regardless ceiling height.
- For the air-conditioned room (master bedroom), the cooling load in air-conditioned room (master bedroom) reduced almost half from the base model (around 43.9%) by applying the combined techniques, i.e. internal insulation and ceiling height of 2.2m. It should be noted that the building unit was facing North/South, and air-conditioning unit is turned on in the night-time only.

Proposal of design guidelines for middle-class high-rise apartment

Potential cooling techniques that are identified from the vernacular houses and results of the numerical simulation are proposed to be implemented in the apartment building through building modifications. The key points are:

- From the field measurement on the existing apartments in Surabaya and some Dutch colonial buildings in Bandung, potential cooling strategies proposed are thermal mass, ceiling height, corridor spaces and comfort ventilation.
- As simulated using CFD STREAM for structural cooling (night ventilation) and comfort ventilation (full-day ventilation), some design guidelines for improving indoor thermal environments are proposed as illustrated in Figures 5.92-93 and summarized in Table 5.14. Basically, there are two types of comfort requirements for respective daytime and night-time, and therefore the proposal of design guidelines for both requirements are different as well.
- For air-conditioned master bedroom, proposed cooling strategies to reduce cooling load in the air-conditioned room are:
 - Orientation: South-North
 - Ventilation strategy: Daytime ventilation, while applying night ventilation in the adjacent room (living room)

- Insulation: Internal insulation
- Ceiling height: 2.2-2.5m

Final conclusions

Based on the previous key findings, the conclusions of this study are as follow:

- An intensive field experiment in the existing apartments in Surabaya and computer simulation have been carried out. The results revealed that indoor thermal environments of the middle-class high-rise apartment in Indonesia are quite severe. Thermal comfort could not be achieved even during the night-time and therefore, it is difficult to achieve it without relying on the air-conditioning system.
- Dutch colonial buildings nicely maintain indoor air temperature lower than the corresponding outdoors and they reveal some cooling techniques that worthwhile of applying to the middle-class high-rise apartment. Some of them are high thermal mass, corridor space, large opening area as well as permanent openings above windows and louver door, and the high ceiling height. Some of those (such as high thermal mass, opening area and ceiling height) then are picked up as cooling techniques for high-rise apartments and their cooling effects are investigated through computer simulation.
- In general, it is concluded that higher thermal mass is effective strategies in providing better indoor thermal environment in naturally ventilated room rather than other examined strategies (i.e. opening ratio, ceiling height and window position). Higher thermal mass effectively lower the daytime indoor air temperature by 0.8-0.9°C compared to that employed lower thermal mass. The cooling effects of ceiling height and window position are almost the same (which is around 0.3-0.4°C lower), while those of opening ratio are found to be the smallest. Nevertheless, larger opening ratio increases indoor wind speed and therefore effectively reduces SET* values particularly when the central windows at both sides are applied.
- Cooling load in the air-conditioned master bedroom would be effectively reduce if the room volume is reducing by lowering the ceiling height while internal insulation is applied. Orientation and ventilation strategies do not contribute in the cooling load reduction significantly. Nonetheless, combining all above techniques obtained the lowest reduction of the cooling load.
- The approach of three dimensional perspective (ventilation strategies, envelope strategies and building volume) revealed a new insight in designing cooling strategies for building particularly high-rise apartment in the hot-humid climatic regions. This approach disclose new possibility for energy-saving guidelines of buildings in the future. Further studies should be undertaken since this study have limitations.

6.2 Study limitations and further studies

The number of sample size for determining factors influencing indoor thermal environments in the occupied units, as presented in Subchapter 3.5 Section 3.5.3. The sample size is considered too small to conclude the predictors for indoor thermal environment and therefore the number of this sample should be extended in order to gain more comprehensive results. Furthermore, the use of statistical test in Section 4.4.3 of Chapter 4 is not sufficient to explain the means difference between two samples. Therefore, other statistical test methods should be considered in the future studies.

Other limitation of this study is the validation results for wind speeds in the CFD STREAM. As explained in the Chapter 5, it is difficult to fit the validation results with the measurement results for indoor wind speeds and therefore the strong relationship between them is difficult to be achieved. Further studies should consider this matter (i.e. wind speed validation) accurately before further running simulation.

This study limited on some parameters as well as limited test conditions, such as single orientation (south-facing). Moreover, this study investigated two extreme values only such as ceiling height (i.e. 3.0m and 5.0) and ratio of openings area to floor area (i.e. 0.05 and 0.15) without considering other values. Therefore, some parameters with other test conditions should be further examined to obtain more comprehensive results on the cooling strategies for high-rise apartment buildings including unit position (i.e. lower floors or higher floor levels). Since windows/openings position is important in structural cooling, this parameter should be included in further studies.

In this thesis, simulation using CFD was conducted in the living room only, under naturally ventilated condition. It is interesting to investigate the indoor thermal environment not only in the living room but also master bedroom and other rooms. In addition, some additional passive techniques such as shading devices should be considered in the future studies. Coupling techniques with another building energy simulation (such as TRNSYS-COMIS, BES, etc.) can be considered for the future studies. This techniques also can be considered to reduce the calculation time in simulation, which is one of disadvantages in using CFD.

Further studies on the thermal behavior of corridor spaces are recommended. Corridor spaces play important roles to indoor air temperatures. Several types of corridor space with several parameters, such as width, depth, and length of corridor space can be examined using CFD, to see its effect to indoor spaces. This including stack effect of atrium or corridor space in the apartment buildings. In the larger scale, investigation of composition of building mass of apartment buildings and its effects to the wind flow are also recommended. It is believed that building configuration affect the wind flow, and thus it is also affect to the performance of ventilation in the apartment buildings.



References

- ADB**, 2016: Housing Policies in Singapore. Asian Development Bank Institute, Tokyo, Japan.
- Adiyanto**, A., Djunaedi, A., Ikaputra and Suryabrata, J.A., 2015: The Architecture of Dutch colonial office in Indonesia and the adaptation to tropical climate. *International Journal of Scientific and Research Publications*, **5** (4).
- Aflaki**, A., N. Mahyuddin and M.R. Baharum, 2016: The influence of single-sided ventilation towards the indoor thermal performance of high-rise residential building: A field study. *Energy and Buildings*, **126**, 146-158.
- Aflaki**, A., N. Mahyuddin, Z.A. Mahmoud and M.R. Baharum, 2015: A review on natural ventilation applications through building façade components and ventilation openings in tropical climates. *Energy and Building*, **101**, 153-162.
- Akeiber**, H., P. Nejat, M.Z. Abdul Majid, M.A. Wahid, F. Jomehzadeh, I.Z. Famileh, J.K. Calautit, B.R. Hughes and S.A. Zaki, 2016: A review on phase change material (PCM) for sustainable passive cooling in building envelopes. *Renewable and Sustainable Energy Reviews*, **60**, 1470-1497.
- Alam**, M., J. Sanjayan, P.X.W. Zou, S. Ramakrishnan and J. Wilson, 2017: Evaluating the passive and free cooling application methods of phase change materials in residential buildings: A comparative study. *Energy and Buildings*, **148**, 238-256.
- Al-Obaidi** K.M., M. Ismail, and A.M. Abdul Rahman, 2014a: Passive cooling techniques through reflective and radiative roofs in tropical houses in Southeast Asia: A literature review. *Frontiers of Architectural Research*, **3**, 283-297.
- Al-Obaidi** K.M., M. Ismail, and A.M. Abdul Rahman, 2014b: A review of the potential of attic ventilation by passive and active turbine ventilators in tropical Malaysia. *Sustainable Cities and Society*, **10**, 232-240.
- Al-Obaidi** K.M., M. Ismail, and A.M. Abdul Rahman, 2014c: Design and performance of novel innovative roofing system for tropical landed houses. *Energy Conversion and Management*, **85**, 488-504.
- Al-Saadi**, S.N., and S. Zhai, 2013: Modelling phase change materials embedded in building enclosure: A review. *Renewable and Sustainable Energy Reviews*, **21**, 659-673.

- Arethusa**, M.T., 2014: *Factors influencing window opening behavior in apartments of Indonesia: Natural ventilation strategies for middle class apartments*. Master's Thesis (unpublished). Graduate School for International Development and Cooperation, Hiroshima University, Hiroshima, Japan.
- Arethusa**, M.T., T. Kubota, A.M. Nugroho, I.G.N. Antaryama, S.N. Ekasiwi and T. Uno, 2014: Factors influencing window opening behaviour in apartments of Indonesia. *PLEA2014*; Ahmedabad.
- ASHRAE**, 2013: *ANSI/ASHRAE Standard 55-2013 Thermal Environmental Conditions for Human Occupancy*. American Society of Heating, Refrigerating and Air-Conditioning Engineers, Inc., Atlanta.
- ASHRAE**, 2017: *2017 ASHRAE Handbook – Fundamentals (SI Edition)*. American Society of Heating, Refrigerating and Air-Conditioning Engineers, Inc., Atlanta.
- Asian Development Bank**, 2010: *Key indicators for Asia and the Pacific 2010, Special chapter: The rise of Asia's Middle Class*. Asian Development Bank
- Awbi**, H., 2003: *Ventilation of Buildings, 2nd edition*. Spon Press, London, England.
- Badan Perencanaan Pembangunan Nasional, Badan Pusat Statistik and United Nations Population Fund**, 2014: *Proyeksi Penduduk Indonesia 2010-2035*. Badan Pusat Statistik, Jakarta.
- Badan Pusat Statistik (BPS)**, 2014: *Surabaya in Figures 2014*. Badan Pusat Statistik Kota Surabaya, Surabaya, Indonesia.
- Balaras**, C., 1996: Cooling in buildings. In: *Passive Cooling of Buildings* [Santamouris, M. and D. Asimakopoulos (eds.)]. James & James (Science Publishers) Ltd., London, pp. 1-34.
- Barbieri**, SU and L. van Duin, 2003: *A Hundred Years of Dutch Architecture 1901-2000*. SUN, Amsterdam, the Netherland.
- Baskaran**, A. and A. Kashef, 1996: Investigation of air flow around buildings using computational fluid dynamics techniques, *Engineering Structures*, 18(11), 861-875.
- Bauer**, M., P. Mösle, and M. Schwarz, 2010: *Green Building – Guidebook for Sustainable Architecture*. Springer-Verlag, Berlin and Heidelberg.
- BCA**, 2004: Guidelines on envelope thermal transfer value for buildings. Building and Construction Authority, Singapore.
- Bojic**, M. and F. Yik, 2005: Cooling energy evaluation for high-rise residential buildings in Hong Kong. *Energy and Buildings*, 37, 345-351.
- Bojic**, M., F. Yik, K. Wan and J. Burnett, 2002: Influence of envelope and partition characteristics on the space cooling of high-rise residential buildings in Hong Kong. *Building and Environment*, 37, 347-355.
- Bojic**, M., F. Yik F and P. Sat, 2001: Influence of thermal insulation position in building envelope on the space cooling of high-rise residential buildings in Hong Kong. *Energy and Buildings*, 33, 569-581.

- Bonta**, D. and S. Snyder, 2008: *New Green Home Solutions: Renewable Household Energy and Sustainable Living*. Gibbs Smith, Utah.
- Boral**. *Technical Manual*. https://www.usgboral.com/in_id/product-resources-and-tools-from-usgboral/the-resource-centre/technical-manual.html, accessed in 01 February 2018.
- Borda-Diaz**, N., P.I. Mosconi, and J.A. Vasquez, 1989: Passive cooling strategies for a building prototype design in a warm-humid tropic climate. *Solar and Wind Technology*, **6**, 389-400.
- Brager**, G.S. and R.J. de Dear, 1998: Thermal adaptation in the built environment: a literature review. *Energy and Buildings*, **27**(1), 83-96.
- Bronner**, S.J., 2006: Building tradition, Control and authority in vernacular architecture. *Vernacular Architecture in the Twenty-First Century, Theory, education and practice Ed. Asquith L. and M. Vellinga*, Taylor and Francis, New York.
- BP Statistical Review of World Energy June 2017**, <https://www.bp.com/content/dam/bp/en/corporate/pdf/energy-economics/statistical-review-2017/bp-statistical-review-of-world-energy-2017-full-report.pdf>, accessed at 01 September 2017.
- BSI**, 2006: *BS EN ISO 7730:2005 Ergonomics of the Thermal Environment – Analytical Determination and Interpretation of Thermal Comfort Using Calculation of the PMV and PPD Indices and Local Thermal Comfort Criteria*. British Standards Institute, London.
- BSN**, 2001: *SNI 03-6572-2001 Tata cara perancangan sistem ventilasi dan pengondisian udara pada bangunan gedung*. BSN, Jakarta, Indonesia.
- BSN**, 2002: *SNI 6882- Spesifikasi mortar untuk pekerjaan pasangan*. Badan Standar Nasional, Jakarta, Indonesia.
- BSN**, 2011: *SNI 6389-2011 Konversi energi selubung bangunan pada bangunan gedung*. BSN, Jakarta, Indonesia.
- BSN**, 2011: *SNI 6390-2011 Konservasi energi sistem tata udara bangunan gedung*. BSN, Jakarta, Indonesia.
- BSN**, 2013: *SNI 2847-2013 Persyaratan beton structural untuk bangunan gedung*. Badan Standar Nasional, Jakarta, Indonesia.
- Cândido**, C., R.J. de Dear, R. Lamberts, and L. Bittencourt, 2010: Air movement acceptability limits and thermal comfort in Brazil's hot humid climate zone. *Building and Environment*, **45**(1), 222-229.
- Cheng**, V., E. Ng and B. Givoni, 2005: Effect of envelope colour and thermal mass on indoor temperatures in hot humid climate. *Solar Energy*, **78**, 528-534.
- Cheung**, C.K., R.J. Fuller and M.B. Luther, 2005: Energy-efficient envelope design for high-rise apartments. *Energy and Buildings*, **37**, 37-48.
- Choi**, I.Y., S.H. Cho and J.T. Kim, 2012: Energy consumption characteristics of high-rise apartment buildings according to building shape and mixed-use development. *Energy and Buildings*, **46**, 123-131.

- Coackley**, D., P. Raftery and M. Keane, 2014: A review of methods to match building energy simulation models to measured data. *Renewable and Sustainable Energy Reviews*, **37**, 123-141.
- Coch**, H., 1998: Chapter 4-Bioclimate in vernacular architecture. *Renewable and Sustainable Energy Reviews*, **2**, 67-87
- Cook**, J. (ed.), 1989: *Passive Cooling*. The MIT Press, Cambridge, Massachusetts and London, England.
- Coordinating Ministry for Economic Affairs**, 2011: *Master plan for acceleration and expansion of Indonesia Economic Development*. Coordinating Ministry of Economic Affairs, Jakarta.
- Crawley**, D.B., J.W. Hand, M. Kummert, and B.T. Griffith, 2008: Contrasting the capabilities of building energy performance simulation programs. *Building and Environment*, **43**, 661-673.
- Cradle**, 2015: *scSTREAM Version 12 User's Guide: Basics of CFD Analysis*. Software Cradle Co., Ltd., Tokyo, Japan.
- Cradle**, 2015: *scSTREAM Version 12 User's Guide: Preprocessor Reference*. Software Cradle Co., Ltd., Tokyo, Japan.
- Cradle**, 2015: *scSTREAM Version 12 User's Guide: Solver Reference*. Software Cradle Co., Ltd., Tokyo, Japan.
- Cradle**, 2015: *scSTREAM Version 12 User's Guide: Postprocessor Reference*. Software Cradle Co., Ltd., Tokyo, Japan.
- Darmawan**, A., 2011: *Analyzing Urban Redevelopment Based on Environmental Behavior: A Case of Rusunawa Residents Behavior in Surabaya City, Indonesia*. Master's Thesis (unpublished), University of Brawijaya, Malang, Indonesia.
- de Dear**, R.J. and G.S. Brager, 2002: Thermal comfort in naturally ventilated buildings: revisions to ASHRAE Standard 55. *Energy and Buildings*, **34**, 549-561.
- de Gracia**, A. and Cabeza, L.F., 2015: Phase change materials and thermal energy storage for buildings. *Energy and Buildings*, **103**, 414-415.
- De Waal**, H.B., 1993: New recommendations for building in tropical climates. *Building and Environment*, **28**, 271-285.
- D'Agostino**, D. and P.M. Congedo, 2014: CFD modelling and moisture dynamics implications of ventilation scenarios in historical buildings, *Building and Environment*, **79**, 181-193.
- Dili**, A.S., M.A. Naseer, and T. Z. Varghese, 2010: Passive environment control system of Kerala vernacular residential architecture for a comfortable indoor environment: a qualitative and quantitative analyses. *Energy and Buildings*, **42**, 917-927.
- Dimoudi**, A., 1996: Passive cooling of buildings. In: *Passive Cooling of Buildings* [Santamouris, M. and D. Asimakopoulos (eds.)]. James & James (Science Publishers) Ltd., London, pp. 35-55.
- Djamila**, H., C.C. Ming and S. Kumaresan, 2015: A generalized thermal perception approach for indoor thermal comfort assessment in the humid tropics of Malaysia, *Energy and Buildings*, **88**, 276-287.

- Dorer, V., A. Haas, and A. Weber (eds.)**, 2005: *COMIS 3.2 – User Guide*. Swiss Federal Laboratories for Materials Testing and Research (EMPA), Dübendorf, Switzerland.
- Energy Information Administration (EIA)**, 2016: *International Energy Outlook 2016*. Energy Information Administration.
- Feriadi, H. and N.H. Wong**, 2004: Thermal comfort for naturally ventilated houses in Indonesia. *Energy and Buildings*, **36(7)**, 614-626.
- Feustel, H.E.**, 1999: COMIS – an international multizone air-flow and contaminant transport model. *Energy and Buildings*, **30**, 3-18.
- Feustel, H.E. and A. Raynor-Hoosen (eds.)**, 1990: *Fundamentals of the Multizone Air Flow Model – COMIS*. Technical Note AIVC 29. Air Infiltration and Ventilation Centre, Coventry, UK.
- Finn, D.P., D. Connolly, and P. Kenny**, 2007: Sensitivity analysis of a maritime located night ventilated library building. *Solar Energy*, **81**, 697-710.
- Fouquier, A., S. Robert, F. Suard, L. Stephan and A. Jay**, 2013: State of the art in building modelling and energy performances prediction: A review. *Renewable and Sustainable Energy Reviews*, **23**, 272-288.
- Geetha, NB and R. Velraj**, 2012: Passive cooling methods for energy efficient buildings with and without thermal energy storage-A review. *Energy Education Science and Technology Part A: Energy Science and Research*, **29(2)**, 913-946
- Geros, V., M. Santamouris, A. Tsangrasoulis, and G. Guarracino**, 1999: Experimental evaluation of night ventilation phenomena. *Energy and Buildings*, **29**, 141-154.
- Givoni, B.**, 1976: *Man, Climate and Architecture, second ed.* Applied Science Publishers Ltd., London.
- Givoni, B.**, 1994: Building design principles for hot-humid regions. *Renewable Energy*, **5(2)**, 908-916.
- Givoni, B.**, 1994: *Passive and Low Energy Cooling of Buildings*. Van Nostrand Reinhold, New York.
- Givoni, B.**, 2004: Adaptive thermal comfort standards in the hot-humid tropics. *Energy and Buildings*, **36**, 628-637.
- Givoni, B.**, 2011: Indoor temperature reduction by passive cooling systems. *Solar Energy*, **85**, 1692-1726.
- Grosso, M.**, 1992: Wind pressure distribution around buildings: a parametrical model. *Energy and Buildings*, **18**, 101-131.
- Grosso, M.**, 1995: *CPCAL⁺ Calculation of Wind Pressure Coefficients on Buildings, Versions 1.1 DOS and 1.1 WIN: User's Manual*. PASCOOL Research Program. Commission of the European Communities, Turin.
- Gunningham, N.**, 2013: Managing the energy trilemma: The case of Indonesia. *Energy Policy*, **54**, 184-193

- Handinoto** and S. Hartono, 2006: Arsitektur transisi di Nusantara dari akhir abad 19 ke awal abad 20 (Studi KAsus Kompleks Bangunan Militer di Jawa pada peralihan abad 19 ke 20). *Dimensi*, **34(2)**, 81-92
- Handinoto**, 2010: *Arsitektur dan Kota-kota di Jawa pada Masa Kolonial*. Graha Ilmu, Yogyakarta, Indonesia.
- Harmanescu**, M. and C. Enache, 2016: Vernacular and Technology, InBetween. *Procedia Environmental Sciences*, **32**, 412-419.
- Hasan, M.H.**, T.M.I. Mahlia and Hadi Nur, 2012a: A review on energy scenario and sustainable energy in Indonesia. *Renewable and Sustainable Energy Reviews*, **16**, 2316-2328.
- Hasan, M.H.**, W.K. Muzammil, T.M.I. Dahlia, A. Jannifar and I. Hasanuddin, 2012b: A review on the pattern of electricity generation and emission in Indonesia from 1987 to 2009. *Renewable and Sustainable Energy Reviews*, **16**, 3206-3219.
- Hassan**, A.S. and M. Ramli, 2010: Natural ventilation of indoor air temperature: a case study of the traditional Malay house in Penang. *American Journal of Engineering and Applied Sciences*, **3(3)**, 521-528.
- Hebel/Bata Ringan AAC**. <http://www.hebelindonesia.com/p/hebel-aac.html>, accessed in 01 February 2018.
- Hirunlabh**, J., W. Kongduang, P. Namprakai and J. Khedari, 1999: Study of natural ventilation of houses by a metallic solar wall under tropical climate. *Renewable Energy*, **18**, 109-119.
- Hirunlabh**, J., S. Wachirapuwadon, N. Pratinthong and J. Khedari, 2001: New configurations of a roof solar collector maximizing natural ventilation. *Building and Environment*, **36**, 383-391.
- Hens**, H., 2012: *Building Physics-Heat, Air and Moisture Second Edition*. Ernst & Sons, Berlin, Germany.
- Hoseini**, A.H.G., U. Berardi, N.D. Dahlan, and A.G. Hoseini, 2014: What can we learn from Malay vernacular houses?, *Sustainable cities and society*, **13**, 157-170.
- Humphreys**, M.A., J.F. Nicol, and I.A. Raja, 2007: Field studies of indoor thermal comfort and the progress of the adaptive approach. *Advances in Building Energy Research*, **1**, 55-88.
- Indraganti**, M., 2010: Using the adaptive model of thermal comfort for obtaining indoor neutral temperature: findings from a field study in Hyderabad, India. *Building and Environment*, **45(3)**, 519-536.
- Indraganti**, M., 2010: Thermal comfort in naturally ventilated apartments in summer: Findings from a field study in Hyderabad, India. *Applied Energy*, **87**, 866-883.
- Indraganti**, M., 2010: Adaptive use of natural ventilation for thermal comfort in Indian apartments. *Building and Environment*, **45**, 1490-1507.
- Indraganti**, M., R. Ooka, H.B. Rijal and G.S. Brager, 2014: Adaptive model of thermal comfort for offices in hot-humid climates of India. *Building and Environment*, **74**, 39-53.
- IEA**, 2008: *Energy efficiency requirements in building codes, energy efficiency policies for new buildings- IEA Information Paper*. International Energy Agency (IEA), Paris, France.

- IEA, 2012: *IEA Statistics 2012 Edition: CO₂ emissions from fuel combustion*. International Energy Agency (IEA), Paris, France.
- International Monetary Fund**, 2014: *World Economic Outlook: Recovery Strengthens, Remains Uneven*. IMF, Washington DC.
- IPCC**, 2014: *IPCC Working Group III – Mitigation of Climate Change, Chapter 9: Buildings*. Cambridge University Press, Cambridge, United Kingdom and New York, NY, USA, 996 pp.
- Jafari, Y., J. Othman, A.H.S. Mohd Nor**, 2012: Energy consumption, economic growth and environmental pollutants in Indonesia. *Journal of Policy Modeling*, **34**, 879-889.
- Jones, P.J. and G.E. Whittle**, 1992: Computational fluid dynamics for building air flow prediction- Current status and capabilities. *Building and Environment*, **3**, 321-338.
- Kang, N.N., S.H. Cho and J.T. Kim**, 2012: The energy-saving effects of apartment residents' awareness and behavior. *Energy and Buildings*, **46**, 112-122.
- Kenisarin, M. and K. Mahkamov**, 2016: Passive thermal control in residential buildings using phase change materials. *Renewable and Sustainable Energy Reviews*, **55**, 371-398.
- Karyono, T.H.**, 2000: Report on thermal comfort and building energy studies in Jakarta – Indonesia. *Building and Environment*, **35**(1), 77-90.
- Khedari, J., N. Yamtraipat, N. Pratintong, and J. Hirulabh**, 2000: Thailand ventilation comfort chart. *Energy and Buildings*, **32**(3), 245-249.
- Khedari, J., J. Waewsak, S. Thepa and J. Hirunlabh**, 2000: Field investigation of night radiation cooling under tropical climate. *Renewable Energy*, **20**, 183-193.
- Khedari, J., M. Rungsiyopas, R. Sarachitti and J. Hirunlabh**, 2004: An new type of vented concrete block for zero cooling energy. *Building and Environment*, **39**, 1193-1197
- Kim, G., H.S. Lim, T.S. Lim, L. Schaefer and T.J. Kim**, 2012: Comparative advantage of an exterior shading devices in thermal performance for residential buildings. *Energy and Buildings*, **46**, 105-111.
- Koenigsberger, O.H., T.G. Ingersoll, A. Mayhew, and S.V. Szokolay**, 1974: *Manual of Tropical Housing and Building. Part 1: Climatic Design*. Longman Group Limited, London.
- Kowaltowski, D.C.C.K., W.V. da Rosa, A.M.G.P. Silvia**, 2007: Tradition and thermal performance: An investigation of New-Vernacular Dwellings in Campinas, Brazil. *TDSR Volume XVII Number II*, 79-92.
- Kubota, T. and D.H.C. Toe**, 2010: Potential of passive cooling techniques for modern houses in tropical climate of Malaysia: analysis of indoor thermal environment with various ventilation strategies. *International Journal of Ventilation*, **9**(1), 11-23.
- Kubota, T., D.H.C. Toe, and S. Ahmad**, 2009: The effects of night ventilation technique on indoor thermal environment for residential buildings in hot-humid climate of Malaysia. *Energy and Buildings*, **41**(8), 829-839.

- Kubota**, T., M.A. Zakaria, S. Abe and D.H.C. Toe, 2017: Thermal function of internal courtyards in traditional Chinese shophouse in the hot-humid climate of Malaysia. *Building and Environment*, **112**, 115-131.
- Kunto**, H., 1986: *Semerbak Bunga di Bandung Raya*. Granesia, Bandung.
- Kwok**, A.G. and N.B. Rajkovich, 2010: Addressing climate change in comfort standards. *Building and Environment*, **45**, 18-22.
- Labaki**, L.C. and D.C.C.K. Kowaltowski, 1998: Bioclimatic and Vernacular Design in Urban Settlements of Brazil, *Building and Environment*, **33**, 63-77.
- Lam**, J.C., 2000: Residential sector air conditioning loads and electricity use in Hong Kong. *Energy Conversion and Management*, **41**, 1757-1768.
- Laussmann**, D and D. Helm, 2011: Air change measurement using tracer gas. *Chemistry, Emission Control, Radioactive Pollution and Indoor Air Quality*, Mazzeo NA (Ed.), InTech, Rijeka, Croatia.
- Lei**, J., K. Kumarasamy, K.T. Zingre, J. Yang, M.P. Wan and W. Yang, 2017: Cool colored coating and phase change materials as complementary cooling strategies for building cooling load reduction in tropics.
- Liping**, W. and N.H. Wong, 2007: The impacts of ventilation strategies and façade on indoor thermal environment for naturally ventilated residential buildings in Singapore. *Building and Environment*, **42**, 4006-4015.
- Liping**, W., N.H. Wong and S. Li, 2007: Façade design optimization for naturally ventilated residential buildings in Singapore. *Energy and Buildings*, **39**, 954-961.
- Manu**, S., Y. Shukla, R. Rawal, L.E. Thomas and R. de Dear, 2016: Field studies of thermal comfort across multiple climate zones for the subcontinent: India Model for Adaptive Comfort (IMAC). *Building and Environment*, **98**, 55-70.
- McDonald** P. A population projection for Indonesia, 2010-2035, 2014: *Bulletin of Indonesian Economic Studies*; **50**(1), 123-29
- Ministry of Energy and Mineral Resources**, 2010: Handbook of Energy and Economic Statistics of Indonesia 2010. Ministry of Energy and Mineral Resources, Jakarta, Indonesia.
- Ministry of Energy and Mineral Resources**, 2014: Handbook of Energy and Economic Statistics of Indonesia 2014. Ministry of Energy and Mineral Resources, Jakarta, Indonesia.
- Ministry of Finance**, 2015: *Peraturan Menteri Keuangan No. 269/PMK.010/2015 tentang Batasan Harga Jual Unit Hunian Rumah Sederhana Milik (Rusunami) dan Penghasilan bagi Orang Pribadi yang Memperoleh Unit Hunian Rumah Susun Sederhana Milik*. Ministry of Finance, Jakarta, Indonesia
- Ministry of Public Works**, 2012: *Rusunawa, Komitmen Bersama Penanganan Permukiman Kumuh*. Ministry of Public Works, Jakarta, Indonesia.
- Ministry of Public Works**, 2014: *Peraturan Menteri Pekerjaan Umum No 05/PRT/M/2007 tentang Pedoman Teknis Pembangunan Rumah Susun Sederhana Bertingkat Tinggi*. Ministry of Public Works, Jakarta, Indonesia.

- Ministry of Public Works and Housing**, 2015: *Peraturan Menteri Nomor 20/PRT/M/2015 tentang Perubahan atas Peraturan Menteri Pekerjaan Umum dan Perumahan Rakyat No. 20/PRT/M/2014 tentang Fasilitas Likuiditas Pembiayaan Perumahan Dalam Rangka Perolehan Rumah Melalui Kredit/Pembiayaan Pemilikan Rumah Sejahtera bagi Masyarakat Berpenghasilan Rendah*. Ministry of Public Works and Housing, Jakarta, Indonesia.
- Ministry of Public Works and Housing**, 2016: *Keputusan Menteri No. 552/KPTS/M/2016 tentang Batasan Penghasilan Kelompok Sasaran KPR Bersubsidi, Batasan Harga Jual Rumah Sejahtera Tapak dan Satuan Rumah Sejahtera Susun, serta Besaran Subsidi Bantuan Uang Muka Perumahan*. Ministry of Public Works and Housing, Jakarta, Indonesia.
- Mirahimi**, S., M.F. Mohamed, L.C. Haw, N.L. Nik Ibrahim, W.F.M. Yusoff and A. Aflaki, 2016: The effect of building envelope on the thermal comfort and energy saving for high-rise buildings in hot-humid climate. *Renewable and Sustainable Energy Reviews*, **53**, 1508-1519.
- Moran**, M.J., H.N. Shapiro, D.D. Boettner and M.B. Bailey, 2011: *Fundamentals of Engineering Thermodynamics Seventh Edition*. John Wiley & Sons, United States of America.
- Mishra**, A.K. and M. Ramgopal, 2013: Field study on human thermal comfort – An overview. *Building and Environment*, **64**, 94-106.
- Mishra**, A.K. and M. Ramgopal, 2015: An adaptive thermal comfort model for the tropical climatic regions of India (Köppen climate type A). *Building and Environment*, **85**, 134-143.
- Mitchell**, R., C. Kohler, L. Zhu, D. Arasteh, J. Carmody, C. Huizenga, and D. Cuicija, 2011: *THERM 6.3/WINDOW 6.3 NFRC Simulation Manual*. LBNL Report 48255. Lawrence Berkeley National Laboratory, California.
- Mujianto**, S. and G. Tiess, 2013: Secure energy supply in 2025: Indonesia's need for an energy policy. *Energy Policy*, **62**, 31-41.
- Nguyen**, A., M.K. Singh, and S. Reiter, 2012: An adaptive thermal comfort model for hot humid South-East Asia. *Building and Environment*, **56**, 291-300.
- Nguyen**, A., Q. Tran, D. Trand and S. Reiter, 2011: An investigation on climate responsive design strategies of vernacular housing in Vietnam, *Building and Environment*, **46**, 2088-2106.
- Nguyen**, A.T. and S. Reiter, 2012: An investigation on thermal performance of a low cost apartment in hot-humid climate in Danang. *Energy and Buildings*, **47**, 237-246.
- Nicol**, F., 2004: Adaptive thermal comfort standards in the hot-humid tropics. *Energy and Buildings*, **36**(7), 628-637.
- Nicol**, J.F. and M.A. Humphreys, 2002: Adaptive thermal comfort and sustainable thermal standards for buildings. *Energy and Buildings*, **34**(6), 563-572.
- Nicol**, F. and M. Humphreys, 2010: Derivation of the adaptive equations for thermal comfort in free-running buildings in European standard EN15251. *Building and Environment*, **45**(1), 11-17.
- Nicol**, F., M. Humphreys, and S. Roaf, 2012: *Adaptive Thermal Comfort: Principles and Practice*. Routledge, London and New York.

- Nielsen, P.V.**, 2015: Fifty years of CFD for room air distribution. *Building and Environment*, **91**, 78-90.
- Nugroho, A.M.**, 2012: A thermal assessment of the traditional house in Flores, Indonesia. *Journal of Basic and Applied Scientific Research*, **2(12)**, 12795-12801.
- Nurfindarti, E. and Zulkaidi, D.**, 2015: Strategi pengelolaan cagar budaya Kota Bandung. *Jurnal Perencanaan Wilayah dan Kota B*, **4(1)**, 83-103
- Ohashi, M.**, 2017: *Investigation of energy-saving techniques by passive cooling strategies for modern houses in hot-humid climate of Malaysia*, Master's thesis (unpublished), Hiroshima University, Hiroshima, Japan.
- Olgyay, V.**, 1963: *Design with Climate: Bioclimatic Approach to Architectural Regionalism*. Princeton University Press, New Jersey.
- Omrani, S., V. Garcia-Hansen, B. Capra and R. Drogemuller**, 2017: Natural ventilation in multi-storey buildings: Design process and review of evaluation tools. *Building and Environment*, **116**, 182-194.
- Oliver, P.**, 2006: *Built to Meet Needs: Cultural Issues in Vernacular Architecture*. Architectural Press, Oxford.
- Orosa, J.A, A.C. Oliveira**, 2011: A new thermal comfort approach comparing adaptive and PMV models. *Renewable Energy*, **36**, 951-956.
- Passchier, C.**, 2007: Colonial Architecture in Indonesia, References and Developments, In *The past in the present, Architecture in Indonesia*, Ed. Nas, J.M. Leiden: KITLV Press.
- Peren, J.I., T. van Hoff, B.C.C. Leite and B. Blocken**, 2015: CFD analysis of cross ventilation of a generic isolated building with asymmetric opening positions: Impact of roof angle and opening location. *Building and Environment*, **85**, 263-276.
- Pires, L., Silva, P.D., and Castro Gomes, J.P.**, 2013: Experimental study of an innovative element for passive cooling of buildings. *Sustainable Energy Technologies and Assessments*, **4**, 29-35.
- Prajongsan, P. and S. Sharples**, 2012: Enhancing natural ventilation, thermal comfort and energy savings in high-rise residential buildings in Bangkok through the use of ventilation shafts. *Building and Environment*, **50**, 104-113.
- Previtali, J.M. and Z. Zhai**, 2016: Short communication, A taxonomy of vernacular architecture, An addendum to "Ancient vernacular architecture: Characteristics categorization and energy performance evaluation" (Zhai and Previtali, 2010). *Energy and Buildings*, **110**, 71-78.
- Priyadarsini R., K.W. Cheong, and N.H. Wong**, 2004: Enhancement of natural ventilation in high-rise residential buildings using stack system. *Energy and Buildings*, **36**, 61-71.
- Rajapakhsa, I, H. Nagai and M. Okumiya**, 2003: A ventilated courtyard as a passive cooling strategy in the warm humid tropics. *Renewable Energy*, **28**, 1755-1778.
- Ramponi, R. and B. Blocken**, 2012: CFD simulation of cross-ventilation for a generic isolated building: Impact of computational parameters. *Building and Environment*, **53**, 34-48.
- Rastogi, V., E. Tamboto, D. Tong and T. Sinburimsit**, 2013: *Asia's Next Big Opportunity:*

- Indonesia's Rising Middle-Class and Affluent Consumers*. The Boston Consulting Group.
- Roaf, S.**, with M. Fuentes and S. Thomas-Rees, 2013: *Ecohouse: A Design Guide, fourth ed.* Routledge, London and New York.
- Roslan, Q.**, S.H. Ibrahim, R. Affandi, M.N. Mohd Nawi and A. Baharun, 2016: A literature review on the improvement strategies of passive design for the roofing system of the modern house in a hot and humid climate region. *Frontiers of Architectural Research*, **5**, 126-133.
- Sabzi, D.**, *et al.*, 2015: Investigation of cooling load in buildings by passive cooling options applied on roof. *Energy and Buildings*, **109**, 135-142.
- Sadafi, N.**, E. Salleh, C.H. Lim, and Z. Jaafar, 2011: Evaluating thermal effects of internal courtyard in a tropical terrace house by computational simulation. *Energy and Buildings*, **43**, 887-893.
- Santamouris, M.** (ed.), 2007: *Advances in Passive Cooling*. Earthscan, London, UK and Sterling, US.
- Santamouris, M.**, 2016: Cooling the buildings-past, present and future. *Energy and Buildings*, **128**, 617-638.
- Santamouris, M.**, *et al.*, 2007: Recent progress on passive cooling techniques, advanced technological developments to improve survivability levels in low-income households. *Energy and Buildings*, **39**, 859-866.
- Sfakianaki, A** *et al.*, 2008: Air tightness measurements of residential houses in Athens, Greece. *Building and Environment*, **42**, 398-485.
- Shanthi Priya, R.**, M.C. Sundarraja, S. Radhakrishnan and L. Vijayalakshmi, 2012: Solar passive techniques in the vernacular buildings of coastal regions in Nagapattinam, Tamilnadu, India-A qualitative and quantitative analysis. *Energy and Buildings*, **49**, 50-61.
- Surahman, U.** and T. Kubota, 2012: Life cycle energy and CO2 emissions in unplanned buildings of Indonesia. *PLEA2012*, Lima, Peru.
- Swami, M.V.** and S. Chandra, 1987: *Procedures for Calculating Natural Ventilation Airflow Rates in Buildings*. Florida Solar Energy Center, Florida, United States of America.
- Szokolay, S.V.**, 2004: *Introduction to Architectural Science: The Basis of Sustainable Design*. Architectural Press, Oxford.
- The World Bank**, 2011: *Indonesia Economic Quarterly: 2008 again?*. The World Bank, Washington DC.
- The World Bank**, 2012: *Indonesia Economic Quarterly: Maintaining resilience*. The World Bank, Washington DC.
- Toe, D.H.C.** and T. Kubota, 2013: Development of an adaptive thermal comfort equation for naturally ventilated buildings in hot-humid climates using ASHRAE RP-884 database. *Frontiers of Architectural Research*, **2**, 278-291.
- Toe, D.H.C.**, 2013: *Application of passive cooling techniques to improve indoor thermal comfort of modern urban houses in hot-humid climate of Malaysia*, PhD thesis (unpublished), Hiroshima University, Hiroshima, Japan.

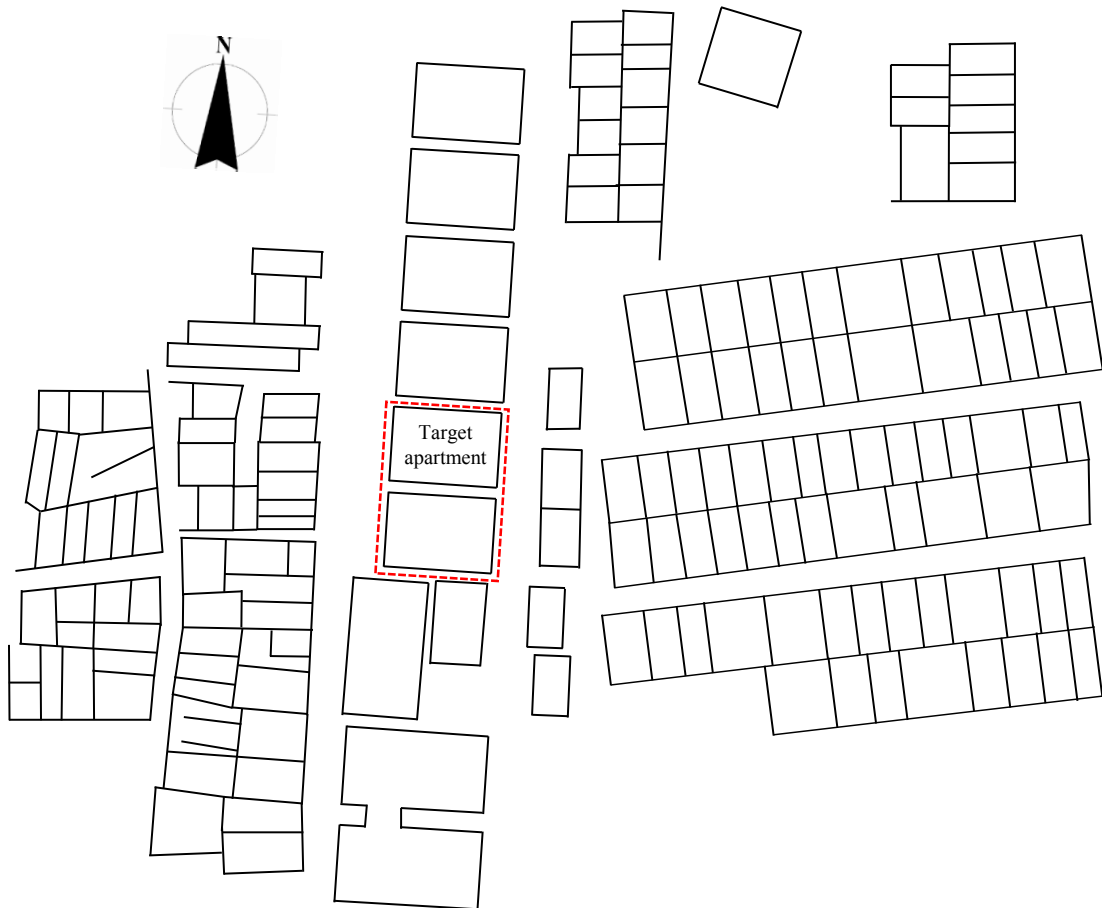
- Toe**, D.H.C. and T. Kubota, 2015: Comparative assessment of vernacular passive cooling techniques for improving indoor thermal comfort of modern terraced houses in hot-humid climate of Malaysia. *Solar Energy*, **114**, 229-258.
- UNEP**, 2009: *Buildings and Climate Change, Summary for decision-makers*. UNEP, Paris, France.
- Van Dullemen**, C.J., 2012: *Tropical Modernity, Life and Work of C.P. Wolf Schoemaker*. Sun, Amsterdam, Netherland.
- Vangtook**, P. and S. Chirattananon, 2007: Application of radiant cooling as a passive cooling option in hot humid climate. *Building and Environment*, **42**, 543-556.
- Veersteeg**, H.K. and W. Malalasekera, 2007: *Introduction to computational fluid dynamics: The finite volume method Second Edition*. Pearson Education Ltd., Edinburgh, United Kingdom.
- Voskuil**, R.P.G.A., *et al.*, 1996: *Bandoeng, Beeld van een stad*. Asia Maior.
- Wan Ismail**, W.H. and J.R. Nadarajah, 2016: Young visitors in the city: Their perceptions of Heritage Buildings. *Procedia Social and Behavioral Science*, **234**, 470-477.
- Wibowo**, A.S., 2015: Understanding the design approach of colonial churches: De Nieuwe Kerk and De Oosterkerk in Bandung. *Procedia Social and Behavioral Science*, **184**, 380-387.
- Widodo**, J. (2007) Modern Indonesian architecture: Transplantation, adaptation, accommodation and hybridization. In *The past in the present, Architecture in Indonesia*. Ed. Nas, J.M. Leiden: KITLV Press.
- Wijaya**, E. and T. Tezuka, 2013: A comparative study of households' electricity consumption characteristics in Indonesia: A techno-socioeconomic analysis. *Energy for Sustainable Development*, **17**, 596-604.
- Wong** N.H. and S. Li, 2007: A study of effectiveness of passive climate control in naturally ventilated residential buildings in Singapore. *Building and Environment*, **42**, 1395-1405.
- Wuisman**, J.J.J.M., 2007: The past in the present, the place and role of Indonesian vernacular architecture traditions and building styles of the past in the present. In *The past in the present, Architecture in Indonesia*. Ed. Nas, J.M. Leiden: KITLV Press.
- Yang**, W. and G. Zhang, 2008: Thermal comfort in naturally ventilated and air-conditioned buildings in humid subtropical climate zone in China. *International Journal of Biometeorology*, **52**(5), 385-398.
- Yang**, X., K. Hong, Y. Kang and T. Yao, 2015: Numerical investigation on the airflow characteristics and thermal comfort in buoyancy-driven natural ventilation rooms. *Energy and Buildings*, **109**, 255-266.
- Yao**, J., 2012: Energy optimization of building design for different housing units in apartment buildings. *Applied Energy*, **94**, 330-337.
- Yildiz**, Y. and Z.D. Arsan, 2011: Identification of the building parameters that influence heating and cooling energy loads for apartment buildings in hot-humid climates. *Energy*, **36**, 4287-4296.

- Zakaria**, M.A., 2017: *Energy-saving Modifications through Passive Cooling for Urban Houses in Hot-Humid Climate of Malaysia*, PhD thesis (unpublished), Hiroshima University, Hiroshima, Japan.
- Zhai**, Z. and J.M. Previtali, 2010: Ancient vernacular architecture: characteristics categorization and energy performance. *Energy and Buildings*, **42**, 357-365.
- Zhou**, D., Zhao, C.Y., and Tian, Y., 2012: Review on thermal energy storage with phase change materials (PCMs) in building applications. *Applied Energy*, **92**, 593-605.

Appendix A

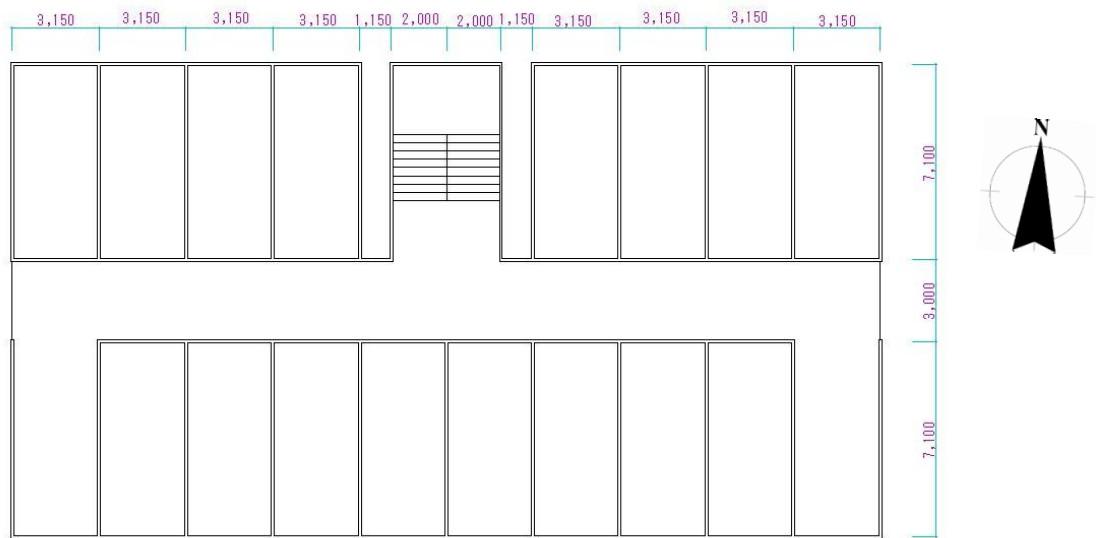
Floor plan and façade of case study apartments

1. Old public apartment

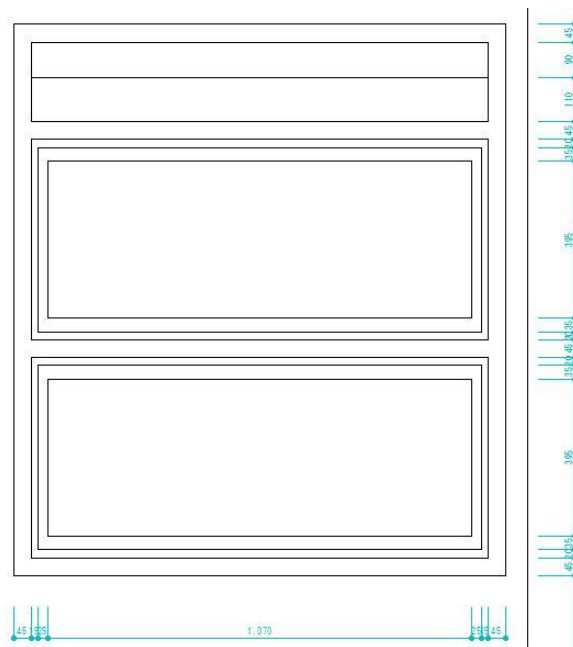


Location of the selected old public apartment and its surrounding

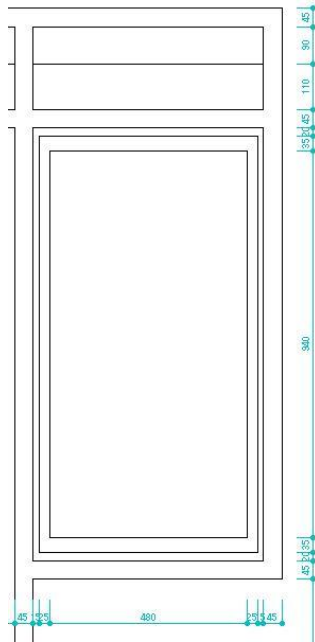
Floor plan and façade of case study apartments



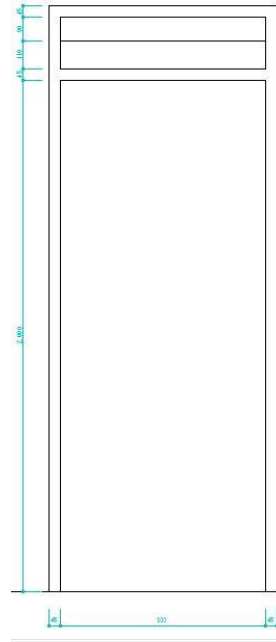
Floor plan of old public apartment (unit in mm)



Profile of front window in the unit of old public apartment (unit in mm)

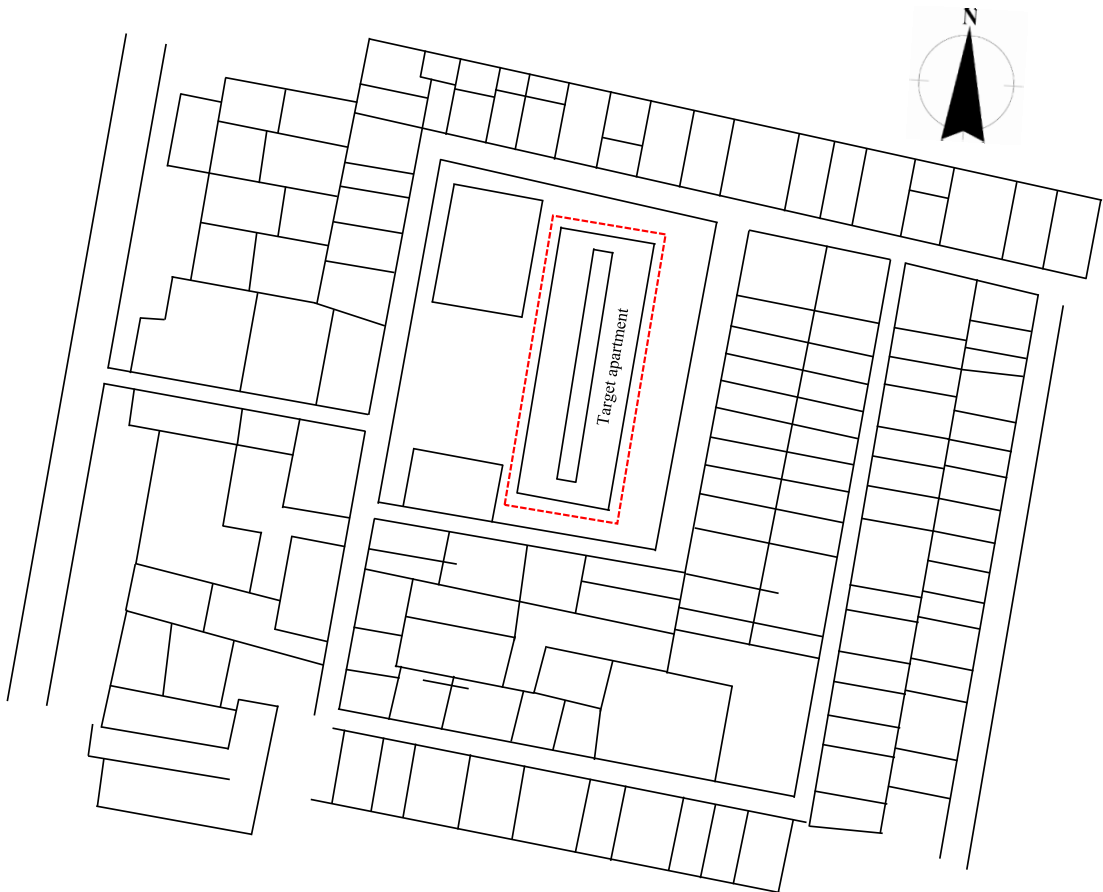


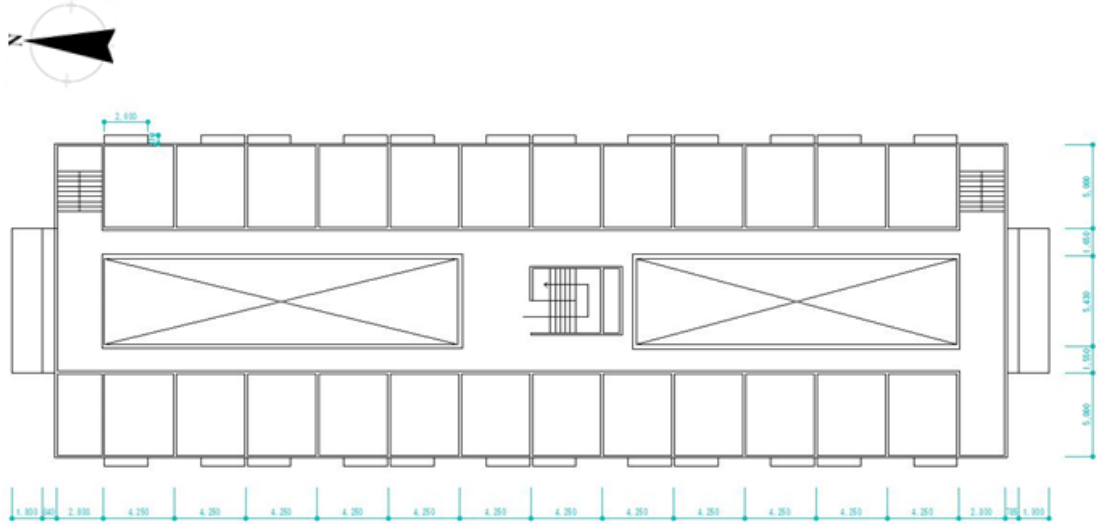
Profile of rear window in the unit of old public apartment (unit in mm)



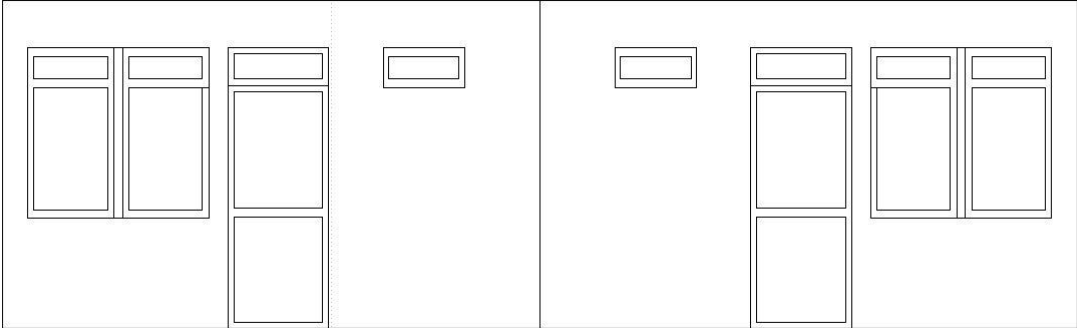
Profile of front/back doors in the unit of old public apartment (unit in mm)

2. New public apartment

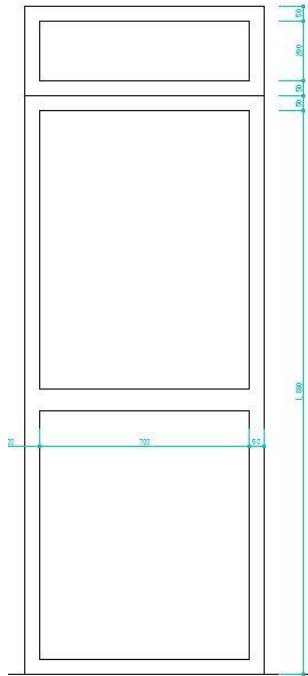




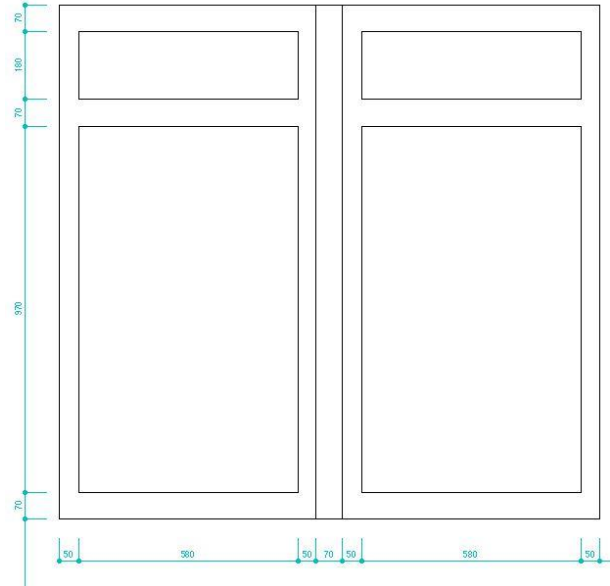
Floor plan of new public apartment (unit in mm)



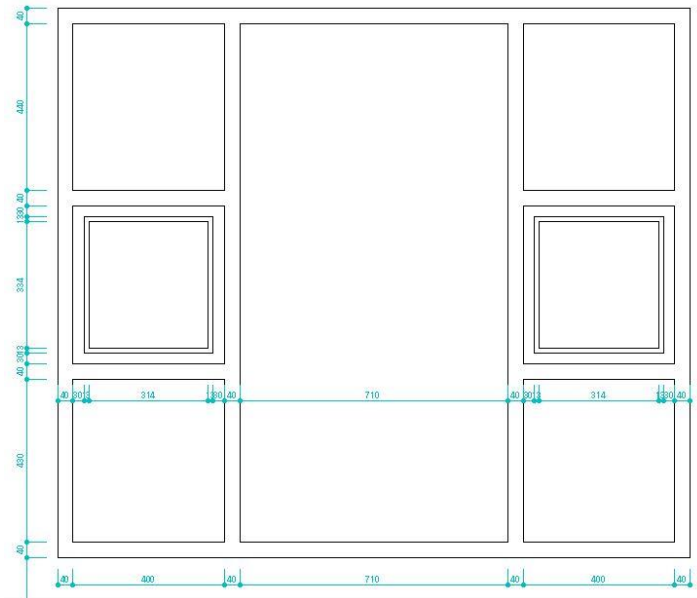
Front façade of new public apartment



Profile of front/back door in the unit of new public apartment

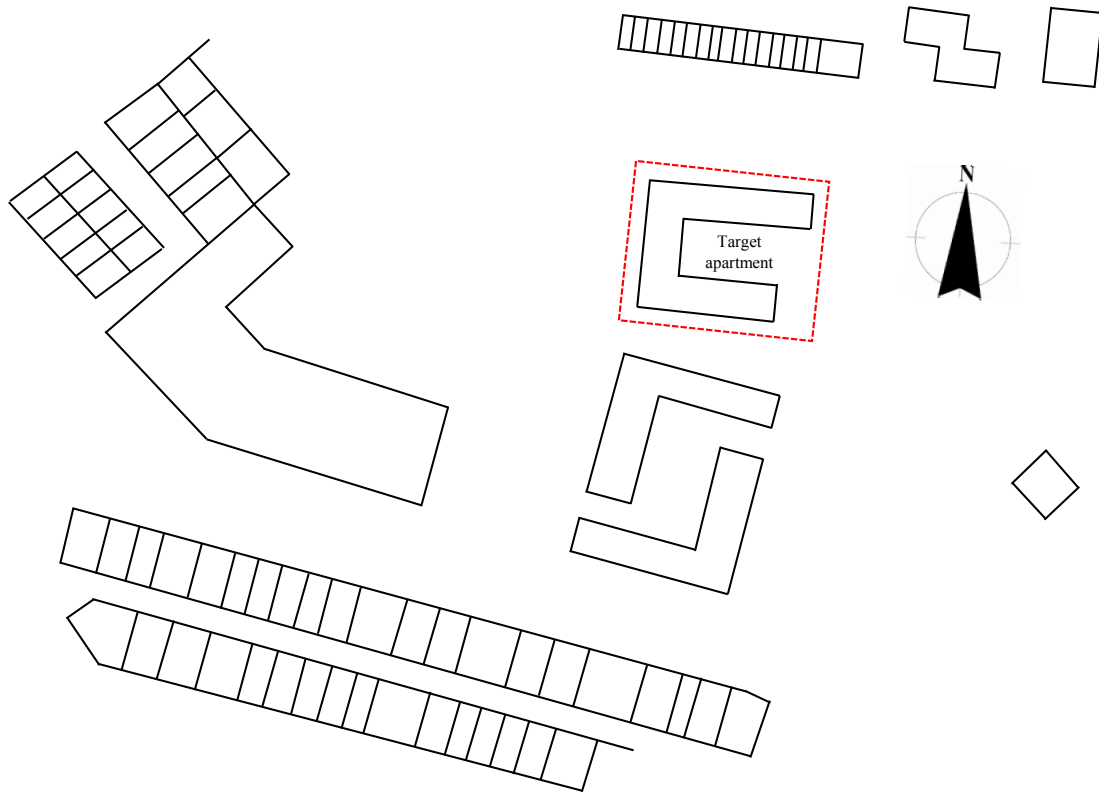


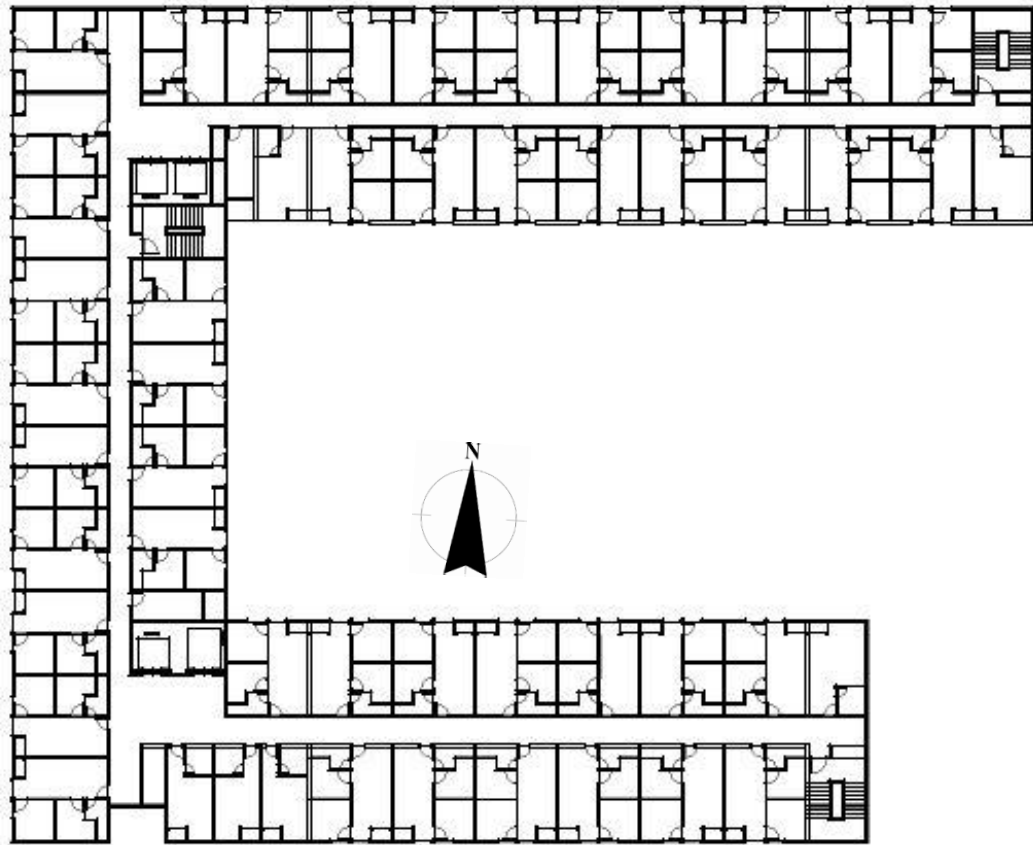
Profile of front window in the unit of new public apartment (unit in mm)



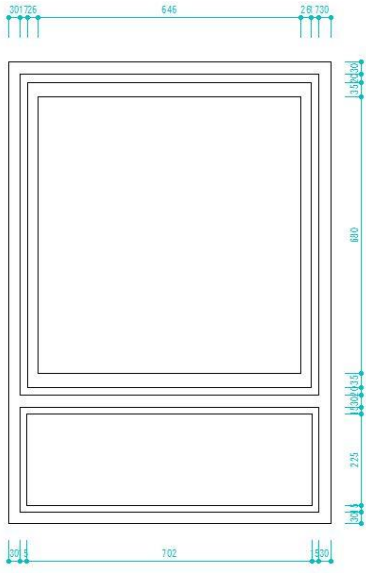
Profile of back window in the master bedroom of new public apartment (unit in mm)

3. Middle-class high-rise apartment (*Rusunami*)

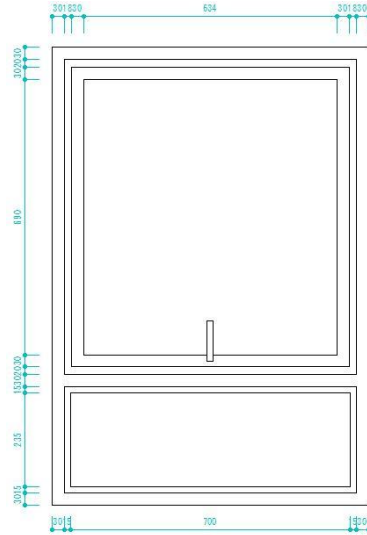




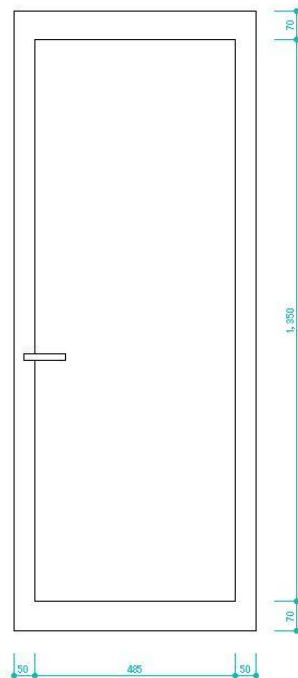
Floor plan of middle-class high-rise apartment



3
Profile of window in master bedroom of middle-class high-rise apartment (unit in mm)



Profile of window in living room of middle-class high-rise apartment (unit in mm)

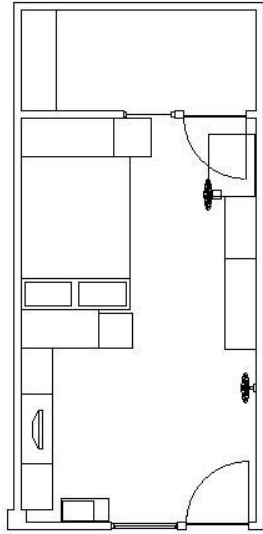


Profile of window in living room of middle-class high-rise apartment (unit in mm)

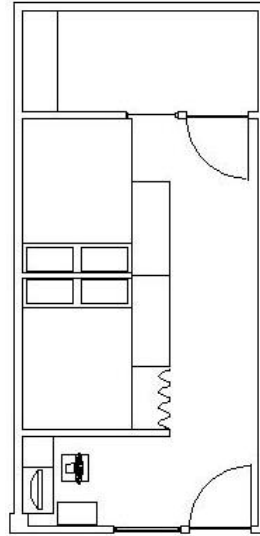
Appendix B

Drawing of occupied units of the public apartments

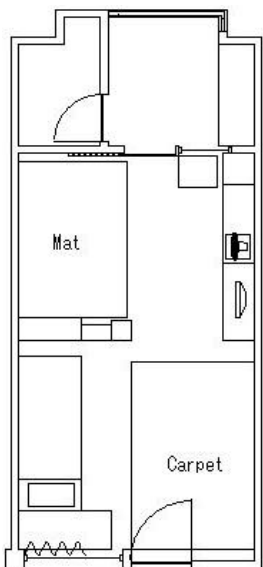
1. Old Public Apartment



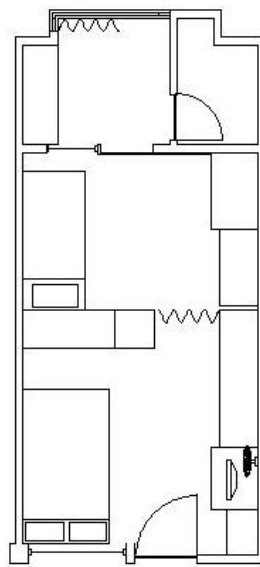
Unit C-302



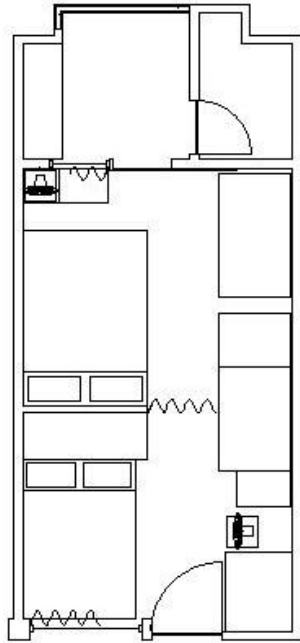
Unit C-407



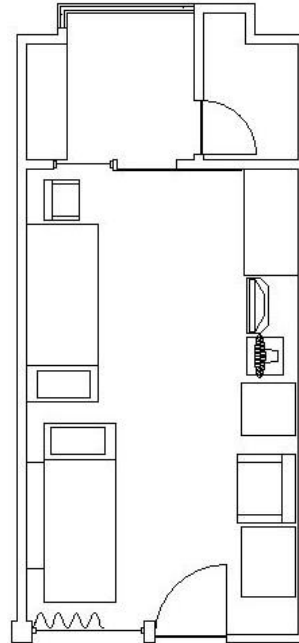
Unit E-208



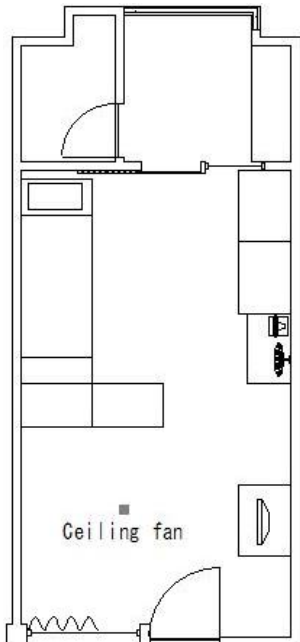
Unit E-212



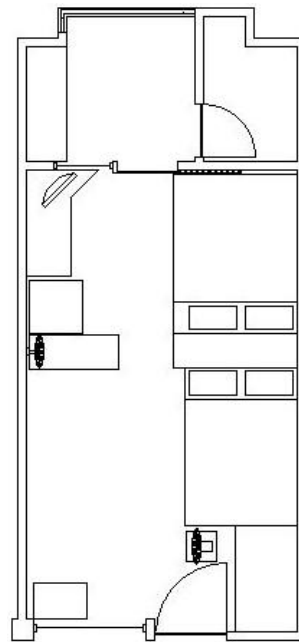
Unit E-214



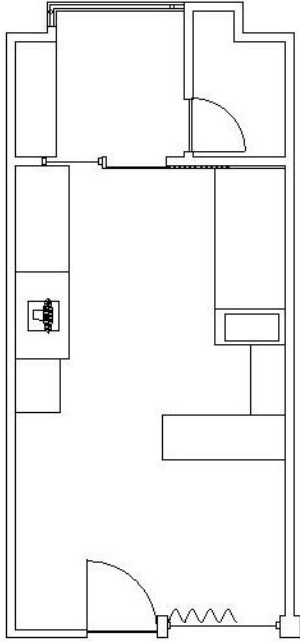
Unit E-304



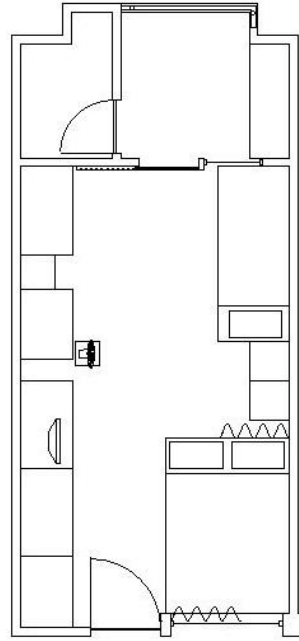
Unit E-306



Unit E-312

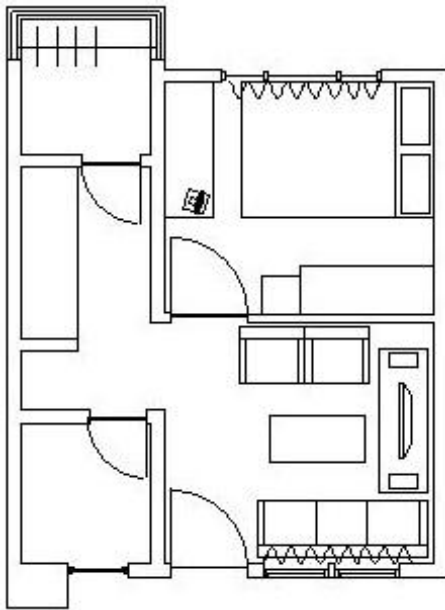


Unit E-401

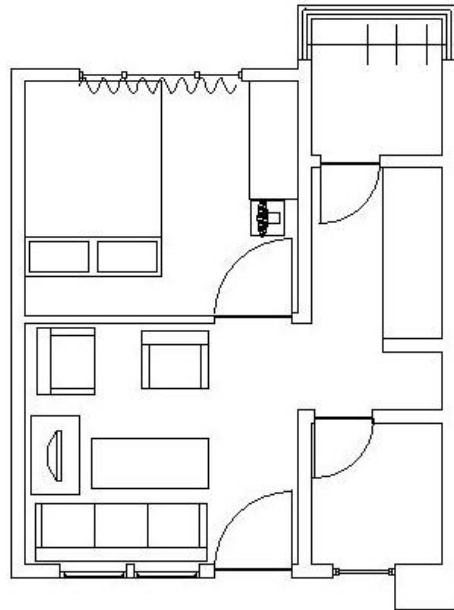


Unit E-415

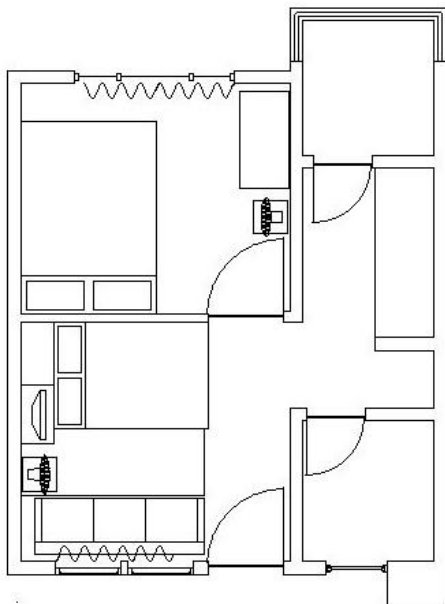
2. New Public Apartment



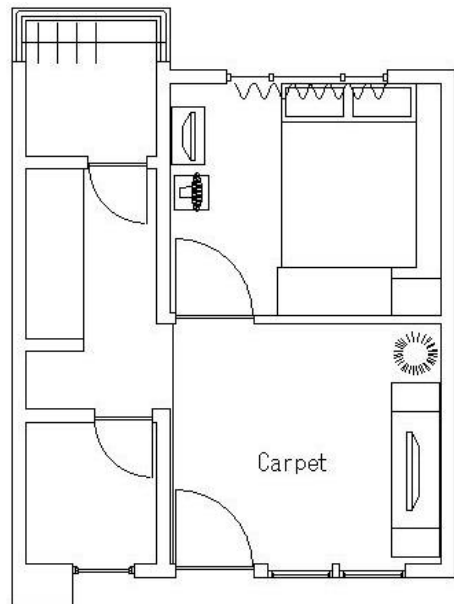
Unit J-308



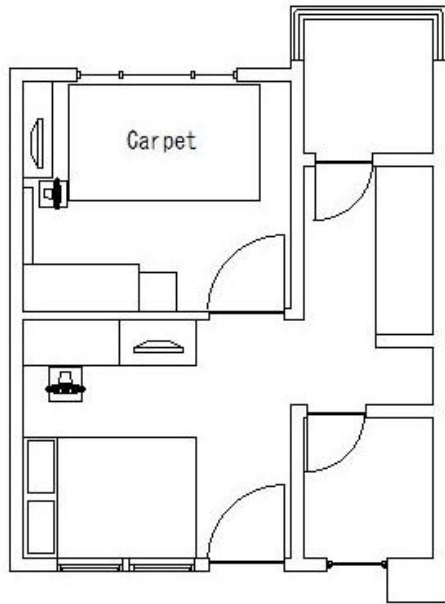
Unit G-203



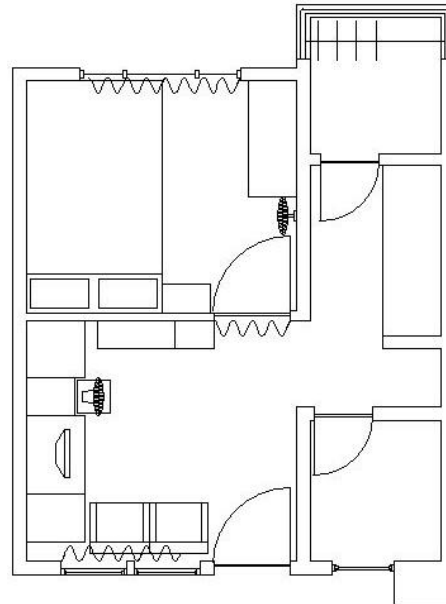
Unit G-205



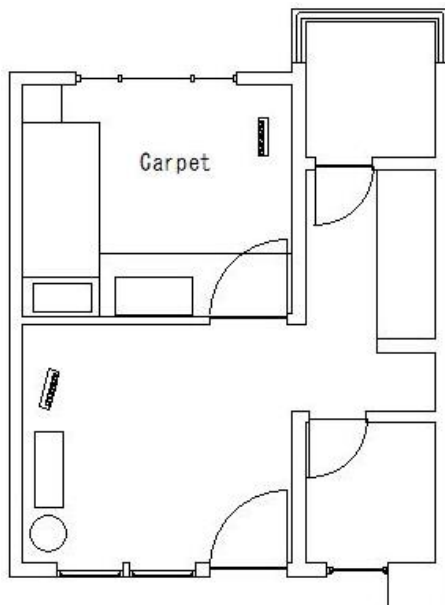
Unit G-216



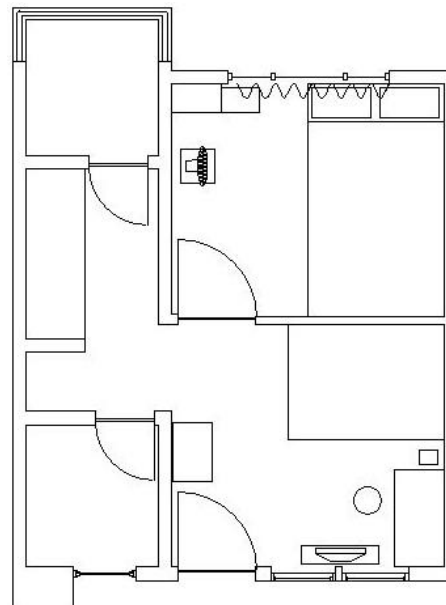
Unit G-301



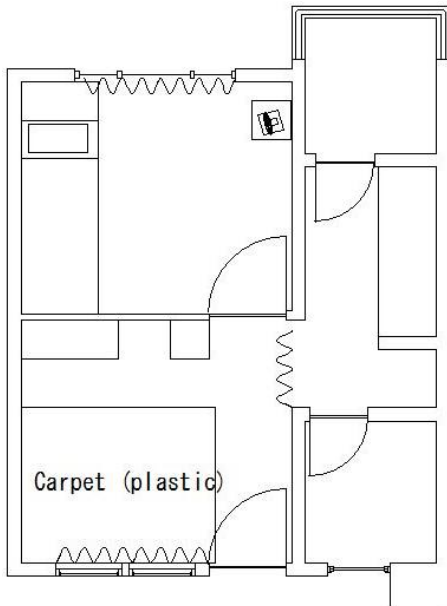
Unit G-313



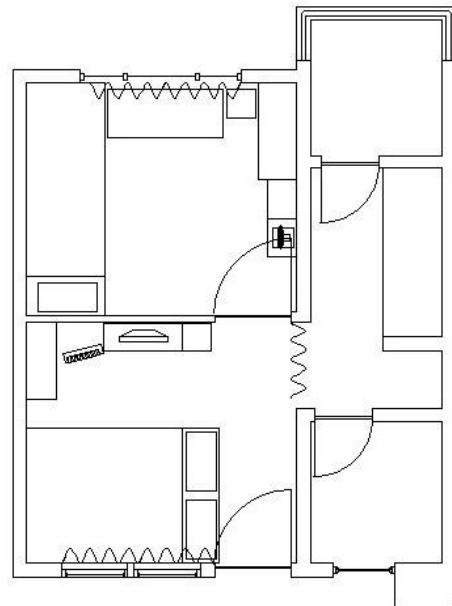
Unit G-407



Unit G-420



Unit G-507



Unit G-515

Appendix C

Questionnaires for occupied units of the public apartments

Questionnaire: Energy consumption and window opening behavior of the occupants of public apartments in Surabaya, Indonesia

Muhammad Nur Fajri Alfata

Naoto Hirata

Main Supervisor: Dr. Kubota Tetsu



Hiroshima University, Japan

Institut Teknologi Sepuluh Nopember (ITS), Surabaya, Indonesia

Universitas Brawijaya (UB), Malang, Indonesia

Mukogawa Women University, Japan

(All information from this questionnaire are confidential and use for the purpose of research only)

Questionnaires for occupied units of the public apartments

Date : Time : From to.....
 Interviewer :

Name of apartment:

Profile of occupants *(Circle the answer by the interviewer)*

(1) No	(2) Sex	(3) Age	(4) Relationship in family	(5) Ethnic	(6) Occupation	(7) Monthly Income
1						
2						
3						
4						

Code:

- | | | |
|-------------------------|---------------------------------|--|
| (2) M: Male / F: Female | (6) 1 Government employee | (7) Please write down the monthly income for each family members |
| (3) Write age | 2 Temporary government employee | |
| (4) 1 Husband | 3 Private employee | |
| 2 Wife | 4 Temporary private employee | |
| 3 Child | 5 Students | |
| 4 Son/daughter in law | 6 Others, | |
| (5) 1 Javanese | | |
| 2 Maduranese | | |
| 3 Chinese | | |
| 4 Others, | | |

Daily occupancy

Please select time you, at least one family member, stay in the house by using arrow sign

Example: One of family members stay in the house every day from 7 pm to 7 am.

Am					Pm										am											
6	7	8	9	0	1	1	1	1	1	1	1	1	1	1	1	2	2	2	2	2	2	1	2	3	4	5

←-----→

Daily occupancy:

Weekday																										
am					pm										am											
6	7	8	9	0	1	1	1	1	1	1	1	1	1	1	1	2	2	2	2	2	2	1	2	3	4	5

Weekend																									
am					pm										am										
6	7	8	9	0	1	1	1	1	1	1	1	1	1	1	2	2	2	2	2	2	1	2	3	4	5

Appendix C

Frequency of daily AC's usage

Living room:

Weekdays (Monday-Friday)

am							pm										am						
6	7	8	9	10	11	12	13	14	15	16	17	18	19	20	21	22	23	24	1	2	3	4	5

Weekends (Saturday-Sunday)

am							pm										am						
6	7	8	9	10	11	12	13	14	15	16	17	18	19	20	21	22	23	24	1	2	3	4	5

Master Bedroom

Weekdays (Monday-Friday)

am							pm										am						
6	7	8	9	10	11	12	13	14	15	16	17	18	19	20	21	22	23	24	1	2	3	4	5

Weekends (Saturday-Sunday)

am							pm										am						
6	7	8	9	10	11	12	13	14	15	16	17	18	19	20	21	22	23	24	1	2	3	4	5

Frequency of daily fan's usage

Living room:

Weekdays (Monday-Friday)

am							pm										am						
6	7	8	9	10	11	12	13	14	15	16	17	18	19	20	21	22	23	24	1	2	3	4	5

Weekends (Saturday-Sunday)

am							pm										am						
6	7	8	9	10	11	12	13	14	15	16	17	18	19	20	21	22	23	24	1	2	3	4	5

Master Bedroom

Weekdays (Monday-Friday)

am							pm										am						
6	7	8	9	10	11	12	13	14	15	16	17	18	19	20	21	22	23	24	1	2	3	4	5

Questionnaires for occupied units of the public apartments

Weekends (Saturday-Sunday)

am							pm								am								
6	7	8	9	10	11	12	13	14	15	16	17	18	19	20	21	22	23	24	1	2	3	4	5

Opening behavior (doors/windows)

1. Are you usually open the doors or windows when you stay in the house?

If yes, please write down when you usually open the doors or windows.

Opening: Windows/Doors (*)

Room:

Weekdays (Monday-Friday)

am							pm								am									
6	7	8	9	10	11	12	13	14	15	16	17	18	19	20	21	22	23	24	1	2	3	4	5	

Weekends (Saturday-Sunday)

am							pm								am									
6	7	8	9	10	11	12	13	14	15	16	17	18	19	20	21	22	23	24	1	2	3	4	5	

Opening: Windows/Doors (*)

Room:

Weekdays (Monday-Friday)

am							pm								am									
6	7	8	9	10	11	12	13	14	15	16	17	18	19	20	21	22	23	24	1	2	3	4	5	

Weekends (Saturday-Sunday)

am							pm								am									
6	7	8	9	10	11	12	13	14	15	16	17	18	19	20	21	22	23	24	1	2	3	4	5	

*) Select one of the options

Thermal comfort in the living room

Air temperature in the living room (or main room if there is only one room)

1. What do you feel related to the air temperature in the living room (or main room) during the daytime? (*Circle the desired answer*)

Hot	Warm	Slightly warm	Neutral	Slightly cool	Cool	Cold
-----	------	---------------	---------	---------------	------	------

2. Related to air temperature, what do you prefer during the daytime? (*Circle the desired answer*)

Much warmer	Warmer	No change	Cooler	Much cooler
-------------	--------	-----------	--------	-------------

3. What do you feel related to the air temperature in the living room (or main room) during the night-time? (*Circle the desired answer*)

Hot	Warm	Slightly warm	Neutral	Slightly cool	Cool	Cold
-----	------	---------------	---------	---------------	------	------

4. Related to air temperature, what do you prefer during the night-time? (*Circle the desired answer*)

Much warmer	Warmer	No change	Cooler	Much cooler
-------------	--------	-----------	--------	-------------

Wind flow in the living room (or main room if there is only one room)

5. What do you feel related to the wind flow in the living room (or main room) during the daytime? (*Circle the desired answer*)

Too breezy	Breezy	Slightly breezy	Neutral	Slightly still	Still	Too still
------------	--------	-----------------	---------	----------------	-------	-----------

6. What do you prefer related to the wind flow in the living room (or main room) during the daytime? (*Circle the desired answer*)

Much higher	Higher	Slightly higher	No change	Slightly lower	Lower	Much lower
-------------	--------	-----------------	-----------	----------------	-------	------------

7. What do you feel related to the wind flow in the living room (or main room) during the night-time? (*Circle the desired answer*)

Too breezy	Breezy	Slightly breezy	Neutral	Slightly still	Still	Too still
------------	--------	-----------------	---------	----------------	-------	-----------

8. What do you prefer related to the wind flow in the living room (or main room) during the night-time? (*Circle the desired answer*)

Much higher	Higher	Slightly higher	No change	Slightly lower	Lower	Much lower
-------------	--------	-----------------	-----------	----------------	-------	------------

Relative humidity in the living room (or main room if there is only one room)

9. What do you perceive related to relative humidity in the living room (or main room) during the daytime? (*Circle the desired answer*)

Too humid	Humid	Slightly humid	Neutral	Slightly dry	Dry	Too dry
-----------	-------	----------------	---------	--------------	-----	---------

10. What do you prefer related to the relative humidity in the living room (or main room) during the daytime? (*Circle the desired answer*)

Much more humid	More humid	No change	Less humid	Much less humid
-----------------	------------	-----------	------------	-----------------

11. What do you perceive related to relative humidity in the living room (or main room) during the night-time? (*Circle the desired answer*)

Too humid	Humid	Slightly humid	Neutral	Slightly dry	Dry	Too dry
-----------	-------	----------------	---------	--------------	-----	---------

12. What do you prefer related to the relative humidity in the living room (or main room) during the night-time? (*Circle the desired answer*)

Much more humid	More humid	No change	Less humid	Much less humid
-----------------	------------	-----------	------------	-----------------

Indoor air quality in the living room (or main room if there is only one room)

13. What do you think about the indoor air quality in the living room at the daytime? (*Circle the desired answer*)

Very bad	Bad	Slightly bad	Neutral	Slightly good	Good	Very good
----------	-----	--------------	---------	---------------	------	-----------

14. What do you think about the indoor air quality in the living room at the night-time?
(Circle the desired answer)

Very bad	Bad	Slightly bad	Neutral	Slightly good	Good	Very good
----------	-----	--------------	---------	---------------	------	-----------

General comfort in the living room (or main room if there is only one room)

15. How do you find the general comfort level during the daytime? (Circle the desired answer)

Very comfortable	Comfortable	Slightly comfortable	Neutral	Slightly uncomfortable	Uncomfortable	Very uncomfortable
------------------	-------------	----------------------	---------	------------------------	---------------	--------------------

16. How do you find the general comfort level during the night-time? (Circle the desired answer)

Very comfortable	Comfortable	Slightly comfortable	Neutral	Slightly uncomfortable	Uncomfortable	Very uncomfortable
------------------	-------------	----------------------	---------	------------------------	---------------	--------------------

Please feel free to write down your opinion about thermal comfort in your apartment unit

Thank you very much for your kind cooperation

Sketch (by interviewer)

Sketch of interior of apartment unit (living room and master bedroom, if possible)


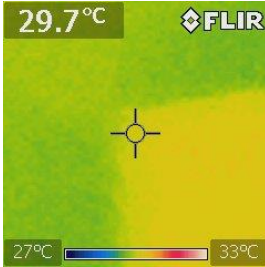

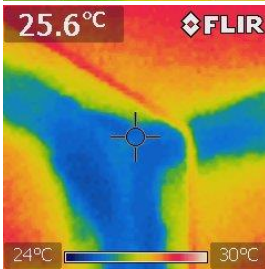
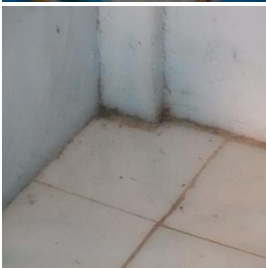
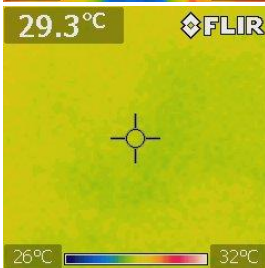

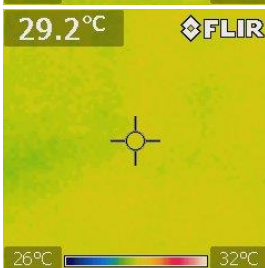

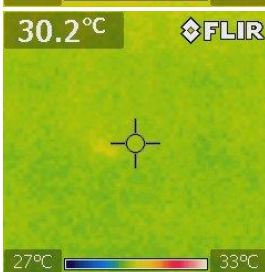
[Room arrangement, partition and dimension of space, furniture (particularly where AC placed in) and the location of window]




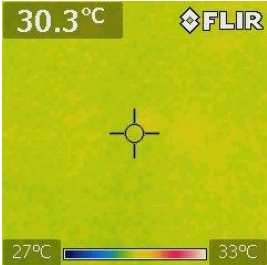

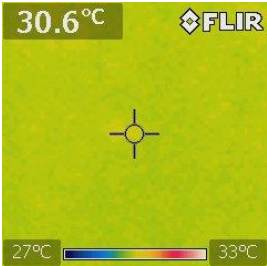

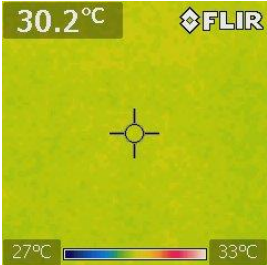
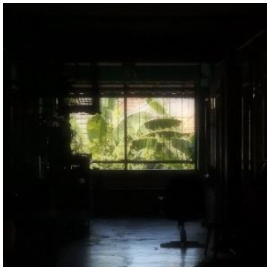
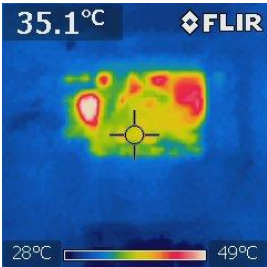
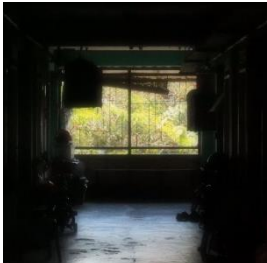
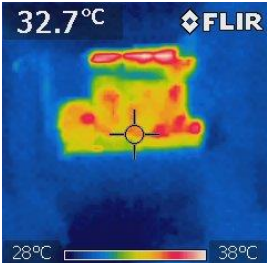
Appendix D


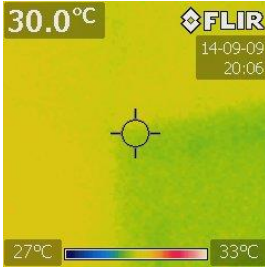

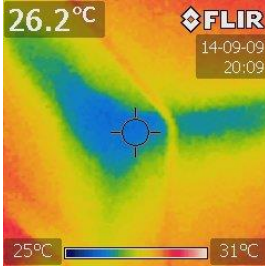

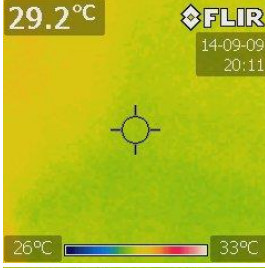

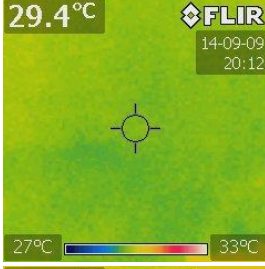

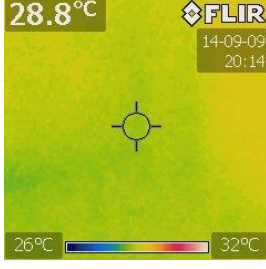
Surface temperatures of the walls in the three types of apartments using thermal camera

Appendix D

Apartment type	Time	Location	Thermal viewer
Old public apartment	12:00		
			
			
			
			


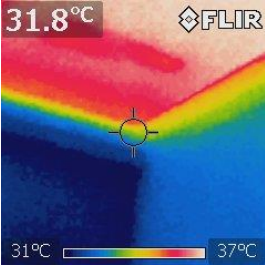

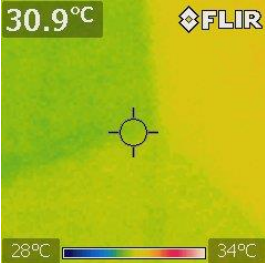

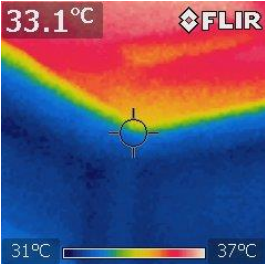

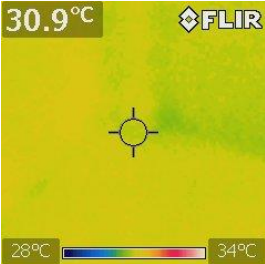

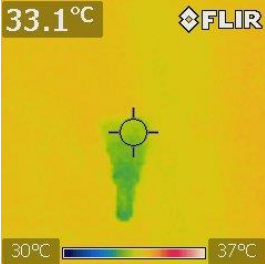
Surface temperatures of the walls in the three types of apartments using thermal camera

Apartment type	Time	Location	Thermal viewer
			
			
			
			
			


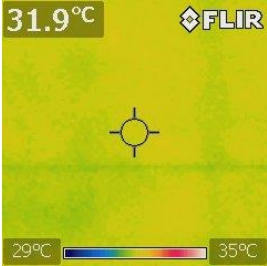

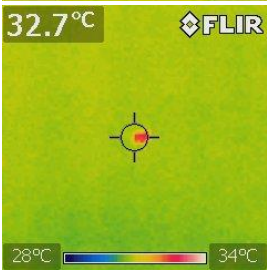

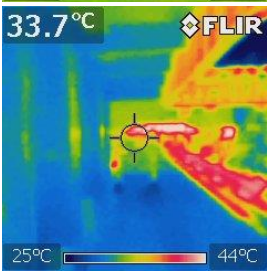
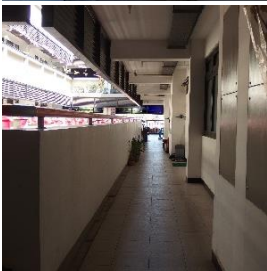
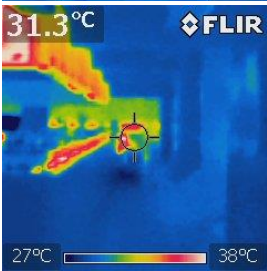
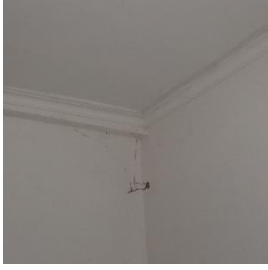
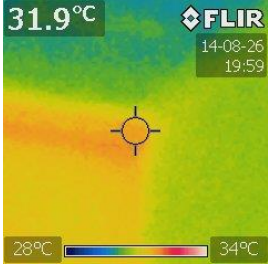
Apartment type	Time	Location	Thermal viewer
	20:00		
			
			
			
			

Surface temperatures of the walls in the three types of apartments using thermal camera

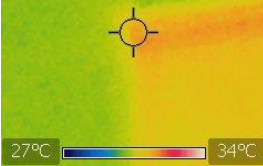
Apartment type	Time	Location	Thermal viewer
			
			
			
			
			

Apartment type	Time	Location	Thermal viewer
New public apartment	15:00		
			
			
			
			


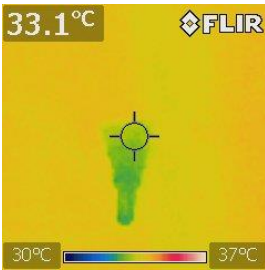

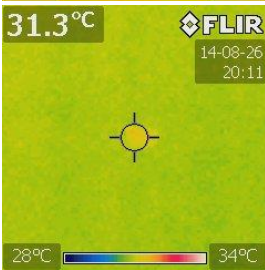

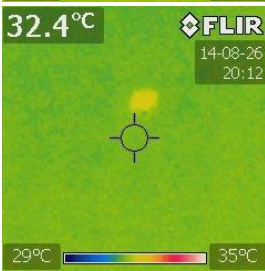

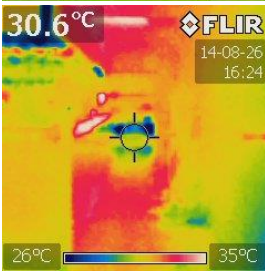

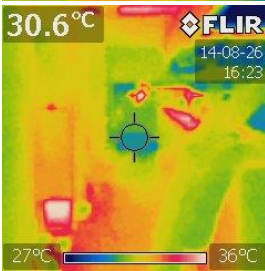
Surface temperatures of the walls in the three types of apartments using thermal camera

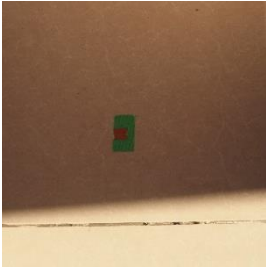
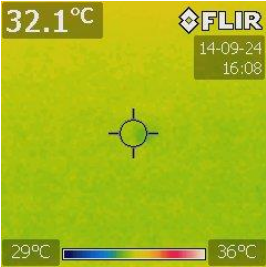
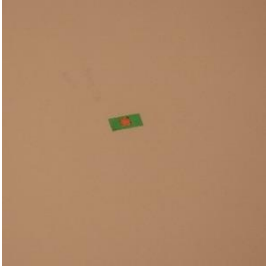
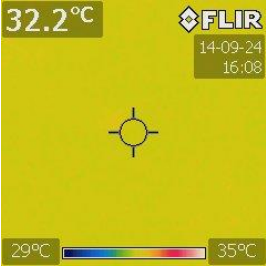

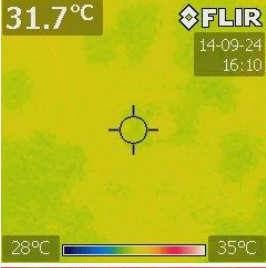

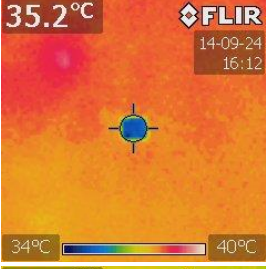
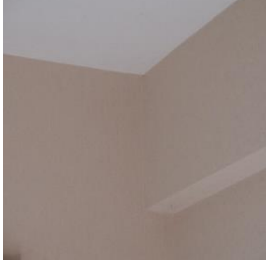
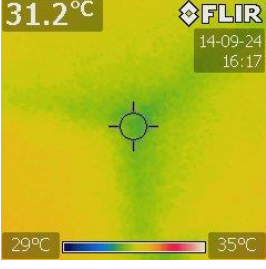
Apartment type	Time	Location	Thermal viewer
			
			
			
			
	20:00		

Appendix D


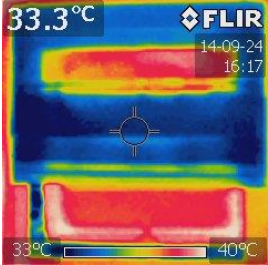

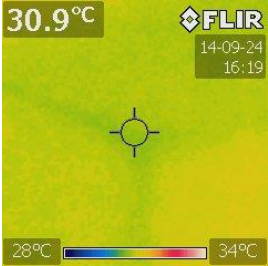

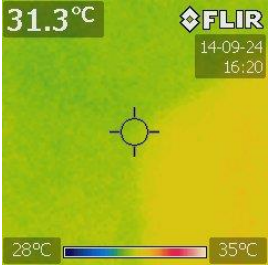

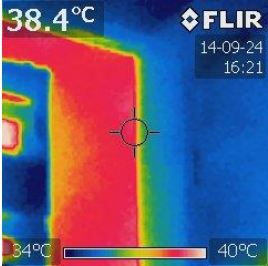

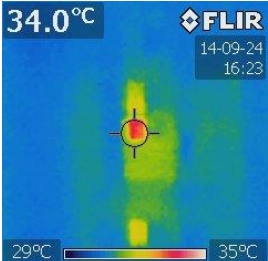
Apartment type	Time	Location	Thermal viewer
	30.7°C	FLIR 14-08-26 20:00	
	30.8°C	FLIR 14-08-26 20:02	
	30.4°C	FLIR 14-08-26 20:02	
	30.8°C	FLIR 14-08-26 20:05	
	30.6°C	FLIR 14-08-26 20:05	


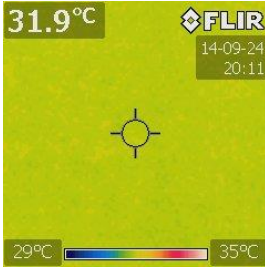

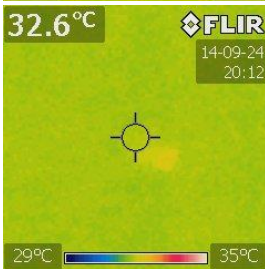

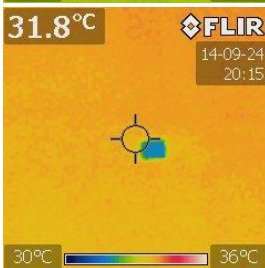

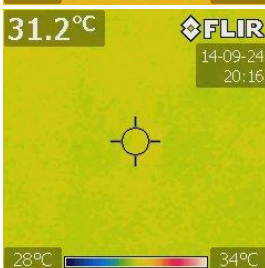
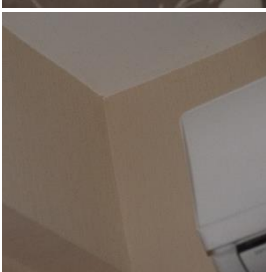
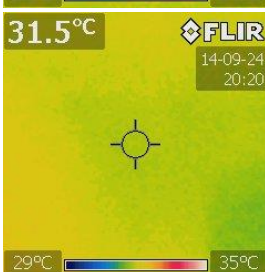
Surface temperatures of the walls in the three types of apartments using thermal camera

Apartment type	Time	Location	Thermal viewer
			
			
			
			
			


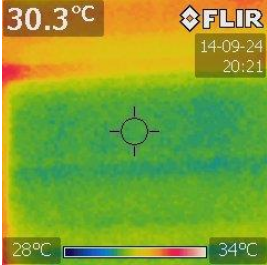

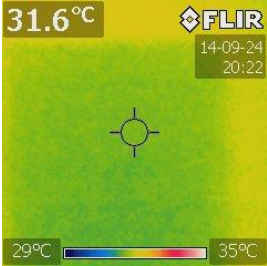


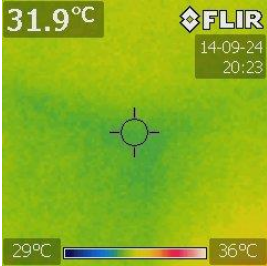

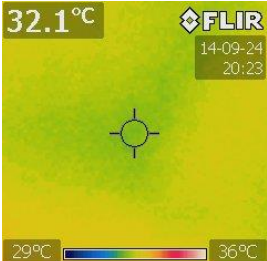
Apartment type	Time	Location	Thermal viewer
Middle-class high-rise apartment	12:00		
			
			
			
			

Surface temperatures of the walls in the three types of apartments using thermal camera




Apartment type	Time	Location	Thermal viewer
			
			
			
			
			

Apartment type	Time	Location	Thermal viewer
	08:00		
			
			
			
			

Surface temperatures of the walls in the three types of apartments using thermal camera

Apartment type	Time	Location	Thermal viewer
			
			
			
			
			

Appendix D

Apartment type	Time	Location	Thermal viewer
	31.5°C	FLIR	14-09-24 20:24
	31.9°C	FLIR	14-09-24 20:24
	30.5°C	FLIR	14-09-24 20:26

Appendix E

Complete results of Multiple Regression Analysis using Enter-method

1. Including outdoor air temperature (Out_AT)

Time	R^2		Adj. R^2		Independent variables	β		r	
0:00	.601	**	.437	**	Outdoor air temperature	.593	**	.654	**
					Open back openings	-.327		-.374	*
					Household size	.256		.321	*
					Open front and back openings	-.163		-.233	
					Window to wall ratio	.126		-.272	
					Orientation facing East/West	-.067		.039	
					Floor level	-.065		-.139	
					Occupancy	-.021		.089	
					Open front opening	-.010		.086	
					1:00	.613	**	.454	**
Open back openings	-.279		-.349	*					
Household size	.252		.307	*					
Open front and back openings	-.151		-.252						
Window to wall ratio	.054		-.297	*					
Orientation facing East/West	-.048		.004						
Occupancy	-.045		.074						
Floor level	-.038		-.131						
Open front opening	.011		.113						
2:00	.575	*	.401	*					
					Household size	.283		.305	*
					Open back openings	-.232		-.277	
					Open front and back openings	-.180		-.275	
					Window to wall ratio	.071		-.268	
					Occupancy	-.070		.037	
					Floor level	-.069		-.171	
					Orientation facing East/West	-.062		-.019	
					Open front openings	-.028		.058	
					3:00	.550	*	.365	*
Household size	.267		.287						
Open back openings	-.227		-.279						
Open front and back openings	-.169		-.263						
Floor level	-.071		-.184						
Open front openings	-.070		.021						
Occupancy	-.061		.025						
Orientation facing East/West	-.042		-.045						
Window to wall ratio	.030		-.300	*					

Complete results Multiple Regression Analysis using Enter-method

Time	R²	Adj. R²	Independent variables	β	r			
4:00	0.525 *	0.330 *	Outdoor air temperature	.584 **	.615 **			
			Household size	.272	.284			
			Open back openings	-.180	-.269			
			Occupancy	-.131	.008			
			Open front openings	-.101	.037			
			Window to wall ratio	-.084	-.337 *			
			Open front and back openings	-.069	-.186			
			Floor level	-.021	-.178			
			Orientation facing East/West	-.001	-.049			
			5:00	.493 *	.286 *	Outdoor air temperature	.488 *	.577 **
Household size	.269	.288						
Open front openings	.190	.223						
Window to wall ratio	-.128	-.362 *						
Occupancy	.111	.121						
Open front and back openings	-.079	-.250						
Floor level	-.048	-.169						
Orientation facing East/West	-.035	-.044						
Open back openings	-.027	-.105						
6:00	.422	.185				Outdoor air temperature	.577 **	.567 **
			Household size	.205	.213			
			Window to wall ratio	-.168	-.339 *			
			Open back openings	.158	-.100			
			Orientation facing East/West	.068	-.008			
			Occupancy	-.062	.008			
			Floor level	-.021	-.179			
			Open front openings	.020	.173			
			7:00	.355	-.161	Window to wall ratio	-.506 *	-.388 *
						Solar radiation	.434	.280
Orientation facing East/West	.285	.015						
Open front openings	.139	.202						
Occupancy	-.107	-.007						
Open back openings	.069	-.132						
Household size	.059	.128						
Floor level	-.033	-.167						
8:00	.221	-.050				Window to wall ratio	-.520 *	-.352 *
						Outdoor air temperature	-.244	-.162
			Orientation East/West	.204	.083 *			
			Open back openings	.148	-.110			
			Occupancy	.096	.029			
			Open front openings	-.080	.102			
			Floor level	.030	-.100			

Appendix E

Time	R^2	Adj. R^2	Independent variables	β	r
9:00	.253	-.007	Window to wall ratio	-.448 *	-.254
			Orientation facing	.404	.188
			East/West		
			Outdoor air temperature	-.265	-.244
			Open front openings	-.176	.024
			Open back openings	.155	-.005
			Floor level	.137	.017
			Occupancy	-.084	.078
			Household size	.052	.146
10:00	.349	-.172	Window to wall ratio	-.542	-.182
			Orientation facing	.542	.302 *
			East/West		
			Open back openings	.393	.155
			Floor level	.223	.097
			Occupancy	.119	.190
			Outdoor air temperature	-.117	.055
			Household size	-.089	.153
			Open front openings	.011	.097
11:00	.348	-.174	Orientation facing	.428	.343 *
			East/West		
			Window to wall ratio	-.286	-.174
			Floor level	.267	.193
			Open back openings	.215	.045
			Outdoor air temperature	.186	.329
			Occupancy	.115	.217
			Open front openings	.054	.162
			Household size	-.027	.184
12:00	.550 **	.419 **	Outdoor air temperature	.594 **	.516 **
			Floor level	.359 *	.289
			Orientation facing	.336 *	.362 *
			East/West		
			Household size	.077 *	.165
			Open back openings	.052	-.164
			Occupancy	.047	.216
			Open front openings	.016	.236
13:00	.668 **	.572 **	Outdoor air temperature	.660 **	.625 **
			Floor level	.414 **	.343 *
			Orientation facing	.220	.333 *
			East/West		
			Household size	.068	.149
			Open back openings	-.059	-.375 *
			Occupancy	.021	.258
			Open front openings	.008	.285

Complete results Multiple Regression Analysis using Enter-method

Time	R²	Adj. R²	Independent variables	β	r				
14:00	.710	**	.609	**	Outdoor air temperature	.715	**	.661	**
					Floor level	.390	**	.368	*
					Window to wall ratio	.204		-.061	
					Occupancy	.167		.424	**
					Open front openings	.115		.326	*
					Orientation facing	.049		.358	*
					East/West				
					Household size	-.040		.114	
					Open back openings	.033		-.455	**
15:00	.629	**	.499	**	Outdoor air temperature	.596	**	.632	**
					Floor level	.343	*	.366	*
					Occupancy	.136		.368	*
					Window to wall ratio	.134		.028	
					Open back openings	-.075		-.444	**
					Open front openings	.062		.336	*
					Orientation facing	.050		.397	*
					East/West				
					Household size	-.012		.112	
16:00	.566	**	.416	**	Outdoor air temperature	.586	**	.629	**
					Floor level	.266		.301	*
					Open back openings	-.154		-.407	**
					Window to wall ratio	.128		.063	
					Occupancy	.108		.314	*
					Orientation facing	.027		.389	*
					East/West				
					Open front openings	.013		.229	
					Household size	-.003		.112	
17:00	.618	**	.506	**	Outdoor air temperature	.845	**	.690	**
					Open back openings	-.295		-.213	
					Open front openings	-.290		.228	
					Floor level	.153		.235	
					Occupancy	-.098		.143	
					Orientation facing	.055		.334	*
					East/West				
					Household size	-.027		.112	
					18:00	.672	**	.558	**
Open front openings	-.224		.320	*					
Floor level	.180		.134						
Window to wall ratio	-.177		-.195						
Occupancy	-.143		-.114						
Orientation facing	.069		.212						
East/West									
Open front and back openings	.063		-.505	**					
Household size	.033		.139						

Appendix E

Time	R^2		Adj. R^2		Independent variables	β		r	
19:00	.816	**	.741	**	Outdoor air temperature	.736	**	.801	**
					Open front and back openings	-.445	**	-.692	**
					Open front openings	-.401	*	.327	*
					Open back openings	-.321	*	.112	
					Occupancy	-.205		-.087	
					Household size	.129		.164	
					Window to wall ratio	-.121		-.279	
					Floor level	.102		.040	
					Orientation facing East/West	.069		.122	
					20:00	.825	**	.764	**
Open front openings	-.494	**	.179						
Open front and back openings	-.482	**	-.663	**					
Open back openings	-.333	**	.112						
Household size	.203	*	.195						
Occupancy	-.150		.094						
Floor level	.091		-.006						
Window to wall ratio	-.046		-.298	*					
21:00	.704	**	.601	**	Outdoor air temperature	.602	**	.752	**
					Open front and back openings	-.415	**	-.663	**
					Open back openings	-.166		.093	
					Open front openings	-.165		.161	
					Household size	.150		.231	
					Window to wall ratio	.042		-.307	*
					Floor level	.029		-.026	
					Occupancy	-.021		.136	
22:00	.681	**	.570	**	Outdoor air temperature	.515	**	.689	**
					Open front and back openings	-.476	**	-.625	**
					Household size	.207		.305	*
					Open back openings	-.186		.026	
					Window to wall ratio	.099		-.296	*
					Open front openings	-.079		.047	
					Occupancy	.032		.076	
					Floor level	-.015		-.066	
23:00	.591	**	.449	**	Outdoor air temperature	.572	**	.619	**
					Open back openings	-.360	*	-.349	*
					Household size	.279		.353	*
					Open front and back openings	-.120		-.174	
					Floor level	-.104		-.125	
					Window to wall ratio	.083		-.273	
					Open front openings	.019		.116	
					Occupancy	-.004		.111	

2. Excluding outdoor air temperature (Out_AT)

Time	R ²	Adj. R ²	Independent variables	β	r			
0:00	.351	.125	Open back openings	-.420	-.374 *			
			Open front and back openings	-.341	-.233			
			Household size	.218	.321 *			
			Occupancy	.147	.089			
			Floor level	-.133	-.139			
			Orientation facing East/West	.067	.039			
			Window to wall ratio	-.049	-.272			
			Open front openings	-.036	.086			
			1:00	.330	.096	Open back openings	-.368	-.349 *
						Open front and back openings	-.340	-.252
Household size	.219	.307 *						
Occupancy	.130	.074						
Floor level	-.112	-.131						
Window to wall ratio	-.084	-.297 *						
Orientation facing East/West	.040	.004						
Open front openings	-.008	.113						
2:00	.298	.054				Open front and back openings	-.356	-.275
						Open back openings	-.296	-.277
			Household size	.260	.305 *			
			Floor level	-.143	-.171			
			Occupancy	.093	.037			
			Window to wall ratio	-.052	-.268			
			Open front openings	-.050	.058			
			Orientation facing East/West	-.005	-.019			
			3:00	.294	.048	Open front and back openings	-.336	-.263
						Open back openings	-.283	-.279
Household size	.246	.287						
Floor level	-.142	-.184						
Window to wall ratio	-.094	-.300 *						
Occupancy	.094	.025						
Open front openings	-.089	.021						
Orientation facing East/West	-.017	-.045						

Appendix E

Time	R^2	Adj. R^2	Independent variables	β	r
4:00	0.262	0.005	Open front and back openings	-0.261	-0.186
			Open back openings	-0.232	-0.269
			Window to wall ratio	-0.228	-0.337 *
			Household size	.224	.284
			Open front openings	-0.093	.037
			Floor level	-0.085	-0.178
			Orientation facing East/West	.021	-0.049
			Occupancy	-0.011	.008
			5:00	.307	.066
Window to wall ratio	-0.283	-0.362 *			
Open front openings	.226	.223			
Open front and back openings	-0.223	-0.250			
Floor level	-0.073	-0.169			
Orientation facing East/West	.071	-0.044			
Occupancy	.035	.121			
Open back openings	-0.018	-0.105			
6:00	.321	.084			
			Household size	.184	.213
			Floor level	-0.119	-0.179
			Open back openings	-0.111	-0.100
			Open front openings	.092	.173
			Orientation facing East/West	.024	-0.008
			Occupancy	-0.001	.008
			7:00	.355	-0.161
Solar radiation	.434	.280			
Orientation facing East/West	.285	.015			
Open front openings	.139	.202			
Occupancy	-0.107	-0.007			
Open back openings	.069	-0.132			
Household size	.059	.128			
Floor level	-0.033	-0.167			
8:00	.184	-0.054			
			Orientation facing East/West	.259	.083 *
			Household size	.036	.120
			Open back openings	.030	-0.110
			Occupancy	.024	.029
			Open front openings	-0.017	.102
			Floor level	.007	-0.100

Complete results Multiple Regression Analysis using Enter-method

Time	R ²	Adj. R ²	Independent variables	β	r
9:00	.201	-.032	Orientation facing	.458	.188
			East/West		
			Window to wall ratio	-.457 *	-.254
			Occupancy	-.112	.078
			Floor level	.110	.017
			Open front openings	-.108	.024
			Open back openings	.070	-.005
			Household size	.059	.146
10:00	.339	-.082	Orientation facing	.523	.302 *
			East/West		
			Window to wall ratio	-.477	-.182
			Open back openings	.386	.155
			Floor level	.222	.097
			Occupancy	.106	.190
			Household size	-.073	.153
			Open front openings	.038	.097
11:00	.335	.141	Orientation facing	.492 *	.343 *
			East/West		
			Window to wall ratio	-.448 *	-.174
			Floor level	.269	.193
			Open back openings	.224	.045
			Occupancy	.142	.217
			Household size	-.065	.184
			Open front openings	.044	.162
12:00	.253	.074	Floor level	.287	.289
			Orientation facing	.243	.362 *
			East/West		
			Open front openings	.208	.236
			Occupancy	.111	.216
			Household size	.061	.165
			Open back openings	.003	-.164
13:00	.328	.167	Floor level	.298 **	.343 *
			Open back openings	-.216	-.375 *
			Open front openings	.208	.285
			Orientation facing	.128	.333 *
			East/West		
			Household size	.112	.149
			Occupancy	.103	.258
14:00	.475 *	.322 *	Floor level	.395 *	.368 *
			Occupancy	.309	.424 **
			Open front openings	.251	.326 *
			Window to wall ratio	-.228	-.061
			Orientation facing	.207	.358 *
			East/West		
			Open back openings	-.080	-.455 **
			Household size	-.063	.114

Appendix E

Time	R^2	Adj. R^2	Independent variables	β	r			
15:00	.419 *	.250 *	Floor level	.344 *	.366 *			
			Occupancy	.195	.368 *			
			Orientation facing East/West	.193	.397 *			
			Open back openings	-.190	-.444 **			
			Open front openings	.183	.336 *			
			Window to wall ratio	-.135	.028			
			Household size	.025	.112			
			16:00	.306	.103	Floor level	.274	.301 *
Orientation facing East/West	.230	.389 *						
Open back openings	-.207	-.407 **						
Occupancy	.174	.314 *						
Open front openings	.127	.229						
Window to wall ratio	-.084	.063						
Household size	.022	.112						
17:00	.201	.009				Orientation facing East/West	.265	.334 *
			Floor level	.224	.235			
			Open front openings	.219	.228			
			Occupancy	.094	.143			
			Household size	.041	.112			
			Open back openings	.039	-.213			
			18:00	.406	.233	Open front and back openings	-.506 **	-.505 **
						Orientation facing East/West	.289	.212
Floor level	.263	.134						
Window to wall ratio	-.233	-.195						
Occupancy	-.111	-.114						
Household size	.084	.139						
Open front openings	-.046	.320 *						
19:00	.591 **	.448 **				Open front and back openings	-.800 **	-.692 **
			Open back openings	-.269	.112			
			Window to wall ratio	-.181	-.279			
			Household size	.180	.164			
			Orientation facing East/West	.159	.122			
			Open front openings	-.146	.327 *			
			Occupancy	-.130	-.087			
			Floor level	.116	.040			

Complete results Multiple Regression Analysis using Enter-method

Time	R²	Adj. R²	Independent variables	β	r
20:00	.507 *	.363 *	Open front and back openings	-805 **	-.663 **
			Open back openings	-.295	.112
			Open front openings	-.231	.179
			Household size	.157	.195
			Window to wall ratio	-.077	-.298 *
			Occupancy	-.073	.094
			Floor level	.018	-.006
21:00	.471 *	.317 *	Open front and back openings	-.673 **	-.663 **
			Open back openings	-.135	.093
			Household size	.135	.231
			Open front openings	-.067	.161
			Window to wall ratio	-.044	-.307 *
			Occupancy	.026	.136
			Floor level	-.001	-.026
22:00	.491 *	.343 *	Open front and back openings	-.679 **	-.625 **
			Household size	.233	.305 *
			Open back openings	-.160	.026
			Open front openings	-.110	.047
			Occupancy	.105	.076
			Floor level	-.049	-.066
			Window to wall ratio	.022	-.296 *
23:00	.349	.159	Open back openings	-.409 *	-.349 *
			Open front and back openings	-.284	-.174
			Household size	.270	.353 *
			Occupancy	.191	.111
			Floor level	-.176	-.125
			Window to wall ratio	-.076	-.273
			Open front openings	-.017	.116

Appendix F

Detail of questionnaires for the classrooms in Dutch colonial buildings

FOR STUDENT

Questionnaire

Application of passive cooling techniques in Dutch colonial building to apartments for emerging middle classes in Indonesia

A. Introduction

Greetings,

The purpose of this questionnaire survey is to understand comfort level of the occupants of Dutch colonial building in Indonesia. This questionnaire result will be **confidentially use for research purpose only**. It is guaranteed that **no personal data will be delivered to public, in any condition**. Therefore, please comfortably answer the questions.

Thank you very much for your participation.

B. Personal Identification

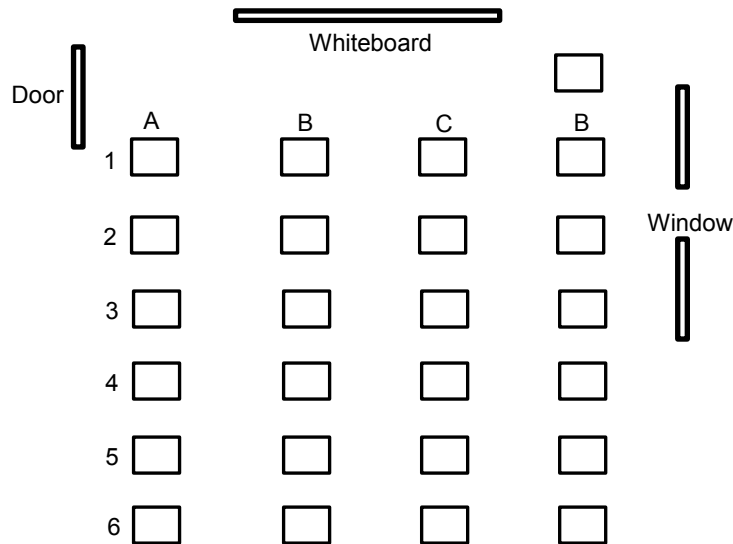
1. Location : Room 4 / Room 7
2. Date :
3. Time :
4. Gender Male Female

If you are female, are you wearing *hijab* (Moslem clothes for woman)?

- Yes
- No

5. Age : _____ years

6. Position of desk (put check (√) on the desk where you sit):

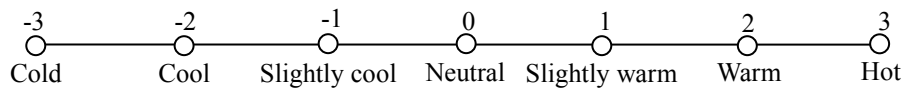


C. Thermal sensation and thermal preference

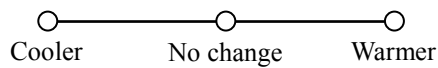
Please put check (√) on the following scale to express what you feel in this room

Morning

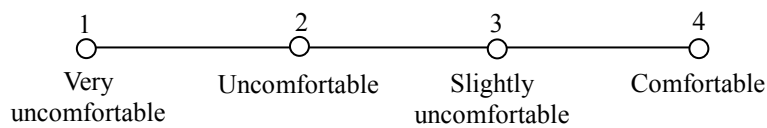
1 How do you feel about the thermal condition in this room in the morning?



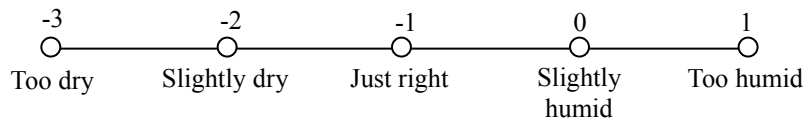
2. What kind of thermal condition do you prefer to have in this room in the morning?



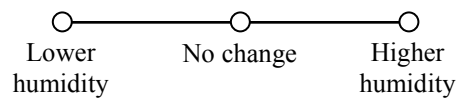
3. How would you rate your overall comfort when you are in this room in morning?



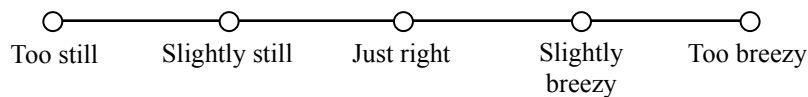
4. How do you feel about the relative humidity in this room in the morning?



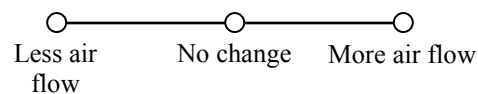
5. What kind of humidity do you prefer to have in this room in the morning?



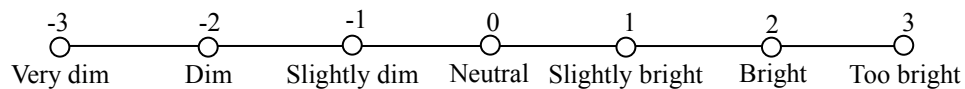
6. How do you feel about the wind flow in this room in the morning:



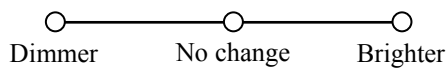
7. What kind of wind flow do you prefer to have in this room in the morning?



8. How do you feel about the lighting in this room in the morning?

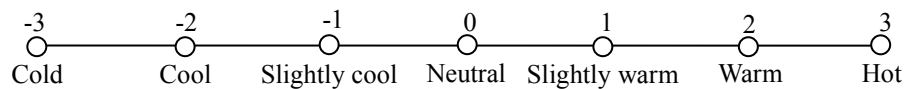


9. What kind of lighting do you prefer to have in this room in the morning?

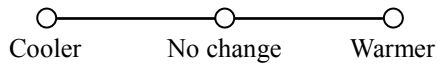


Afternoon

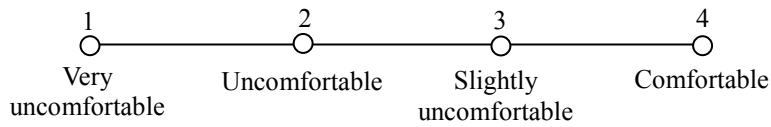
10. How do you feel about the thermal condition in this room in the afternoon?



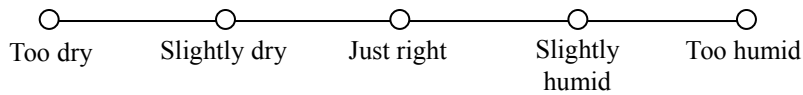
11. What kind of thermal condition do you prefer to have in this room in the afternoon?



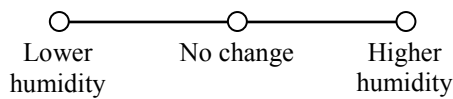
12. How would you rate your overall comfort when you are in this room in afternoon?



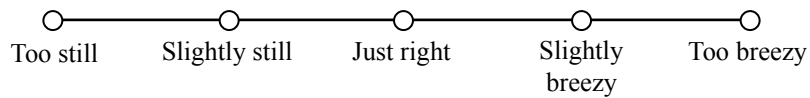
13. How do you feel about the relative humidity in this room in the afternoon?



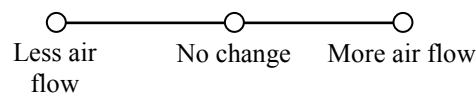
14. What kind of humidity do you prefer to have in this room in the afternoon?



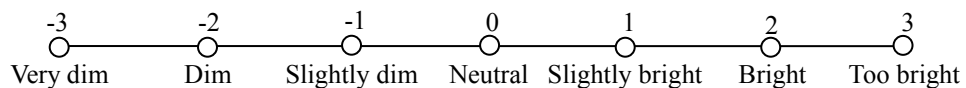
15. How do you feel about the wind flow in this room in the afternoon?



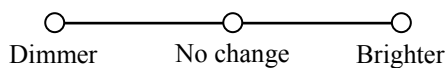
16. What kind of wind flow do you prefer to have in this room in the afternoon?



17. How do you feel about the lighting in this room in the afternoon?



18. What kind of lighting do you prefer to have in this room in the afternoon?



FOR TEACHER

Questionnaire

Application of passive cooling techniques in Dutch colonial building to apartments for emerging middle classes in Indonesia

A. Introduction

Greetings.

The purpose of this questionnaire survey is to understand comfort level of occupants of Dutch colonial building in Indonesia. This questionnaire result will be **confidentially use for research purpose only**. It is guaranteed that **no personal data will be delivered to public, in any condition**. Therefore, please comfortably answer the questions.
Thank you very much for your participation.

B. Personal Identification

1. Location : Room 4 / Room 7
2. Number of students :
3. Date :
4. Time :
5. Gender : Male Female

If you are female, are you wearing hijab (Moslem clothes for woman)?

- Yes
 No

6. Age : _____ years

7. Teaching schedule :

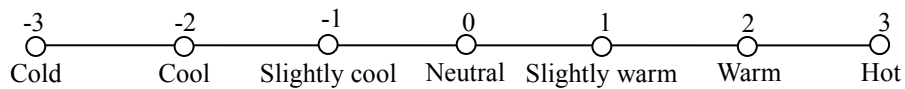
No	Day	Time		
1	Monday			
2	Tuesday			
3	Wednesday			
4	Thursday			
5	Friday			

C. Thermal sensation and thermal preference

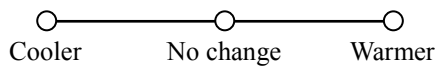
Please put check (√) on the following scale to express what you feel in this room

Morning

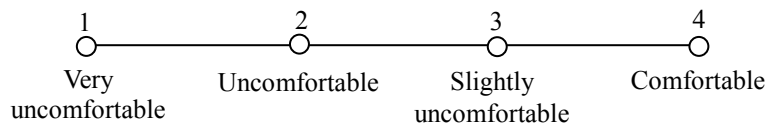
1. How do you feel about the thermal condition in this room in the morning?



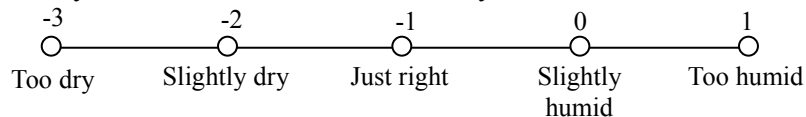
2. What kind of thermal condition do you prefer to have in this room in the morning?



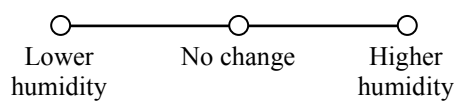
3. How would you rate your overall comfort when you are in this room in morning?



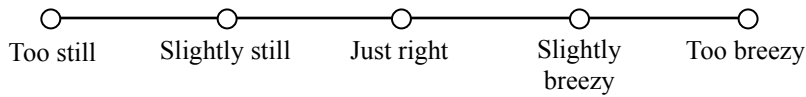
4. How do you feel about the relative humidity in this room in the morning?



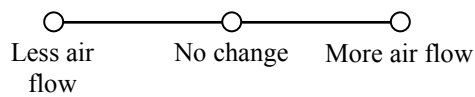
5. What kind of humidity do you prefer to have in this room in the morning?



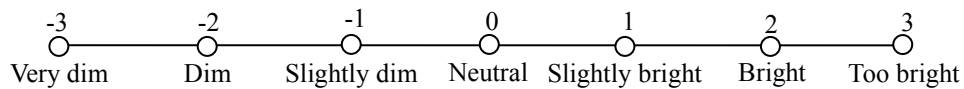
6. How do you feel about the wind flow in this room in the morning:



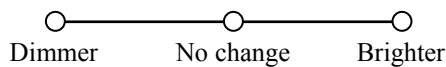
7. What kind of wind flow do you prefer to have in this room in the morning?



8. How do you feel about the lighting in this room in the morning?

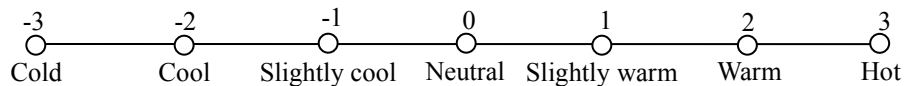


9. What kind of lighting do you prefer to have in this room in the morning?

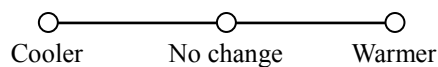


Afternoon

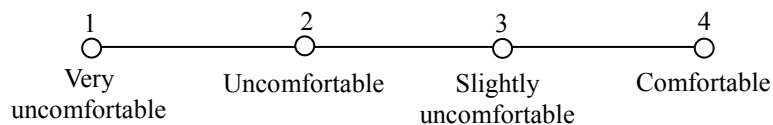
10. How do you feel about the thermal condition in this room in the afternoon?



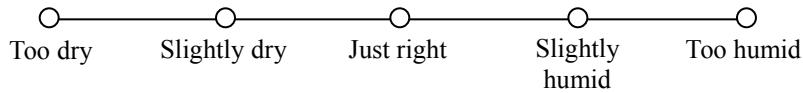
11. What kind of thermal condition do you prefer to have in this room in the afternoon?



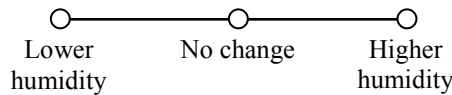
12. How would you rate your overall comfort when you are in this room in afternoon?



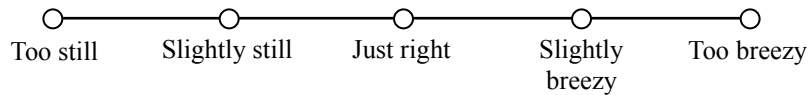
13. How do you feel about the relative humidity in this room in the afternoon?



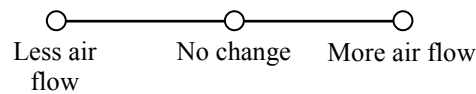
14. What kind of humidity do you prefer to have in this room in the afternoon?



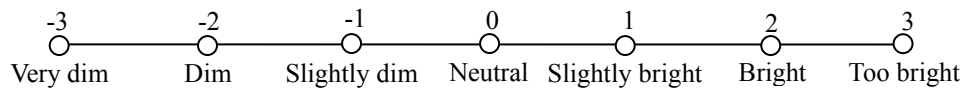
15. How do you feel about the wind flow in this room in the afternoon?



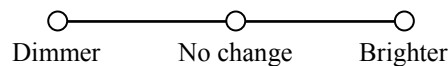
16. What kind of wind flow do you prefer to have in this room in the afternoon?



17. How do you feel about the lighting in this room in the afternoon?



18. What kind of lighting do you prefer to have in this room in the afternoon?



D. Additional comments

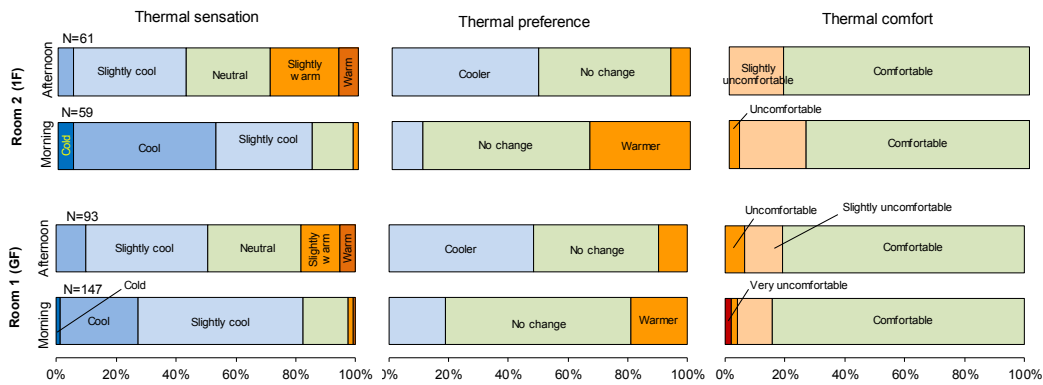
Please write your thought about the thermal environment in this room freely

Appendix G

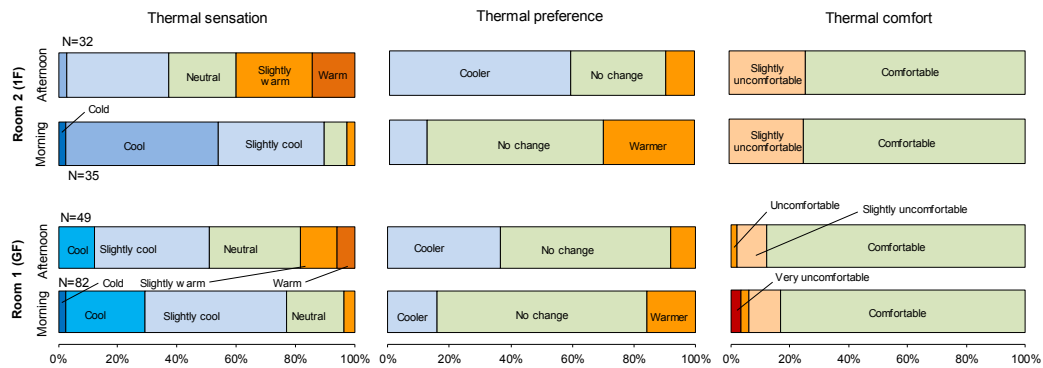
Complete results of questionnaires in Case Study 1: SMAN 3 Bandung

1. Thermal votes

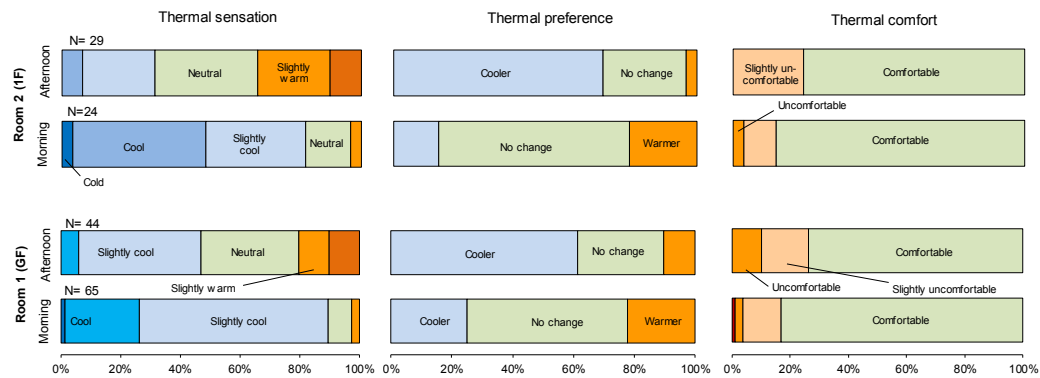
a. Overall samples



b. Samples on the middle-area

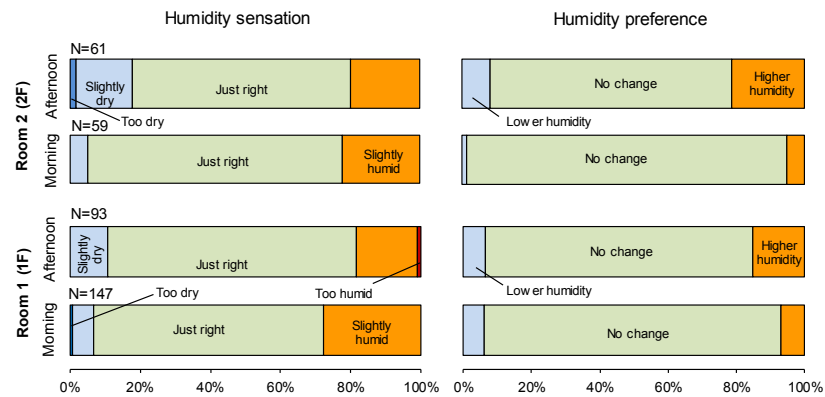


c. Samples on the edge-area (near windows/door)

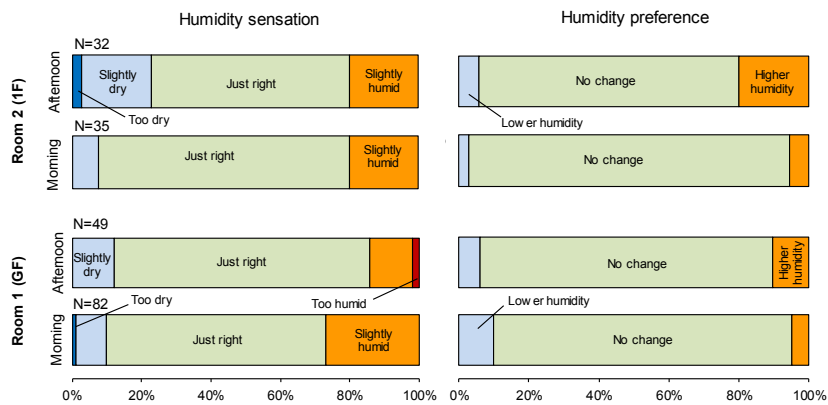


2. Humidity votes

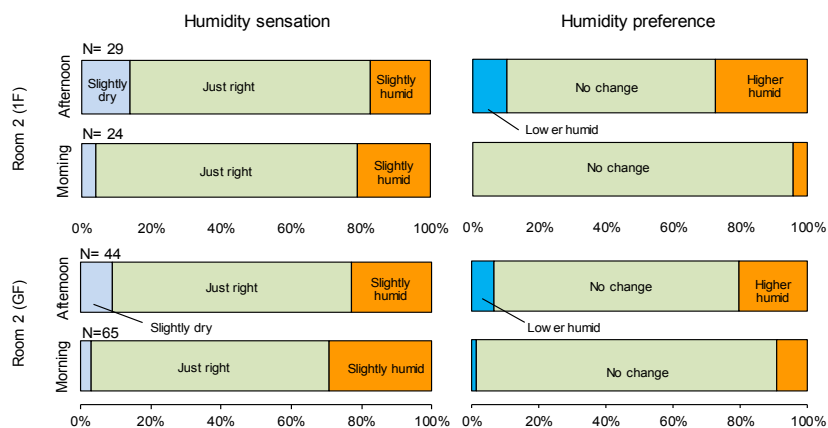
a. Overall samples



b. Samples on the middle-area

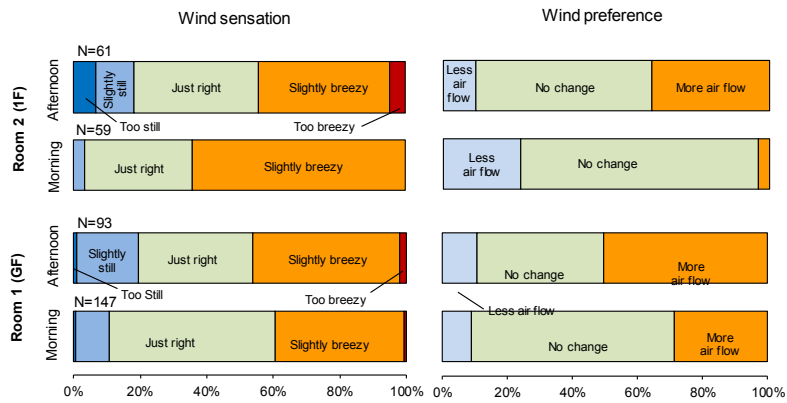


c. Samples on the edge-area (near windows/door)

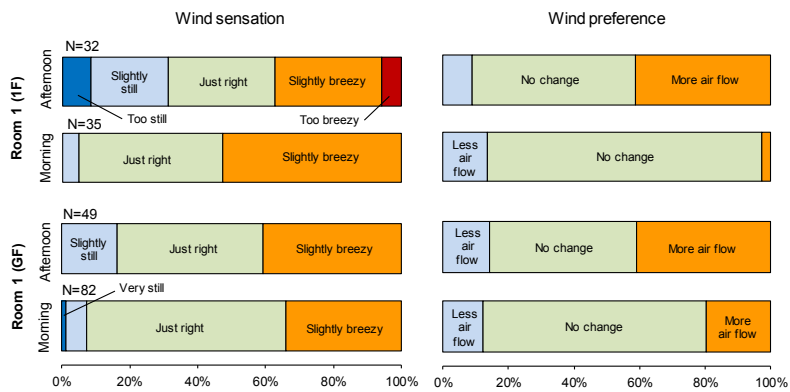


3. Wind speed votes

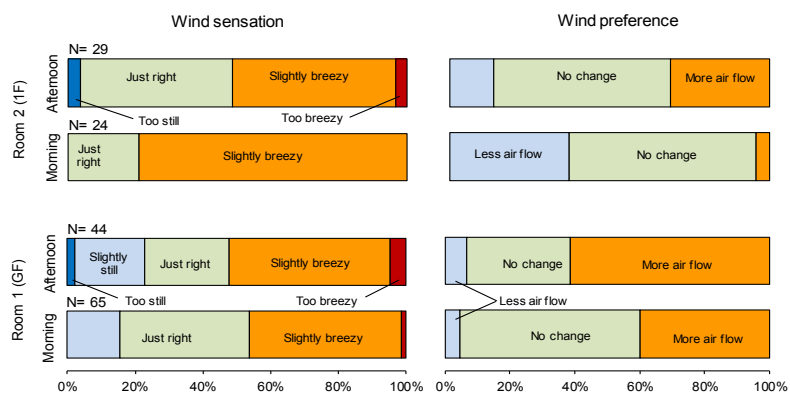
a. Overall samples



b. Samples on the middle-area

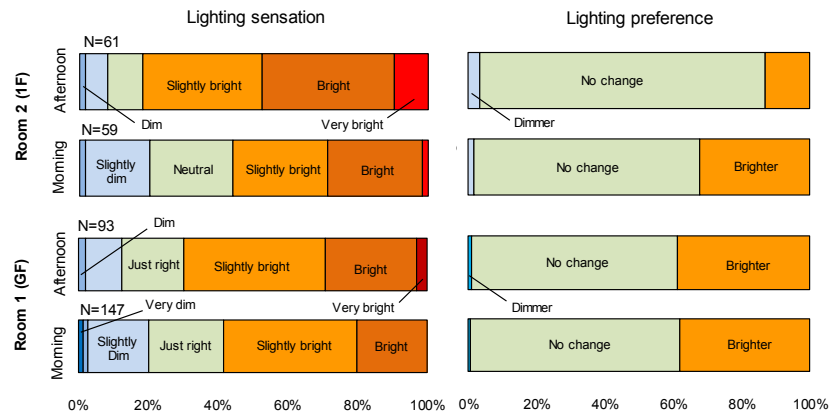


c. Samples on the edge-area (near windows/door)

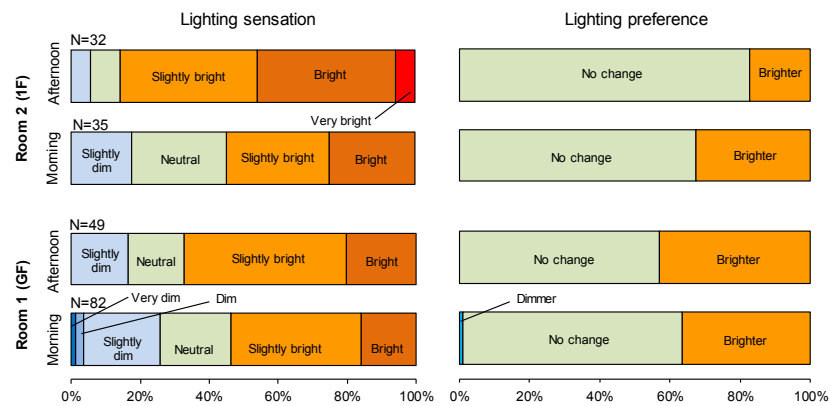


4. Lighting votes

a. Overall samples



b. Samples on the middle-area



c. Samples on the edge-area (near windows/door)

